Copyright Notices

Notice 1

Notice 2

MONASH University

EFFECTS OF GLYCYRRHIZIC ACID ON PEROXISOME PROLIFERATOR-**ACTIVATED RECEPTOR γ**, LIPOPROTEIN **LIPASE AND 11β**-HYDROXYSTEROID DEHYDROGENASE IN RATS

CHIA YOKE YIN

BSc (Biotechnology) (Hons)
MONASH UNIVERSITY

A thesis submitted in fulfillment of the requirements for the degree of
Doctor of Philosophy

Faculty of Science
Monash University

August 2009

TABLE OF CONTENTS

LIST OF FIGURES

LIST OF TABLES

ABSTRACT

The metabolic syndrome is a cluster of metabolic abnormalities comprising of dyslipidaemia and insulin resistance (IR). Peroxisome proliferator-activated receptor gamma (PPARγ) is a ligand-activated transcription factor with a pivotal role in adipocyte differentiation and insulin sensitization. Studies on the ligand binding potential of glycyrrhizic acid (GA), a potential agonist to PPARγ displayed encouraging results in the amelioration of metabolic syndrome. Two isoforms of 11β-hydroxysteroid dehydrogenases, namely 11β-HSD1 and 11β-HSD2, regulate intracellular glucocorticoid levels. Lipoprotein lipase (LPL), a regulator of lipoprotein metabolism, is a downstream gene of PPARγ and its expression is reduced with the occurrence of IR and increased activities of 11β-HSD.

The effects of two different routes of GA administration (oral vs. intraperitoneal), different dosages of GA and treatment periods were studied in rats. It was found that oral administration of 100 mg/kg GA led to optimum improvements in all the studied parameters. GA treatment led to an overall significant decrease in blood glucose and HOMA-IR ($P < 0.05$) as well as serum insulin levels ($P > 0.05$) and improvements in the lipid profile with a decrease in serum TAG, total cholesterol and LDL-cholesterol accompanied by an increase in HDL-cholesterol ($P > 0.05$).

Expression levels of total PPARγ, PPARγ1, PPARγ2 and LPL as well as 11β-HSD1 and 2 activities were measured in six different tissues, i.e., the subcutaneous and visceral adipose tissues, abdominal muscle, quadriceps femoris, liver and kidney. Oral administration of 100 mg/kg GA led to significant increases in the expression levels of total PPARγ, PPARγ1, PPARγ2 and LPL in the subcutaneous and visceral adipose tissues, abdominal muscle and quadriceps femoris ($P < 0.05$) while non-significant increases (i.e., $P > 0.05$) were observed in the liver and kidney. The increase in tissue LPL expression correlated with the improvement of lipid profile in the GA-administered rats. GA administration also led to significant decreases ($P < 0.05$) in 11β-HSD1 activity

in all the studied tissues except for the subcutaneous adipose tissue while 11β-HSD2 activity was significantly decreased in all the six tissues examined ($P < 0.05$).

Overall, this study has shown that GA can possibly be used to ameliorate metabolic syndrome and demonstrated the interlinking roles of PPARγ, 11β-HSD and LPL in glucose homeostasis and lipid metabolism.

STATEMENT OF AUTHORSHIP

The thesis contains no material which has been accepted for the award of any other degree or diploma in any university or other institution. I affirm that, to the best of my knowledge, the thesis contains no material previously published or written by another person, except where due reference is made in the text of the thesis.

Signed:

.....

Chia Yoke Yin

August 2009

ACKNOWLEDGEMENT

First and foremost, allow me to express my gratitude to my supervisor, Dr. Ton So Ha for her continuous support, patience, motivation, enthusiasm and immense knowledge during my Ph.D study and research. Her guidance proved the difference during my research and the writing of this thesis, especially her detailed and constructive comments. Her dedication and interest towards her research group as well as her believe in me truly pushed me to strive for academic excellence. I could not have imagined having a better advisor and mentor for my Ph.D study.

Besides my supervisor, I would like to express my warm and sincere thanks to Dr Yeo Chew Chieng, for his insightful comments and criticisms. Our extensive discussions regarding my work and interesting explorations have been very helpful for this study.

I thank my fellow lab mates in Monash University: Misses Ooi LL, Goh CP, Ng SW, Low KY, Liong SY, Eu ACH and How KY; Messrs Ng MKY, Lim AWY, Tiu KM, Choh LC, Ng IEH, Lim WKA and Wong SM for their support and assistance in time of need, for the sleepless nights working together as well as for their companionship and their antics which made it a joyous journey.

I would like to extend my appreciation to all the Monash University Sunway Campus laboratory and academic staff for their generosity in assistance and technical advice.

Special acknowledgement goes out to Mr. Liew KL for being the guiding light in my journey of research. Words could barely do justice to the encouragement and assistance he offered during the good and the bad times and I cherish him for believing in me even when the chips were down. I would like to express my heartfelt thanks to

Misses Yong ASY and Tsan CSY for their words of advice and encouragement during difficult times.

I am eternally grateful to my family for all the love and care they showered upon me. They were my pillars of strength in my quest for self-improvement and were there when I needed them. I would also like to thank Mr. and Mrs. Liew MK for supporting me spiritually throughout the research years.

The financial support of the Ministry of Science and Technology (MOSTI) (Malaysia) is gratefully acknowledged.

August 2009
Adeline Chia

LIST OF PUBLICATIONS

Journal Papers Accepted/Published:

(1) Chia, Y.Y, Ton, S.H and Khalid B.A.K. (2009) Effects of Glycyrrhizic acid on 11β-Hydroxysteroid Dehydrogenase (11βHSD1 and 2) Activities and HOMA-IR in rats at different treatment periods. *Experimental and Clinical Endocrinology and Diabetes*, 117: 1-8.

(2) Lim, A.W.Y, Chia, Y.Y., Liong, S.Y., Ton, S.H., Khalid, B.A.K. and Sharifah, N.A.S.H. (2009) Lipoprotein Lipase Expression, Serum Lipid and Tissue Lipid Deposition in Orally-administered Glycyrrhizic Acid-treated Rats. *Lipids in Health & Disease*, 8 (1): Article No. 31.

Journal Papers Submitted:

(1) Chia, Y.Y, Ton, S.H and Khalid, B.A.K (2009) Effects of Glycyrrhizic Acid on Peroxisome Proliferator-Activated Receptor Gamma (Total PPARγ, PPARγ1, PPARγ2) Expressions and HOMA-IR in rats. *Asia Pacific Journal of Molecular Biology and Biotechnology*. Manuscript under review.

(2) Chia, Y.Y, Ton, S.H and Khalid, B.A.K (2009) Peroxisome Proliferator-Activated Receptor Gamma (PPARγ), Lipoprotein Lipase (LPL), serum lipid and HOMA-IR in rats given Glycyrrhizic acid. *PPAR Research*. Manuscript under review.

Conference Papers Accepted/Published:

(1) Chia, Y.Y., Ton, S.H. and Khalid B.A.K (2008) Homeostasis model of assessment –insulin resistance (HOMA-IR) and histological analysis on tissues of rats administered with glycyrrhizic acid. *33rd Ann Concf Malaysian Soc for Biochem and Mol Biol*., 27-28th Aug, Kuala Lumpur Pg 147.

(2) Chia, Y.Y., Ton, S.H. and Khalid B.A.K (2008) Effects of the treatment period with glycyrrhizic acid on 11β-hydroxysteroid dehydrogenase type 1 activity in rats. *33rd Ann Concf Malaysian Soc for Biochem and Mol Biol*., 27-28th Aug, Kuala Lumpur Pg 52.

(3) Choh, L.C., Chia, Y.Y., Ton, S.H. and Khalid B.A.K (2008) Effects of glycyrrhizic acid on 11β-hydroxysteroid dehydrogenase type 1 and type 2 activities. *33rd Ann Concf Malaysian Soc for Biochem and Mol Biol*., 27-28th Aug, Kuala Lumpur Pg 54.

(4) Lim, W.Y.A., Liong, S.Y., Chia, Y.Y., Ton, S.H. and Khalid B.A.K (2008) Lipid profile, serum free fatty acids and lipid deposition in glycyrrhizic acid-treated rats. *33rd Ann Concf Malaysian Soc for Biochem and Mol Biol*., 27-28th Aug, Kuala Lumpur Pg 86.

(5) Chia, Y.Y. (2007) Peroxisome proliferator-activated receptor (PPAR) gamma levels in glucose homeostasis and adipogenesis in rats administered with glycyrrhizic acid. *The Inaugural Frontiers in Biotechnology Research* (Seminar Series).

(6) New, J.Y., Chia, Y.Y., Ton, S.H. and Khalid B.A.K. (2007) 11β-hydroxysteroid dehydrogenase type 1 activity in glycyrrhizic acid treated rats. *Chinese Medical Journal*, 120(2): 197. [ISSN: 0366-6999].

(7) Goh, C.P., Chia, Y.Y., Ton, S.H. and Khalid, B.A.K. (2007) Blood glucose and serum insulin levels in glycyrrhizic acid treated rats. *Chinese Medical Journal*, 120(2): 200-201. [ISSN: 0366-6999].

(8) Goh, C.P., Chia, Y.Y., Ton, S.H., Khalid, B.A.K. and Sharifah. N.A. (2007) Blood glucose levels and histological analysis of rats administered with glycyrrhizic acid. *32nd Ann Concf Malaysian Soc for Biochem and Mol Biol*., 5-6th Sept, Petaling Jaya Pg 42.

ABBREVIATIONS

6PG	6-phosphogluconolactone
11β-HSDs	11β-hydroxysteroid dehydrogenases
11β-HSD1	11β-hydroxysteroid dehydrogenase type 1
11β-HSD2	11β-hydroxysteroid dehydrogenase type 2
ABCA1	ATP binding cassette transporter member 1, sub-family ABCA
ABCG1	ATP binding cassette transporter member 1, sub-family ABCG
ACC	acetyl-CoA carboxylase
ACS	acyl-CoA synthase
ADA	American Diabetes Association
AF-2	Activation Function 2
aP2	Fatty acid binding protein
ATP	Adenosine Tri-Phosphate
ATPase	Adenosine triphosphatase
ATP III	Adult Treatment Panel III
ATS	Subcutaneous adipose tissue
ATV	Visceral adipose tissue
BAC	β-actin
BLAST	Basic Local Alignment Searching Tool
BMI	Body mass index
BSA	Bovine serum albumin
CAP	c-Cbl associating protein
C/EBP α	CCATT/enhancer binding protein α
COX-2	Cyclooxygenase type 2
CVD	Cardiovascular diseases
DHAP	Dihydroxyacetone phosphate

EDTA	Ethylenediaminetetraacetate
ELISA	Enzyme-linked immunosorbant assay
FAS	Fatty acid synthase
FAT/CD36	Fatty acid translocase
FATP-1	Fatty acid transport protein-1
FFAs	Free fatty acids
G6Pase	Glucose-6-phosphatase
GA	Glycyrrhizic acid
GC	Glucocorticoid
GE	Glycyrrhetic acid
GLUT-2	Glucose transporter-2
GLUT-4	Glucose transporter-4
GM	Monoglucuronyl-glycyrrhetic acid
GR	Glucocorticoid receptor
GRE	Glucocorticoid response element
GSIS	Glucose-stimulated insulin secretion
H&E	Haematoxylin and Eosin
H6PDH	Hexose-6-phosphate dehydrogenase
HDL	High density lipoprotein
HOMA-IR	Homeostasis Model Assessment of Insulin Resistance
HPLC	High performance liquid chromatography
HRP	Horseradish peroxidise
HSPG	Heparin sulphate proteoglycans
IDF	International Diabetes Federation
IFG	Impaired fasting glucose
IGT	Impaired glucose tolerance
IL-6	Interleukin-6
IP10	Interferon-inducible protein 10
IR	Insulin resistance

IRS-1	Insulin receptor substrate-1
iTAC	Interferon-inducible T-cell alpha chemoattractant
kDa	kilo-Daltons
K	Kidney
K^+	Potassium
KR	Krebs-Ringer
KRB buffer	Krebs-Ringer bicarbonate buffer
L	Liver
LADA	Latent Autoimmune Diabetes of Adults
LDL	Low density lipoprotein
LNA	Locked Nucleic Acid
LPL	Lipoprotein Lipase
MA	Abdominal muscle
mAb	Monoclonal antibody
MC	Mineralocorticoid
mCPT-1	Mitochondria carnitine palmitoyltransferase-1
MetS	Metabolic syndrome
MIG	Monokine induced by interferon γ
MMP-9	Matrix metallopeptidase 9
MR	Mineralocorticoid receptor
MT	Quadriceps femoris
NA^+	Sodium
Na^+/K^+-ATPase	Sodium, potassium-adenosine triphosphatase
NAD	Nicotinamide adenine dinucleotide
NAD^+	Oxidised nicotinamide adenine dinucleotide
NADH	Reduced nicotinamide adenine dinucleotide
NADP	Nicotamide adenine dinucleotide phosphate
$NADP^+$	Oxidised nicotinamide adenine dinucleotide phosphate

NADPH	Reduced nicotinamide adenine dinucleotide phosphate
NCBI	National Centre for Biotechnology Information
NHMS	National Health and Morbidity Survey
NO	Nitric oxide
PI3K	Phosphatidylinositol-3-kinase
PAI-1	Plasminogen activator inhibitor-1
PAS	Periodic acid Schiff's
PEPCK	Phosphoenolpyruvate carboxykinase
PPARγ	Peroxisome Proliferator-Activated Receptor gamma
PPRE	Peroxisome Proliferator Response Elements
qRT-PCR	Real-time reverse transcription polymerase chain reaction
RAS	Renin-angiotensin system
RER	Rough endoplasmic reticulum
RXR	Retinoid X Receptor
SBP	Systolic blood pressure
SPSS	Statistics Package for the Social Sciences
SREBP	Sterol regulator element-binding protein
T2DM	Type 2 diabetes mellitus
TAG	Triacylglycerol
TNF-α	Tumour necrosis factor-α
TZD	Thiazolidinedione
U	Unit
VLDL	Very low density lipoprotein
WHO	World Health Organisation

CHAPTER 1

Introduction

Chapter 1

INTRODUCTION

1.1 Metabolic syndrome

A Swedish physician, Eskil Kylin, first reported metabolic syndrome as a clinical entity in 1923 based on the manifestation of a constellation of conditions such as gout, hypertension and hyperglycaemia. Worldwide concerns and awareness were heightened as the understanding of the disorder deepened to include the presence of other complications (Balkau *et al.*, 2007). Metabolic syndrome reflects the major role of visceral (abdominal or central variant) obesity (Carr *et al.*, 2004) and insulin resistance in association with dyslipidaemia, glucose intolerance and hypertension (Moller and Kaufman, 2005), ultimately leading to inflammatory, dyslipidaemic, pro-thrombic states and increase risk of ischaemic heart disease (Grundy *et al.*, 2005; Babu and Fogelfield, 2006).

1.1.1 Epidemiology of the metabolic syndrome

Clinical definitions of the metabolic syndrome has been proposed by multiple organizations, with the latest being defined by the American Diabetes Association (ADA) in 2008, preceding the pioneer proposal by World Health Organization (WHO) in 1998 and International Diabetes Federation (IDF) in 2005 (Balkau *et al.*, 2007; American Diabetes Association, 2008). In between, the National Cholesterol Education Program – Adult Treatment Panel III (ATP III) put forward a differing definition of metabolic syndrome, which would eventually be used as a guideline for the most recent definition of metabolic syndrome (Alberti *et al.*, 2005). The current clinical definition by ADA in 2008 involves the suppression of the emphasis placed on diabetes and

insulin resistance as core criteria in earlier definitions and the emergence of central obesity as a core criterion for the syndrome. The threshold of all the other variables were similar to those of the ATP III definition, with the exception of the impaired fasting glucose threshold (5.6 mmol/L [100mg/dL]), adapted from the most recent diagnostic levels by the ADA. Despite the presence of multiple clinical definitions, the differing definitions essentially evolve around similar core cardio-metabolic risk factors such as central obesity, hyperglycaemia, dyslipidaemia and hypertension but differ in their cut-off points and threshold values (Table 1.1) (Chew *et al.*, 2006).

Metabolic syndrome is a prevalent disorder that increases with age (Eckel *et al.*, 2005) and obesity (Batsis *et al.*, 2007). The incidence of metabolic syndrome is also dependent on gender (van Zwieten and Mancia, 2006) and ethnicity (Miranda *et al.*, 2005), with men and Hispanics more susceptible compared to women and blacks or whites respectively. A worrying trend in the 21st century is the increasing prevalence of obesity in children and adolescents, thus increasing their risk of developing metabolic syndrome (Eckel *et al.*, 2005; Chew *et al.*, 2006).

However, the prevalence of obesity and metabolic syndrome cannot be directly extrapolated to Asians as studies on these populations are less comprehensive when compared to studies of Caucasians, with constant underestimation of the prevalence rates due to variations in the definition of the syndrome (Nestel *et al.*, 2007). In a study on the three major ethnic groups (Chinese, Malay and Indians) in Singapore , minor modifications such as a specific reduction in the BMI and waist circumference criteria tailored to represent the Asian population proved to be more accurate and could be extrapolated to represent the Asian community as a whole (Tan *et al.*, 2004).

Table 1.1: Clinical definitions of metabolic syndrome by various organizations

		WHO (1998)				ATP III (2001)		ADA (2008)		
Central obesity		BMI > 30kg/m^2 and/or				Waist circumference (cm) (gender and ethnic specific)				
		Waist/Hip ratio				Asian	Caucasian	Europid	South Asians	Japanese
Men		> 0.90				≥ 90	≥ 102	≥ 94	≥ 90	≥ 85
Women		> 0.85				≥ 80	≥ 88	≥ 80	≥ 80	≥ 90
Triglyceride (mmol/L)		≥ 1.7				≥ 1.7 or specific treatment for hypertriglyceridaemia				
HDL (mmol/L)	Men	≤ 0.9				< 1.03 or specific treatment for low HDL-cholesterol level				
	Women	≤ 1.0				< 1.3 or specific treatment for low HDL-cholesterol level				
Blood pressure (mmHg)		≥ 160/90 (systolic/diastolic)				≥ 130/85 (systolic/diastolic) or specific treatment of known hypertension				
Fasting plasma glucose (mmol/L)			T2DM	IGT	IFG	≥ 6.1		≥ 6.9 or previously diagnosed T2DM		
		Fasting	≥ 7.0	< 7.0	6.1-7.0					
		2-hrs post	≥ 11.1	7.8-11.1	< 7.8					
Urinary protein		Microalbuminuria: ≥ 20μg/min				-		-		
Criteria required for diagnosis		Glucose intolerance, T2DM and two of the others above				Three or more of the five criteria above		Central obesity and two others of the above		

WHO: World Health Organization, ATP III: National Cholesterol Education Program – Adult Treatment Panel III, IDF: International Diabetes Federation, BMI: body mass index, HDL: high-density lipoprotein, T2DM: type 2 diabetes mellitus, IGT: impaired glucose tolerance, IFG: impaired fasting glycaemia
(Chew *et al.*, 2006; Batsis *et al.*, 2007 and American Diabetes Association, 2008)

1.1.2 Pathophysiology of the metabolic syndrome

Insulin resistance has been hypothesized as the best pathophysiological process used to explain the metabolic syndrome (Eckel *et al.*, 2005) although their direct consequential relationship remains debatable (Miranda *et al.*, 2005). Obesity and insulin resistance has been shown to be the two predominant underlying mechanisms that lead to the development of the syndrome (Misra and Khurana, 2008).

1.1.2.1 Obesity

Obesity is caused by imbalances between energy intake and expenditure leading to increased storage of triacylglycerol (TAG) by the body (Miranda *et al.*, 2005). Genetic and environmental factors such as sedentary lifestyles, smoking and poor dietary habits are common factors that promote the incidence of obesity (Cummings and Schwartz, 2003; Milnar *et al.*, 2007). Obesity-related cases of metabolic syndrome are depot specific and more prominent when the fat is accumulated around the subcutaneous and visceral (intra-abdominal) area (Grundy *et al.*, 2005). The accumulation of fat at the latter is associated with greater detrimental effects and would eventually lead to an increase in the release and accumulation of free fatty acids from the adipose tissues to peripheral tissues (Eckel *et al.*, 2005). Increased accumulation of visceral fat would lead to a parallel increase in the secretion of pro-inflammatory cytokines, thus vindicating its role to promote or further elevate insulin resistance (Bagry *et al.*, 2008).

1.1.2.2 Insulin resistance (IR)

Insulin resistance, an insufficient response or biological effect of target (adipose, liver and skeletal muscle) cells to physiological plasma insulin levels (Milnar *et al.*, 2007), plays a pivotal, if not the main role in the pathogenesis of metabolic syndrome (Bagry *et al.*, 2008). Insulin is a hormone responsible for the stimulation of peripheral

glucose uptake and inhibition of hepatic glucose production to regulate plasma glucose levels (Wassink *et al.*, 2007).

The aetiology of IR, similar to those of obesity and type 2 diabetes mellitus, involves a complex interplay between genetic predispositions, environmental factors, stress (Bagry *et al.*, 2008) and aging (Milnar *et al.,* 2007), leading to hyperinsulinaemia, hyperglycaemia as well as lipid and lipoprotein dysregulation (Bagry *et al.*, 2008). The presence of the previously mentioned conditions and concomitant elevated serum free fatty acid levels provide a positive feedback to sustain the pathologic state and perpetuate the severity of IR (Fujumoto, 2000; Bagry *et al.*, 2008). Figures 1.1a and b depict the derogatory effects of adipocyte dysfunction towards metabolic syndrome; elevated secretion of pro-inflammatory cytokines and circulatory free fatty acid levels while Table 1.2 compares the complementary causative roles of insulin resistance and obesity.

Although obesity is a common predisposing factor preceding insulin resistance, it must however be noted that insulin resistant individuals are not necessarily obese but possesses abnormal upper body fat distribution (Grundy *et al.*, 2005). Likewise, individuals of normal weight are also susceptible to insulin resistance (Eckel *et al.*, 2005).

1.1.3 Clinical significance of the metabolic syndrome

Metabolic syndrome could also serve as a predictive tool for the early detection of two prevalent clinical entities that are becoming increasingly related; cardiovascular disease (CVD) and type 2 diabetes mellitus (T2DM). Patients had reported a (i) threefold increased risk of developing myocardial infarction or stroke (Bagry *et al.*, 2008), (ii) fivefold increased risk of developing T2DM (Bagry *et al.*, 2008), further enhancing the risk of CVD (Chew *et al.*, 2006) and (iii) sevenfold increased risk for non-diabetic patients to develop T2DM (Chew *et al.*, 2006).

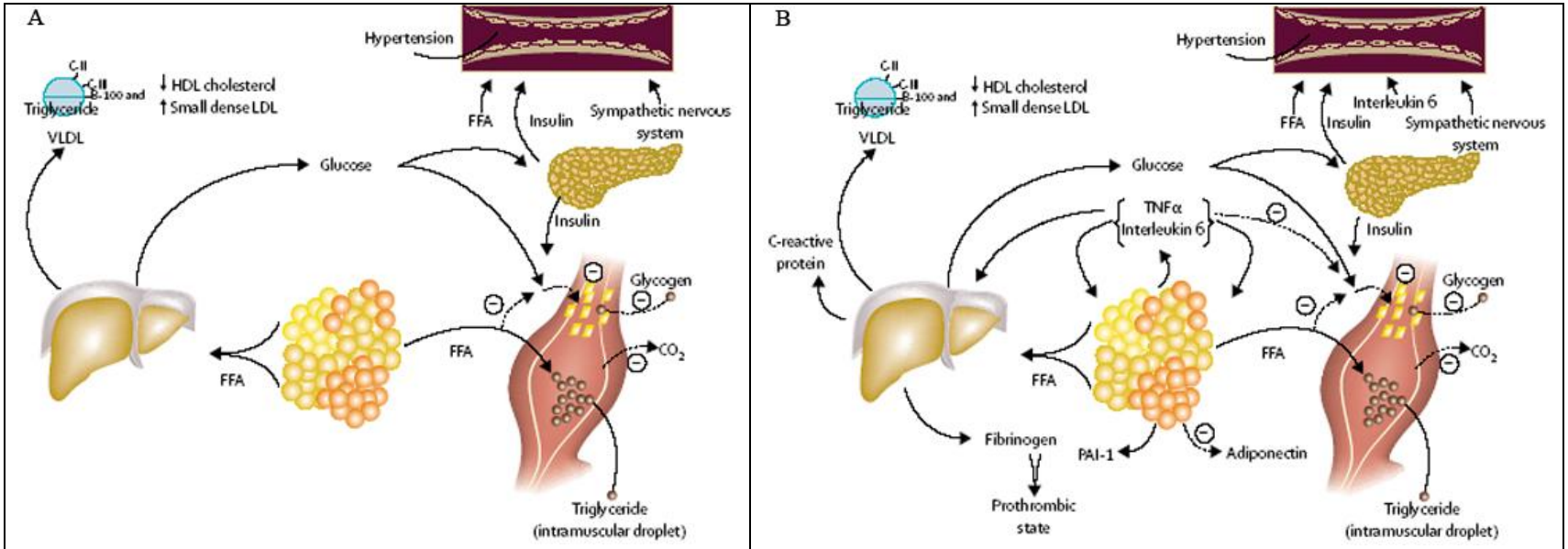

(a) Increase in adiposity mediates excessive free fatty acid (FFA) release into the circulation which would stimulate increased production of glucose, triacylglycerol (TAG) and very low density lipoproteins (VLDL). Insulin-mediated glucose uptake by muscles is also inhibited due to reduced insulin sensitivity. Associated defects encompass a reduction in glucose partitioning to glycogen and increased triacylglycerol lipid accumulation. Hyperinsulinaemia ensue due to increased pancreatic insulin secretion in concert with increase in circulatory glucose and a certain extent FFA. Resulting hyperinsulinaemia enhances sodium reabsorption and sympathetic nervous system (SNS) activity, which contributes to hypertension (Eckel *et al.*, 2005).

(b) Paracrine and endocrine effect of the pro-inflammatory state is contributed by excessive FFA. Enhanced secretion of cytokines such as interleukin-6 (IL-6) and tumor necrosis factor alpha (TNF-α) by adipocytes increases insulin resistance and lipolysis of adipose tissue TAG stores to circulating FFA. Increase in circulatory cytokines would lead to enhanced hepatic glucose and VLDL production by the liver and increases insulin resistance in muscle. Both cytokines and FFA also increase liver fibrinogen and plasminogen activator inhibitor-1 (PAI-1) production to match the overproduction of PAI-1 by adipose tissue which results in a prothrombic state. Reduction in anti-inflammatory and insulin sensitizing cytokine adiponectin production is associated with metabolic syndrome and might contribute to the pathophysiology of the syndrome (Eckel *et al.*, 2005).

Figures 1.1: Pathophysiology of metabolic syndrome

Table 1.2: Complementary roles of insulin resistance and obesity in the development of metabolic syndrome (Miranda *et al.*, 2005)

Insulin resistance	Obesity
Insulin resistance ↓ Compensatory hyperinsulinaemia to maintain euglycaemia ↓ Obesity, β-cell exhaustion and diabetes, dyslipidaemia (high fatty acid flux) ↓ Metabolic syndrome ↓ Increased atherosclerosis and cardiovascular disease	Triacylglycerol and fatty acids ↓ Triacylglycerol stored in small peripheral adipocytes ↓ Energy in > energy out ↓ During obesity, excess triacylglycerol transferred to hepatocytes, skeletal monocytes and visceral adipocytes to cause abnormally large peripheral adipocytes ↓ Excess triacylglycerol causes insulin resistance and metabolic syndrome with increased risk for cardiovascular disease

1.1.4 Possible remedy for the metabolic syndrome

Since an absolute cause for the syndrome has yet to be identified, the current strategy employed to combat the syndrome is targeted at the amelioration of risk factors (Balkau *et al.*, 2007). Although lifestyle modifications such as weight loss, regular exercise and a healthy diet have been suggested by researchers to mitigate the syndrome, it has proven to be insufficient (Fulop *et al.*, 2006).

1.2 Diabetes mellitus

Diabetes mellitus is a metabolic condition with impairment in insulin secretion, action or both, resulting in chronic hyperglycaemia as well as disturbances in carbohydrate, fat and protein mechanism (Alberti and Zimmet, 1998). There are several different manifestations of diabetes mellitus such as type 1 diabetes mellitus, type 2 diabetes mellitus and gestational diabetes which are the most common (Permutt *et al.*, 2005). Among others are insulin-resistant type 1 diabetes (double diabetes), latent autoimmune diabetes of adults (LADA) and maturity onset diabetes of the young (MODY) (Tan and Lim, 2001; American Diabetes Association, 2002).

1.2.1 Type 2 diabetes mellitus

T2DM, or previously known as non-insulin-dependent diabetes mellitus due to classification of patients based on their treatment rather than pathogenesis of the disease (Alberti and Zimmet, 1998), is the most prevalent form of diabetes, encompassing approximately 95% of all diabetic cases (Permutt *et al.*, 2005). As opposed to the absolute insulin deficiency due to autoimmune destruction of pancreatic β-cells associated with type 1 diabetes mellitus, T2DM involves the impairment of insulin action and secretion from the pancreatic β-cells (Richter *et al.*, 2007).

1.2.1.1 Epidemiology of T2DM

According to statistics recorded by the WHO, there were a reported 135 million diabetic individuals worldwide in 1995, with more than half the cases reported in India, China and the United States alone. Based on these statistics, it was projected that by 2025, the number would escalate to approximately 300 million individuals, with Asians expected to contribute to half the number (Cockram, 2000). It was also estimated that the number of diabetic individuals in developed and lesser-developed countries would increase by 42% from 51 million to 72 million and 170% from 84 million to 228 million individuals respectively (Fujimoto, 2000). The Malaysian National Health and Morbidity Survey (NHMS) III performed in 2006 indicated that the prevalence of diabetes mellitus in Malaysia was 14.9%, a staggering 86% increase over a decade from 8% in 1996. This has now proven to be an underestimate as the prevalence in 2006 was already 12% (Table 1.3). An estimate by WHO has indicated that by 2030, Malaysia would have a total 2.48 million diabetics (prevalence of 10.8%) compared to the 0.94 million diabetics in 2000, indicating an increase of 164% (Mastura *et al.*, 2008).

The incidence of diabetes mellitus is attributed to both genetic and environmental factors. T2DM displays a polygenic inheritance pattern (Ostenson, 2001) and the genes associated with T2DM are listed in Table 1.4. Defects or mutations in any of the mentioned genes would lead to the proliferation of T2DM (Groop, 1999). The prevalence of T2DM increases with age, with the middle-aged and adults older than 65 years being the most susceptible groups to the disease (Permutt *et al.*, 2005). The ethnicity and race of an individual has also been found to be a risk factor for the development of diabetes, with the minority ethnic and racial groups migrating from lesser-developed areas to urbanized regions more susceptible respectively (Fujimoto, 2000). Studies on nutritional and lifestyle trends (Groop, 1999) have highlighted the roles of both factors in the development of T2DM in obese, insulin resistant (Permutt *et al.*, 2005) and individuals with unfavourable body fat distribution (Harris, 1995), more

so with the presence of conditions such as impaired glucose tolerance (IGT) and impaired fasting glucose (IFG) (Permutt *et al.*, 2005).

1.2.1.2 Pathophysiology of T2DM

Although researchers have disputed that impaired insulin secretion is the chief cause of T2DM, evidence has proven that T2DM is a heterogenous disorder which could not be attributed to any single pathological mechanism but instead to a cluster of metabolic abnormalities (Groop, 1999; Mahler and Adler, 1999). As the majority of diabetic individuals are overweight or exhibiting traits of visceral obesity, the ability of insulin to perform its usual function would be impaired (Mahler and Adler, 1999). Obese individuals would exhibit antagonism towards insulin action through an increase in the secretion of adipocytokines (Korc, 2003) and elevated lipolytic rate which in turn releases free fatty acids. Increased levels of free fatty acids would reduce the potency of insulin to suppress glucose production in the liver and cause a positive feedback for fatty acid synthesis (Saltiel, 2001). Continuation of the mentioned condition would eventually lead to deterioration in glucose homeostasis through abnormal increases in hepatic glucose production and a reduction in glucose uptake efficiency (Groop, 1999). Thus, it has been proven that the main regulators for the incidence of T2DM are the combined effects of impaired insulin sensitivity and peripheral insulin resistance (Mahler and Adler, 1999). The metabolic staging of T2DM is summarized in Figure 1.2.

Table1. 3: Prevalence of selected health problems: Comparison between NHMS II (1996) and NHMS III (2006) (Mastura *et al.*, 2008)

	NHMS II	NHMS III
Diabetes mellitus (among adult 30 years old & above)	8.3% (95% CI: 7.8 – 8.7)	14.9% (95% CI: 14.4 – 15.5)
Hypertension (among adult 30 years & above)	29.9% (95% CI: 29.1 – 30.7)	42.6% (95% CI: 41.8 – 43.3)
Overweight (among adult 18 years old & above)	16.6% (95% CI: 16.1 – 17.1)	29.1% (95% CI: 28.6 – 29.7)
Obesity (among adult 18 years old & above)	4.4% (95% CI: 4.1 – 4.7)	14.0% (95% CI: 13.6 – 14.5)
Current smoker (among adult 18 years old & above)	24.8% (95% CI: 24.1 – 25.4)	22.8% (95% CI: 22.3 – 23.3)

Table 1.4: Several genes that are associated with T2DM and their functions (Permutt *et al.*, 2005)

Gene	Gene name	Function
ABCC8	ATP-binding cassette, subfamily C, sulfonylurea receptor	Regulator of potassium channels and insulin release
CAPN10	Calpain 10	Protease
GCGR	Glucagon receptor	Controls hepatic glucose production and insulin secretion
GCK	Glucokinase	Glucose metabolism
KCNJ11	Potassium inwardly-rectifying channel, subfamily J, member 11	Regulation of insulin secretion
PPARG	Peroxisome proliferator-activated receptor γ	Transcription factor
HNF4A	Hepatocyte nuclear factor 4 α	Transcription factor
SLC2A1	Glut 1	Glucose transporter

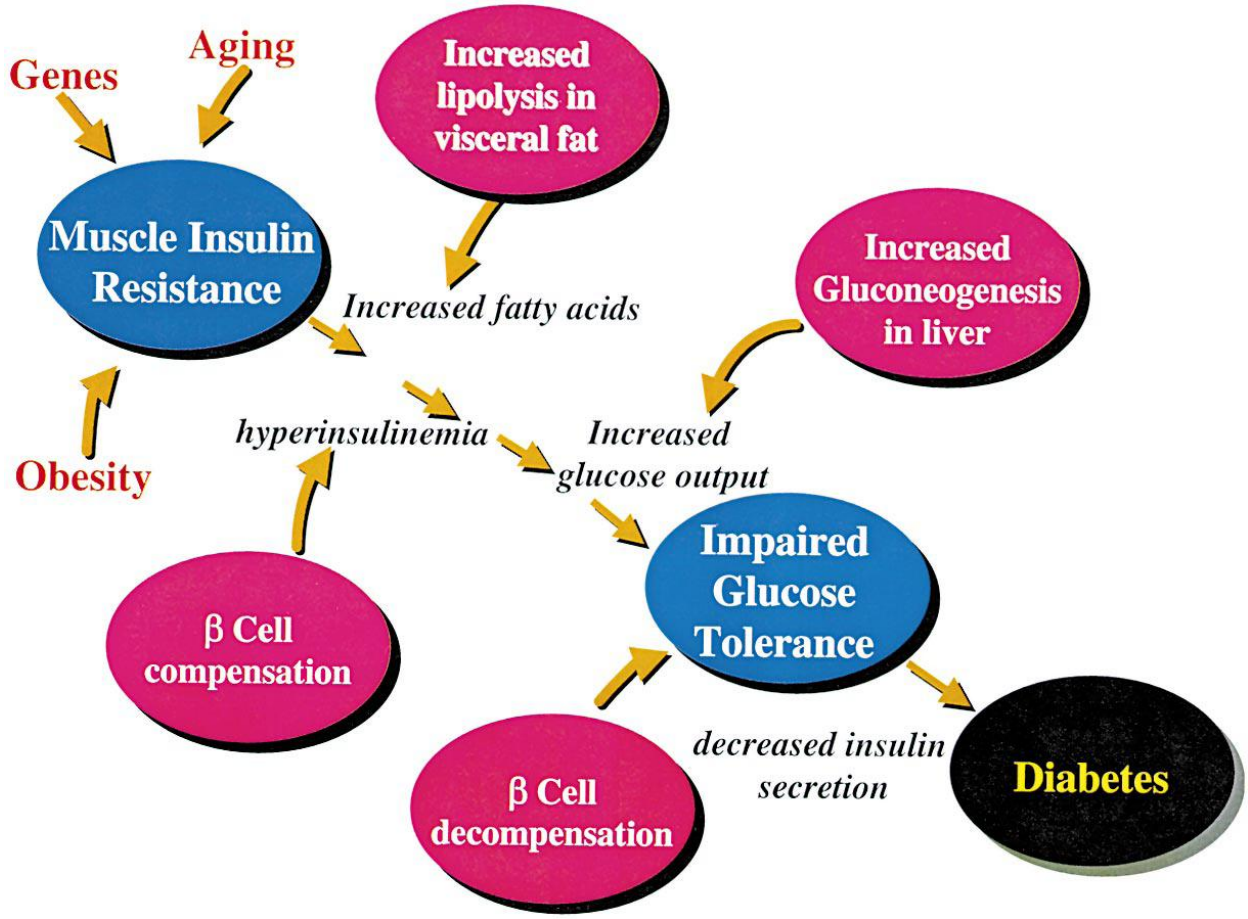

Figure 1.2: Metabolic staging of type 2 diabetes mellitus.

T2DM is preceded by a progressive decrease in insulin action and the subsequent inability of the β-cell to compensate for the ensuing IR. Incidence of IR in visceral fat mediates an increase in FFA production which worsens IR in liver and muscle. Initially the β-cell would compensate for IR by increasing insulin secretion until the threshold is reached and the compensatory mechanism could not cope with the degeneration, thus leading to impaired glucose tolerance and ultimately diabetes (Saltiel, 2001).

1.2.2 Therapeutic agents

Since 1942, sulfonylureas have been used to treat type 2 diabetes mellitus. It requires functional pancreatic β-cells for their hypoglycaemic effect. All the current available sulfonylureas in the market would bind to specific receptors on β-cells, thus resulting in the closure of potassium adenosine tri-phosphate (ATP) channels. As a result, the calcium channel will open and lead to an increase in the cytoplastic calcium that stimulates insulin release (Mahler and Adler, 1999).

Biguanides are glucose lowering drugs that work primarily by decreasing hepatic glucose production and to lesser extent by decreasing peripheral insulin resistance. This drug acts by causing the translocation of glucose transporters from the microsomal fraction to the plasma membrane of hepatic and muscle cells. Biguanides also improve the lipid profile by causing a decline in total and very low density lipoprotein triacylglycerol, total cholesterol and very low density cholesterol levels and an increase in high density lipoprotein cholesterol levels (Mahler and Adler, 1999).

Other therapeutic agents currently being used are α-glucosidase inhibitors and thiazolidinedione (TZD). α-glucosidase inhibitors act by slowing the absorption of carbohydrates from the intestines, minimizing the postprandial rise in blood glucose (Mahler and Adler, 1999). On the other hand, TZDs are insulin sensitizers that work in tandem with peroxisome proliferator-activated receptor gamma (PPARγ) to lower blood glucose and insulin levels with the ultimate aim of improving insulin sensitivity (Jermendy, 2007). TZDs are selective synthetic ligands with a high affinity for PPARγ (Kota *et al.*, 2005). Binding of TZD to PPARγ would cause a conformational change to its structure resulting in its activation (Dubuquoy *et al.*, 2002). The activation of PPARγ by TZD causes (i) proliferation and differentiation of pre-adipocytes to smaller and more insulin-sensitive adipocytes, (ii) a decrease in free fatty acid and TAG levels together with a redistribution of free fatty acids from visceral to subcutaneous adipose tissues, and (iii) improvement in β-cell function, both directly and indirectly (Jermendy,

2007). Therefore, activation of PPARγ by TZDs would lead to the presence of its insulin sensitization properties (Dubuquoy *et al.*, 2002).

As the activation of PPARγ by cognate ligands leads to the emergence of its insulin sensitization properties, the potential of natural ligands are being unearthed in view of replacing their synthetic counterparts. In spite of rave reviews regarding the insulin sensitizing capabilities and the potential shown by TZDs, there are several drawbacks in its use as a therapeutic drug to improve insulin sensitivity. During its heyday, there were three different drugs marketed as TZDs; troglitazone, rosiglitazone and pioglitazone. However, only two of the TZDs remain in the market as troglitazone has been removed due to reports of severe idiosyncratic hepatotoxicity, side effects unique only to troglitazone (Jermendy, 2007; Rubenstrunk *et al.*, 2007). Several side effects constantly associated with the use of TZDs include the presence of fluid retention and weight gain due to an increase in adipose tissue mass and body fluid expansion, the latter being further associated with hemodilution and peripheral edema (Rubenstrunk *et al.*, 2007). The most worrying adverse effect involves an increase in the risk of heart failure with a hazard ratio of 1.7 (Guo and Tabrizchi, 2006), probably due to an increase in cardiac workload and subsequent cardiac insufficiency generated from fluid retention (Rubenstrunk *et al.*, 2007).

1.3 Natural solution – Glycyrrhizic acid

Glycyrrhizic acid (GA), the principal bioactive component found in commercial licorice products, constituting 3-5% of fresh root (*Liquiriti radix*) and 10-25% of its extract (*Glycyrrhizae extractum crudum* or *Succus liquiritiae*) is the focus of this study as it has been successfully proven to exhibit PPARγ-ligand binding activity through ligand binding assays (Kuroda *et al.*, 2003; Mae *et al.*, 2003). The licorice plant, genus name *Glycyrrhiza* [Greek: *glykos* (sweet) and *rhiza* (root)], have been an integral part of traditional medicinal interventions, dating back to its use by the ancient Romans and

Greeks for treatment of asthma, dry cough and the prevention of thirst. The Chinese have also harvested its potential to treat ailments such as tuberculosis and peptic ulcers (Isbrucker and Burdock, 2006) while the Tibetians and Indians used it to combat inflammatory and pulmonary complications (Baltina, 2003). In the 21st century, GA is still being widely used by the community as conditioning and flavouring agents in tobacco, sweets, chocolates, chewing gum and certain alcoholic beverages (Ploeger *et al.*, 2001). More importantly, GA possesses a wide range of biological activities which encompasses anti-inflammatory, anti-ulcer, anti-allergic, antidote, anti-oxidant, anti-viral and anti-tumor properties (Baltina, 2003).

1.3.1 Pharmacokinetics of GA

GA is a water-soluble saponin compound naturally available as a mixture of potassium-calcium-magnesium salts. It comprises of glycyrrhetic acid (GE), a tri-terpenoid aglycone, conjugated to a disaccharide of glucoronic acid (Figure 1.3) (Ploeger *et al.*, 2001).

Upon oral ingestion of GA, it undergoes pre-systemic de-glucuronidation by intestinal bacteria (such as *Eubacterium* sp. (strain GHL), *Ruminococcus* sp. PO1-3 and *Clostridium* innocuum ES2406, all containing a specialized β-glucoronidase) (Ploeger *et al.*, 2001) and completely absorbed as monoglycone 18-β-glycyrrhetic acid (GM) and GE (Wang *et al.*, 1995) without any evidence suggestive of systemic hydrolysis (Takeda *et al.*, 1996). Thus, GA would be completely absorbed as GE and would result in low oral bioavailability of GA, which is evident as GA is undetectable in rat and human plasma at oral doses below 50mg/kg and 100mg/kg respectively (Ploeger *et al.*, 2000).

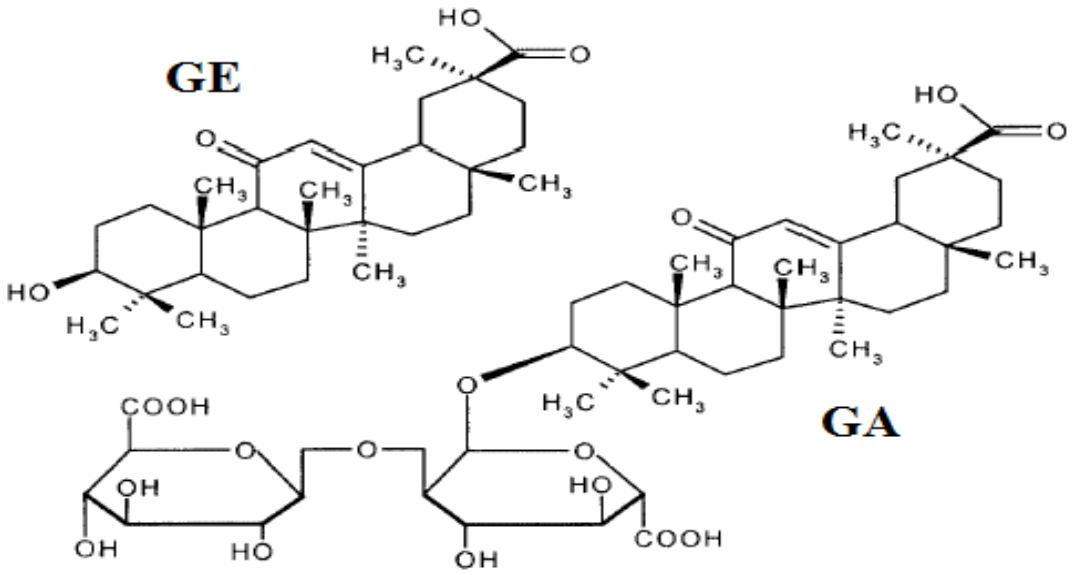

Figure 1.3: Chemical structure of glycyrrhizic acid (GA) and glycyrrhetic acid (GE) (Ploeger *et al.*, 2001)

Systemic analysis of both GA and GE revealed similar pharmacokinetic properties and both bind extensively to specific and non-specific binding sites of human and rat plasma albumin. Capacity-limited processes mediate sinusoidal and canalicular transport of compounds, as well as distribution, metabolism and excretion which affect their dose-dependent clearance from plasma (Ploeger *et al.*, 2001).

1.3.2 Enterohepatic recirculation

Enterohepatic recirculation of GE and its glucuronide metabolites occur due to further conjugation or reduction following excretion into the bile and subsequently re-metabolized by the afore-mentioned commensal bacteria. The enterohepatic recirculation rate is proportional to the amount of GE present in the system (Ploeger *et al.*, 2001) and although GA and GE accumulation in tissues are minimal, the recycling may lead to potential systemic accumulation which becomes more apparent when administered daily (Isbrucker and Burdock, 2006). The enterohepatic recirculation of GE is responsible for the delay in the terminal plasma clearance of GE (Ploeger *et al.*, 2001). A summary of the pharmacokinetics of GA is displayed in Figure 1.4.

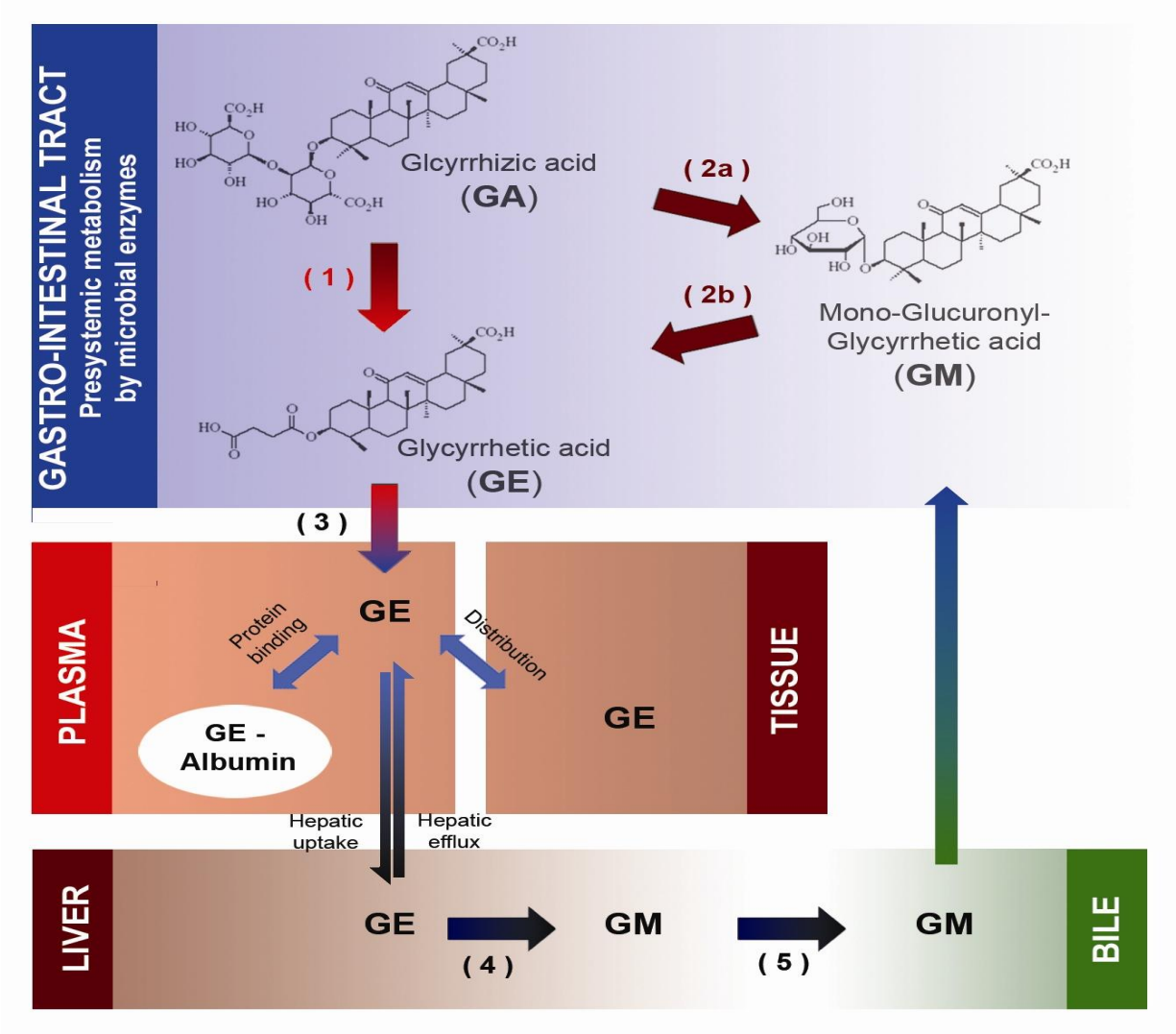

Figure 1.4: Pharmacokinetics of glycyrrhizic acid (GA).

GA is hydrolyzed by intestinal microbes either completely (step 1) or through a two-step intermediary process (steps 2a and 2b) upon oral ingestion. The sinusoidal transport of GA is mediated by a capacity limited carrier protein (step 3) and GE is extensively bound to albumin with minimal distribution to peripheral tissues. GE is then hydrolyzed almost completely to glucoronide and sulfate conjugates (GM) and excreted into the bile by cMOAT (step 5). Biliary excretion of GE metabolites is also mediated by canalicular multispecific organic anion transporter (cMOAT), whereby the metabolites are reabsorbed as GE after excretion into duodenum and subjected to bacterial hydrolysis (steps 2a and 2b) (Ng, 2008).

1.3.3 Pharmacodynamics of GA

Both GA and GE exhibit non-selective competitive inhibition of the enzyme 11β-hydroxysteroid dehydrogenase (11β-HSD) activity, the latter 200 to 1000 times more potent than the former (Isbrucker and Burdock, 2006). Two distinct 11β-HSD isoforms, type 1 and 2, catalyze the interconversion of hormonally active 11-hydroxy glucocorticoids (cortisol in human and corticosterone in rodents) and their inert 11-keto derivatives (cortisone in human and 11-dehydrocorticosterone in rodents) (Tomlinson *et al.*, 2004).

Chronic exposure to GA has been associated with corticosteroid-like effects and changes in cortisol metabolism in the tissues which may cause hypermineralocorticoid-like effects such as electrolyte imbalance, hypertension and depression of the renin-angiotensin-aldosterone system (Ploeger *et al.*, 2000; Isbrucker and Burdock, 2006). However, the effects are reversible upon withdrawal of GA (Isbrucker and Burdock, 2006). Clinical studies have revealed the principal mechanism to be excess tissue corticosteroids acting on mineralocorticoid receptors through competitive inhibition of 11β-HSD enzymatic activity, thus allowing the interaction between glucocorticoids and the mineralocorticoid receptors in the kidneys (Tanahashi *et al.*, 2002).

1.4 Peroxisome proliferator-activated receptor gamma

PPARγ is a ligand-activated transcription factor originating from the nuclear hormone receptor superfamily (Guo and Tabrizchi, 2006). PPARγ is a class II nuclear receptor comprising six structural regions in four functional domains (Figure 1.5). The four functional domains were identified as A/B, C, D and E/F. The A/B region positioned at the variable NH_2-terminal contains a ligand-independent activation function 1 (AF-1), responsible for the covalent modification of PPARγ through phosphorylation (Guo and Tabrizchi, 2006). The C domain contains the DNA-binding

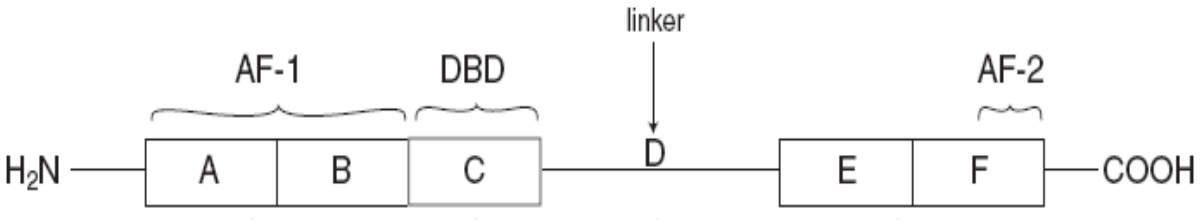

Figure 1.5: Structural and functional domains of PPARγ.

PPARγ possesses six structural regions contained in four functional domains (Guo and Tabrizchi, 2006).

Abbreviations: AF-1, activated function-1 domain; AF-2, activation function-2 domain; DBD, DNA-binding domain; PPRE, peroxisome proliferator response element

domain, the most conserved domain characteristic of all nuclear receptors. It contains two zinc finger motifs (Li and Glass, 2004) which mediate the recognition of sequence-specific nucleotides within regulatory regions of the peroxisome proliferator response elements (PPREs) (Guo and Tabrizchi, 2006). Besides being a co-factor docking domain (Kota *et al.*, 2005), the D domain also allows the rotation of the DNA-binding domain as well as connects the DNA-binding domain to the E/F region (Guo and Tabrizchi, 2006). Meanwhile, the E/F domain is the ligand binding domain which confers ligand specificity and possesses ligand-dependent activation function 2 (AF-2) which is responsible for the recruitment of co-factors to activate the receptors bound to PPRE and the gene transcription mechanism (Kota *et al.*, 2005).

1.4.1 PPARγ gene transcription mechanism

The regulation of the PPARγ expression is governed by two different transcriptional activites, with or without the presence of ligands in the ligand-binding domain (Li and Glass, 2004). Prior to the activation of PPARγ, there would be conformational changes present in the AF-2 region (Houseknecht *et al.*, 2002) which mediates the heterodimerization of PPARγ to the retinoid X receptor (RXR). Similar to PPARγ, RXR is a nuclear receptor present in many tissues and its activation is also governed by the presence of cognate ligands such as 9 *cis*-retinoic acid (Brown and Plutzky, 2007). The PPARγ/RXR complex would then bind to specific PPRE sequences containing direct repeat (DR)-1 elements of two hexanucleotides with a single nucleotide spacer separating the AGGTCA sequence through their respective DNA-binding domains (Kota *et al.*, 2005; Brown and Plutzky, 2007).

Binding of the PPARγ/RXR complex to the PPRE in the absence of ligands involves post-translational modification of the PPARγ structure by phosphorylation (Brown and Plutzky, 2007). The binding would in turn induce the recruitment of co-repressors such as nuclear receptor co-repressor and the silencing mediator of retinoic acid and thyroid receptors to form co-repressor complexes to ultimately repress basal gene transcription (Figure 1.6a) (Li and Glass, 2004; Gurnell, 2005). The co-repressor complex possesses histone deacetylase activity to repress the transcription process through the condensation of nucleosomes (Auwerx, 1999).

Activation of gene transcription could also be governed by ligand-dependent-allosteric changes in the ligand binding domain complexes which would lead to the recruitment of co-activators either in the absence of the co-repressor complex or as a replacement for the co-repressors (Figure 1.6b) (Li and Glass, 2004; Gurnell, 2005). Increase in gene transcription is attributed to the histone acetylation activities of the co-activator complex which promotes the unfolding of the chromatin structure to increase accessibility to the promoter regions (Gurnell, 2005).

1.4.2 **Isoforms of PPARγ**

In both human and rats, there are two distinct protein isoforms of PPARγ; PPARγ1 and PPARγ2, originating from a similar PPARγ gene through alternative splicing of 5 exons in the NH_2-terminal region and differential promoter action (Fernyhough *et al.*, 2007). Both the protein isoforms differ only at the NH2-terminal of PPARγ2, with human and mice having additional 28 and 30 amino acids respectively (Smith, 2003), thus increasing the transcriptional activator potency of PPARγ2 (Heikkinen *et al.*, 2007). Despite having only two protein isoforms, there are four mRNA isoforms arising from the PPARγ gene (Fernyhough *et al.*, 2007). Due to the translated proteins for both PPARγ3 and PPARγ4 being similar to the PPARγ1 protein (Gurnell, 2005), the PPARγ1, PPARγ3 and PPARγ4 mRNA encodes for the PPARγ1

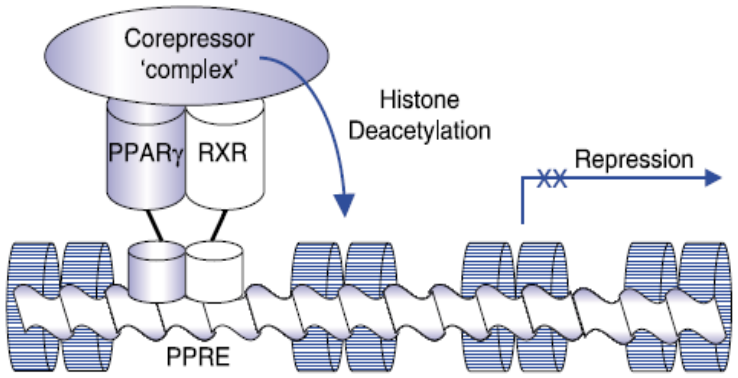

(a) In the absence of exogenous ligands, PPARγ recruits co-repressors with histone deacetylation properties to target genes to repress basal transcription activity (Gurnell, 2005).

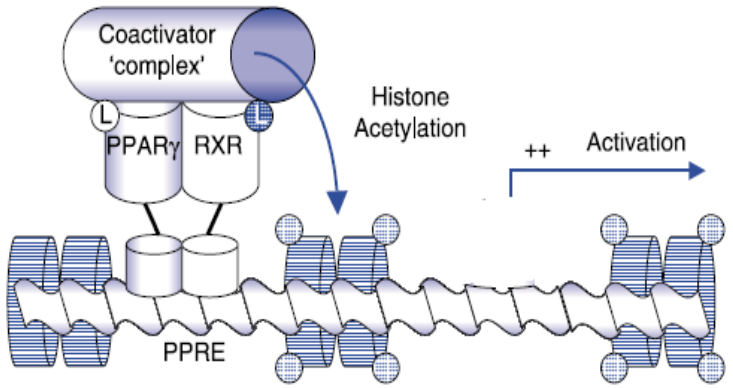

(b) Presence of cognate ligands for both PPARγ and RXR induces a conformational change in the receptor and promotes co-repressor release. Upon release of co-repressor, recruitment of co-activators (steroid receptor co-activator-1 and cAMP response element (CREB) – binding protein) occurs (Gurnell, 2005).

Figures 1.6: PPARγ gene transcription mechanism

Abbreviations: Peroxisome proliferator-activated receptor gamma (PPARγ), Peroxisome proliferator response element (PPRE), Retinoid X receptor (RXR).

protein while the PPARγ2 mRNA encodes for the PPARγ2 protein (Figure 1.7) (Auwerx, 1999; Fernyhough *et al.*, 2007).

1.4.3 Tissue distribution of PPARγ

Due to differences in their function and protein structures, both isoforms display distinct expression patterns (Heikkinen *et al.*, 2007). PPARγ1 is the predominant isoform and is abundantly available in the adipose tissues and large intestines while moderate amounts are localized in the kidney, liver and small intestine. Only small amounts of PPARγ1 are expressed in the muscle tissues. The distribution pattern of PPARγ2 is similar to those of PPARγ1 but at lower expression levels when compared to PPARγ1. The only exception might be in the adipose tissues where the expression of PPARγ2 might occasionally be higher than those of PPARγ1 (Guo and Tabrizchi, 2006).

1.4.4 Biological functions of PPARγ

PPARγ acts as a metabolic transcriptional nodal point by regulating multiple gene cassette expression in different pathways to produce a coordinated response to intracellular or extracellular stimulus (Table 1.5) (Evans *et al.*, 2004; Brown and Plutzky, 2007). The regulation of gene cassettes by PPARγ affects several pathways including glucose homeostasis, lipid and lipoprotein metabolism, inflammatory and immune responses (Ricote and Glass, 2007) as well as adipogenesis (Brown and Plutzky, 2007). The high expression of PPARγ in adipose tissues indicates its importance as lipid sensors activated by dietary fatty acids and their metabolites to enhance metabolism (Evans *et al.*, 2004).

---[A1]-----[A2]----[B]----------[1]---[2]---[3]-----[4]---[5]-----[6] Human/ Rat PPARγ gene

[A1][A2][1][2][3][4][5][6]	mRNA isoform 1	→	[1-6] PPARγ1 protein
[B][1][2][3][4][5][6]	mRNA isoform 2	→	[B] [1-6] PPARγ2 protein
[A2][1][2][3][4][5][6]	mRNA isoform 3	→	[1-6] PPARγ1 protein
[1][2][3][4][5][6]	mRNA isoform 3	→	[1-6] PPARγ1 protein

Figure 1.7: Human PPARγ gene together with the protein and mRNA isoforms.

Rat PPARγ gene has only the PPARγ 1 and 2 protein and mRNA isoforms (Auwerx, 1999).

Table 1.5: PPARγ target pathways activated through regulation of specific gene cassettes (Brown and Plutzky, 2007)

PPARγ target pathways	Genes activated
Adipogenesis	aP2, adiponectin, adipsin, C/EBP α
Lipid metabolism	LPL, ABCA1, ABCG1, fatty acid binding protein 4
Glucose control	GLUT4, thioredoxin-binding protein-2, resistin
Inflammation/vascular	Interferon-γ, chemokines (MIG, iTAC, IP10), chemokine receptors (CCR2), tumor necrosis factor-α, MMP-9

Abbreviations: Fatty acid binding protein (aP2), CCATT/enhancer binding protein α (C/EBP α), Lipoprotein lipase (LPL), ATP binding cassette transporter member 1, sub-family ABCA (ABCA1), ATP binding cassette, subfamily G member 1 (ABCG1), Glucose transporter 4 (GLUT4), Monokine induced by interferon γ (MIG), Interferon-inducible T-cell alpha chemoattractant (iTAC), Interferon-inducible protein 10 (IP10), Matrix metallopeptidase 9 (MMP-9).

1.4.4.1 PPARγ and lipid metabolism

PPARγ is the master regulator of fat cell function that governs differentiation of pre-adipocyte precursor cells into mature adipocytes capable of lipid filling as well as the mediation of hormone and cytokine expression (Kota *et al.*, 2005; Dahlman and Arner, 2007). In addition to an increase in smaller and more insulin sensitive adipocytes, PPARγ activation also promotes apoptosis of mature, lipid-filled visceral adipocytes and a redistribution of the free fatty acids towards the subcutaneous adipose tissues (Guo and Tabrizchi, 2006). The increase in adipocyte number increases the lipid storage capacity and indirectly confers protection towards non-adipose tissues in the event of excessive lipid accumulation (Camp *et al.*, 2002). PPARγ also acts synergistically with two transcription factors, CCAAT/enhancer binding protein α (C/EBPα) and sterol regulatory element-binding protein (SREBP) to transactivate adipose-specific genes, leading to promotion of adipogenesis and TAG storage (Cartwright *et al.*, 2007; Dahlman and Arner, 2007).

1.4.4.2 PPARγ and glucose homeostasis

A pivotal component in glucose homeostasis is the glucose-induced stimulation of insulin secretion to mediate the uptake of glucose. Activation of PPARγ would subsequently improve insulin sensitivity in the muscles and liver as it triggers muscle glucose disposal and inhibition of hepatic glucose output through an increase in insulin action. Inhibition of hepatic glucose output is achieved through fluctuations in the secretion of signaling molecules by adipocytes upon PPARγ activation (Evans *et al.*, 2004). Although the adipose tissue accounts for only approximately 10% of insulin-stimulated glucose disposal (Evans *et al.*, 2004), it has been proven to be the main target for insulin sensitizing effects as researchers have shown that mice without adipose tissues are refractory to anti-diabetic effects of TZD (Rangwala and Lazar, 2004).

PPARγ also regulates several genes that are central to the maintenance of glucose homeostasis in the body. For example, PPARγ regulates the expression of genes that encode the insulin-responsive glucose transporter known as GLUT4 and c-Cbl associating protein (CAP). Both are required for GLUT4 translocation to the cell surface and CAP acts as the stimulator for glucose transport (Evans *et al.*, 2004). PPARγ activation would subsequently increase the expression of GLUT4 and increase glucose uptake into adipocytes to reduce the levels of circulatory glucose (Fernyhough *et al.*, 2007).

1.5 Lipoprotein lipase

Lipoprotein lipase (LPL) is a water-soluble enzyme that liberates free fatty acids through the hydrolysis of ester bonds of water-soluble substrates such as TAG, phospholipids and cholesterol esters (Wong and Schotz, 2002; Brown and Rader, 2007). LPL is a 55-kDa glycoprotein consisting of 450 amino acids (Dugi *et al.*, 1992; van Tilbeurgh *et al.*, 1994) and although the tertiary protein structure of LPL has not been documented, the molecular structure was based on the elucidated three-dimensional structure of pancreatic lipase (Santamarina-Fojo and Brewer Jr., 1994; Brown and Rader, 2007) [Figure 1.8]. The similarity between both the lipases has been attributed to the high primary sequence homology and disulfide linkages for structural stability (Santamarina-Fojo and Brewer Jr., 1994).

The catalytically active enzyme exists as a homodimer, with each monomer organized into distinct structural domains; a larger NH_2-terminal consisting of the catalytic centre and the apoC-II interaction site and a smaller COOH-terminal involved in the regulation of substrate specificity (van Tilbeurgh *et al.*, 1994; Mead *et al.*, 2002) [Figure 1.9].

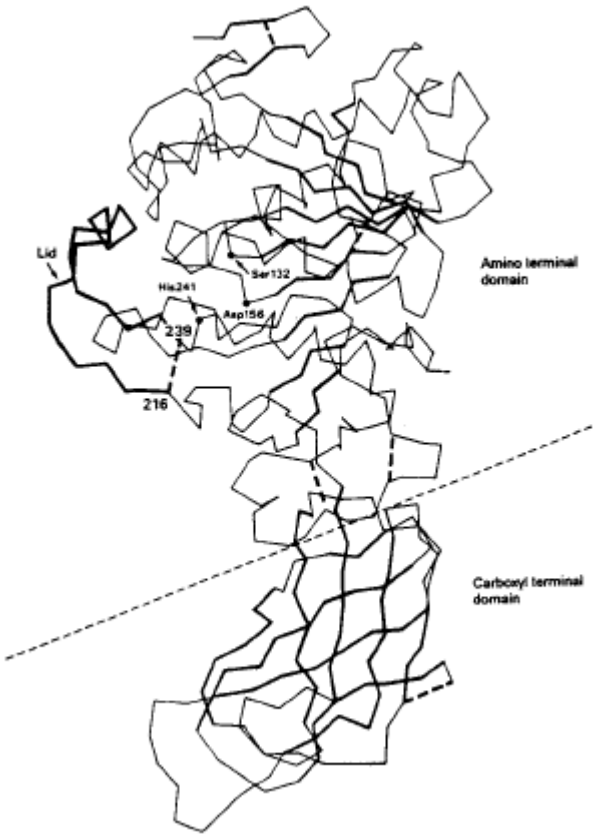

Figure 1.8: The three-dimensional structure of lipoprotein lipase with the location of amino and carboxyl terminal domains as well as the lid and catalytic triad residues (Santamarina-Fojo and Brewer Jr., 1994).

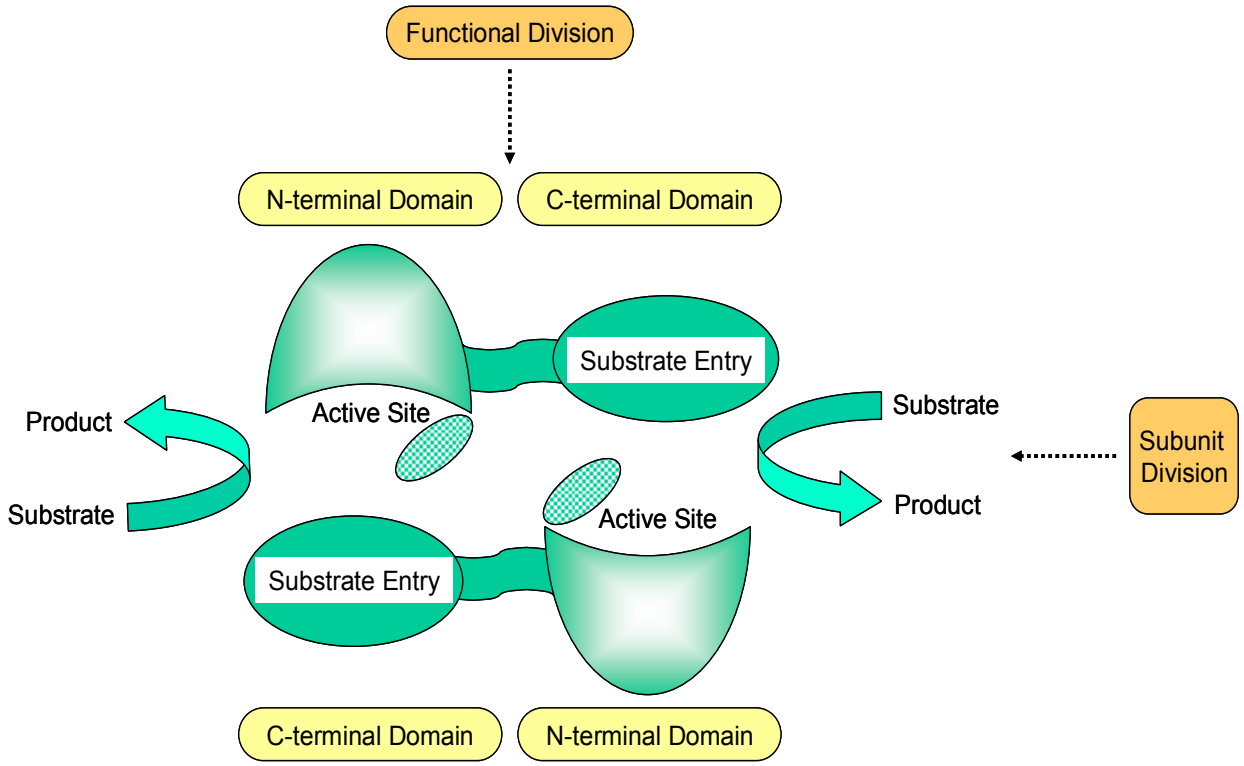

Figure 1.9: LPL model of the catalytically active enzyme exists as a larger NH_2-terminal consisting of the catalytic centre and a smaller COOH-terminal (Wong *et al.*, 1994).

1.5.1 Physiological function of LPL

LPL is responsible for the hydrolysis of circulating TAG moiety of TAG-rich lipoproteins, namely chylomicrons and very-low-density lipoprotein (VLDL) in addition to playing an active role in overall lipoprotein metabolism [Figure 1.10]. The heparin sulfate proteoglycans (HSPG) are responsible for anchoring the enzyme to its physiological site of action, the luminal surface of capillary endothelial cells (Preiss-Landi *et al.*, 2002). As LPL regulates the plasma TAG concentration, disturbances to LPL activity would result in dire metabolic consequences for lipoprotein metabolism (Kageyama *et al.*, 2003).

1.5.2 Synthesis and site of LPL expression

Endothelial LPL protein originates from the tissue parenchymal cells prior to translocation to the site of action (Braun and Severson, 1992). LPL is synthesized and highly expressed in the adipose tissues, cardiac and skeletal muscle, kidney and mammary glands while lower levels are present in the liver, adrenal and brain (Zhang *et al.*, 2001).

Following transcription of the LPL gene, post-translational modification such as N-linked glycosylation occurs in the rough endoplasmic reticulum (RER) to bestow catalytic activity to the nascent LPL polypeptide. The carbohydrate moiety undergoes further modification as it transverses through the RER and Golgi apparatus. The sorting process occurs within the trans-Golgi cisternae and the LPL glycoprotein would be incorporated into secretory vesicles. The glycoprotein would then be either delivered to the lysosomes for intracellular degradation or to the plasma membrane of parenchymal cell surface for exocytosis and translocation to functional heparin sulfate proteoglycans (HSPG) binding sites (Braun and Severson, 1992; Mead *et al.*, 2002) [Figure 1.11].

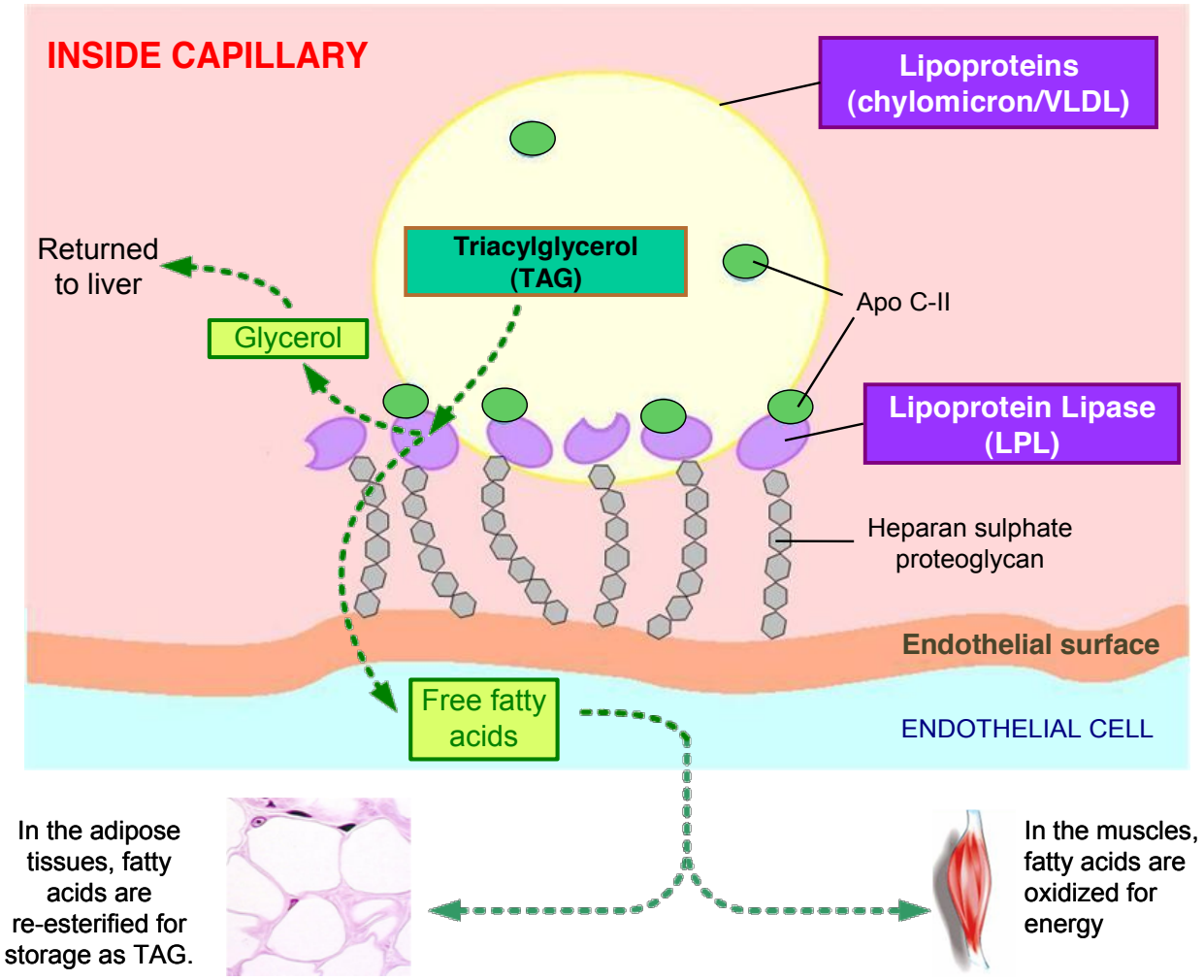

Figure 1.10: Binding of a lipoprotein to LPL on the inner surface of a capillary.

Apo C-II of lipoproteins will activate LPL thus leading to the hydrolysis of the core TAG to FFA and glycerol. The FFA are either re-esterified for storage as TAG in the adipose tissues or oxidized for energy in skeletal and cardiac muscles while glycerol is returned to the liver (Mathews *et al.*, 2000).

[LPL: lipoprotein lipase; apo: apolipoprotein; VLDL: very-low-density lipoprotein; TAG: triacylglycerol; FFA: free fatty acids]

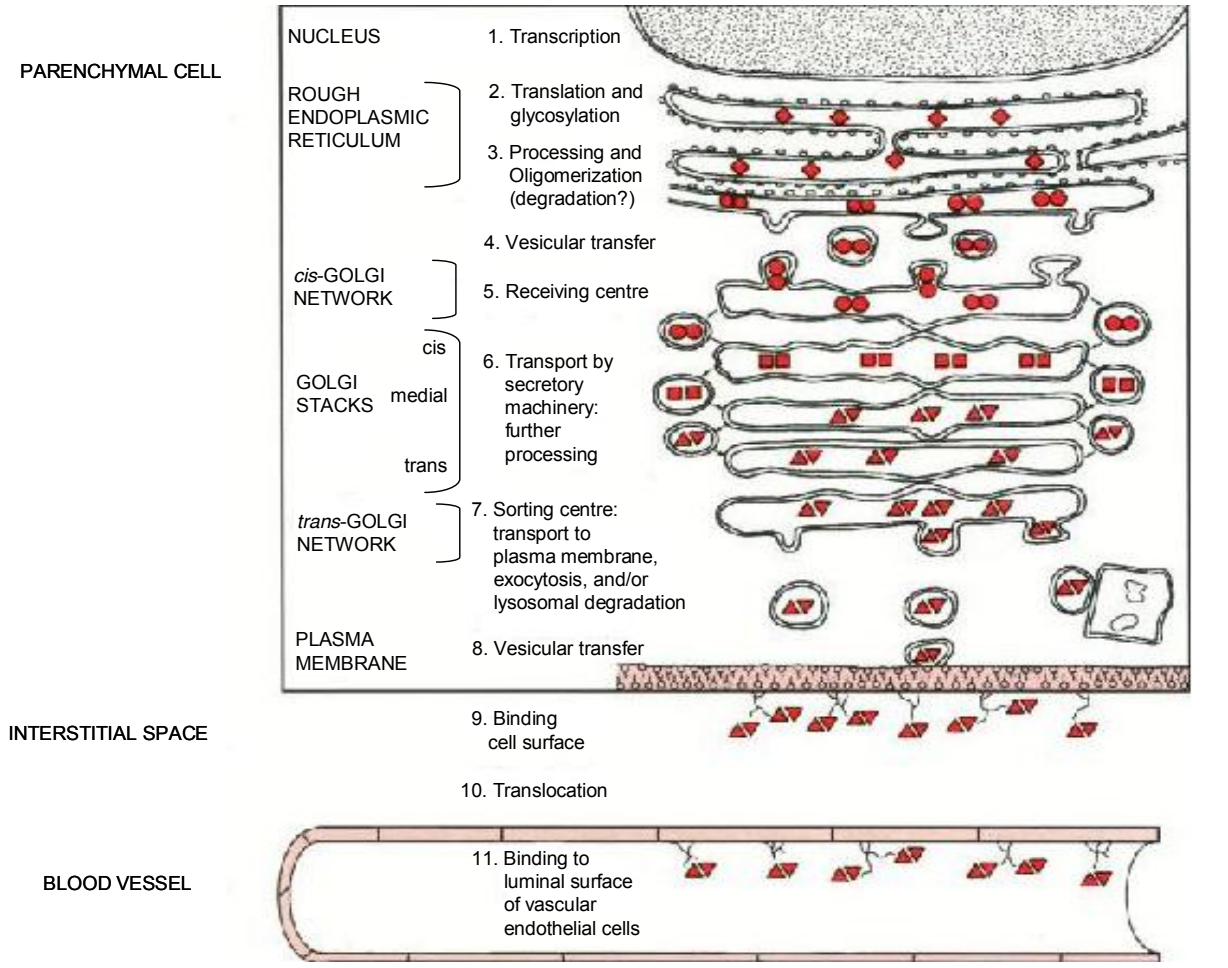

Figure 1.11: The synthesis of LPL (Braun and Severson, 1992).

Nascent LPL protein Dimerized LPL LPL undergoing Golgi processing

Active, glycosylated LPL

1.5.3 *In vivo* regulation and transcriptional control of LPL expression

The regulation of LPL activity is tissue-specific with reciprocal changes to assist direct fatty acid utilization based on the specific metabolic demands of each tissue (Braun and Severson, 1992). Both dietary and hormonal changes are responsible for the regulation of LPL activity through transcriptional and post-transcriptional mechanisms. Fasting or exercise would cause a decrease and increase in adipose tissue and muscle LPL activity respectively; this is likely an attempt by the latter to compensate for a calorie-deprived condition (Mead *et al.*, 2002). Lactation would lead to a marked increase in mammary gland LPL activity which in turn directs the circulating TAG for milk synthesis (Braun and Severson, 1992). Thus, the tissue-specific regulation of LPL ensures localized control of free fatty acid (FFA) uptake and distribution of nutrients to tissues.

Interaction between specific transcription factors and the *cis*-acting elements in the regulatory regions upstream and downstream of the LPL gene is required for its transcriptional control (Mead *et al.*, 2002). The expression of LPL is governed by the activation of PPARγ by cognate ligands as LPL is a downstream gene of PPARγ. The PPARγ/RXR complex would bind to the PPRE present in the promoter region of the LPL gene and increases the LPL gene expression (Mead *et al.*, 2002; Kota *et al.*, 2005). The induction of lipoprotein lipase synthesis by PPARγ is mainly in the mature adipocytes in order to increase local generation of free fatty acids (Rangwala and Lazar, 2004).

Cortisol can also exert chronic effects on lipid metabolism, where excess cortisol would promote an increase in the LPL activity. This effect involves an increased level of LPL mRNA leading to increased relative LPL synthesis and additional post-translational regulation. Furthermore, the anti-lipolytic action of insulin during hyperinsulinaemic

conditions can cause lipid mobilization, resulting in increased lipid accumulation (Rosmond *et al.*, 2006).

1.5.4 Dyslipidaemia and LPL – Protective role against dyslipidaemia

Dyslipidaemia is associated with a cluster of inter-related plasma lipid and lipoprotein abnormalities, amounting to it being a hallmark risk factor in metabolic syndrome (Kolovou *et al.*, 2005). There are four characteristics of dyslipidaemia; increased flux of FFA, elevated TAG levels (hypertriglyceridaemia), reduced high density lipoprotein (HDL) levels and increased small, dense low density lipoprotein (LDL). The most significant characteristic which contributes to the development of dyslipidaemia is the elevation in plasma FFA concentration (Krauss, 2004; Kolovou *et al.*, 2005).

Dyslipidaemia is widely established as an independent risk factor for cardiovascular disease. Low HDL cholesterol and hypertriglyceridaemia have been found to be significantly related to myocardial infarction/stroke in patients with metabolic syndrome (Kolovou *et al.*, 2005). As mentioned earlier in Section 1.1.2.2, although obesity is a common finding in insulin resistant individuals, those individuals are not necessarily obese but possess abnormal upper body fat distribution (Grundy *et al.*, 2005). It must also be stressed that normal weight individuals are also susceptible to insulin resistance (Eckel *et a*l., 2005), thus cementing the importance of dyslipidaemic conditions in the development of metabolic syndrome.

Obesity-induced secretion of adipocytokines is responsible for hypertriglyceridaemia as it increases the flux of adipose tissue-derived FFA towards the liver via the portal vein, which in turn stimulates hepatic TAG synthesis to ultimately increase the secretion of VLDL particles (Kolovou *et al.*, 2005; Fulop *et al.*, 2006). Sustained elevation of FFA levels would promote insulin resistance and cause a positive

feedback to sustain the pathologic state of insulin resistance as mentioned in Section 1.1.2.2, leading to a reduction in LPL expression and eventually retards the LPL activity (Mead *et al.*, 2002; Kageyama *et al.*, 2003).

The hypertriglyceridaemic condition arises from three different sources; (i) lipolysis of TAG store from adipose tissues causing elevation in the flux of FFA to the liver, (ii) decreasing LPL levels which leads to the inhibition of lipolysis of chylomicrons and VLDL and (iii) increased hepatic *de novo* TAG synthesis due to insulin resistance (Lann and LeRoith, 2007). However, it has been proven that stimulation of LPL activity would lower plasma TAG and increase HDL levels (Mukherjee, 2003) as humans with enhanced LPL activity tend to develop low plasma TAG and high HDL levels, rendering protection from myocardial infarction while humans deficient in LPL develop hypertriglyceridaemia (Pillarisetti and Saxena, 2003; Tsutsumi, 2003).

1.5.4.1 Cumulative beneficial effects of PPARγ and LPL activity

Thus, it could be said that binding of a cognate ligand to PPARγ would cause its activation and subsequently cause an increase in the LPL activity by binding to the PPRE in the promoter region. Activation of PPARγ and LPL enhances insulin sensitivity by reducing circulatory free fatty acid levels through an increase in the number of adipocytes together with an increase in net flux of free fatty acids into adipocytes (Figure 1.12). This would prevent the accumulation of free fatty acids in non-adipose tissues and control the levels of circulating TAG with the ultimate aim of ameliorating the risk factors for metabolic syndrome (Rangwala and Lazar, 2004).

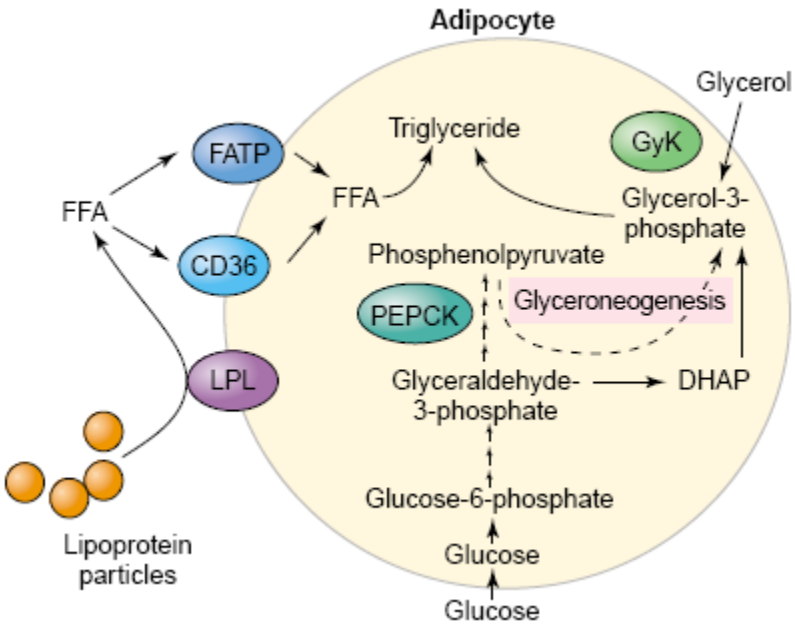

Figure 1.12: Effects of PPARγ activation on fatty acid metabolism in adipocytes.

Activation of PPARγ upon cognate ligand binding increases the expression of both lipoprotein lipase (LPL) and levels of fatty acid transporters [fatty acid transport protein (FATP) and CD36], which releases FFA and causes greater influx of FFA into adipocytes respectively. Glycerol-3-phosphate required for esterification of the FFA to triacylglycerol is provided by glyceroneogenesis via phosphoenol pyruvate carboxykinase (PEPCK) in addition to phosphorylation of exogenous glycerol via glycerol kinase (GyK) (Rangwala and Lazar, 2004).

Abbreviations: DHAP, dihydroxyacetone phosphate

1.6 Corticosteroid hormones

Corticosteroid hormones, derived from the common precursor cholesterol with a common structure consisting of a single cyclopentane and three cyclohexane rings, are synthesized by the adrenal cortex. The hormones are functionally divided into three classes according to their principal effects; namely glucocorticoid (GC; cortisol and corticosterone), mineralocorticoid (MC; aldosterone and deoxycorticosterone) and androgens (Seckl, 1997).

1.6.1 Mechanism of corticosteroid action

Corticosteroids are lipid-soluble hormones that readily transverse cell membranes via passive diffusion (Björntorp and Rosmond, 2000) and their actions are mediated through intracellular protein receptors belonging to a superfamily of ligand-activated transcription factors (Evans, 1988). The receptors are predominantly localized within the cytoplasm and could be divided into mineralocorticoid receptors (MR) (Hollenberg *et al.*, 1985) and glucocorticoid receptors (GR) (Krozowski and Funder, 1983). The cytoplasmic corticosteroids are exposed to intracellular metabolism by 11β-HSD which modifies the final active cytosolic concentration and effects (Björntorp and Rosmond, 2000).

Binding of MR and GR with their respective hormones would result in the attachment of hormone-receptor complex to specific DNA sequences known as the glucocorticoid response element (GRE). The GREs act as regulatory nuclear transcription factors to induce or repress target gene transcription as well as alter mRNA synthesis for proteins that mediate their multiple physiological effects. The non-classical mode of GR action involves ligand activation with other transcription factors or the

RNA polymerase II complex rather than direct binding with the GRE (Björntorp and Rosmond, 2000).

1.6.1.1 Role of mineralocorticoids and glucocorticoids

MC has two functions; (i) regulation of renal epithelial sodium transport and indirectly, the circulatory volume homeostasis through concomitant water reabsorption from the nephron (Miller and Chrousos, 2001) and (ii) the control of potassium homeostasis. The binding of MC to MR in the cytosol of epithelial cells causes modification of apical sodium ion channel and basal lateral NA^+/K^+-adenosine triphosphatase (ATPase), leading to increased sodium ion transport across cell membrane (Dluby *et al.*, 2003).

The physiologically active cortisol and corticosterone are responsible for 95% of all GC activity in human and rodents respectively (Miller and Chrousos, 2001). GCs play an important role in the regulation of intermediary metabolism and possess extensive influences on carbohydrate, protein and lipid metabolism. They play a protective secondary role against glucose deprivation, coordinated by anabolic effects on hepatic tissues and catabolic effects on extra-hepatic tissues. GCs also stimulate the differentiation and proliferation of pre-adipocytes to adipocytes through the transcriptional activation of key differentiation genes in addition to increasing the expression and activity of 11β-HSD1 (Hauner *et al.*, 1989).

1.6.2 **11β**-hydroxysteroid dehydrogenases

As mentioned in Section 1.3.3, 11β-HSDs are enzymes sharing 21% homology primarily within conserved regions of the short-chain dehydrogenase / reductase superfamily but are derived from separate gene products (Tomlinson *et al.*, 2004).

11β-HSD type 1 is predominantly reduced by nicotinamide adenine dinucleotide phosphate (NADPH)-dependent 11-oxo-reductase *in vivo.* It regenerates active GCs, thus amplifying intracellular GC action while the nicotinamide adenine dinucleotide phosphate ($NADP^+$)-dependent 11-dehydrogenase activity catalyses the reverse direction, converting cortisone to cortisol in humans and 11-dehydrocorticosterone to corticosterone in rodents (Draper and Stewart, 2005). However, the directionality is dependent on the availability of the NADPH and $NADP^+$ co-factors respectively.

11β-HSD type 2 is an exclusive nicotinamide adenine dinucleotide (NAD)-dependent dehydrogenase converting active cortisol into inactive cortisone and inactivates intracellular GCs. It is highly expressed in MC targeted tissues, such as the kidney and colon while minimally expressed in the spleen (Krozowski *et al.*, 1999). The distinct differences between both isozymes are summarized in Table 1.6 and illustrated in Figure 1.13 (Draper *et al.*, 2003).

1.6.2.1 Physiological roles of 11β-HSD1 and 11β-HSD2

The tissue-specific expression of both isoforms play a pivotal role in pre-receptor metabolism of corticosteroid hormones, thus regulating intracellular levels of GCs and MC activities *in vivo* and downstream activation of GR and MR (Draper and Stewart, 2005).

1.6.2.1.1 Regulation of 11β-HSD by PPARγ

Excess GCs have been proven to enhance visceral obesity, hyperlipidaemia and insulin resistance in addition to being responsible for the upregulation of 11β-HSD

expression (Berthiaume *et al.*, 2004). Activation of PPARγ has been noted to inhibit the levels of 11β-HSD1 expression, thus rendering anti-diabetic effects *in vivo* and improve glucose homeostasis (Berger *et al.*, 2001). Inhibition of 11β-HSD1 also reduces the risk of hyperglycaemia, hyperlipidaemia and hyperinsulinaemia constantly associated with GC metabolism (Berger *et al.*, 2001; Berthiaume *et al.*, 2007).

Table 1.6: Features and characteristics of 11β-HSD 1 and 2 isozymes

	11β-HSD1	11β-HSD2
Protein size	292 amino acids 34 kDa	405 amino acids 44 kDa
Function	Controls and amplifies intracellular levels of cortisol to GR	Protects non-selective MR from illicit activation by cortisol leaving free access for aldosterone
Direction of reaction	Bi-directional 11-oxo-reductase (predominates *in vivo*), bi-directional (*in vitro*)	Uni-directional Dehydrogenase (only)
Co-factor	$NADP^+$ (dehydrogenase direction) NADPH (oxo-reductase direction)	Exclusive NAD^+ dependent
Substrate affinity	Low affinity Km ≈ μM range	High affinity (100x more than type 1) Km ≈ 50 nM (cortisol) & 5 nM (corticosterone)
Tissue expression	Liver, adipose, brain, gonads, vasculature, lung, immune cells, bone	MC target tissues such as; kidney, colon, salivary glands, placenta
Diurnal variation	Morning ≈ 500 nM Evening ≈ 100 nM	No marked diurnal variation ≈ 70 nM

(kDa: kilo-daltons, NADPH: reduced nicotinamide adenosine dinucleotide phosphate, $NADP^+$: nicotinamide adenine dinucleotide phosphate, NAD^+: nicotinamide adenine dinucleotide)

(Draper and Stewart, 2005)

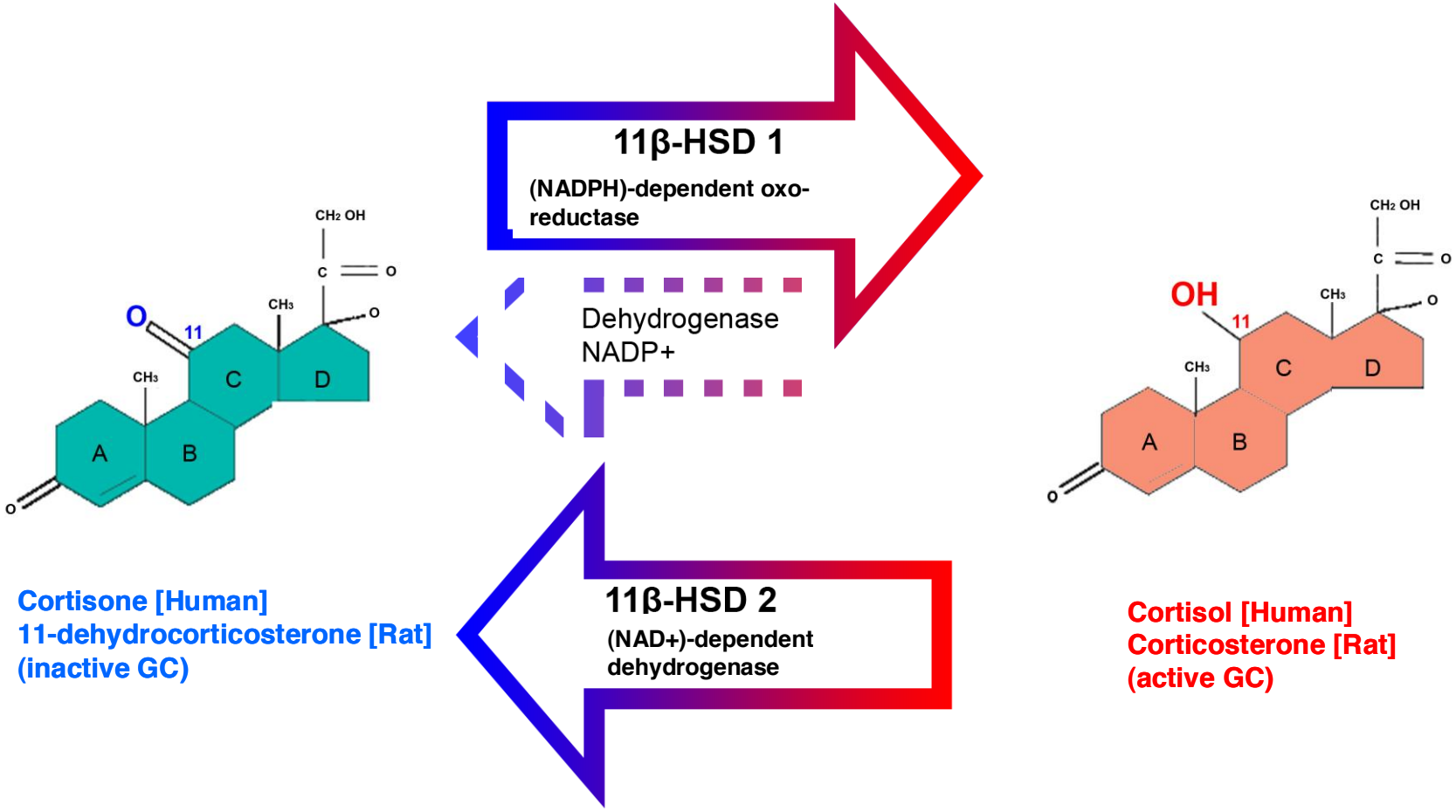

Figure 1.13: Directionality of 11β-HSD 1 and 2.

The enzymatic action of 11β-HSD on its glucocorticoid substrates, interconversion between cortisone and cortisol (Adapted from Draper and Stewart, 2005).

1.7 Aims

Despite the rapid advancement in medical technology, the WHO has stated that diabetes mellitus has reached epidemic proportions and its prevalence would be one of the main human threats in the 21st century and beyond (Permutt *et al.*, 2005). Closer to home, the prevalence of diabetes mellitus in both Malaysia and Singapore has been doubling every decade since the mid-1970s (Cockram, 2000). In 1997, a National Survey was performed in Malaysia and it was determined that the prevalence of diabetics among the adult population to be exceeding 8% (Cockram, 2000). The most recent NHMS III survey indicated that the prevalence of diabetes mellitus in Malaysia has increased by over 86% between years 1996-2006 to 14.9%, almost doubling in its magnitude over the last decade (Mastura *et al.*, 2008). Based on the projections, the disease would be afflicting a larger population as time passes. Thus, it is of the utmost importance to develop a solution and prevent the situation from further deteriorating.

The collective beneficial effects exerted by PPARγ, 11β-HSD and LPL have been implicated to improve the metabolic risk factors associated with diabetes mellitus and metabolic syndrome. The potential of GA as an agonist of PPARγ and an inhibitor of 11β-HSD activities has not been fully utilized and documented. Although the ligand binding potential of GA towards PPARγ has provided a positive correlation, very little research has been conducted to elucidate the role of GA as a ligand for PPARγ to improve insulin sensitivity (Kuroda *et al.*, 2003).

In the absence of PPARγ activation, elevated GC activity together with increased secretion of adipocytokines would lead to an insulin resistant state in humans (Fulop *et al.*, 2006; Qi and Rodrigues, 2006). Research on the activation of PPARγ indicates promise in ameliorating the effects of insulin resistance due to its role in adipogenesis and insulin sensitization. Oral feeding of GA for seven weeks to genetically diabetic KK-A^y mice resulted in reduction in blood glucose levels, displaying its insulin sensitizing properties (Takii *et al.*, 2001). Treatment of experimental animals with

carbenoxolone, a synthetic GE analog led to a dose-dependent reduction in plasma TAG and FFA in obese, hyperlipidaemic mice following subcutaneous administration (Nuotio-Antar *et al.*, 2007) while oral administration of the same compound to obese Zucker rats caused a decrease in plasma TAG (Livingstone and Walker, 2003). Thus, the transcriptional activation of PPARγ, the inhibition of 11β-HSD activity and the subsequent transcriptional activation of LPL might improve insulin sensitivity and ameliorate the risk factors for metabolic syndrome.

To date, there has not been much research done on the cumulative effects of GA on PPARγ, 11β-HSD and LPL to ameliorate insulin resistance and lipid dysregulation. Thus the objectives of this study are to:

(a) Determine and compare the following parameters between treated and non-treated rats:

  (i) two different routes of administration (intraperitoneal and oral)

  (ii) different dosages of glycyrrhizic acid (25, 50, 100 and 150mg/kg)

  (iii) different treatment periods of glycyrrhizic acid upon administration (12, 24, 48 hours and 1 week)

(b) Determine the levels of glucose, serum insulin and Homeostasis Model of Assessment for Insulin Resistant (HOMA-IR) in the above rats.

(c) Quantify the expression of PPARγ1, PPARγ2, total PPARγ, LPL levels and activities of 11β-HSD isoforms 1 and 2 in visceral and subcutaneous adipose tissue, abdominal muscle, quadriceps femoris, liver and kidney of the above rats.

(d) Study histological changes in the liver and the size of visceral and subcutaneous adipose tissue adipocytes of GA-administered rats.

CHAPTER 2

Materials and Methods

Chapter 2

MATERIALS AND METHODS

2.1 Animal and Treatment

2.1.1 Animal ethics

Prior to the commencement of the project, approval was sought from the Monash University Animal Ethics Committee in accordance to the 2004 Australian Code of Practice for the Care and Use of Animal for Scientific Purposes and Relevant Victorian Legislation (Prevention of Cruelty to Animals Act 1986). The project was only undertaken after approval was obtained (AEC Approval Number SOBSB/MY/2006/46).

2.1.2 Sample size determination

Eight animals were allocated to each treatment group as computation displayed more than 80% power ($1 - \beta$) to detect a 5% significance level (α) via comparisons of means (unpaired data) (Appendix 1) (Campbell and Machin, 2002).

2.1.3 Animal housing and diet

Male Sprague Dawley rats (*Rattus novergicus*) weighing between 160g to 200g were purchased from the University Malaya animal facility and were bred in the animal facility of the Monash University Sunway campus. The rats were individually housed in polypropylene cages at approximately 23°C with a 12- hour light and dark cycle (lights on at 0700 hours and lights out at 1900 hours). Each cage was littered with paper shavings as bedding and the rats were given Glenn Forest stock-feeder rat chow and tap water *ad libitum*.

2.1.4 Experimental design

Rats were randomly assigned to two groups designated the control and GA-administered groups (Figure 2.1) and the initial body weight (grams) of all rats were taken. Rats in the control group were given tap water without GA while the rats in the GA-administered group were given GA dissolved in distilled water via different routes of administration (intraperitoneal and oral), different dosages (25, 50, 75, 100 and 150 mg/kg body weight of rat) and different time durations (12, 24 and 48 hours as well as 1 week). Daily food and fluid consumption was measured for determination of weight gain.

2.1.5 Determination of systolic blood pressure

A week prior to the start of GA administration of 100 mg/kg for 1 week, all rats were subjected to tail-cuff blood pressure measurement to allow habituation that increases rat compliance.

Blood pressure was measured using the NIBP controller (ADInstruments, Australia). Conscious rats were placed into a plastic restrainer of which the depth was adjusted to fit the animal comfortably but restricting their movements. A tail-cuff with a pulse transducer was applied onto the tail of the restrained animal and the tail was heated using a table lamp with 60W bulb for 20-30 minutes. Blood pressure was measured by inflating the tail-cuff once the heart rate had stabilized. The recording and determination of blood pressure were performed using the Chart recording software. This procedure was performed every alternate day.

Similar protocol was then conducted to determine the systolic blood pressure of all rats throughout the one week duration of treatment.

2.1.6 Sample collection

Upon completion of the projected treatment period, the rats were fasted for 12 hours prior to humane sacrifice between 0800 to 1000 hours under the influence of anaesthesia via intraperitoneal administration of pentobarbital sodium [Nembutal] (150mg/kg), following the approved institutional animal ethics guidelines (AEC Approval Number SOBSB/MY/2006/46).

2.1.6.1 Blood and serum collection

Immediately upon dissection, blood was drained from the cardiac ventricle via the apex of each rat using a 5 mL syringe and 22G needle. Then, five drops of blood were added into a microtube containing 0.5 g of ethylenediamine tetraacetic acid (EDTA) and sodium fluoride (1:2 w/w). The contents were then mixed thoroughly prior to the determination of plasma glucose levels.

Another 5 mL of blood was allowed to clot at room temperature (25°C) for 30 minutes prior to centrifugation at 4°C and 12,000 x g for 10 minutes. The serum was then aliquoted into microtubes before storage at -80°C until required for analysis (Figure 2.1).

2.1.6.2 Tissue harvesting

Tissues of interest such as liver (L), kidney (K), subcutaneous and visceral adipose tissues (ATS and ATV), abdominal and quadriceps femoris muscles (MA and MT) were identified and promptly harvested. All the tissues were equally cut into three sections; (i) the first section was placed into individual cryovials (Nalgene, USA), immediately snap-frozen in liquid nitrogen and stored at -80°C prior to real time PCR analysis, (ii) the second section was placed into 15 mL polypropylene conical tubes prior to homogenization for analysis of 11β-HSD activity and

(iii) the remaining sections were trimmed into cubes approximately 5×5×5 mm prior to fixation for histology analysis (Figure 2.1).

2.2 Blood and Serum Biochemical Analysis

2.2.1 Blood glucose determination using Trinder's Glucose Oxidase method

100 μL of blood in the microtube from Section 2.1.6.1 was added to 2.9 mL of protein precipitant in a Falcon tube. The solution was mixed well and later centrifuged at 894 x g for 10 minutes. 0.5 mL of the resulting supernatant was transferred into an aluminum foil-wrapped test tube. Then, 1.5 mL of Colour Reagent (containing 0.09M NaH_2PO_4: 0.02M NaN_3: 0.002M $C_{11}H_{13}N_3O$: 900U glucose oxidase: 50U peroxidase) was added and the test tubes were subjected to incubation at 37°C for 20 minutes. Later, 0.2 mL of the solution was transferred into a microtitre plate, with duplicates done for each tube. A series of standards ranging from 5 mmol/L to 20 mmol/L were prepared. The microtitre plate was read at 515 nm using BIO-TEK Powerwave XS Microplate Scanning Spectrophotometer. Quantification of blood glucose levels were based on a reference curve derived from the absorbance unit at 515 nm against different concentration of standards (Appendix 2; Figure A2.1).

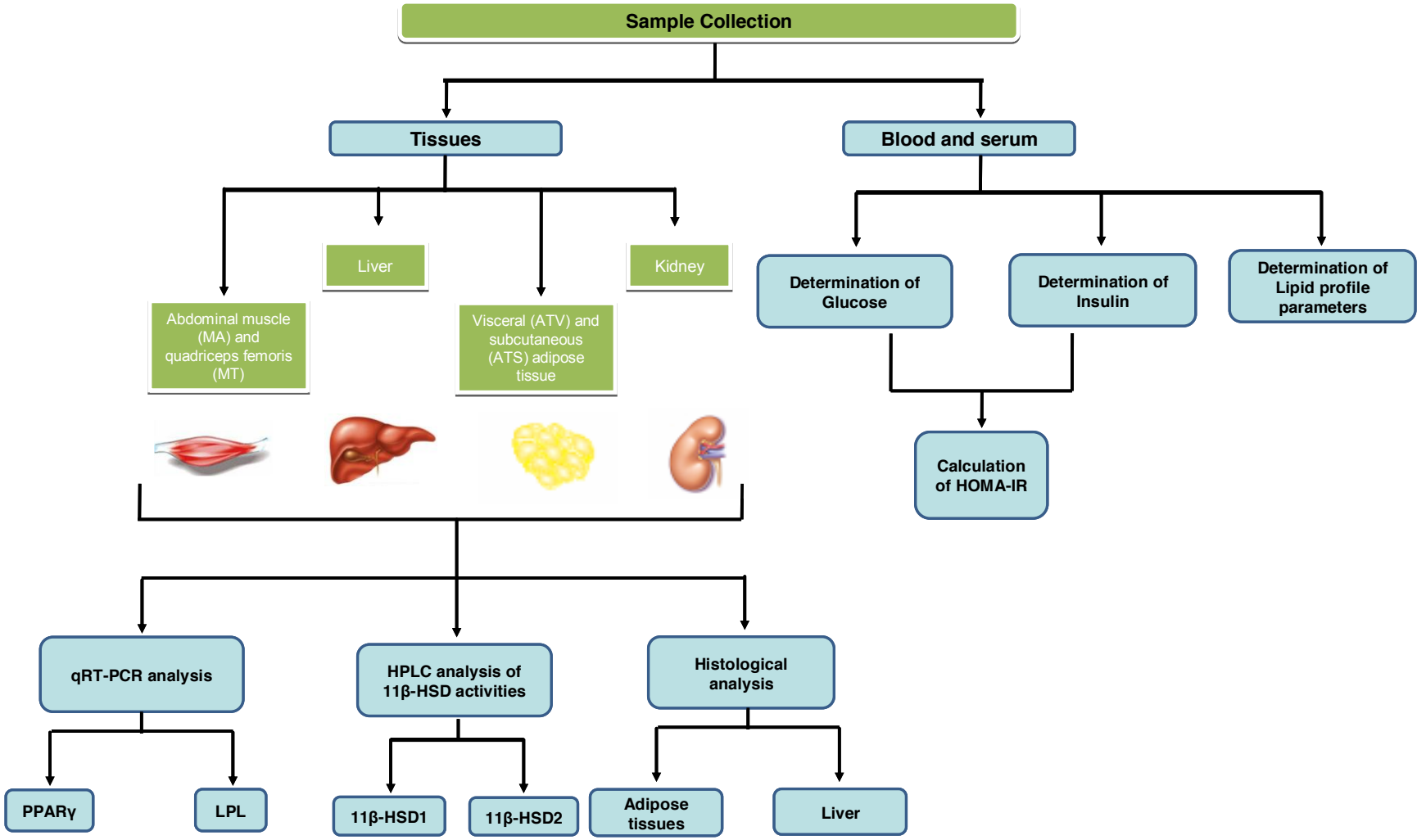

Figure 2.1: Flow chart for experimental design.

2.2.2 Serum insulin determination by ELISA

Determination of serum insulin levels was done using the Rat/Mouse Insulin ELISA Kit (Linco Research, USA) that employs the sandwich ELISA assay concept. All analyses were performed in duplicates in a 96-well microtitre plate. The microtitre plate was coated with mouse monoclonal anti-rat insulin antibodies and subjected to three washes with 300 μL of Wash Buffer (as provided by the manufacturer) per wash. This was followed by the sequential addition of 10 μL of Assay Buffer (as per manufacturer) and 10 μL of Matrix Solution (as per manufacturer) to all wells and the subsequent addition of 10 μL of insulin standards, control and samples to their respective wells. 80 μL of biotinylated anti-insulin detection antibodies were then added to all wells and the plate was sealed, agitated and incubated for 2 hours at room temperature. The plate was again washed three times with 300 μL of Wash Buffer per wash and 100 μL of streptavidin-horseradish peroxidase conjugate was added to all wells. The plate was sealed, agitated and incubated for 30 minutes at room temperature before being subjected to six washes with 300 μL of Wash Buffer per wash. This was followed by the addition of 100 μL of 3,3'5,5'-tetramethylbenzidine substrate to the all wells. The plate was sealed for a final round of 15 minutes incubation at room temperature. Lastly, 100 μL of Stop Solution (as per manufacturer) was added to all the wells and the absorbance was measured at 450 nm and 590 nm with BIO-TEK Powerwave XS Microplate Scanning Spectrophotometer within 5 minutes (Figure 2.2).

The increase in absorbance from 590 nm to 450 nm is directly proportional to the level of insulin present and quantification of insulin level was done using the standard curve generated from a series of insulin standards ranging from 0.2 to 10 ng/mL (Appendix 2; Figure A2.2).

The microtitre plate was washed with 3x 300 µl of wash buffer

⇩

10 µl of assay buffer were added to the blank and sample wells

⇩

10 µl of matrix solution were added to the blank, standard and the control

⇩

10 µl of the standards, controls and samples were added to the wells

⇩

80 µl of the monoclonal mouse anti-rat insulin antibody were added to all

⇩

The plate was sealed, agitated and incubated for 2 hours at room temperature

⇩

100 µl of streptavidin-horseradish peroxidase conjugate were added to all

⇩

The plate was sealed, agitated and incubated for 2 hours at room temperature

⇩

Each well was washed six times with 300 µl wash buffer

⇩

100 µl of diluted 3,3',5,5'-tetramethylbenzidine were added to all wells

⇩

The plate was sealed, agitated and incubated for 15 minutes at room

⇩

Each well was washed three times with 300 µl wash buffer

⇩

100 µl of 0.3M hydrochloric acid was added to each well

⇩

Absorbance of each well was read at 450 nm and 590 nm

Figure 2.2: Flow-chart of insulin determination by Enzyme-linked Immunosorbent assay (ELISA).

2.2.3 Calculation of homeostasis model assessment of insulin resistance (HOMA-IR)

The insulin resistance of each rat was determined using HOMA-IR indices, which involves the product of fasting plasma glucose and fasting serum insulin in mmol/L and ng/mL respectively divided by 22.5 (Konrad *et al.*, 2007).

2.2.4 Determination of serum triacylglycerol (TAG)

Serum TAG was quantified using the Wako Triglyceride E kit (Wako, Japan). 15 µL of serum samples, blank and TAG standards (ranging form 0.50 – 3.00 mmol/L) were added to individual aluminium foil-wrapped test tubes containing 2.25 mL of Working Solution and the mixtures were incubated at 37°C for 5 minutes. 200 µL of the coloured solution was pipetted into a microtitre plate in duplicates and the plate was read at 600 nm using the BIO-TEK Powerwave XS Microplate Scanning Spectrophotometer. The level of serum TAG was determined with reference to the standard curve generated (Appendix 2; Figure A2.3).

2.2.5 Determination of serum total cholesterol

Serum total cholesterol was quantified using the Randox CH200 Cholesterol kit (Randox, UK). 10 µL of serum samples, blank and cholesterol standards (ranging from 1.00 to 5.00 mmol/L) were added to individual aluminium foil-wrapped test tubes containing 1.0 mL of reagent R1 and the mixture was incubated at 37°C for 5 minutes. 200 µL of the coloured solution was pipetted into a microtitre plate in duplicates and the plate was read at 500 nm using the BIO-TEK Powerwave XS Microplate Scanning Spectrophotometer. The level of serum cholesterol was determined with reference to the standard curve generated (Appendix 2; Figure A2.4).

2.2.6 Determination of serum HDL- and LDL-cholesterol

HDL-cholesterol was first separated from the LDL and VLDL fraction by precipitation of the latter two using the Randox CH203 HDL Precipitant (Randox, UK). 35 µL of serum samples, blank and HDL standards (ranging from 0.20 to 1.40 mmol/L) were added to 87.5 µL of diluted precipitant and allowed to sit at room temperature for 10 minutes, followed by centrifugation at 4000 rpm for 10 minutes.

Cholesterol assay was then performed using the Randoz CH200 Cholesterol kit (Randox, UK) aforementioned in section 2.2.5. 25 µL of the clear supernatants from samples, blank and HDL standards were added to 250 µL of reagent R1 and incubated at 37°C for 5 minutes. 100 µL of the coloured solution was pipetted into a microtitre plate in duplicates and the plate was read at 500 nm using the BIO-TEK Powerwave XS Microplate Scanning Spectrophotometer. The level of serum HDL cholesterol was determined with reference to the standard curve generated (Appendix 2; Figure A2.5).

LDL-cholesterol was calculated using the Friedewald formula below, using the levels of total cholesterol, TAG and HDL-cholesterol obtained (Friedewald *et al.*, 1972):

$$\text{LDL-cholesterol} = \text{Total Cholesterol} - \frac{\text{TAG}}{2.2} - \text{HDL-Cholesterol}$$

2.3 Real-time Reverse Transcription Polymerase Chain Reaction (qRT-PCR) quantification **of total PPARγ, PPARγ2 and LPL expression (Qiagen and Sigma**-Proligo, USA)

2.3.1 Total mRNA extraction from tissue samples

Total mRNA extraction from kidney, liver and both abdominal and quadriceps femoris muscles were performed using the Qiagen RNeasy Mini Kit while the Qiagen RNeasy Lipid Tissue Mini Kit was used for the total mRNA extraction from subcutaneous and visceral adipose tissues. The protocols for extraction of total mRNA from these different tissues were obtained from the manufacturer of the extraction kits and are shown in Appendices 3 to 5.

2.3.2 Storage of extracted mRNA

Purified mRNA was stored at -20^{O}C until required.

2.3.3 Quantification and purity analysis of extracted mRNA

The concentration of eluted mRNA was estimated through measurements of absorbance at 260 nm (A_{260}) using a Perkin Elmer Lambda 25 UV/VIS spectrometer. The concentration of RNA could be determined using an absorbance of 1 unit at A_{260} corresponding to 44 μg of RNA per ml (Qiagen, 2006).

Extracted mRNA samples were diluted 50 times by adding 10 μL of the isolated RNA to 490 μL of RNase-free water. RNA analysis was performed by measuring the absorbance of the diluted RNA with a PerkinElmer Lambda 25 UV/VIS Spectrometer (PerkinElmer, USA). RNase-free water was used as a blank. The concentration of mRNA could be obtained by using the following equation:

RNA concentration $= A_{260}$ x 44µg/mL x dilution factor

For analysis of RNA purity, another reading at 280 nm (A_{280}) was obtained. The ratio of A_{260}/A_{280} was then compared with known pure RNA range of 1.9 to 2.1 (Qiagen, 2006). RNase-free water was again used as the blank.

2.3.4 Analysis of RNA integrity

Extracted RNA samples were subjected to agarose gel electrophoresis for the determination of quality and integrity of extracted RNA. 1.2% (w/v) native agarose for electrophoresis was prepared by completely dissolving 0.36 g of agarose powder in 30 mL of 1X TBE buffer. The solution was then allowed to cool prior to casting of the gel. The gel was then left for approximately 20 minutes to solidify. The gel tanks were filled with 1X TBE buffer and the RNA samples were loaded into the wells together with two sets of ssRNA ladder markers (New England Biolabs). The electrophoresis process was performed with a potential difference of 80V. The resulting gel was treated with ethidium bromide (0.5 mg/mL) for approximately 20 minutes prior to documentation with a SynGene GeneGenius Bio Imaging system. The estimation of RNA integrity was observed through the degree of smearing of 18S and 28S ribosomal RNA bands present in the gel image.

2.3.5 RNase-free DNase treatment

The extracted RNA samples were treated with RNase-free DNase (Promega RQ1 RNase-free DNase) by incubating with the RNase-free DNase reaction mixture (Appendix 6) at 37°C for 30 minutes. Then, 1 μL of RQ1 DNase Stop Solution (as provided by the manufacturer) was added followed by incubation at 65°C for a further 10 minutes.

2.3.6 cDNA synthesis

Synthesis of cDNA was conducted using Qiagen Omniscript Reverse Transcriptase (Qiagen, USA). The preparation of cDNA synthesis reaction mixture is shown in Appendix 7. The samples from Section 2.3.5 were incubated with the reaction mixture at 37°C for one hour and were subsequently stored at -80°C until required for analysis.

2.3.7 Primer and probe design for rat total PPARγ, PPARγ2, LPL and β-actin

Gene specific forward and reverse primers were designed for rat total PPARγ, PPARγ2, LPL and β-actin (BAC) using PRIMER3 software for partial amplification of each gene. The design of primers was in accordance to several basic requirements noted below (Nolan *et al.*, 2006):

(a) Primer size was set within a range of 15 to 25 nucleotides, with the optimum value of 20 nucleotides.

(b) Melting temperature (T_m) was set between 55°C to 65°C, with an optimum of 60°C.

(c) Guanosine and cytosine (GC) content was set between 40 to 60 percent.

Analyses of the designed primers were performed using the Nucleotide-nucleotide Basic Local Alignment Searching Tool (BLAST) program available from the National Centre for Biotechnology Information (NCBI) website. The presence of possible palindromic sequences and primer-dimer formation were also checked using the Primer Premier 5 program prior to the synthesis of the primers. The profiles of all the primers are shown in Appendix 8.

Upon synthesis of primers by Sigma-Proligo (Sigma, USA), the T_m of each primer was manually rechecked using the equation given below (Nolan *et al.*, 2006):

$$T_m = 2^{\circ}C \times (A+T) + 4^{\circ}C \times (G+C)$$

Locked Nucleic Acid (LNA) Dual-labeled Fluorogenic Probes were also designed for rat total PPARγ, PPARγ2, LPL and BAC and obtained from Sigma Proligo. The profiles of each probe are shown in Appendix 8.

2.3.8 Real-time Reverse Transcription Polymerase Chain Reaction (Nolan *et al.*, 2006)

All the optimization involved in qRT-PCR for total PPARγ, PPARγ2, LPL and BAC were performed using the DNA Engine Opticon 2 Continuous Fluorescence Detector from MJ Research® Incorporated. The parameters involved in the optimization process included both primer concentrations, Locked Nucleic Acid (LNA) probe concentration as well as annealing (50°C - 60°C) and elongation (60°C - 75°C) temperatures. Reaction mixtures contained 12.5 µL of Jumpstart™ *Taq* ReadyMix™ (2.5 Units of Jumpstart *Taq* DNA Polymerase, 10 mM Tris-HCl, 50 mM KCl, 1.7 mM $MgCl_2$ and 0.2 mM of dNTPs), forward and reverse primers for each respective gene, specific LNA Dual-labeled Fluorogenic Probe, cDNA template (from Section 2.3.6) and RNase-free water adding up to a total of 25 µL reaction mixture. The optimized reaction mixtures (Appendix 9) were later used for the quantification of total PPARγ, PPARγ2, LPL and BAC expression in the liver (L), kidney (K), subcutaneous and visceral adipose tissues (ATS and ATV), abdominal and quadriceps femoris muscles (MA and MT).

2.3.9 Calibration of standard curve

Construction of calibration curves for both total PPARγ and PPARγ2 were done using purified recombinant plasmids containing total PPARγ and PPARγ2 insertions (Lee *et al.*, 2008). The T/A cloning method was used to clone the PPARγ2 fragments. The PPARγ2 fragment obtained by PCR were ligated into pDrive vectors at the multiple cloning site and transformed on LB agar plates containing ampicillin, IPTG and X-Gal. Recombinant clones were selected based on the blue-white X-Gal IPTG induction method and grown on LB media. Extraction of the plasmid DNA was performed using QIAprep Spin Miniprep Kit (Tiu, 2008). A similar procedure was used to obtain the total PPARγ plasmids. The total PPARγ plasmid is a recombinant containing both PPARγ1 and PPARγ2. Sequencing of recombinant pDrive plasmid was performed to verify the identity of insertion as total PPARγ and PPARγ2. Upon subjecting the sequencing results to nucleotide sequence similarity search using BLASTN (Altschul *et al.*, 1990), the identity of the insert in the recombinant pDrive plasmid was confirmed (Appendix 10).

The plasmids were quantified spectrophotometrically and the copy number of the respective total PPARγ and PPARγ2 plasmids was obtained through the product of the respective mass of the PPARγ fragment and pDrive plasmid (Lee *et al.*, 2008):

$$\text{DNA (copy)} = \frac{6.02 \times 10^{23} \text{ (copies mol}^{-1}\text{)} \times \text{DNA amount (g)}}{\text{DNA length (bp)} \times 660 \text{ (g mol}^{-1} \text{ bp}^{-1}\text{)}}$$

A hundred fold dilution series was performed for both plasmids. The standard curve was constructed with the logarithm of initial template copy numbers against the respective C_t values of the diluted plasmids (Appendix 10.8, Figure A10.7 and A10.8).

2.3.10 Quantification of total PPARγ, PPARγ2 and LPL expression (Nolan *et al.*, 2006)

Upon optimization of qRT-PCR parameters, expression of the respective genes was quantified using the optimized temperature profile (Appendix 11) in 25 µL of reaction mixtures. All qRT-PCR were carried out on a Peltier Thermal Cycler PTC-100 (MJ Research, UK) and analysis was performed using the DNA Engine Opticon® 2 Continuous Fluorescence Detection system (MJ Research, UK).

2.3.11 Absolute quantification of total PPARγ, PPARγ1 and PPARγ2 expression

Absolute quantification was performed through the substitution of the raw C_t readings for all the tissue samples into the calibrated standard curve in Section 2.3.9. The quantification of PPARγ1 was performed by subtracting the copy number of PPARγ2 from total PPARγ (Ameshima *et al.*, 2003).

2.3.12 Relative quantification of LPL expression

The comparison of LPL expression between control and GA-administered rats were performed using the Comparative C_t ($\Delta\Delta C_t$) Method that is based on the expression ratio of the target gene relative to a reference gene (Plaffl *et al.*, 2002). C_t is the 'threshold cycle', which by definition refers to the cycle number where amplification levels rises above the background. To ensure valid comparison of LPL expression, C_t values were fixed at the same position across all samples (Vaerman *et al.*, 2004).

2.3.13 Agarose gel electrophoresis of amplified PCR products - **(total PPARγ, PPARγ2, LPL and β-actin)**

Random amplified products were subjected to 4% agarose gel (w/v) electrophoresis to determine the presence of the desired products (total PPARγ, PPARγ2, LPL and β-actin). Preparation of gel was similar to that in Section 2.3.4 with the exception of using 1.2 g of agarose powder diluted in 30 mL of 1X TBE buffer and the use of a 25 bp DNA step ladder obtained from Promega, USA. Amplicons and the 25 bp ladder were run on the agarose gel which was subsequently stained with 0.5 mg/mL ethidium bromide for approximately 15 minutes, followed by destaining under running water for 2 minutes. The gel was viewed and captured using SynGene Gene Genius Bio Imaging System. The presence of the desired bands was noted with reference to the DNA ladder markers used (Appendix 10.8.3).

2.4 **11β**-hydroxysteroid dehydrogenases **(11β**-HSDs) activities

2.4.1 Homogenization of tissues

All reagents were freshly prepared prior to dissection. All tissue samples, buffers and homogenates were kept on ice and procedures were performed in duplicates at 4°C throughout the experiment unless otherwise stated.

Krebs-Ringer (KR) bicarbonate buffer was prepared as described in Appendix 12. The harvested tissues were homogenized, in a ratio of 1.0 g of tissue to 2.0 mL of KR buffer, with a Heidolph DIAX 900 rotor stator homogenizer. The rotor was rinsed with 70% ethanol followed by KR buffer prior to homogenization of the next sample.

2.4.2 Determination of protein concentration

A series of protein standards varying from 0.3 to 1.8 mg/mL was prepared by diluting a stock bovine serum albumin (BSA) (2 mg/mL) with KR buffer (Appendix 13). The homogenised lysates were centrifuged in a Hettich Zentrifugen Universal 32R centrifuge at 14,000 x g for 20 minutes at 4°C.

10 µL of afore-mentioned BSA standards, homogenates supernatants and KR buffer were placed into a 96-well microtitre plate for assay of protein content using modified Lowry's method (Okutucu *et al.*, 2007). 25 µL and 200 µL of Bio-Rad Reagents A and B respectively, were added into each well, mixed properly and incubated at room temperature for 15 minutes before spectrophotometric measurement at 650 nm by a BIO-TEK Powerwave XS microtitre plate reader. A standard protein curve was prepared from the corresponding results of blanks (KR buffer) and known protein concentrations of BSA solutions for the determination of unknown protein concentrations of the homogenates (Appendix 12). A standard curve was constructed for every assay to prevent batch to batch variation.

2.4.3 **Conditions for incubation of 11β-HSD**

50 mg of tissue protein were incubated with 0.1 mM corticosterone in the presence of excess cofactor (0.35 mM NADP+ for 11β-HSD type 1 and 0.35 mM NAD+ for 11β-HSD type 2) in a microtube. KR buffer (containing 0.2% glucose and 0.2% BSA) was added to a final volume of 500 µL and the mixture was incubated at 37°C in a Memmert water-bath for one hour. The reaction was terminated by storage of microtubes at -20ºC (Morton *et al.*, 2004).

2.4.4 Extraction of glucocorticoid (11-dehydrocorticosterone)

800 µL of ethyl acetate was added to each microtube and was placed horizontally on a rotating Protech orbital shaker at 100 rpm for 30 minutes, prior to centrifugation in an Eppendorf microentrifuge 5415R at 22ºC, 16,000 x g for 10 minutes. The resulting upper organic layer was transferred into a new microtube, evaporated under flow of nitrogen gas and reconstituted with 400 µL of High Performance Liquid Chromatography (HPLC) mobile phase (20% methanol, 30% acetonitrile and 50% water v/v) prior to analysis (Nwe *et al.*, 2000).

2.4.5 Quantification by High Performance Liquid Chromatography

Various concentrations of 17α-hydroxy-11-dehydrocorticosterone (17α-hydroxy-11-DHB) ranging from 1 to 10 µM (Appendix 14) were used to determine retention time and standard product curve for quantification of 11-DHB from the tissue samples.

A Hamilton syringe was used to inject 100 µL of the above sample into a sample loop of the Perkin Elmer Series 200 Liquid Chromatography Pump which was connected to the Vacuum Degasser, for analysis on a reverse phase Waters Symmetry® C18 5 µm (3.9 x 150 mm) column by gradient elution. The first five minutes of the gradient elution used was from 10:15:75 (v/v) methanol:acetonitrile:water and was later switched to 20:30:50 (v/v) methanol:acetonitrile:water. This was followed by isocratic elution for the next 10 minutes. The mobile phase flow rate was set constant at 1 mL/min. A Perkin Elmer Series 200 Diode Array Detector was used for spectrophotometric measurement at 254 nm (Nwe *et al.*, 2000).

Enzyme activities of 11β-HSD types 1 and 2 were expressed as: 1 Unit (U) of 11β-HSD was the formation of 11-dehydrocorticosterone (ρmole), under the above-mentioned pre-defined experimental conditions of 50 mg of tissue protein at an incubation time of one hour at 37°C (Lavery *et al.*, 2007).

2.5 Histological analysis

2.5.1 Fixation of tissues

Each tissue sample was fixed by immersion in a universal bottle containing 10% (v/v) neutral-buffered formalin to facilitate better penetration by the fixative. Immersed tissues were left at room temperature for 48 hours with replacement of fixative every 2 days until the tissues hardened.

2.5.2 Impregnation and infiltration of tissues

Tissue impregnation consisted of two steps, namely dehydration and clearing. Dehydration involved removal of water within tissues by sequential immersion in increasing concentrations of ethanol (50%, 70%, 80%, 95% and 100% v/v) in water for 1 hour each at room temperature followed by absolute ethanol for another hour. Clearing involved immersion of tissues in a mixture of xylene and absolute ethanol (1:1 ratio v/v) followed by pure xylene, each lasting 24 hours until the tissues became transparent. Flow-chart for this procedure is shown in Figure 2.3.

Tissue infiltration consisted of serial addition of paraffin flakes to tissues immersed in xylene and incubated in a Memmert oven at gradually increasing temperatures (40°C, 50°C and 55°C) for 24 hours each. The paraffin-xylene mixture was discarded and replaced with fresh (molten or liquid) paraffin. The tissues were incubated in uncapped universal bottles at 60°C for three days with daily changes of fresh liquid paraffin (Figure 2.3).

2.5.3 Embedding of tissues

Embedding consisted of immersion of tissues in semi molten paraffin that was previously poured into a cardboard box placed on a tray left on ice. This allowed cooling and solidification of the paraffin base while the upper layers were kept warm and molten by gently skimming the surface with a warm spatula. Tissues were gently lowered into

the semi-molten paraffin once the paraffin base started becoming translucent. The whole block was allowed to solidify at room temperature before hardening at 4°C in a refrigerator for half an hour.

2.5.4 Sectioning of tissues

The hardened paraffin block was trimmed into smaller blocks of individual tissues prior to mounting on a Leica rotary microtome Modell RM2135 for sectioning at a thickness of 6 μm and an angle of 10°. The tissue sections were placed afloat in a water-bath maintained at 45°C and fished onto microscopic glass slides. The slides were dried overnight before dewaxing and rehydration (Figure 2.3).

2.5.5 Dewaxing and rehydration

The slides were de-paraffinized by immersion in xylene followed by a mixture of xylene and absolute ethanol (1:1 v/v) for half an hour and 15 minutes respectively. The slides were then immersed in decreasing concentrations of ethanol, 100%, 95%, 80% and 70%, each lasting 10 minutes before immersion in distilled water for five minutes (Figure 2.3).

2.5.6 Staining

Staining methods, as illustrated in Figure 2.4, were performed at 27ºC, whilst each wash, rinse and immersion lasted 30 seconds, one and five minutes respectively unless stated otherwise.

FIXATION	
⇩	
Immersion in 10% neutral-buffered formalin	
⇩	
Replaced every 2 days until tissue is hardened	
DEHYDRATION	
⇩	
Sequential immersion of tissues in ethanol 50%, 60%, 70%, 80% and	1 hour
⇩	
Immersion of tissues in absolute ethanol. Repeat step	1 hour
CLEARING	
⇩	
Immersion of tissues in a mixture of xylene and ethanol (1:1)	24 hours
⇩	
Immersion of tissues in xylene (repeat until tissues are hardened)	24 hours
INFILTRATION	
⇩	
Addition of paraffin flakes into xylene immersed tissue at increasing	24 hrs
⇩	
At 60 ºC (with daily replacement of paraffin)	3 days
EMBEDDING & SECTIONING	
⇩	
Tissue embedded in paraffin block and cooled at 8 ºC	
⇩	
Sectioned to thickness of 6 µm	
⇩	
Dried on microscope glass slides	
DEWAXING & REHYDRATION	
⇩	
Immersion in xylene	30 mins
⇩	
Immersion in xylene: ethanol mixture (1:1)	15 mins
⇩	
Immersion in absolute ethanol	10 mins
⇩	
Sequential immersion in ethanol 95 %, 80 %, 70 % (v/v),	5 mins
⇩	
Immersion in water	5 mins

Figure 2.3: Flow chart illustrating histological protocol.

2.5.6.1 Haematoxylin and Eosin (H&E) stain

De-paraffinized slides were immersed in haematoxylin for one minute, followed by washing in distilled water, H&E decolorizing acid solution, H&E bluing solution, 70% ethanol, 90% ethanol and water. The slides were subsequently rinsed in eosin for one minute, followed by washing twice in 95% ethanol and twice in absolute ethanol. Finally, they were rinsed in xylene before air-dried.

2.5.6.2 **Periodic acid Schiff's (PAS) stain**

De-paraffinized slides were serially immersed in periodic acid solution, distilled water and Schiff's reagent for 10, 5 and 15 minutes respectively and another rinse in distilled water for five minutes. The slides were subsequently washed in haematoxylin for 10 seconds, distilled water for 30 seconds and ammonia water for 10 seconds, followed by washing in distilled water, 70% ethanol, 95% ethanol and absolute ethanol. Finally, they were rinsed in xylene before air-dried.

2.5.6.3 Mounting and analysis

Formalin fixed paraffin embedded tissue sections were mounted with one drop of Depex mounting medium on the centre of the slide before placement of a cover slip. H&E and PAS stained slides were photographed in triplicate using a Nikon Eclipse E200 microscope connected to Nikon Digital Sight DS-U2.

All slides were examined under 100x and 400x magnification. Adipocyte morphology was characterized by analysis of mean cell area (μm^2) of 100 adipocytes under 400x magnification per slide using the software Motic Image Plus 2.0. The scaling factor was pre-calibrated by a Motic technician.

HAEMATOXYLIN & EOSIN	
Haematoxylin	1-2 mins
⇩	
Distilled Water	30 secs
⇩	
H&E decolourising acid	30 secs
⇩	
H&E blueing solution	30 secs
⇩	
70% alcohol	30 secs
⇩	
90% alcohol	30 secs
⇩	
Distilled Water	30 secs
⇩	
Eosin	1 mins
⇩	
95% alcohol	2 x 30 secs
⇩	
100% alcohol	2 x 30 secs
⇩	
Xylene	1 min
⇩	
Air dry	

Figure 2.4 A

PERIODIC ACID SCHIFF'S	
Periodic Acid solution	10 mins
⇩	
Distilled Water	5 mins
⇩	
Schiff's reagent	15 mins
⇩	
Distilled Water	5 mins
⇩	
Haematoxylin	30 secs
⇩	
Distilled Water	30 secs
⇩	
Ammonia Water	30 secs
⇩	
Distilled Water	30 secs
⇩	
70% alcohol	30 secs
⇩	
95% alcohol	30 secs
⇩	
100% alcohol	30 secs
⇩	
Xylene	1 min
⇩	
Air dry	

Figure 2.4 B

Figure 2.4: Flow-chart for (A) Haematoxylin and Eosin and (B) Periodic Acid Schiff's staining respectively.

2.6 Statistical analysis

Analyses of all data were performed using Statistical Package for the Social Sciences (SPSS) for Windows, version 16 with the exception of relative LPL expression. Prior to the test, the normality of the data was tested to determine the distribution of the data, with significance value of $P \leq 0.05$. Statistical analysis for LPL expression was performed using Relative Expression Software Tool (REST©) MCS Beta 2006. A p-value ≤ 0.05 was considered significant (Campbell and Machin, 2002).

Results for blood glucose (mmol/L), serum insulin (ng/mL), HOMA-IR, total PPARγ, PPARγ1 and PPARγ2 expression levels, 11β-HSD1 and 2 activities were presented as medians and subjected to analysis by Mann-Whitney U-test. The use of median to represent data was to negate the adverse effects of outliers towards the final data since relatively large variations were observed (Campbell and Machin, 2002).

CHAPTER 3

Results

(Part A)

Chapter 3

RESULTS

3.1 Effects of oral vs. intraperitoneal administration of glycyrrhizic acid in rats

50 mg/kg of GA were given to rats either orally or intraperitoneally for 12 hours.

3.1.1 Blood glucose, serum insulin and HOMA-IR

Results for the blood glucose levels, serum insulin levels and the HOMA-IR indices for rats given GA either orally or intraperitoneally are listed in Table 3.1 and shown in Figures 3.1, 3.2 and 3.3 respectively. Slight decreases in the blood glucose and serum insulin levels as well as the HOMA-IR values were observed after 12 hours of GA treatment. Nevertheless, no significant differences were observed in all three parameters when compared between the two routes of administration.

Table 3.1: Median blood glucose and serum insulin levels as well as the HOMA-IR indices of rats administered with GA orally and intraperitoneally

Subject	Median blood glucose levels		Median serum insulin levels		HOMA-IR index	
	(mmol/L)	*P* value	(ng/mL)	*P* value		*P* value
Rats given GA orally	7.37 (5.69 – 10.25)	0.15	2.98 (1.68 – 3.49)	0.47	1.30 (0.54 – 1.71)	0.10
Control	9.49 (7.37 – 10.50)		3.21 (2.31 – 4.87)		1.68 (1.00 – 2.22)	
Rats given GA intraperitoneally	5.69 (5.06 – 7.67)	0.10	2.63 (1.49 – 3.50)	0.08	0.57 (0.52 – 0.90)	0.27
Control	7.88 (5.02 – 9.82)		3.21 (2.52 – 3.73)		0.82 (0.43 – 1.22)	

Only a P value of ≤ 0.05 is considered statistically significant and marked with an asterisk (*)

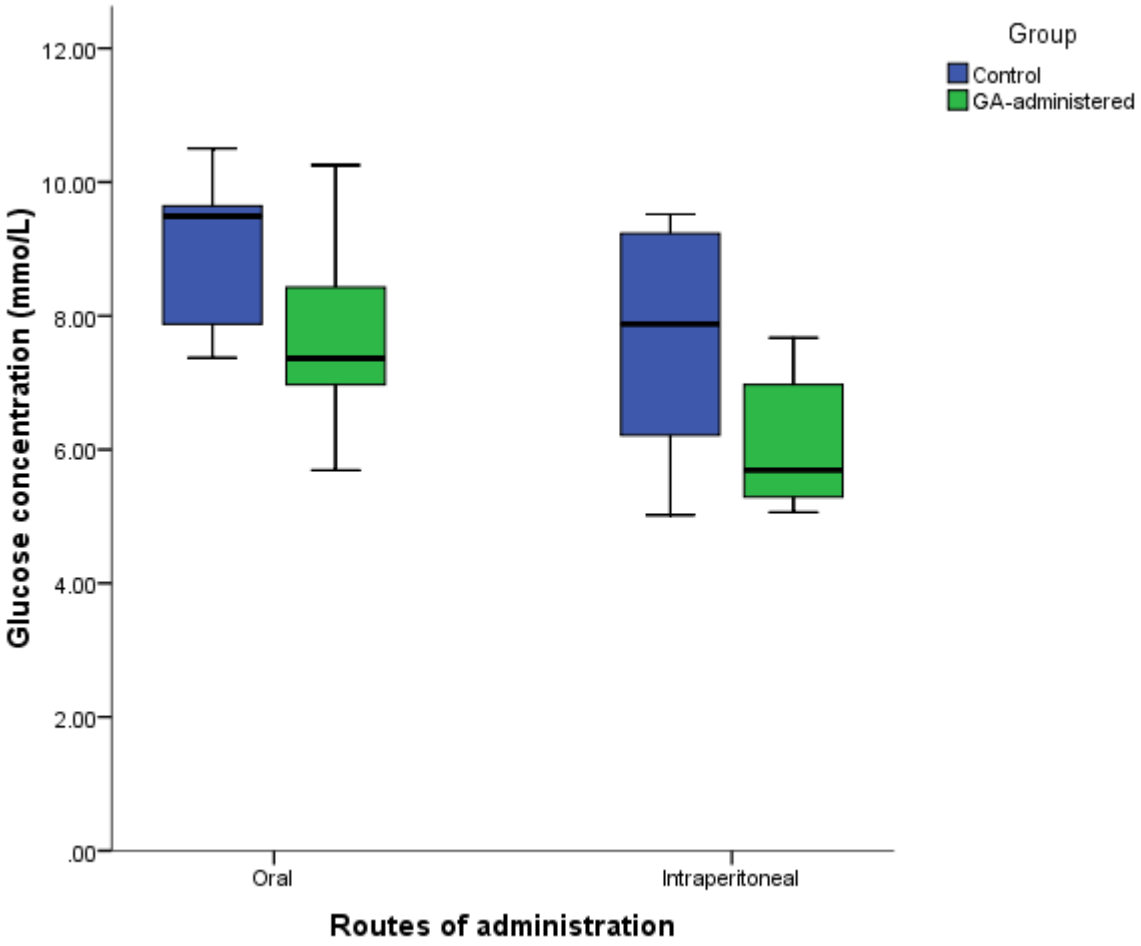

Figure 3.1: Blood glucose levels in rats given GA orally or intraperitoneally.

No significant difference ($P > 0.05$) was observed between the two routes of GA administration.

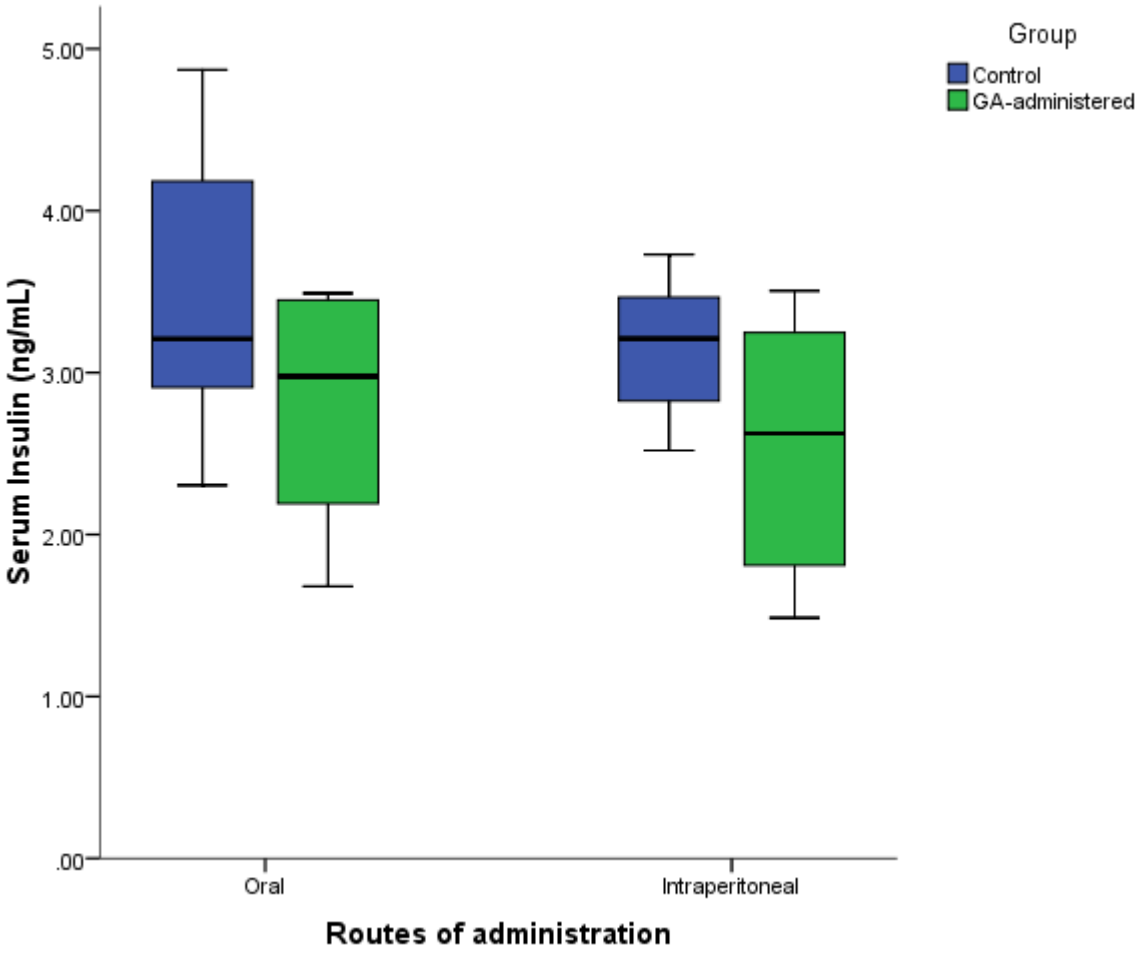

Figure 3.2: Serum insulin levels in rats given GA orally or intraperitoneally.

No significant differences were observed ($P > 0.05$) for both groups.

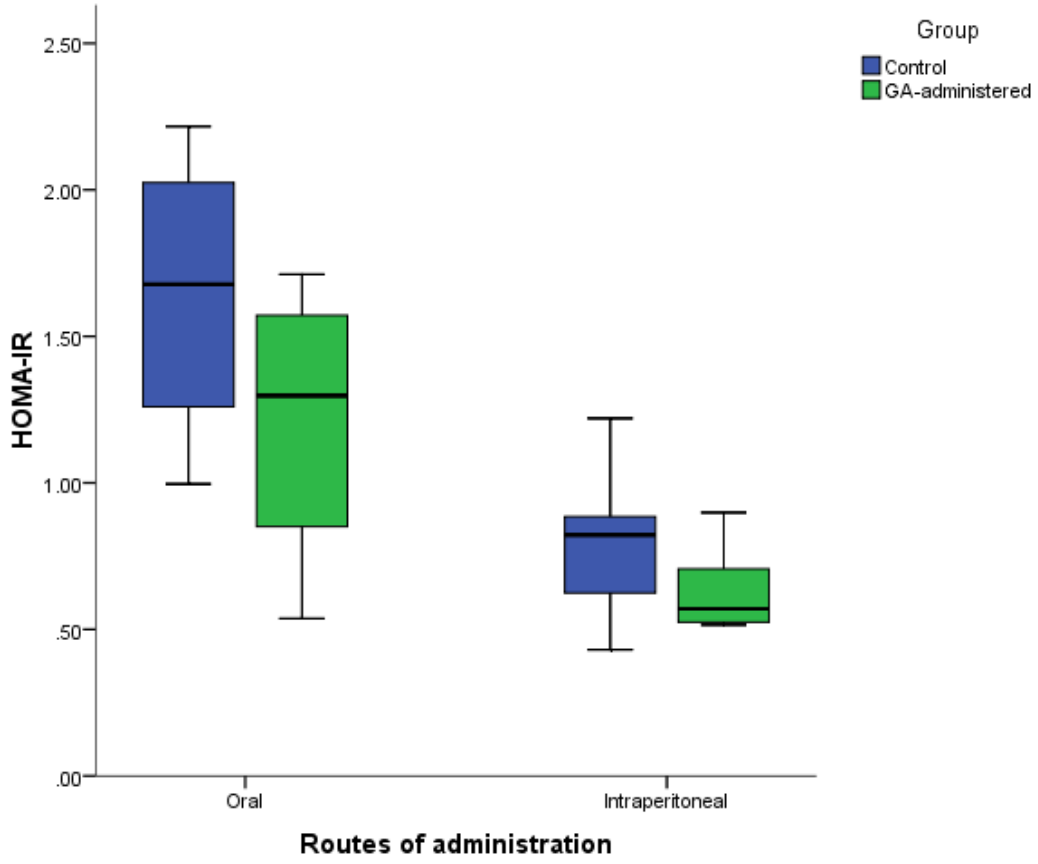

Figure 3.3: HOMA-IR in rats given GA orally or intraperitoneally.

The differences in the HOMA-IR for both groups were not statistically significant ($P > 0.05$).

3.1.2 Quantification of PPARγ and LPL expression

3.1.2.1 Expression of total PPARγ, PPARγ1 and PPARγ2 in studied tissues

The gene expression of total PPARγ, PPARγ1 and PPARγ2 were quantified based on the substitution of the C_t values obtained from the qRT-PCR of various tissues into the equation obtained from the standard curve (Appendix 10.8). The qRT-PCR analysis was based on *Taqman* LNA Dual-labeled Fluorogenic Probe. All the expression values were normalized through standardizing the use of 1µg of total RNA for reverse transcription to cDNA in all tissues and ultimately expressed as copy number per µg of mRNA (Lee *et al.*, 2008). The gene expression for PPARγ1 was obtained through the subtraction of the PPARγ2 gene expression from that of total PPARγ (Ameshima *et al.*, 2003). The differences in the copy numbers per µg of total RNA between the control and GA-administered rats were expressed as fold differences (Alonso, personal communication, July 22nd 2009).

3.1.2.2 Total PPARγ expression

All tissues from the orally or intraperitoneally GA-administered rats displayed a higher expression of total PPARγ compared to the control group (Figures 3.4a and b; Table 3.2), with the visceral adipose tissue displaying the highest expression levels followed by the subcutaneous adipose tissue, quadriceps femoris, liver, abdominal muscle and kidney. However the increased expression levels in all tissues were not statistically significant for both routes ($P > 0.05$). Interestingly, it is in the subcutaneous adipose tissues that the largest increase in total PPARγ levels was observed (i.e., 49-fold increase) and not in the visceral adipose tissues which displayed only a 9.2-fold increase (Table 3.2).

Table 3.2: Fold increase of total PPARγ expression in rats orally and intraperitoneally-administered with GA.

Although there was a general increase in total PPARγ levels for all tissues in GA-administered rats, the increased levels were statistically not significant ($P > 0.05$).

Tissue	Fold-difference in total PPARγ expression	
	Oral	Intraperitoneal
ATS	49.0	32.3
ATV	9.2	6.1
MA	11.2	3.9
MT	17.4	6.8
L	16.4	8.2
K	7.2	3.4

Abbreviations: ATS, subcutaneous adipose tissue; ATV, visceral adipose tissue; MA, abdominal muscle; MT, quadriceps femoris muscle; L, liver; K, kidney.

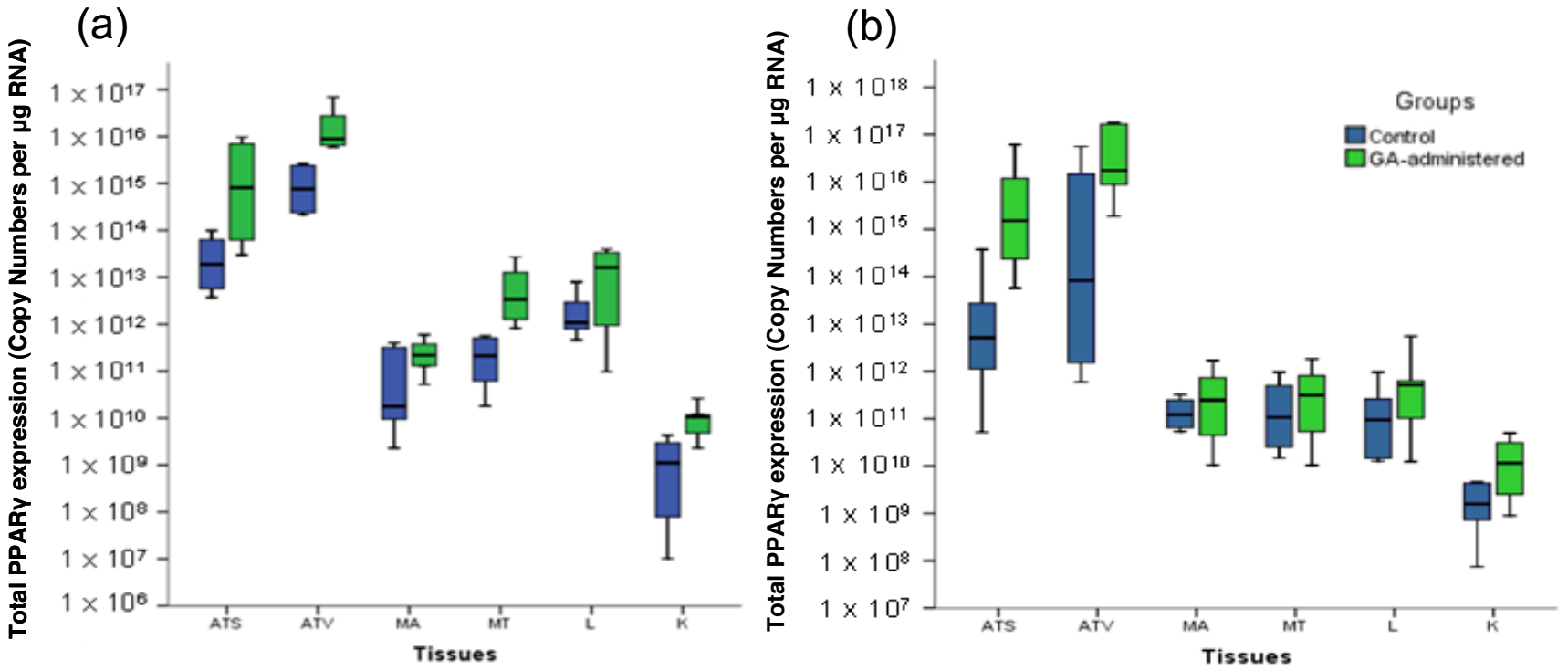

Figures 3.4: Total PPARγ expression levels in various tissues of the control and GA-administered rats (a) orally and (b) intraperitoneally.

Although there was a general increase in PPARγ levels for all tissues in GA-administered rats, the increased levels were statistically not significant ($P > 0.05$). Abbreviations: ATS, subcutaneous adipose tissue; ATV, visceral adipose tissue; MA, abdominal muscle; MT, quadriceps femoris muscle; L, liver; K, kidney.

3.1.2.3 PPARγ1 expression

Similar to that of the total PPARγ expression levels, all tissues from the orally or intraperitoneally GA-administered rats displayed higher expression of PPARγ1 compared to the control group (Figures 3.5a and b; Table 3.3), with visceral adipose tissue displaying the highest expression levels and the kidney displaying the lowest expression levels. The increase in PPARγ1 expression levels in all the tissues was however, not statistically significant between both routes ($P > 0.05$).

3.1.2.4 PPARγ2 expression

All tissues from the orally or intraperitoneally GA-administered rats displayed an increase in median PPARγ2 expression levels compared to the control group (Figures 3.6a and b; Table 3.4). The distribution of PPARγ2 seemed to be tissue-specific, with the visceral and subcutaneous adipose tissues displaying much higher expression levels compared to the other studied tissues. However, the increased expression levels in all the tissues were not statistically significant with both routes ($P > 0.05$).

3.1.2.5 Relative LPL expression in the various studied tissues

The expression of LPL in the various studied tissues was determined by fold difference based on the $2^{-\Delta\Delta Ct}$ method. BAC was used as the endogenous reference gene, with the control group as the calibrator. Since the control group was used as the calibrator, the LPL expression of all tissues was given a baseline value of 1.00 (Plaffl *et al.*, 2002).

Table 3.3: Fold increase of PPARγ1 expression in rats orally and intraperitoneally-administered with GA.

Even though there was a general increase in the expression levels of PPARγ1 in the tissues of GA-administered rats, the increase was not significant ($P > 0.05$).

Tissue	Fold-difference in PPARγ1 expression	
	Oral	Intraperitoneal
ATS	31.7	11.9
ATV	21.7	14.8
MA	30.9	18.5
MT	36.8	15.2
L	33.1	26.2
K	19.0	29.6

Abbreviations: ATS, subcutaneous adipose tissue; ATV, visceral adipose tissue; MA, abdominal muscle; MT, quadriceps femoris muscle; L, liver; K, kidney.

Table 3.4: Fold increase of PPARγ2 expression in rats orally and intraperitoneally-administered with GA.

An increase in PPARγ2 expression levels was observed for all tissues in the GA-administered rats, albeit statistically not significant ($P > 0.05$).

Tissue	Fold-difference in PPARγ2 expression	
	Oral	Intraperitoneal
ATS	24.2	11.2
ATV	28.9	10.6
MA	6.3	6.5
MT	28.5	13.4
L	18.5	21.7
K	10.9	14.4

Abbreviations: ATS, subcutaneous adipose tissue; ATV, visceral adipose tissue; MA, abdominal muscle; MT, quadriceps femoris muscle; L, liver; K, kidney.

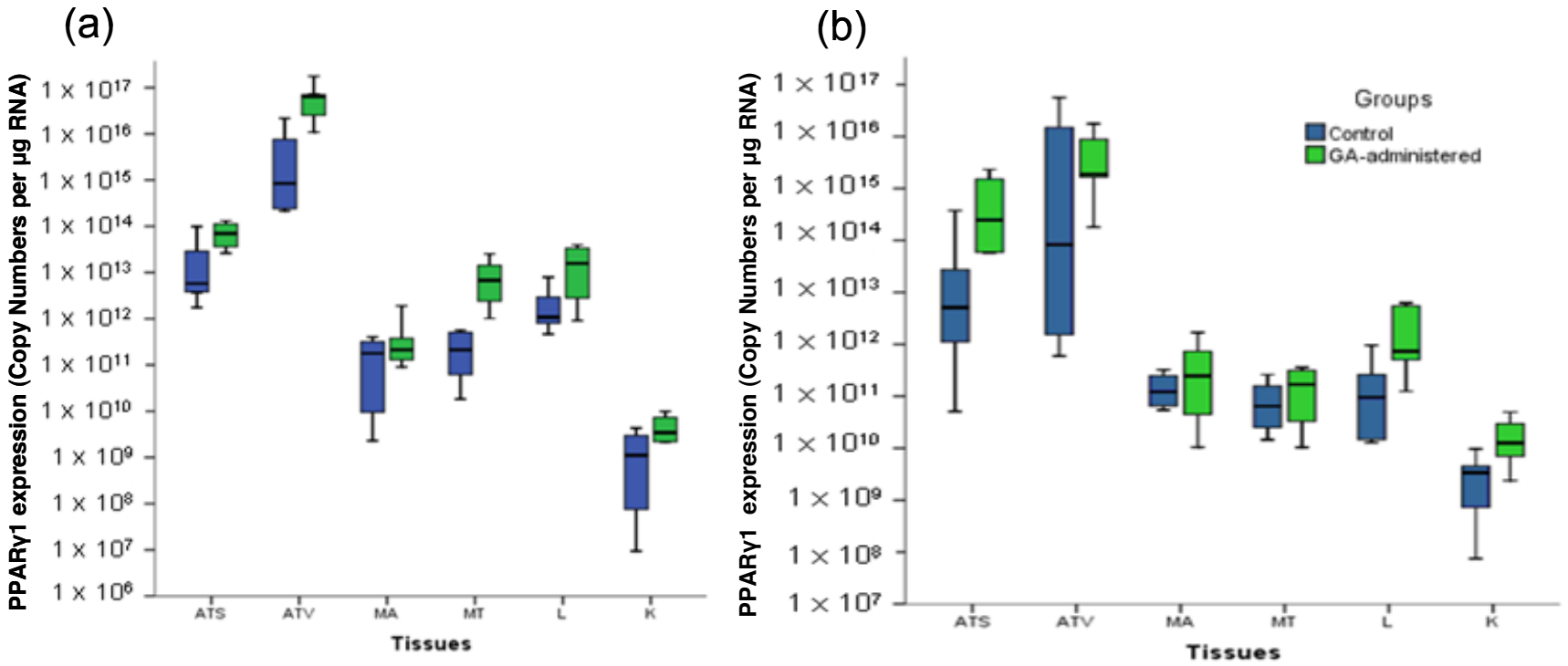

Figures 3.5: PPARγ1 expression levels in various tissues of the control and GA-administered rats (a) orally and (b) intraperitoneally.

Even though there was a general increase in the expression levels of PPARγ1 in the tissues of GA-administered rats, the increase was not significant ($P > 0.05$). Abbreviations: ATS, subcutaneous adipose tissue; ATV, visceral adipose tissue; MA, abdominal muscle; MT, quadriceps femoris muscle; L, liver; K, kidney.

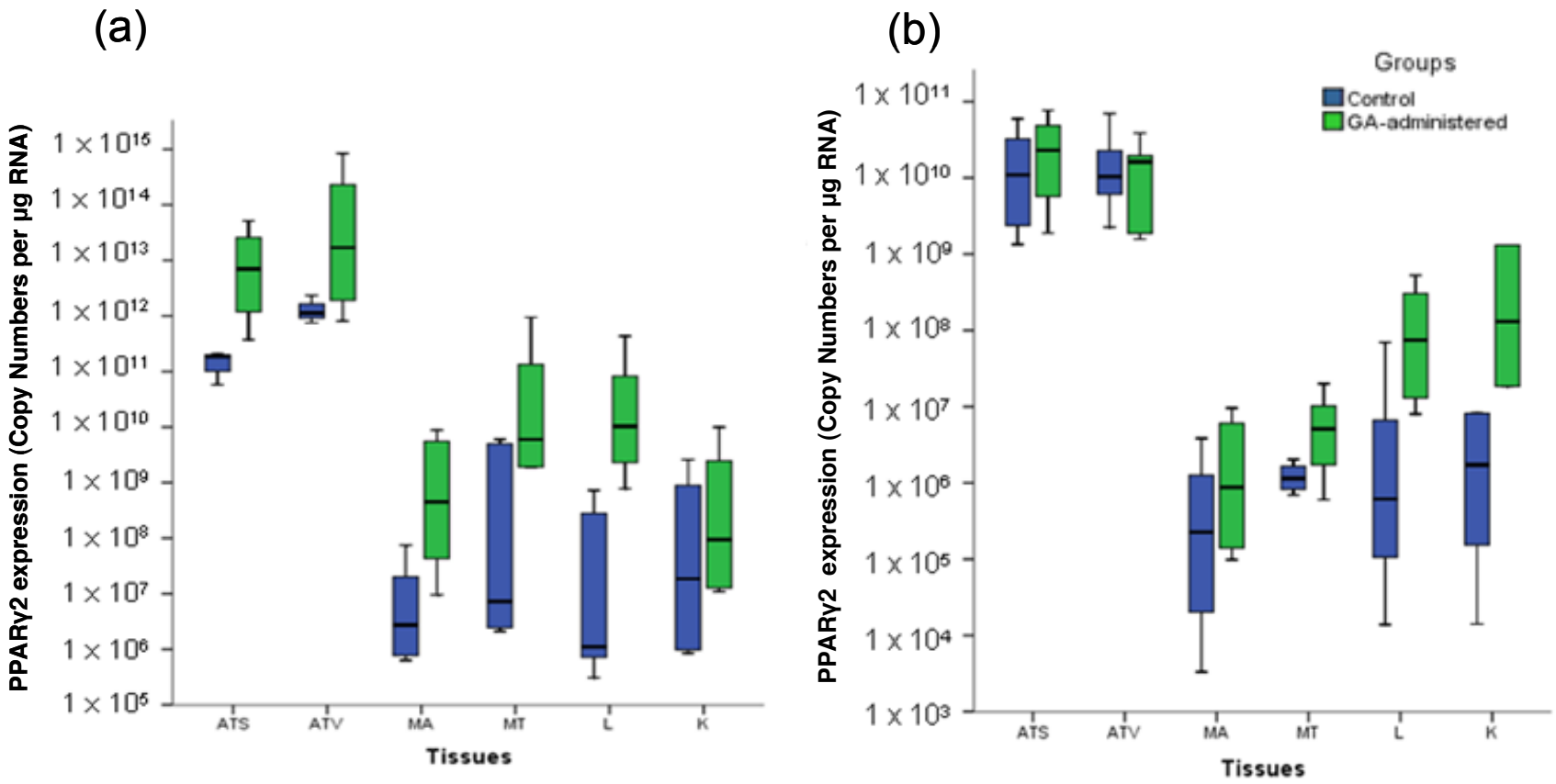

Figures 3.6: PPARγ2 expression levels in various tissues of the control and GA-administered rats (a) orally and (b) intraperitoneally.

An increase in PPARγ2 expression levels was observed for all tissues in the GA-administered rats, albeit statistically not significant ($P > 0.05$). Abbreviations: ATS, subcutaneous adipose tissue; ATV, visceral adipose tissue; MA, abdominal muscle; MT, quadriceps femoris muscle; L, liver; K, kidney.

For the orally-administered rats, LPL expression was increased in all the studied tissues of the GA-administered rats compared to the control group (Figure 3.7a). Of the six tissues studied, the quadriceps femoris displayed the highest increase in LPL expression (i.e., 52.8%) followed by the abdominal muscle (48.2%), liver (42.4%), visceral (27.1%) and subcutaneous adipose tissues (13.1%) and the lowest increase in the kidneys (5.1%). None of the increase in the fold differences was however statistically significant ($P > 0.05$).

For the intraperitoneally-administererred rats, the increase in LPL expression was noted in all the studied tissues of the GA-administered rats compared to the control group (Figure 3.7b). Similar to the orally-administered rats, the quadriceps femoris displayed the highest increase, with 40.8% increase, followed by the abdominal muscle (35.1%), subcutaneous adipose tissue (19.2%), liver (14.3%), visceral adipose tissue (9.2%) and kidney (5.4%). Although there was an increase in LPL expression in all tissues, none of the increase was statistically significant ($P > 0.05$). The increased expression levels in all the tissues were also not statistically significant when compared between both routes ($P > 0.05$).

3.1.3 **11β-HSD1 and 11β-**HSD2 activities

The separation of glucocorticoids (GC) was accomplished by reverse phase chromatography. The product, 11-dehydrocorticosterone (11-DHB), is more hydrophilic than the substrate, corticosterone, due to the presence of an 11-keto group in the former. 17α-hydroxy-11-DHB was used as the representative standard for 11-DHB as it contains an additional 17α hydroxyl group, qualifying it as the most hydrophilic GC. The GCs were eluted in order of increasing hydrophobicity, i.e., 17α-hydroxy-11-DHB, 11-DHB and corticosterone, due to increased interactions between the alkyl carbon chains of the C-18 column and hydrophobic groups (Pácha *et al.*, 1997). The most hydrophobic GC, corticosterone, possessed retention times between 10.3 to 10.6 minutes while a

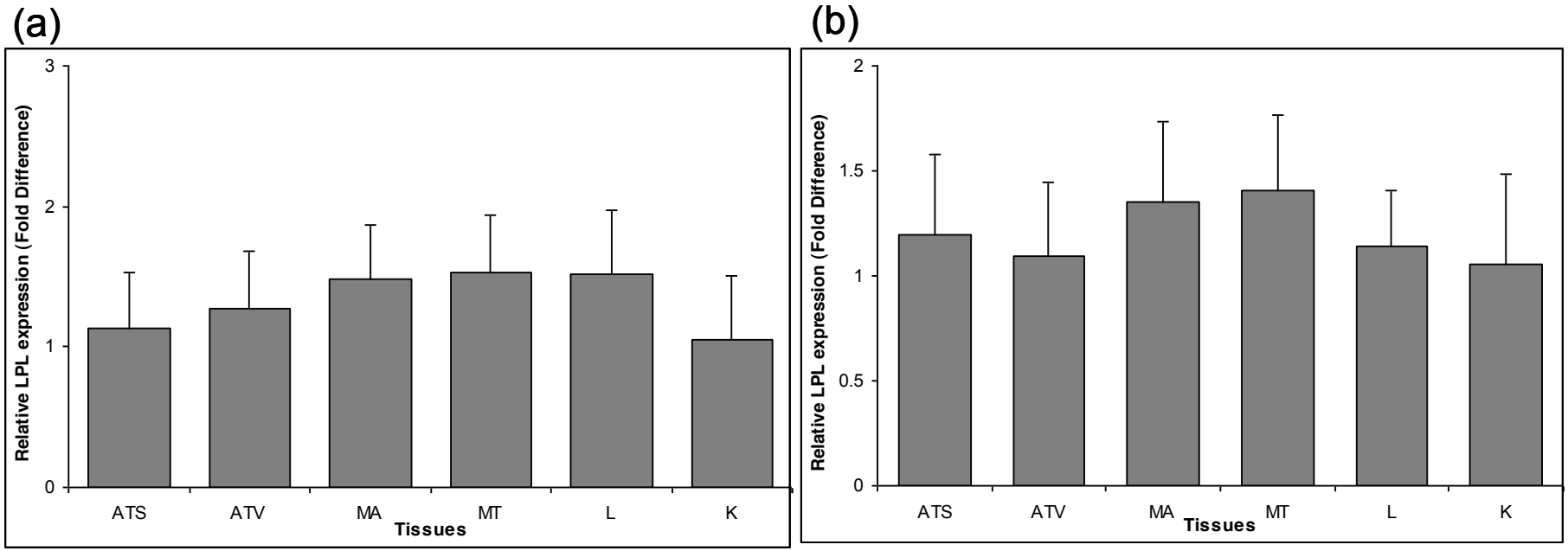

Figures 3.7: Relative expression (fold difference) for LPL in various tissues in GA-administered rats (a) orally and (b) intraperitoneally with β-actin as reference, GA-administered group as target and control group as calibrator.

Although all tissues showed increased LPL expression following GA-administration, the increased levels were not statistically significant ($P > 0.05$). Abbreviationss: ATS, subcutaneous adipose tissue; ATV, visceral adipose tissue; MA, abdominal muscle; MT, quadriceps femoris muscle; L, liver; K, kidney.

consistent peak with retention times of 9.1 to 9.2 minutes was deduced to be 11-DHB (Appendix 14; Figure A14.2).

3.1.3.1 **11β**-HSD1 activities

All the tissues of the rats orally- and intraperitoneally-administered with GA displayed a decrease in the 11β-HSD1 activities, with all but the liver tissue displaying a non-significant decrease ($P > 0.05$). Results for the percentage reduction of 11β-HSD1 activities in rats given GA either orally or intraperitoneally are listed in Table 3.5 and shown in Figures 3.8a and b respectively. Although the percentage reduction of 11β-HSD1 activities in rats given GA intraperitoneally was higher than that of rats orally-administered with GA, the comparison between the GA administered rats for both routes of administration displayed no significant difference.

3.1.3.2 **11β**-HSD2 activities

Similar to what was observed for 11β-HSD1 activities, all the tissues of rats that were orally- and intraperitoneally-administered with GA displayed a decrease in 11β-HSD2 activities with only the liver tissue showing a statistically significant ($P < 0.05$) reduction. Results for the percentage reduction of 11β-HSD2 activities in rats given GA either orally or intraperitoneally are listed in Table 3.6 and shown in Figures 3.9a and b respectively. The liver showed the largest reduction in 11β-HSD2 activities with a 34.17% reduction for rats given GA orally and a 40.81% reduction for rats given GA intraperitoneally. The percentage reduction of 11β-HSD2 activities in rats that were given GA orally- and intraperioneally-administered were similar while the comparison between the GA administered rats for both routes of administration displayed no significant difference.

Table 3.5: Percentage decrease of 11β-HSD1 activities of rats administered with GA orally and intraperitoneally

Subject	Subcutaneous adipose tissue		Visceral adipose tissue		Abdominal muscle		Quadriceps femoris		Liver		Kidney	
	% reduction	*P* value	% reduction	*P* value	% reduction	*P* value	% reduction	*P* value	% reduction	*P* value	% reduction	*P* value
Rats given GA orally	17.90	0.16	17.62	0.16	18.92	0.19	9.45	0.18	18.93	0.04*	12.35	0.45
Rats given GA intraperitoneally	25.13	0.17	48.42	0.17	29.44	0.12	35.83	0.19	47.63	0.03*	27.71	0.16

Only a P value of ≤ 0.05 is considered statistically significant and marked with an asterisk (*)

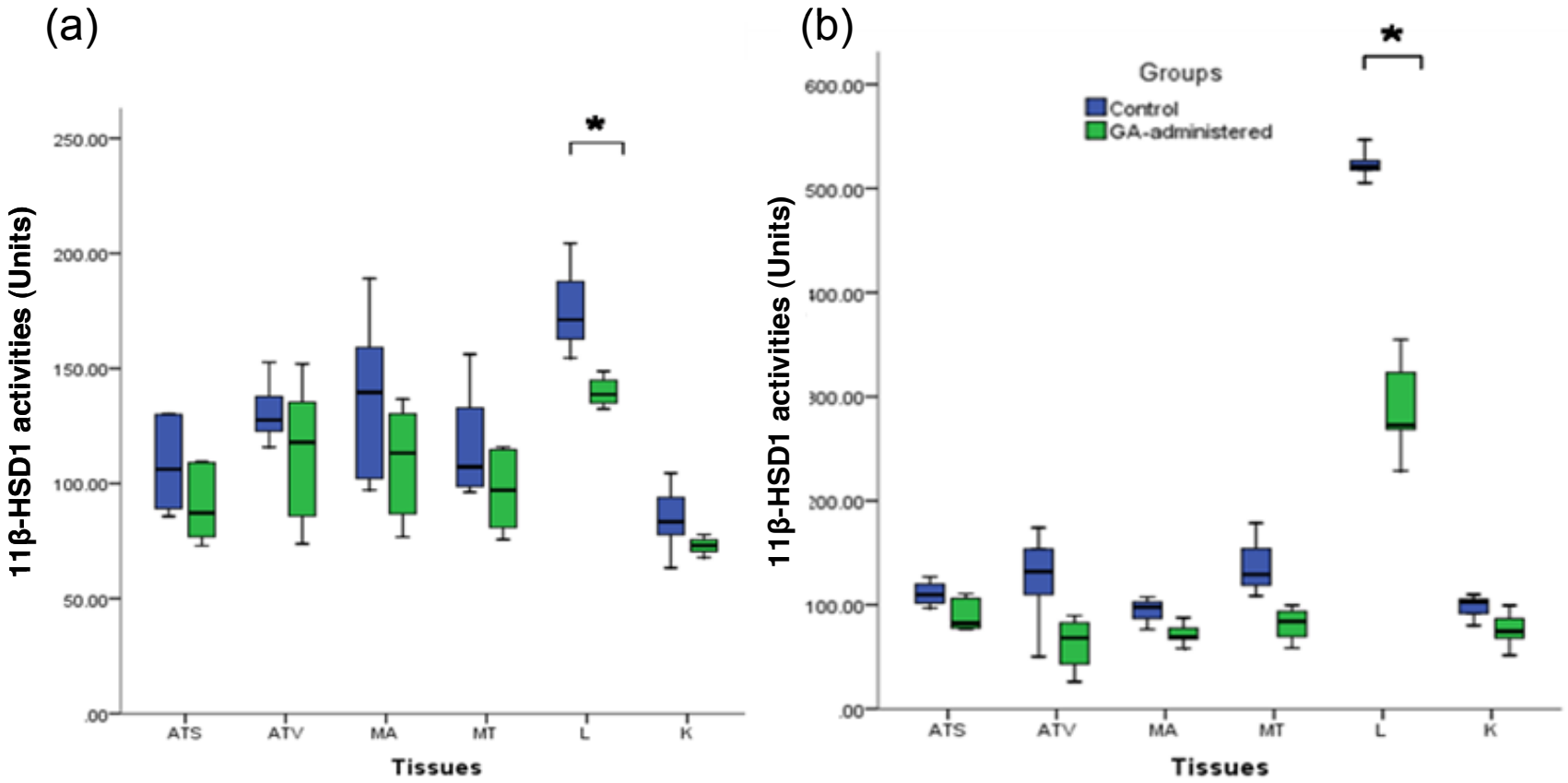

Figures 3.8: 11β-HSD1 activities in various tissues of the control and GA-administered rats (a) orally and (b) intraperitoneally.

All tissues showed reduction in 11β-HSD1 activities with the liver displaying a statistically significant reduction (* indicates $P < 0.05$). Abbreviations: ATS, subcutaneous adipose tissue; ATV, visceral adipose tissue; MA, abdominal muscle; MT, quadriceps femoris muscle; L, liver; K, kidney.

Table 3.6: Percentage decrease of 11β-HSD2 activities of rats administered with GA orally and intraperitoneally

Subject	Subcutaneous adipose tissue		Visceral adipose tissue		Abdominal muscle		Quadriceps femoris		Liver		Kidney	
	% reduction	*P* value	% reduction	*P* value	% reduction	*P* value	% reduction	*P* value	% reduction	*P* value	% reduction	*P* value
Rats given GA orally	27.25	0.16	20.37	0.13	17.31	0.15	12.32	0.16	34.17	0.04*	9.10	0.45
Rats given GA intraperitoneally	19.59	0.20	25.78	0.16	15.33	0.13	18.75	0.17	40.81	0.03*	4.97	0.16

Only a P value of ≤ 0.05 is considered statistically significant and marked with an asterisk (*)

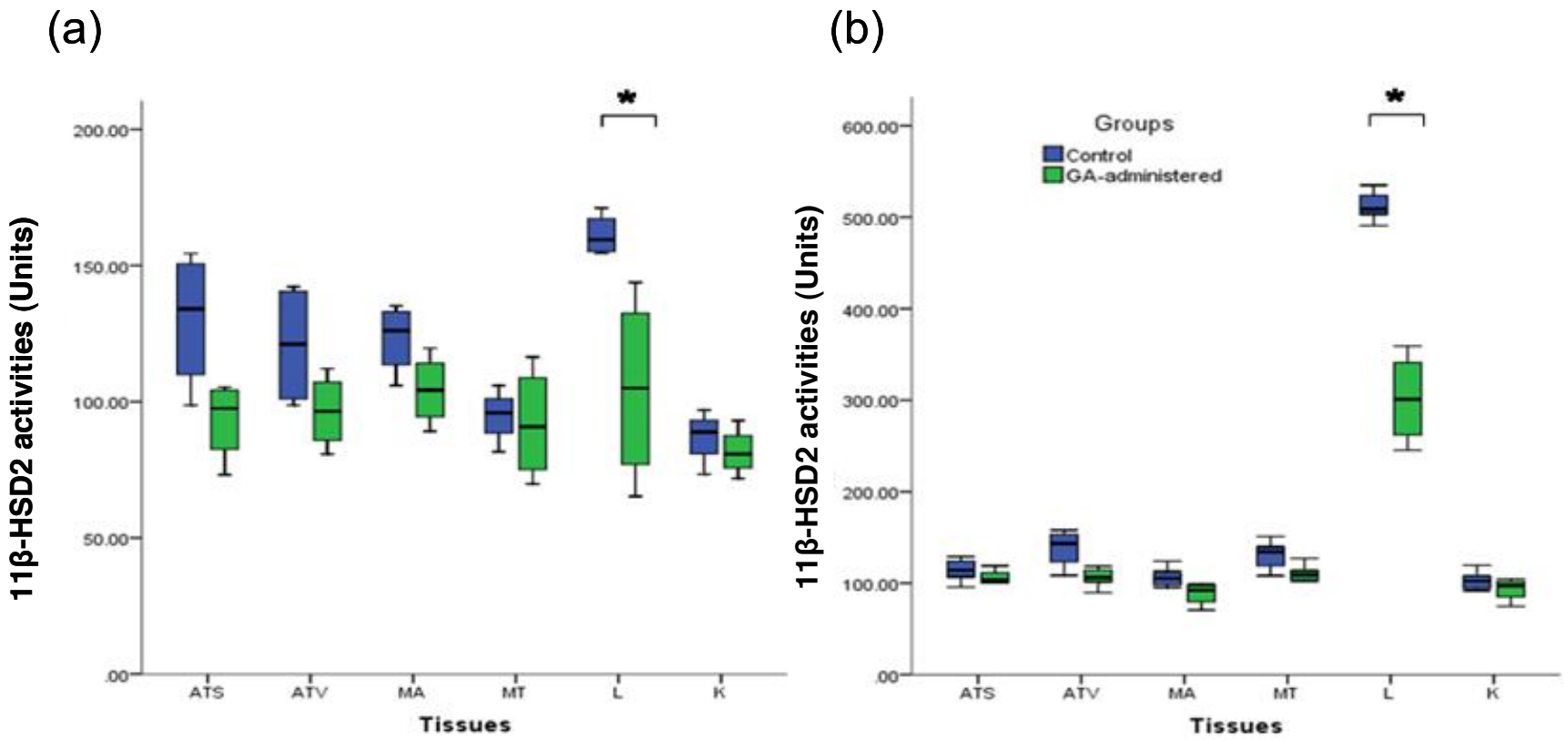

Figures 3.9: 11β-HSD2 activities in various tissues of the control and GA-administered rats (a) orally and (b) intraperitoneally.

Although all tissues showed a general reduction in 11β-HSD2 activities following GA-administration, only the liver showed a statistically significant reduction (* indicates $P < 0.05$). Abbreviations: ATS, subcutaneous adipose tissue; ATV, visceral adipose tissue; MA, abdominal muscle; MT, quadriceps femoris muscle; L, liver; K, kidney.

Chapter 3

Results

(Part B)

3.2 Effects of different dosages of orally-administered glycyrrhizic acid

3.2.1 Effects of different dosages of GA administered

Based on the results from Section 3.1, no significant difference was demonstrated between both the two routes of GA administration. Since there was no significant difference observed, therefore subsequent work was done using oral administration of GA.

Dosages of 25, 50, 75, 100 and 150 mg/kg of GA were chosen for the subsequent part of the study. Oral administration of all the studied dosages of GA for 12 hours resulted in improvement of all the parameters studied, albeit no significant differences noted between all the different studied dosages. Since there was no significant difference noted between the different dosages administered for 12 hours, therefore similar dosages were orally administered to rats for 24 hours.

3.2.2 Blood glucose, serum insulin and HOMA-IR

Significant decrease in the blood glucose levels were seen in rats given GA between 50, 75, 100 and 150 mg/kg ($P = 0.05$, 0.03, 0.02 and 0.01 respectively; $P < 0.05$) (Figure 3.10) for 24 hours while no significant difference in the serum insulin levels was observed between the different dosages used ($P > 0.05$) (Figure 3.11).

Significant decrease in HOMA-IR was seen in rats given 100 and 150mg/kg of GA compared to the control ($P = 0.05$; $P \leq 0.05$). However, no significant difference was detected when the HOMA-IR of rats given 100 and 150 mg/kg GA was compared (Figure 3.12).

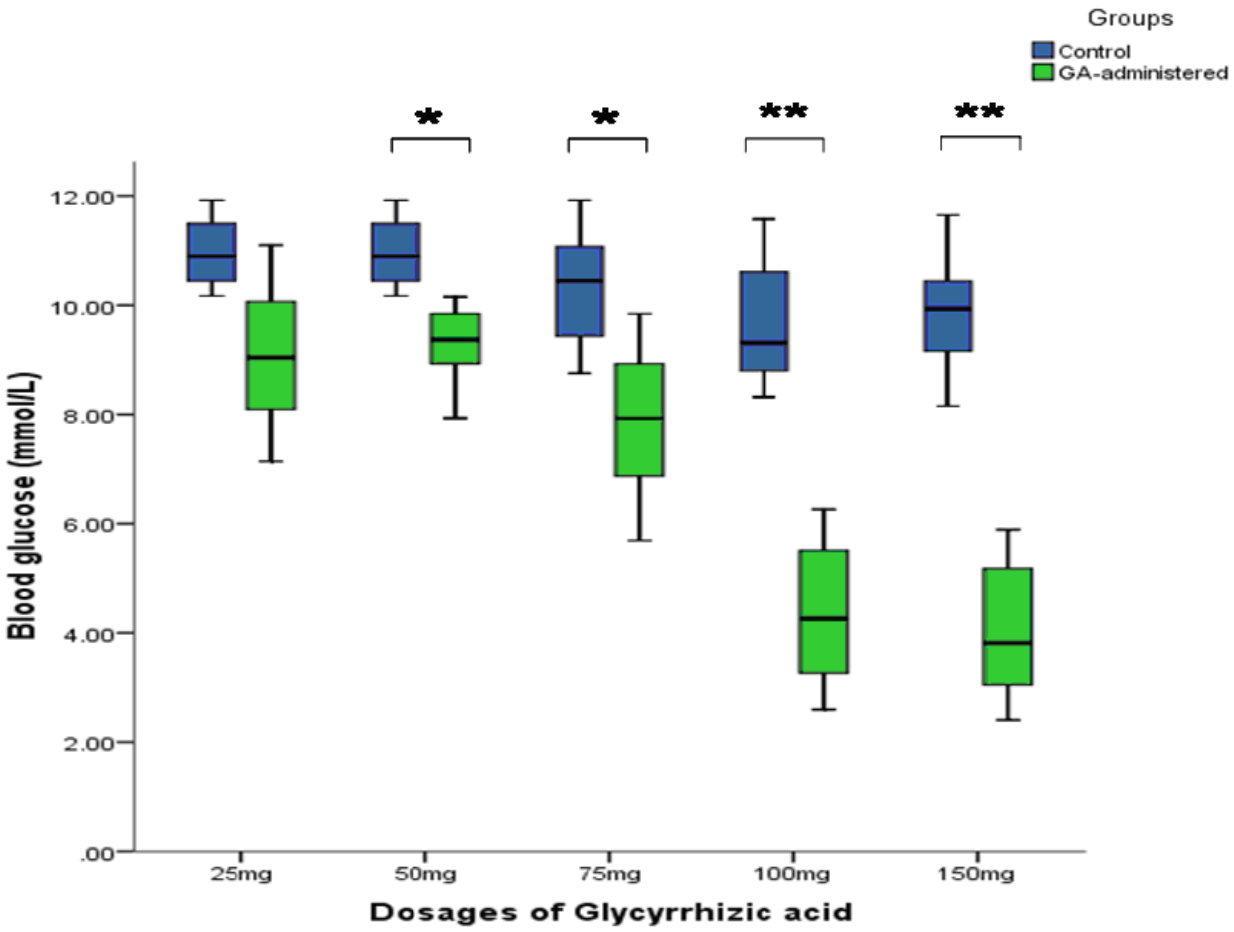

Figure 3.10: Blood glucose levels in GA-treated and control rats given 25, 50, 75, 100 and 150 mg/kg GA.

Decreased blood glucose levels were observed for all GA-administered rats with significant levels observed for dosages of 50 – 150 mg/kg (* indicates $P < 0.05$ and ** $P < 0.01$).

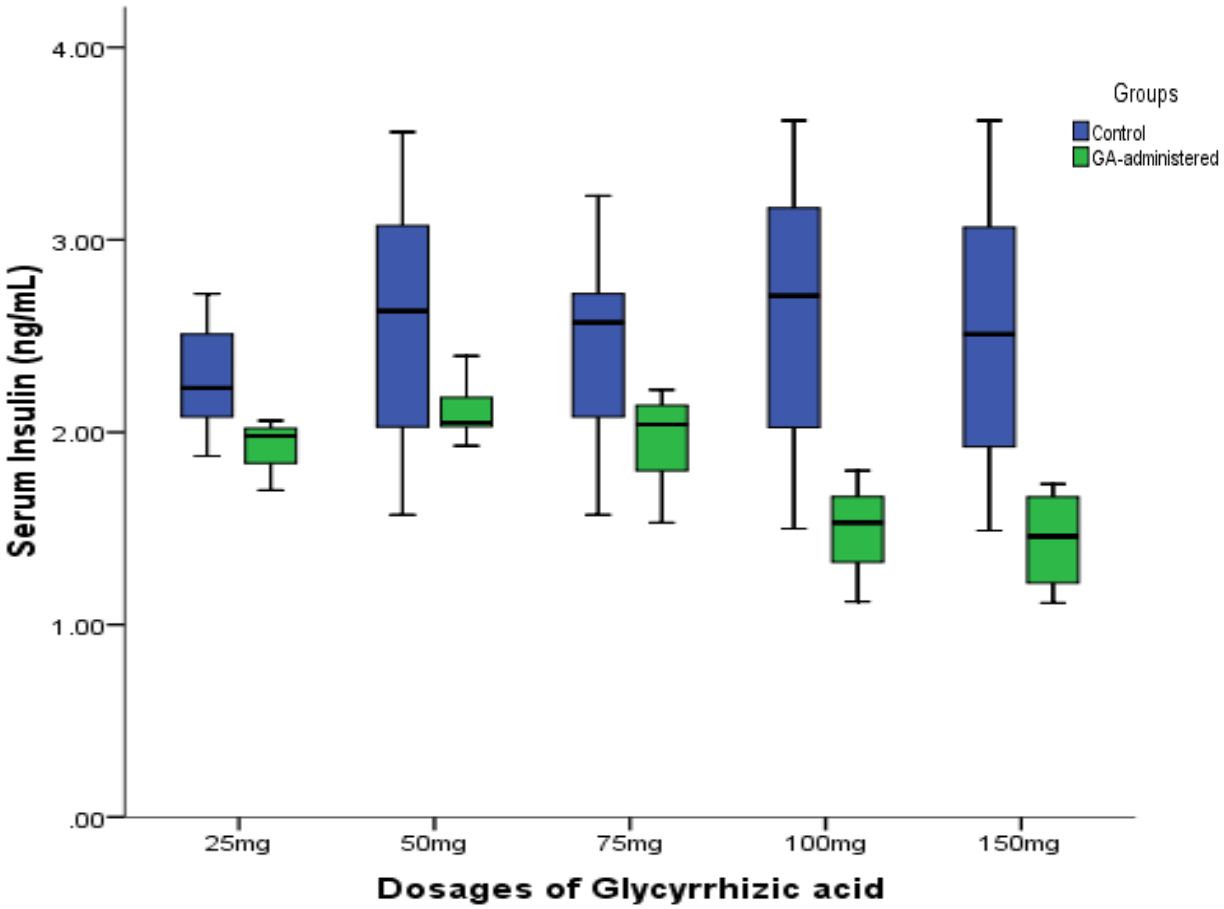

Figure 3.11: Serum insulin levels in GA-treated and control rats given 25, 50, 75, 100 and 150 mg/kg GA.

No significant decrease in insulin levels were observed following GA treatment ($P >$ 0.05 for all dosages).

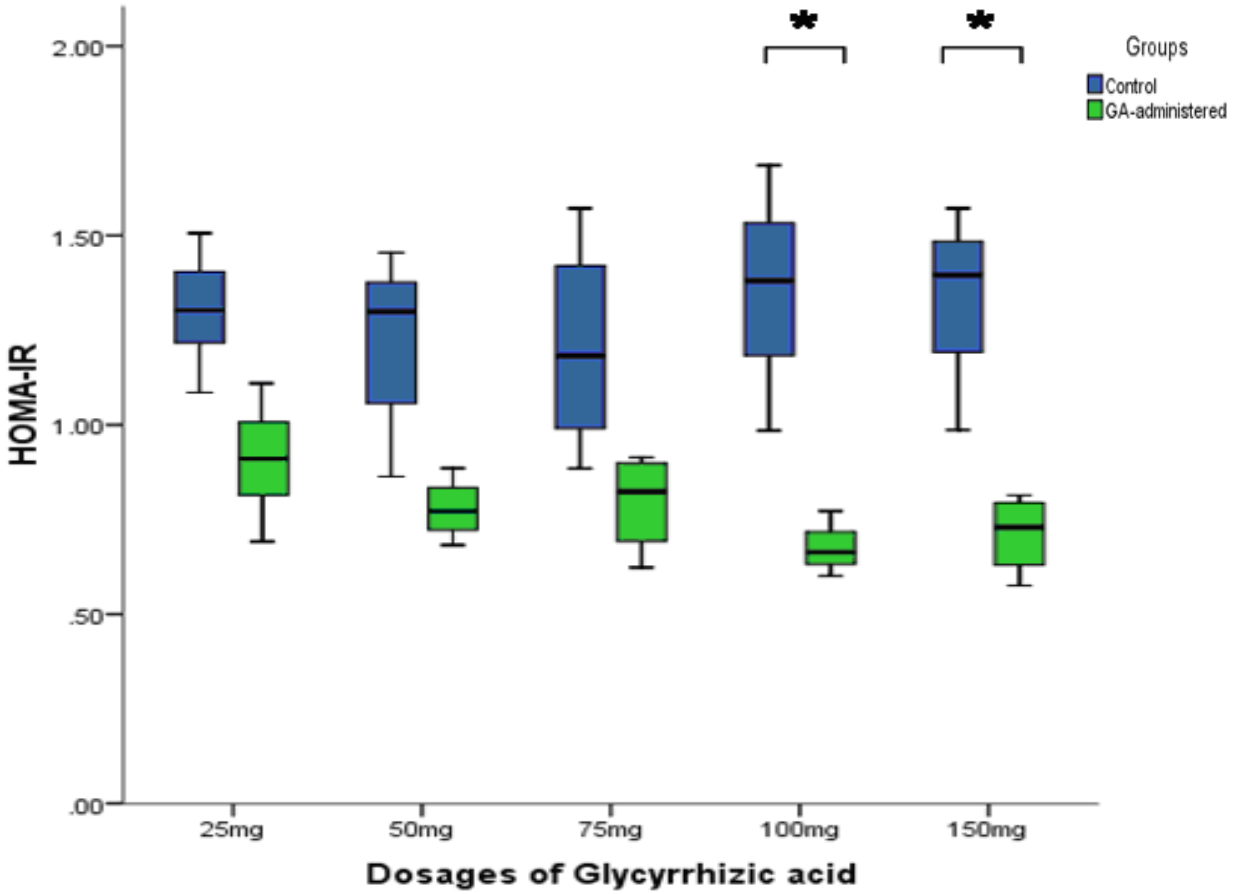

Figure 3.12: HOMA-IR in GA-treated and control rats given 25, 50, 75, 100 and 150 mg/kg GA.

Decreased HOMA-IR values were obtained for all GA-administered rats with rats given 100 and 150 mg/kg GA showing statistically significant decreased values (* indicates $P < 0.05$).

3.2.3 Serum lipid profile

Consistent improvement in all lipid parameters were observed in the GA-administered rats relative to the control with the different dosages (25, 50, 75, 100 and 150 mg/kg) used ($P > 0.05$) (Figure 3.13). There was a general trend of further reduction in serum TAG, total cholesterol and LDL-cholesterol with increasing dosages of GA administered (Table 3.7). Conversely, the amount of HDL-cholesterol increased with GA treatment.

With the various dosages used, no statistical difference between rats given the 100 and 150 mg/kg GA was obtained.

3.2.4 **Total PPARγ expression**

3.2.4.1 Subcutaneous and visceral adipose tissues

Regardless of the dosage of GA administered, the total PPARγ expression levels in the subcutaneous and visceral adipose tissues were higher in the GA-administered rats compared to the control rats (Figures 3.14 a and b; Table 3.8). However, the increase in the expression levels in the subcutaneous adipose tissue with the various dosages was statistically insignificant ($P > 0.05$). Although there was an increase in total PPARγ expression levels in the visceral adipose tissue, significant increase was only noted in the rats administered with 100 ($P = 0.04$) and 150 mg/kg ($P = 0.02$) of GA ($P < 0.05$) where an approximately 80-fold increase was observed. No significant difference was seen between rats given 100 and 150 mg/kg GA.

Table 3.7: Effects on the serum lipid profile of rats administered with GA given in various dosages

Lipid parameter	25 mg/kg GA		50 mg/kg GA		75 mg/kg GA		100 mg/kg GA		150 mg/kg GA	
	% change	*P* value	% change	*P* value	% change	*P* value	% change	*P* value	% change	*P* value
Serum TAG	–18.85	0.21	–20.35	0.20	–20.87	0.18	–28.68	0.16	–29.17	0.13
Total cholesterol	–5.29	0.16	–11.39	0.15	–14.14	0.14	–21.57	0.11	–19.80	0.11
LDL – cholesterol	–4.35	0.19	–8.45	0.16	–17.10	0.16	–21.87	0.14	–29.33	0.14
HDL – cholesterol	6.48	0.18	3.80	0.20	10.08	0.14	18.18	0.13	22.22	0.12

Only a P value of ≤ 0.05 is considered statistically significant and marked with an asterisk (*)

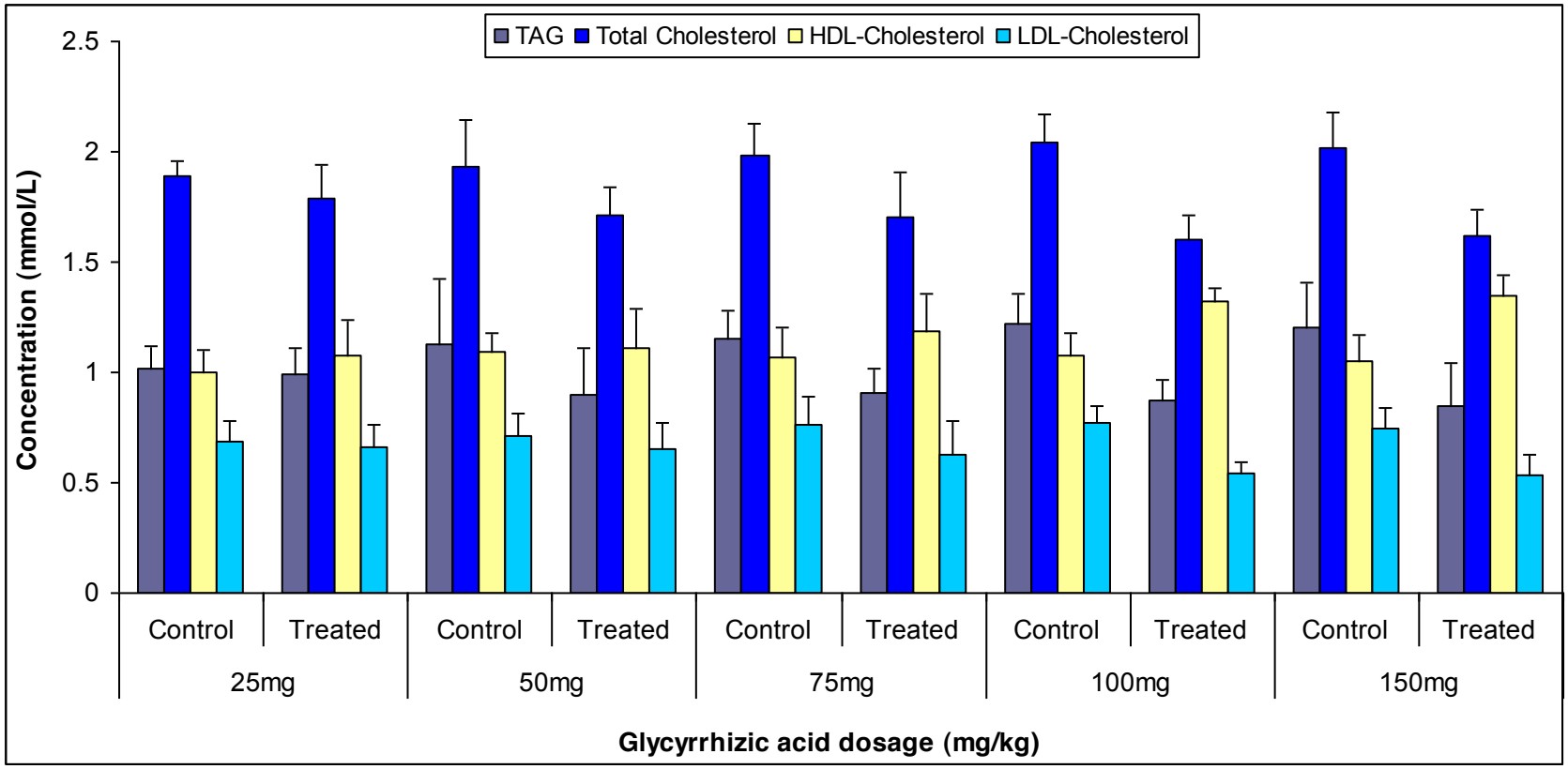

Figure 3.13: Mean serum TAG, total cholesterol, HDL-cholesterol and LDL-cholesterol of control rats and rats administered with various dosages of GA ($P > 0.05$ for all parameters).

Table 3.8: Fold difference in total PPARγ expression in rats administered with various dosages of GA as indicated (in mg/kg).

An increase in total PPARγ expression levels was observed in both tissues following GA-administration (* indicates $P < 0.05$).

Tissue	Fold-difference in total PPARγ expression				
	25 mg/kg	50 mg/kg	75 mg/kg	100 mg/kg	150 mg/kg
ATS	38.7	37.1	29.4	35.8	25.1
ATV	51.8	61.1	61.3	78.2 *	80.0 *
MA	0.85	7.6	11.2	33.3 *	36.9 *
MT	18.7	49.2 *	53.9 *	88.2 *	93.2 *
L	7.3	9.4	13.3	35.5	35.0
K	25.3	30.5	31.2	30.9	33.6

Abbreviations: ATS, subcutaneous adipose tissue; ATV, visceral adipose tissue; MA, abdominal muscle; MT, quadriceps femoris muscle; L, liver; K, kidney.

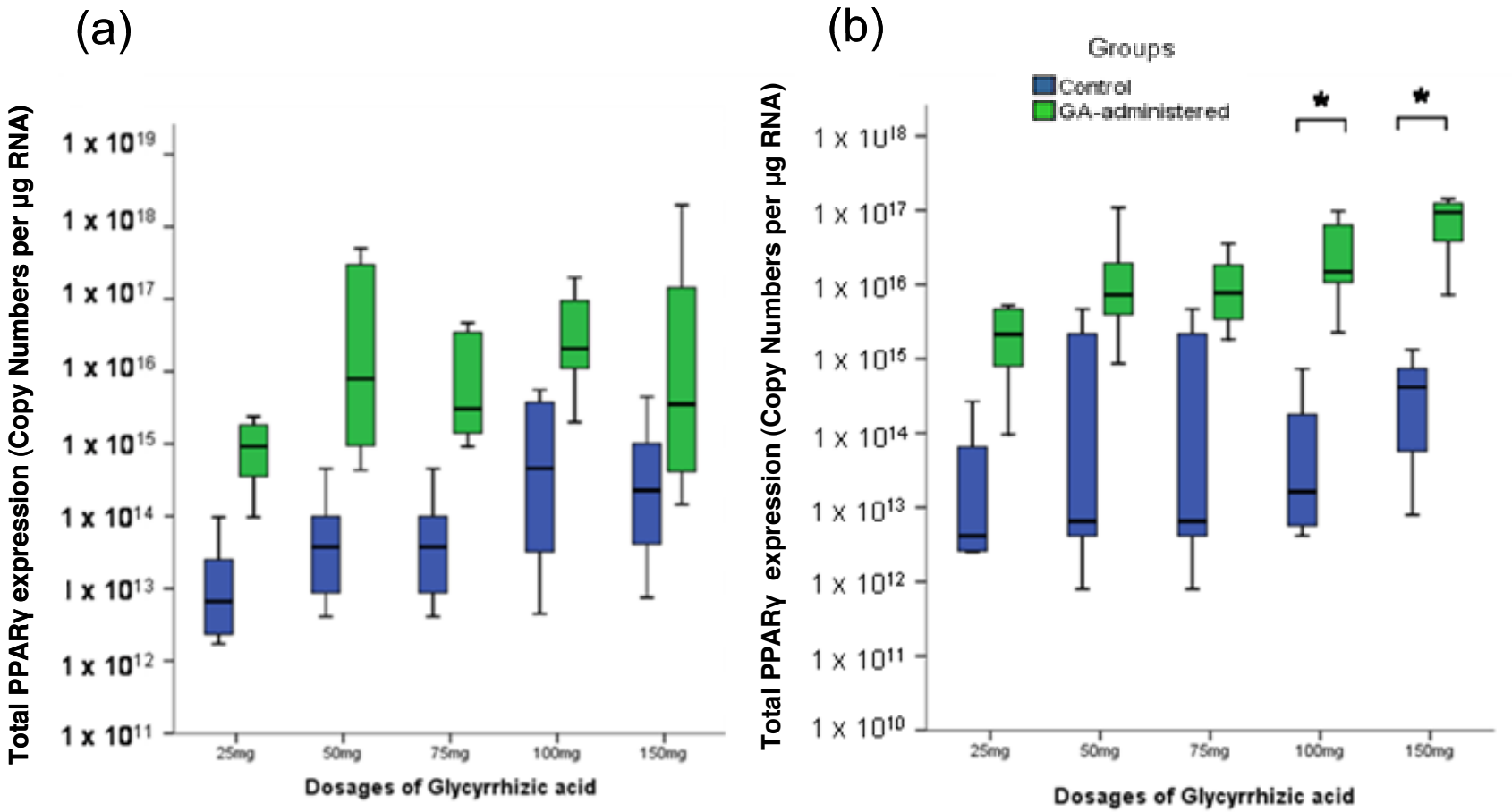

Figures 3.14: Total PPARγ expression levels in (a) subcutaneous and (b) visceral adipose tissues of rats administered with various dosages of glycyrrhizic acid.

An increase in PPARγ expression levels was observed in both tissues following GA-administration (* indicates $P < 0.05$).

3.2.4.2 Abdominal muscle and quadriceps femoris

An increase in total PPARγ expression levels following GA-administration was observed for both the abdominal muscle and quadriceps femoris regardless of the different dosages of GA given (Figure 3.15). In both cases, the increase in PPARγ expression levels was statistically significant ($P < 0.05$) for rats given 100 and 150 mg/kg GA. The quadriceps femoris showed the largest increase in PPARγ expression levels of approximately 90-fold for both dosages of GA whereas the increase in the abdominal muscle was only roughly 35-fold (Table 3.8). However, no significant difference was observed when comparing the PPARγ expression levels of rats given 100 and 150 mg/kg GA.

3.2.4.3 Liver and kidney

As was observed for the abdominal muscle and quadriceps femoris, GA-administration led to increased PPARγ expression levels in both the liver (Figure 3.16) and kidney (Figure 3.17) of rats given various dosages of GA when compared to the control rats. However, in both cases, the increased expression levels were not statistically significant ($P > 0.05$).

3.2.5 **PPARγ1 expression**

3.2.5.1 Subcutaneous and visceral adipose tissues

Similar to total PPARγ expression, PPARγ1 also displayed higher expression levels in the subcutaneous and visceral adipose tissues compared to the control rats (Figures 3.18 a and b; Table 3.9). However, the increase in the expression levels in the subcutaneous adipose tissue with the various dosages was statistically insignificant ($P >$

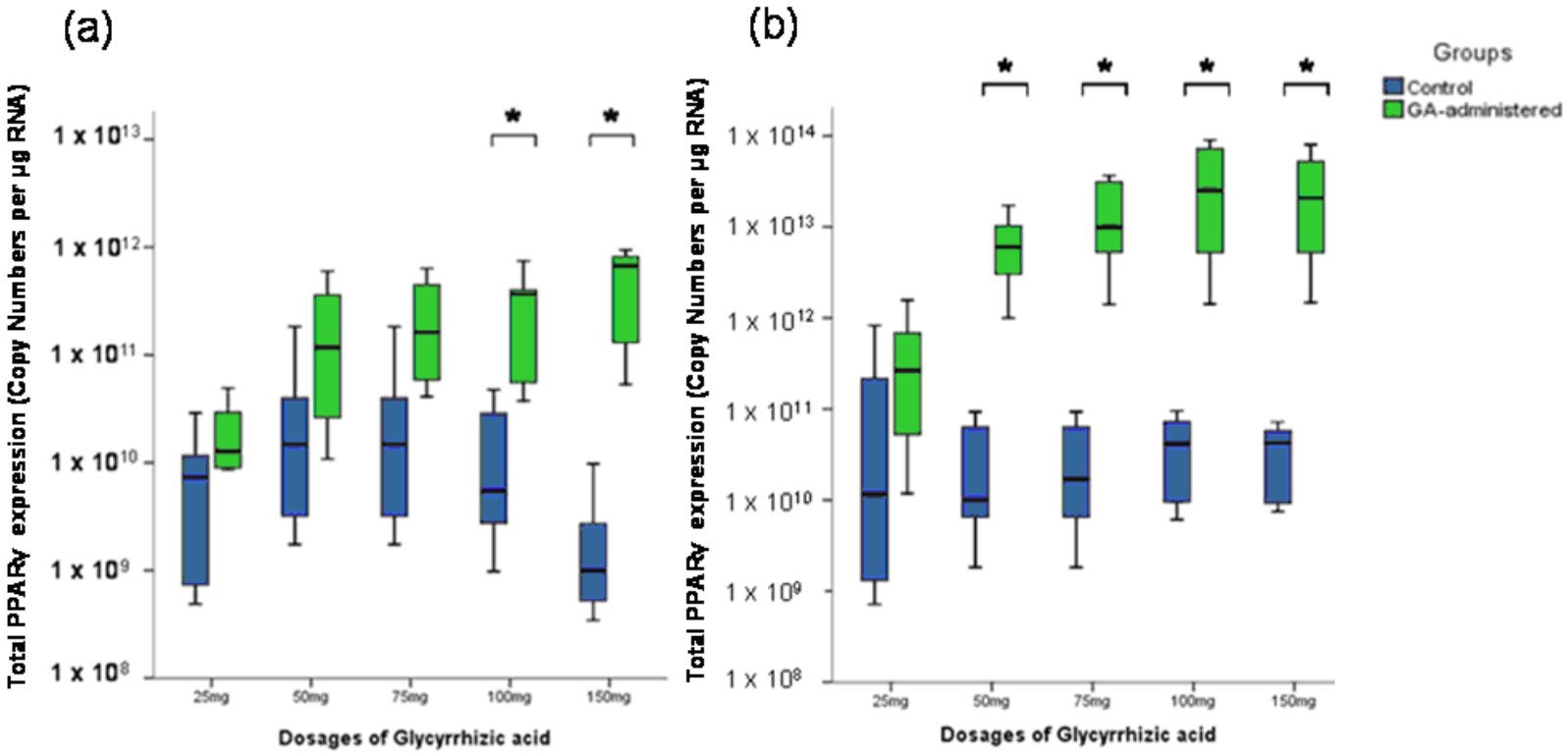

Figures 3.15: Total PPARγ expression levels in (a) abdominal muscle and (b) quadriceps femoris of rats administered with various dosages of glycyrrhizic acid.

GA administration led to increased PPARγ expression levels with rats given 100 and 150 mg/kg GA showing statistically significant increases (* indicates $P < 0.05$).

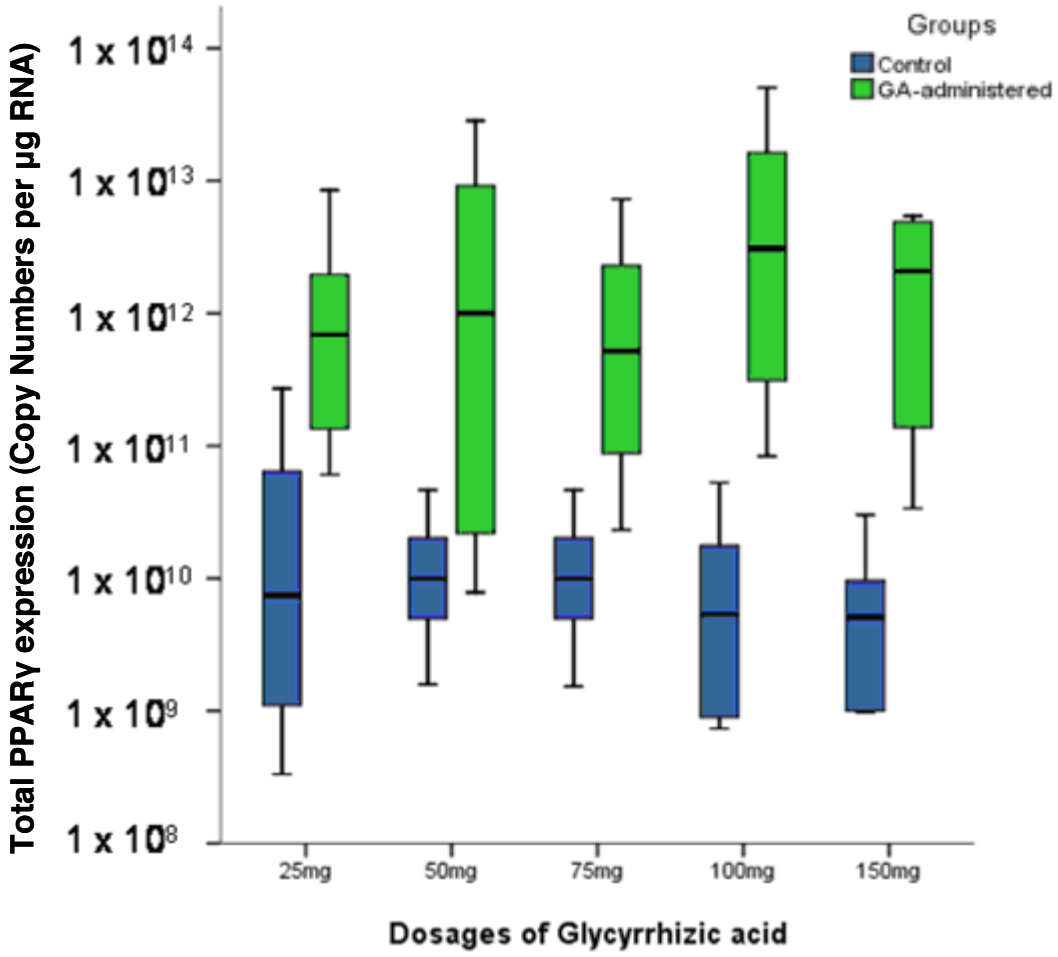

Figure 3.16: Total PPARγ expression levels in liver tissue of rats administered with various dosages of glycyrrhizic acid.

Increased PPARγ expression levels were observed following GA-administration for all dosages albeit $P > 0.05$.

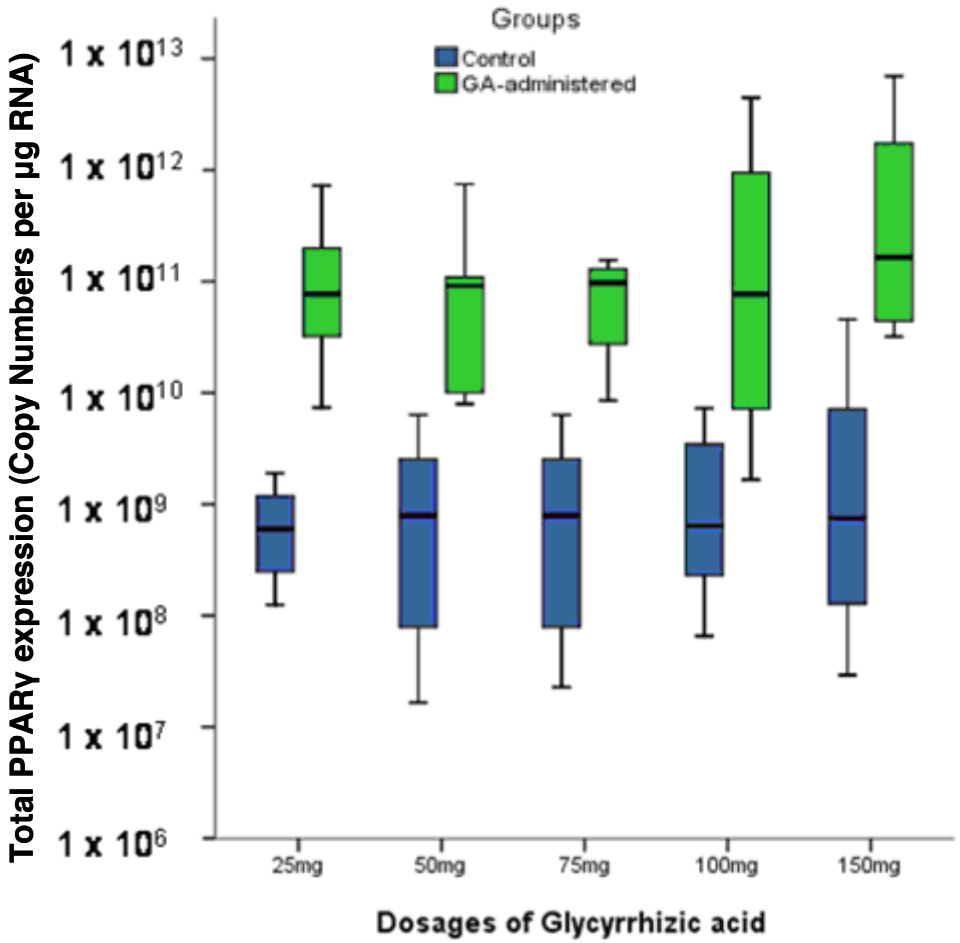

Figure 3.17: Total PPARγ expression levels in kidney of rats administered with various dosages of glycyrrhizic acid.

Note the higher expression levels of PPARγ for all dosages of GA given although $P > 0.05$ for all.

0.05). There was an increase in total PPARγ expression levels in the visceral adipose tissue and significant increase was only noted in the rats administered with 100 (P = 0.05) and 150 mg/kg of GA (P = 0.04) (P < 0.05). No difference between rats given the 100 and 150 mg/kg GA was seen.

3.2.5.2 Abdominal muscle and quadriceps femoris

An increase in PPARγ1 expression levels following GA-administration was observed for both the abdominal muscle and quadriceps femoris regardless of the different dosages of GA given (Figure 3.19a and b). In both cases, the increase in PPARγ expression levels was statistically significant (P < 0.05) for rats given 100 and 150 mg/kg GA. However, no significant difference was observed when comparing the PPARγ expression levels of rats given 100 and 150 mg/kg GA.

3.2.5.3 Liver and kidney

As was observed for the abdominal muscle and quadriceps femoris, GA-administration led to increased PPARγ expression levels in both the liver (Figure 3.20) and kidney (Figure 3.21) of rats given various dosages of GA when compared to the control rats. However, in both cases, the increased expression levels were not statistically significant (P > 0.05).

Table 3.9: Fold difference of PPARγ1 expression in rats administered with various dosages of GA.

An increase in PPARγ1 expression levels was observed in both tissues following GA-administration (* indicates $P < 0.05$).

Tissue	Fold difference in PPARγ1 expression				
	25 mg/kg	50 mg/kg	75 mg/kg	100 mg/kg	150 mg/kg
ATS	9.7	10.7	8.9	17.5	19.8
ATV	49.6	36.5	37.7	52.2 *	57.2 *
MA	1.5	7.3	11.2	26.5 *	34.0 *
MT	29.9	51.1 *	50.5 *	68.5 *	74.1 *
L	6.0	4.6	8.7	16.2	23.4
K	7.8	4.9	13.1	18.3	18.0

Abbreviations: ATS, subcutaneous adipose tissue; ATV, visceral adipose tissue; MA, abdominal muscle; MT, quadriceps femoris muscle; L, liver; K, kidney.

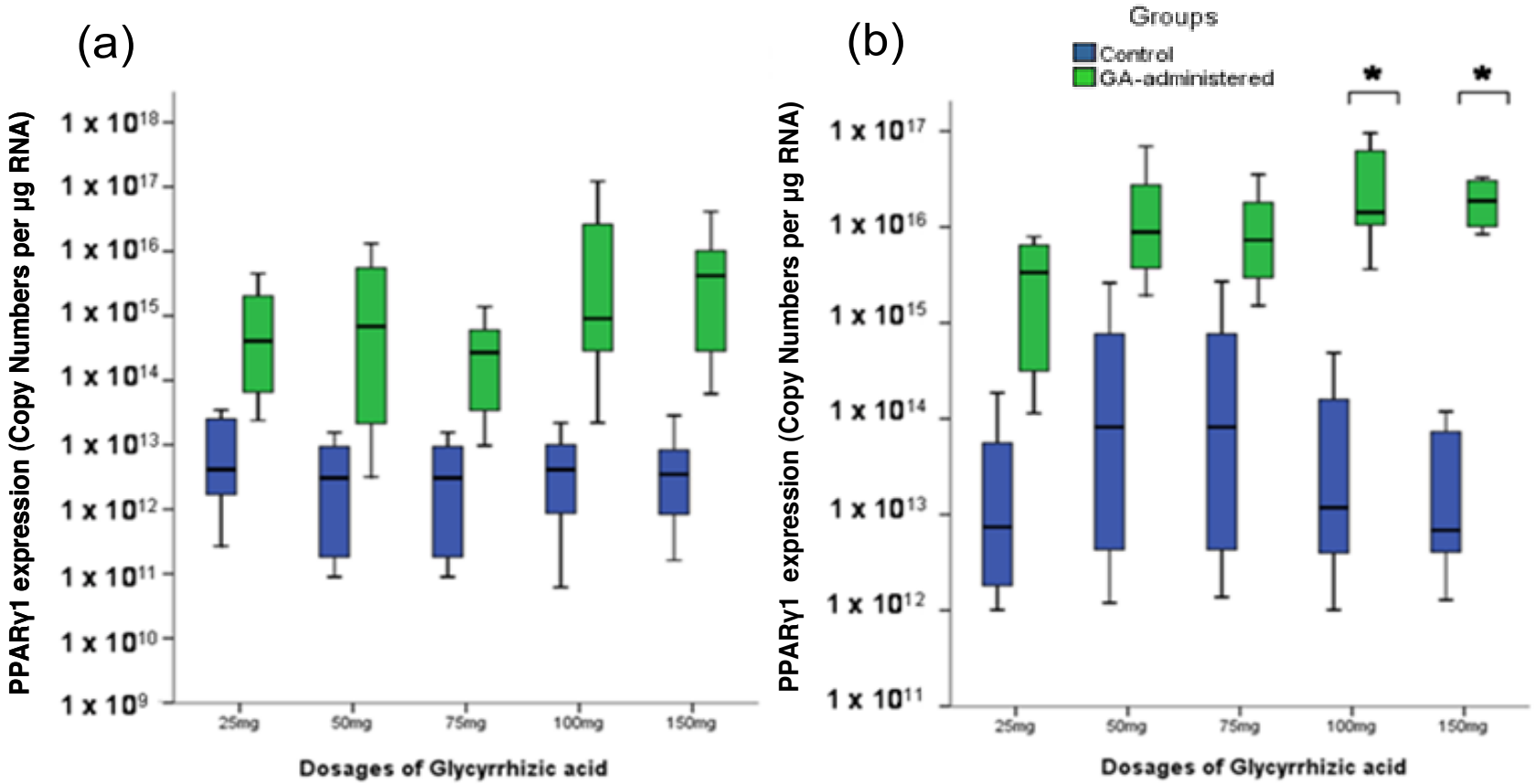

Figures 3.18: PPARγ1 expression levels in (a) subcutaneous and (b) visceral adipose tissues of rats administered with various dosages of glycyrrhizic acid.

An increase in PPARγ expression levels was observed in both tissues following GA-administration (* indicates $P < 0.05$).

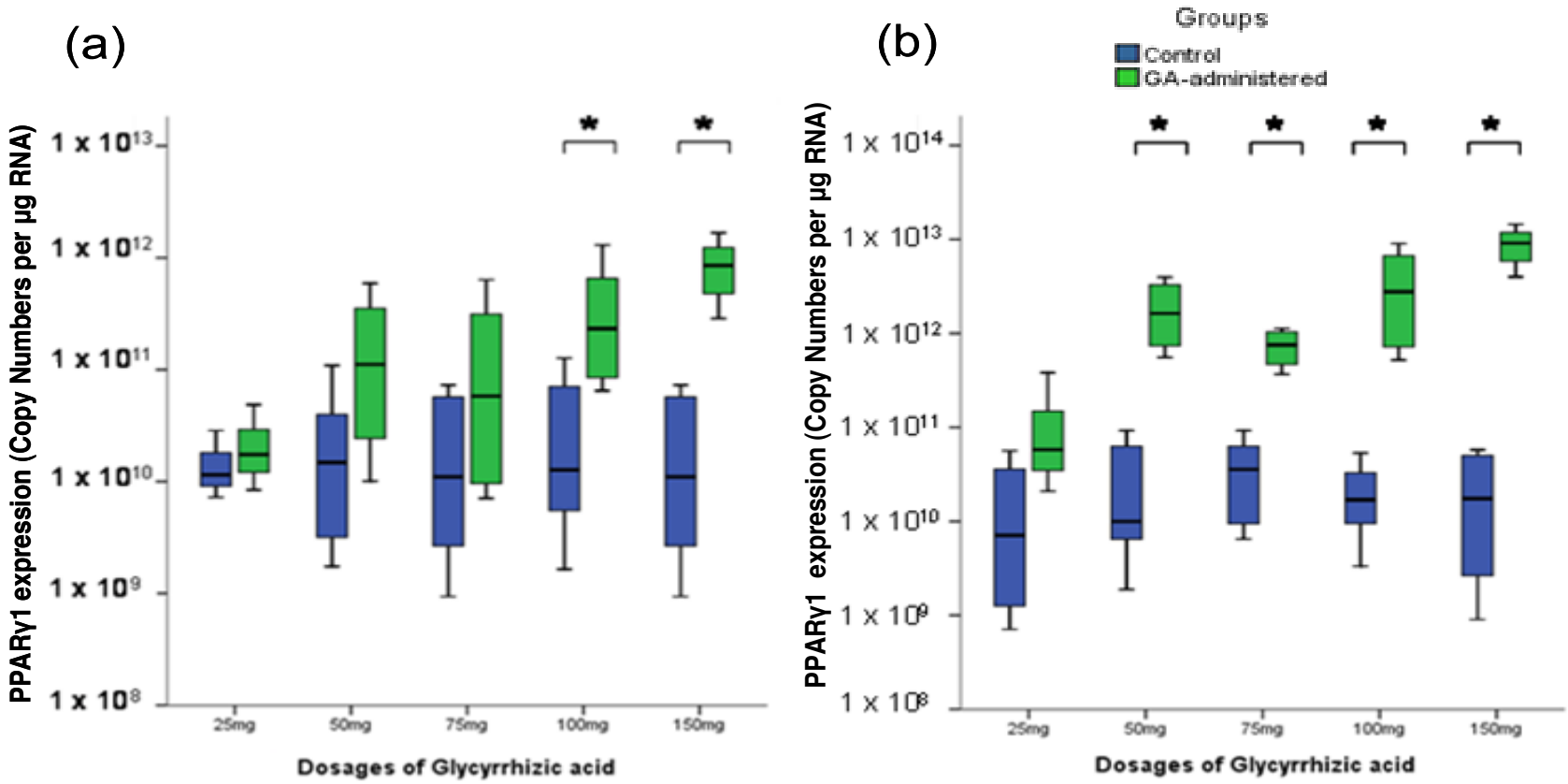

Figures 3.19: PPARγ1 expression levels in (a) abdominal muscle and (b) quadriceps femoris of rats administered with various dosages of glycyrrhizic acid.

GA administration led to increased PPARγ expression levels with rats given 100 and 150 mg/kg GA showing statistically significant increases (* indicates $P < 0.05$).

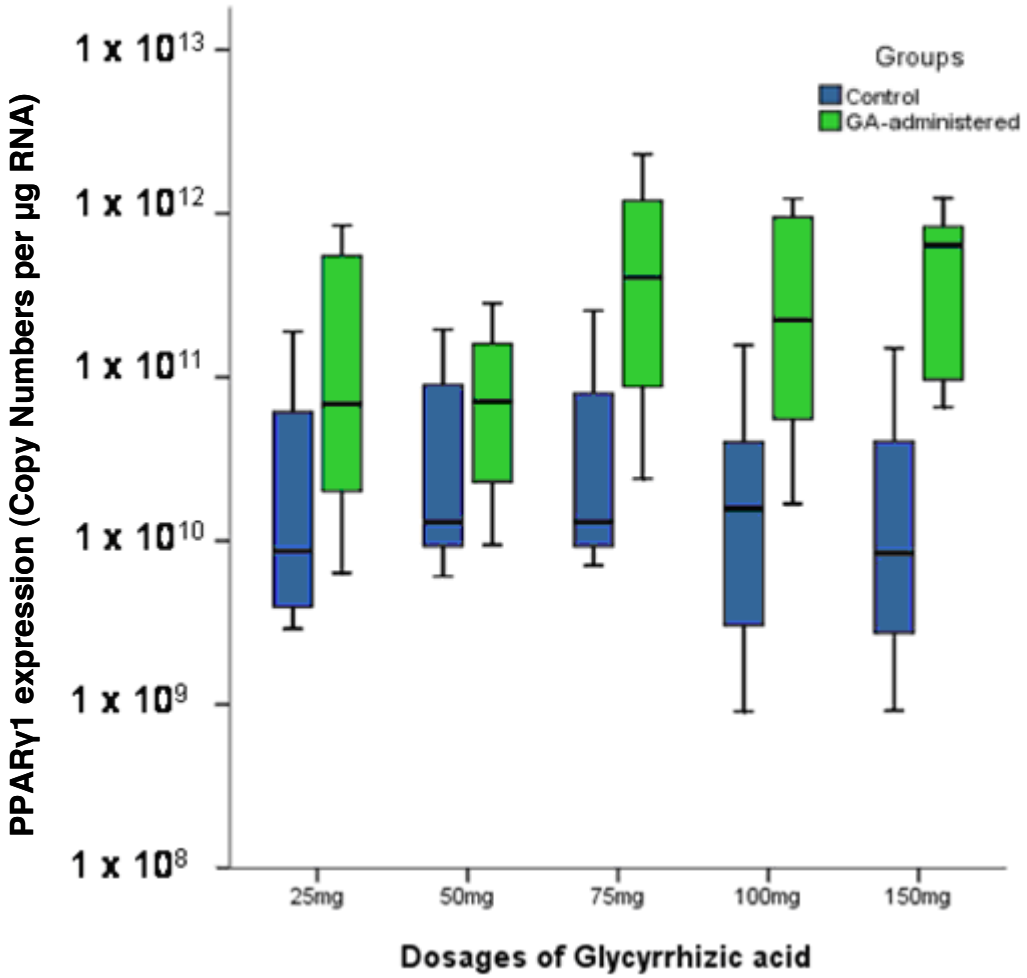

Figure 3.20: PPARγ1 expression levels in the liver tissue of rats administered with various dosages of glycyrrhizic acid.

Increased PPARγ expression levels were observed following GA-administration for all dosages albeit $P > 0.05$.

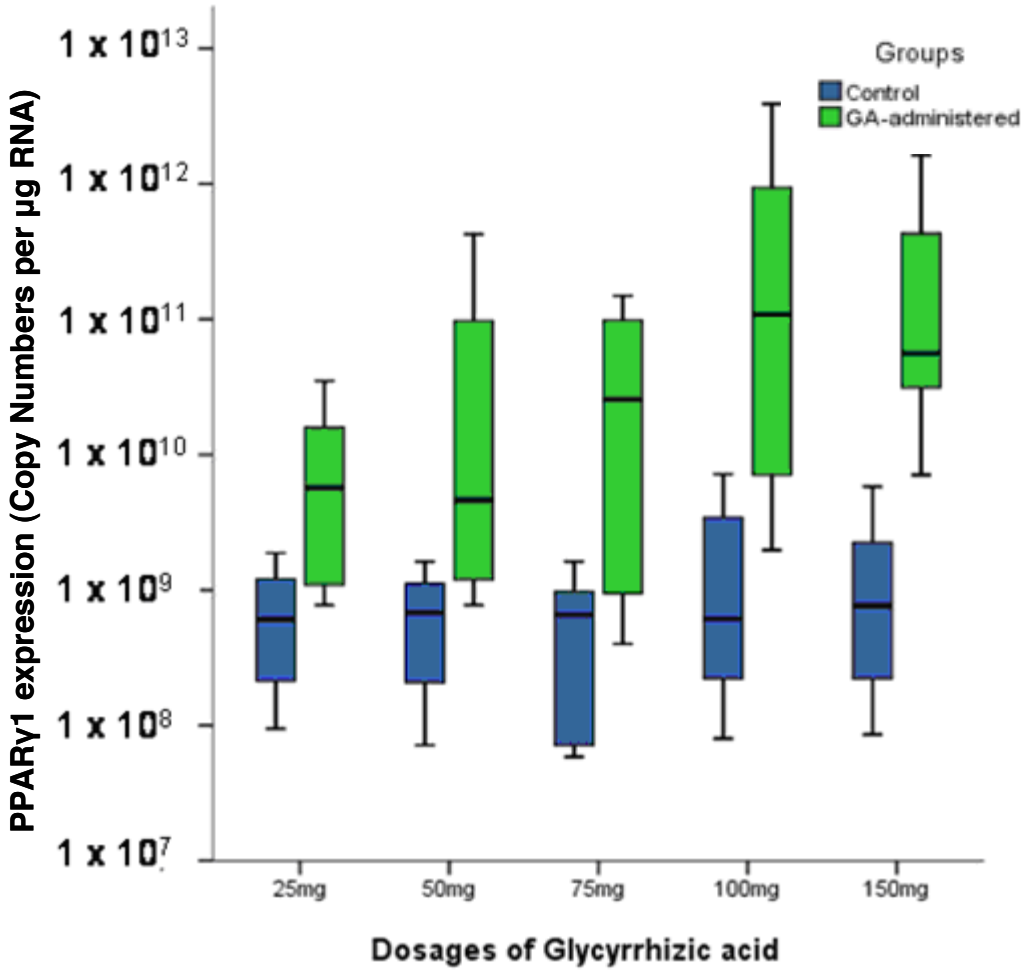

Figure 3.21: PPARγ1 expression levels in the kidney of rats administered with various dosages of glycyrrhizic acid.

Note the higher expression levels of PPARγ for all dosages of GA given although $P > 0.05$ for all.

3.2.6 **PPARγ2 expression**

3.2.6.1 Subcutaneous and visceral adipose tissues

Similar to total PPARγ and PPARγ1 expression, PPARγ2 also displayed higher expression levels in the subcutaneous and visceral adipose tissues compared to the control rats (Figures 3.22 a and b; Table 3.10). However the increase in the subcutaneous adipose tissue with various dosages was statistically insignificant ($P > 0.05$). There was an increase in PPARγ2 expression levels in the visceral adipose tissue and significant increase was only noted in the treated rats with 100 and 150 mg/kg of GA ($P = 0.03$; $P < 0.05$). No difference between rats given the 100 and 150 mg/kg GA was obtained.

3.2.6.2 Abdominal muscle and quadriceps femoris

An increase in PPARγ2 expression levels following GA-administration was observed for both the abdominal muscle and quadriceps femoris regardless of the different dosages of GA given (Figure 3.23a and b). In both cases, the increase in PPARγ expression levels was statistically significant ($P < 0.05$) for rats given 100 and 150 mg/kg GA. However, no significant difference was observed when comparing the PPARγ expression levels of rats given 100 and 150 mg/kg GA.

Table 3.10: Fold difference in PPARγ2 expression in rats administered with various dosages of GA (as indicated in mg/kg).

An increase in PPARγ2 expression levels was observed in all tissues following GA-administration (* indicates $P < 0.05$).

Tissue	Fold difference in PPARγ2 expression				
	25 mg/kg	50 mg/kg	75 mg/kg	100 mg/kg	150 mg/kg
ATS	1.23	7.8	7.1	8.9	9.7
ATV	23.3	80.1	83.6	111.8 *	130.5 *
MA	1.86	9.6	12.6	27.2 *	36.8 *
MT	16.9	38.7 *	35.2 *	61.5 *	72.4 *
L	8.5	8.4	9.8	9.7	10.9
K	8.9	9.7	10.9	13.6	13.8

Abbreviations: ATS, subcutaneous adipose tissue; ATV, visceral adipose tissue; MA, abdominal muscle; MT, quadriceps femoris muscle; L, liver; K, kidney.

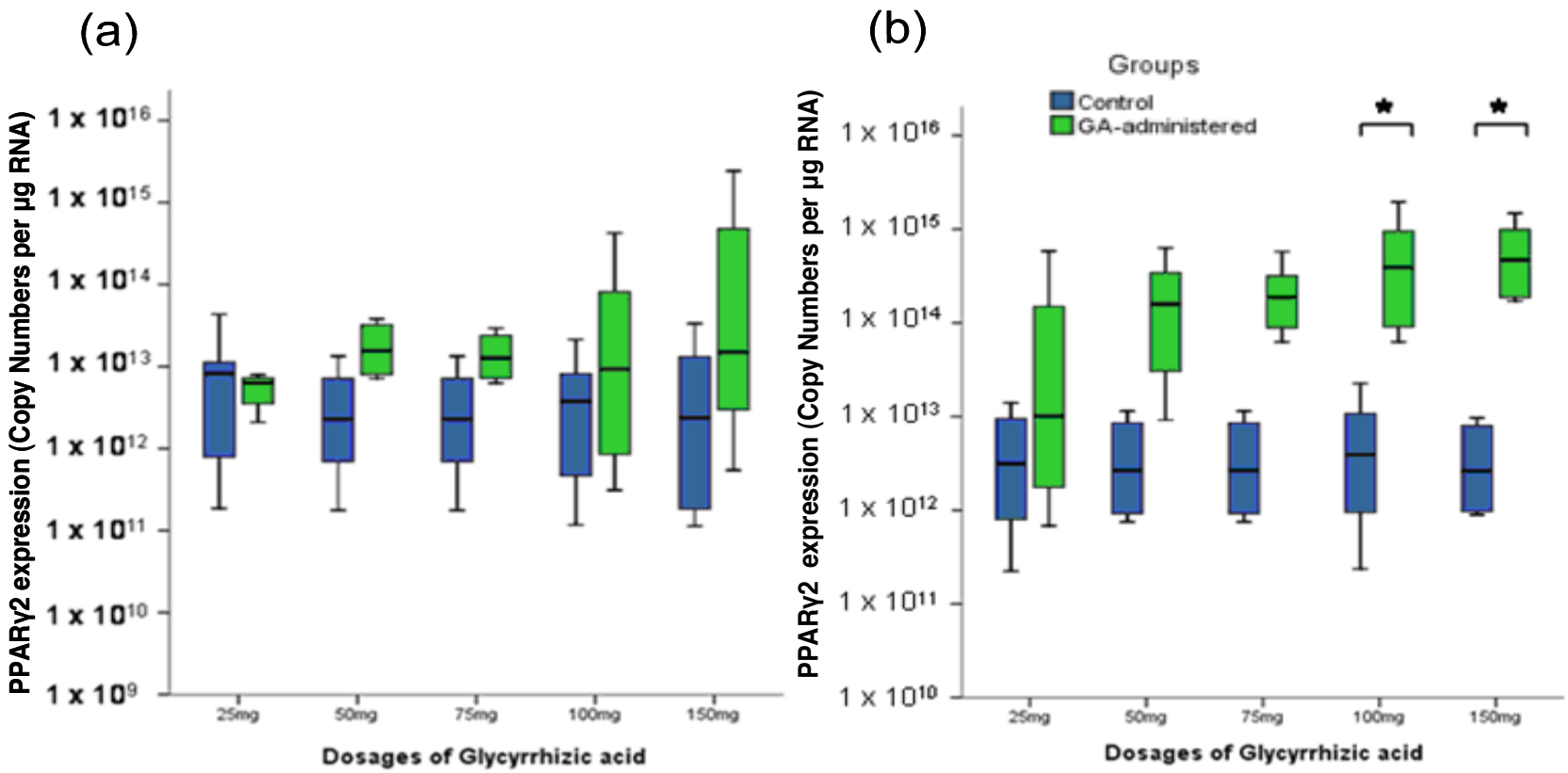

Figures 3.22: PPARγ2 expression levels in (a) subcutaneous and (b) visceral adipose tissues of rats administered with various dosages of glycyrrhizic acid.

An increase in PPARγ expression levels was observed in both tissues following GA-administration (* indicates $P < 0.05$).

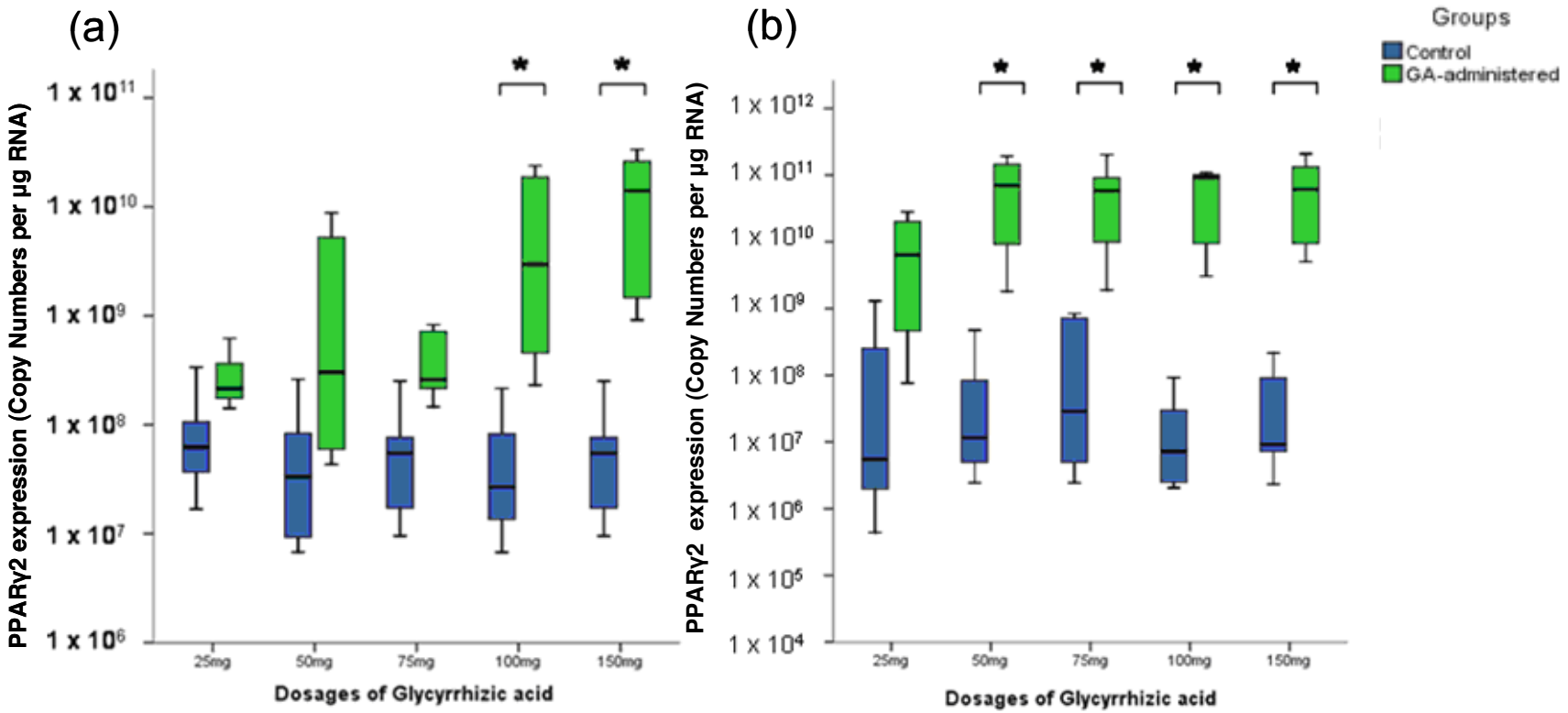

Figures 3.23: PPARγ2 expression levels in (a) abdominal muscle and (b) quadriceps femoris of rats administered with various dosages of glycyrrhizic acid.

GA administration led to increased PPARγ expression levels with rats given 100 and 150 mg/kg GA showing statistically significant increases (* indicates $P < 0.05$).

3.2.6.3 Liver and kidney

As observed for the abdominal muscle and quadriceps femoris, GA-administration led to increased PPARγ expression levels in both the liver (Figure 3.24) and kidney (Figure 3.25) of rats given various dosages of GA when compared to the control rats. However, in both cases, the increased expression levels were not statistically significant ($P > 0.05$).

3.2.7 Relative LPL expression in the various studied tissues

Regardless of the dosage of GA administered, the LPL expression levels in the subcutaneous and visceral adipose tissues were higher in the GA-administered rats compared to the control rats. However, the increase in the expression levels in the subcutaneous adipose tissue with the various dosages was statistically insignificant ($P > 0.05$). Although there was an increase in LPL expression levels in the visceral adipose tissue, significant increase was only noted in the rats administered with 100 ($P = 0.05$) and 150 mg/kg ($P = 0.05$) of GA ($P \leq 0.05$). Although the percentage increase of LPL expression in rats given 150 mg/kg of GA was higher than that of rats administered with 100 mg/kg GA, the comparison between both the dosages displayed no significant difference.

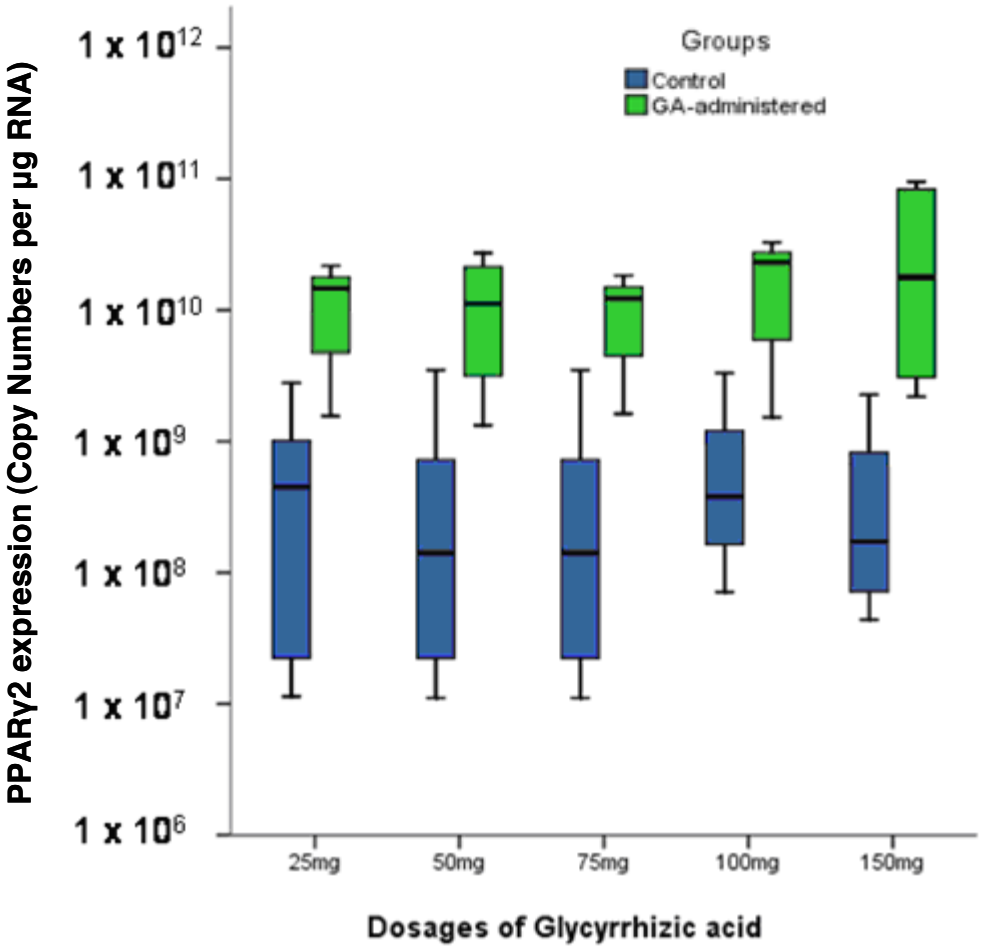

Figure 3.24: PPARγ2 expression levels in the liver tissue of rats administered with various dosages of glycyrrhizic acid.

Increased PPARγ expression levels were observed following GA-administration for all dosages albeit $P > 0.05$.

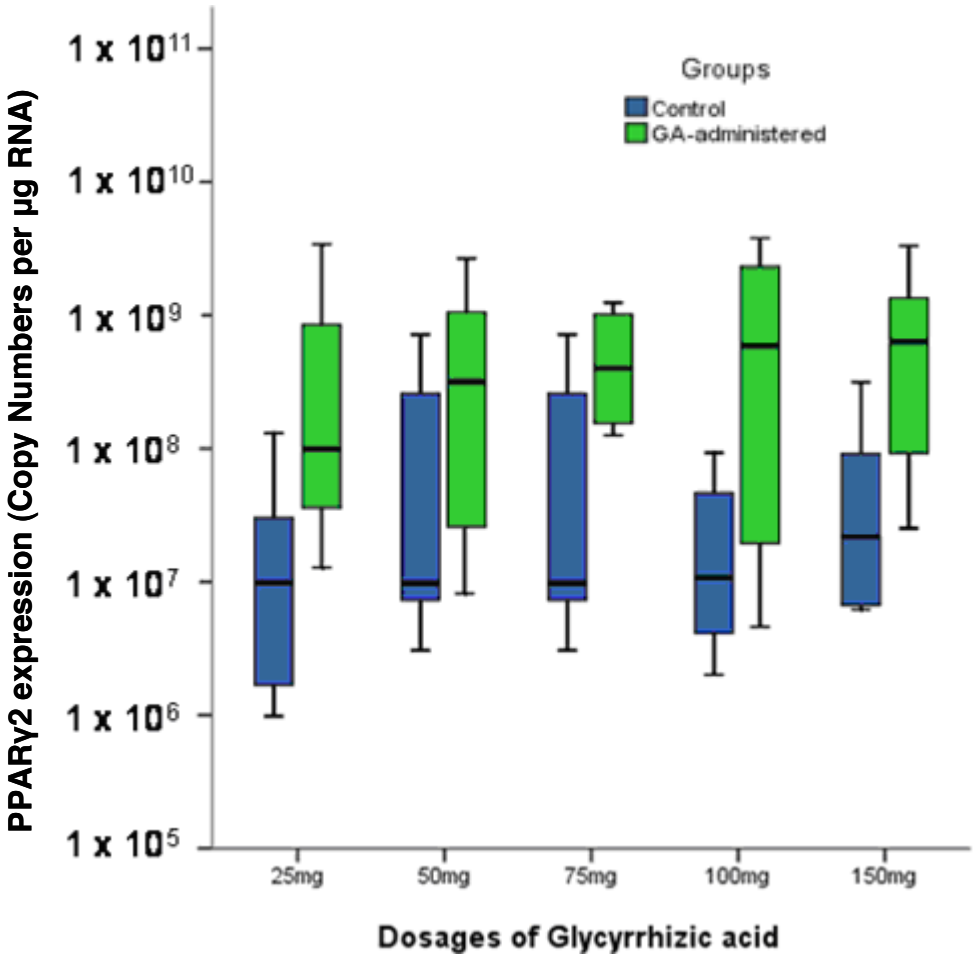

Figure 3.25: PPARγ2 expression levels in kidney of rats administered with various dosages of glycyrrhizic acid.

Note the higher expression levels of PPARγ for all dosages for all dosages of GA given although $P > 0.05$ for all.

An increase in LPL expression levels following GA-administration was observed for both the abdominal muscle and quadriceps femoris regardless of the different dosages of GA given. In both cases, the increase in LPL expression levels was statistically significant ($P < 0.05$). However, no significant difference was observed when comparing the LPL expression levels n the abdominal muscle and quadriceps femoris of rats given 100 and 150 mg/kg GA.

Similarly, treatment with increasing dosages of GA led to increasing levels of LPL expression in both the liver and kidneys of rats, with 47% and 37% higher levels of LPL in the liver and kidneys respectively with administration of 150 mg/kg GA. Nevertheless, the increased LPL expression level in both the liver and kidneys were not statistically significant ($P > 0.05$) (Table 3.11 and Figure 3.26).

3.2.8 **11β-HSD1 and 11β-**HSD2 activities

3.2.8.1 **11β-**HSD1 activities

Figures 3.27 – 3.29 showed the 11β-HSD1 activities in the subcutaneous and visceral adipose tissues, abdominal muscle, quadriceps fermoris, liver and kidney of rats given different dosages of glycyrrhizic acid (25, 50, 75, 100 and 150 mg/kg). In all the tissues examined, administration of GA led to reduction in 11β-HSD1 activities. A much larger decrease in 11β-HSD1 activities was noted in the visceral adipose tissues (ranging from 16.3% – 39.14%) when compared to the subcutaneous adipose tissues (decreased by 6.28% – 14.4%) (Figure 3.27). The reduction in 11β-HSD1 activities was only statistically significant in the visceral adipose tissues of rats given 100 and 150 mg/kg GA.

Table 3.11: Percentage increase of LPL expression in the various tissues of rats administered with various dosages of GA.

Subjects	25 mg/kg		50 mg/kg		75 mg/kg		100 mg/kg		150 mg/kg	
	% increase	*P* value	% increase	*P* value	% increase	*P* value	% increase	*P* value	% increase	*P* value
Subcutaneous adipose tissue	8	0.18	14	0.16	12	0.14	27	0.12	49	0.09
Visceral adipose tissue	9	0.15	19	0.11	11	0.12	53	0.05	63	0.05
Abdominal muscle	31	0.11	34	0.10	44	0.05	51	0.05	67	0.04
Quadriceps femoris	24	0.12	35	0.09	46	0.05	62	0.04	71	0.03
Liver	5	0.16	12	0.14	29	0.12	36	0.12	47	0.09
Kidney	7	0.17	11	0.14	13	0.14	22	0.11	37	0.10

Only a P value of ≤ 0.05 is considered statistically significant and marked with an asterisk (*)

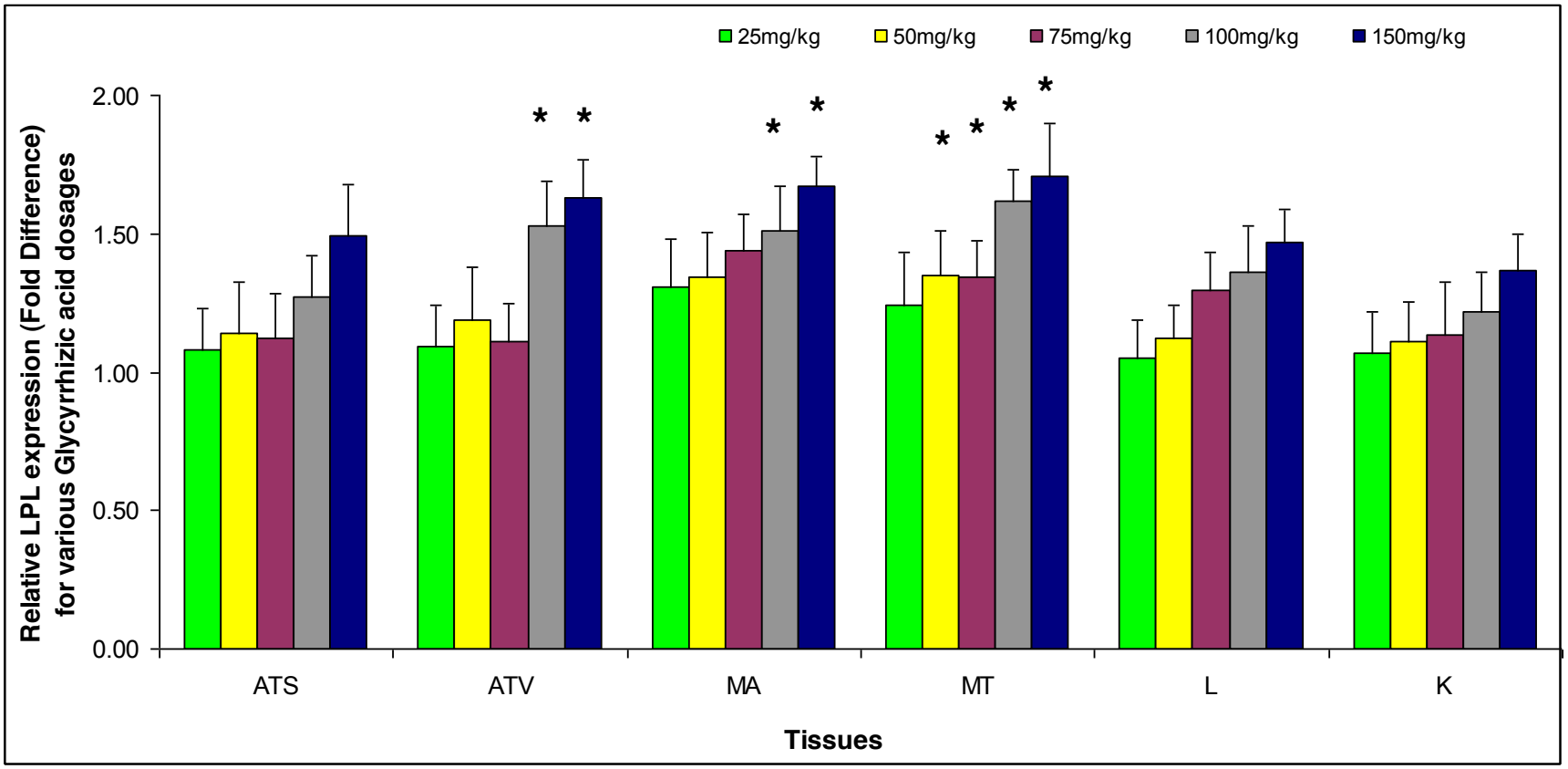

Figure 3.26: Relative expression (Fold difference) for LPL in various tissues of GA-administered rats with various dosages with β-actin as reference, GA-administered group as target and control group as calibrator.

LPL expression increased with increasing dosage of GA administered in all tissues examined (* indicates $P < 0.05$). Abbreviations: ATS, subcutaneous adipose tissue; ATV, visceral adipose tissue; MA, abdominal muscle; MT, quadriceps femoris muscle; L, liver; K, kidney.

Both the abdominal muscle and quadriceps femoris showed similar trends of decreasing 11β-HSD1 activities with increasing dosages of GA administered. The amount of decrease in 11β-HSD1 activities in both tissues were roughly similar with the activity in the abdominal muscle decreasing from 13.06% – 38.59% whereas the activity in quadriceps femoris decreased by 14.6% – 31.5% (Figure 3.28). The decrease in 11β-HSD1 activities was statistically significant in the abdominal muscle of rats given 100 and 150 mg/kg GA whereas for quadriceps femoris, the reduction in 11β-HSD1 activities was significant for all dosages of GA except 25 mg/kg. Likewise, 11β-HSD1 activities were decreased in the liver and kidneys of rats administered with GA, with decreased activities that ranged from 21.4% – 36.6% in the liver and 16.14% – 21.33% in the kidneys (Figure 3.29). The decrease in 11β-HSD1 activities in the kidneys were however, not statistically significant whereas in the liver, the reduction in 11β-HSD1 activities was significant for all dosages of GA except 25 mg/kg.

3.2.8.2 **11β**-HSD2 activities

As in the case of 11β-HSD1 activities, 11β-HSD2 activities were found to be reduced in all the tissues examined (i.e., subcutaneous and visceral adipose tissues, abdominal muscle, quadriceps femoris, liver and kidney) for rats that had been given different dosages of GA (Figures 3.30 – 3.32).

(a) Subcutaneous adipose tissue

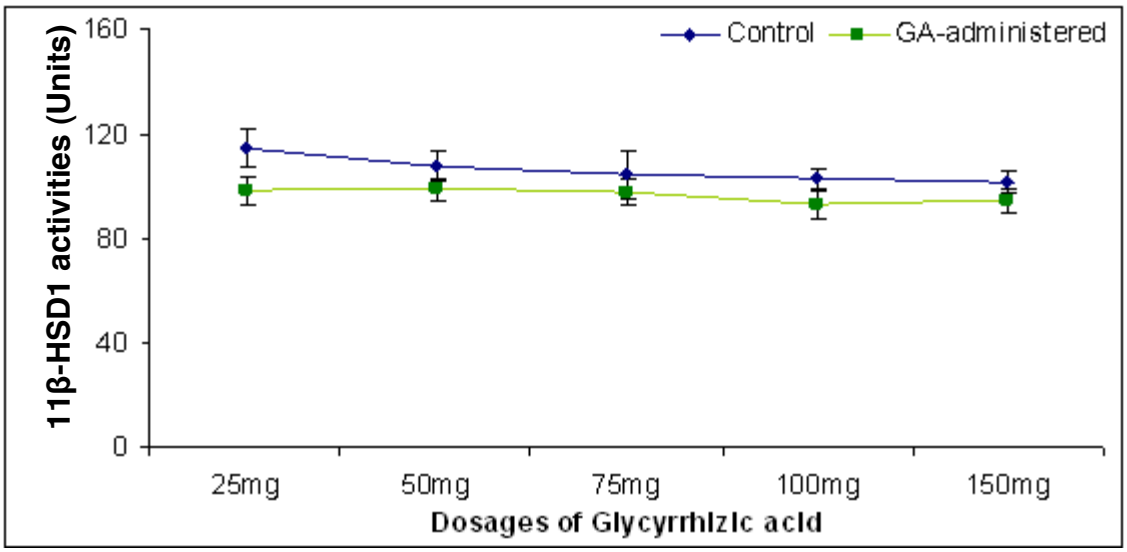

(b) Visceral adipose tissue

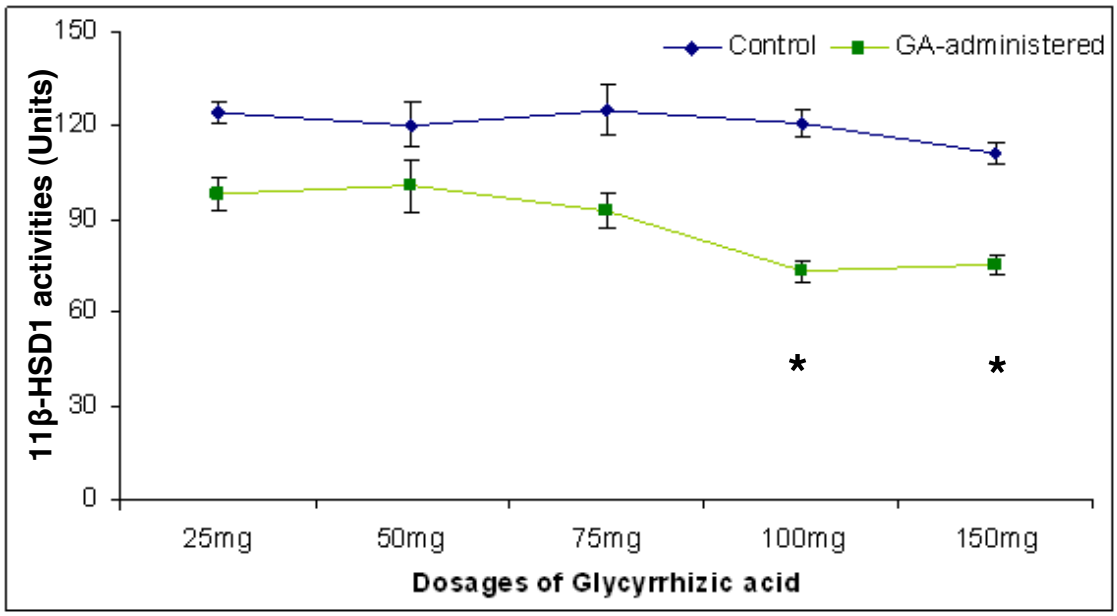

Figures 3.27: 11β-HSD1 activities in (a) subcutaneous and (b) visceral adipose tissues of rats administered with various dosages of glycyrrhizic acid.

In all cases, reduction in 11β-HSD1 activities were observed in rats given GA (* indicates $P < 0.05$).

(a) Abdominal muscle

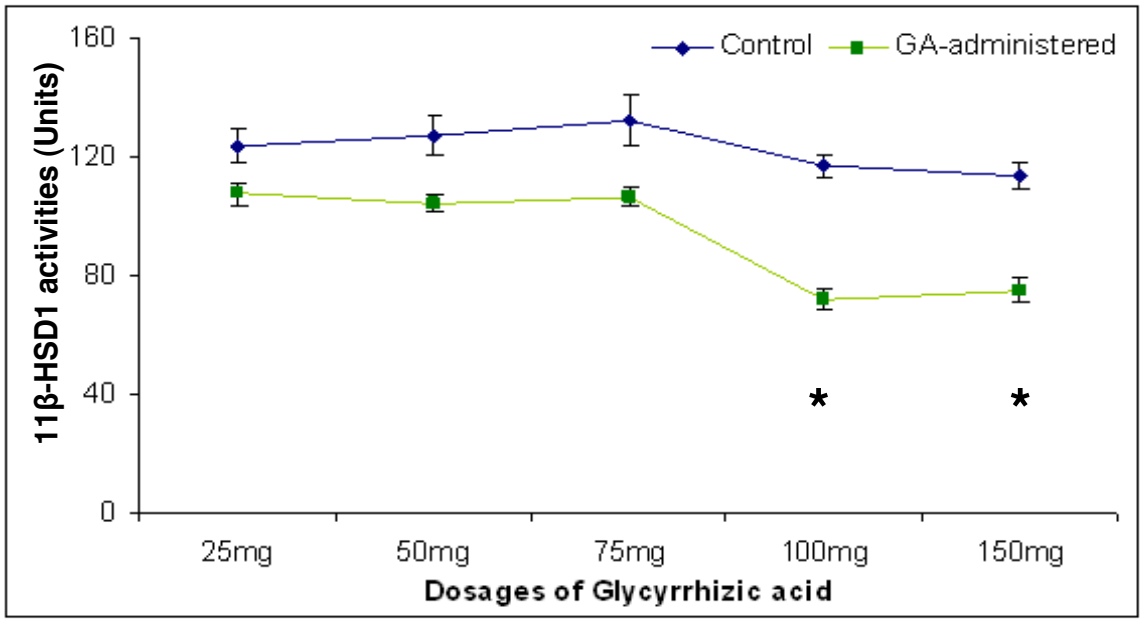

(b) Quadriceps femoris

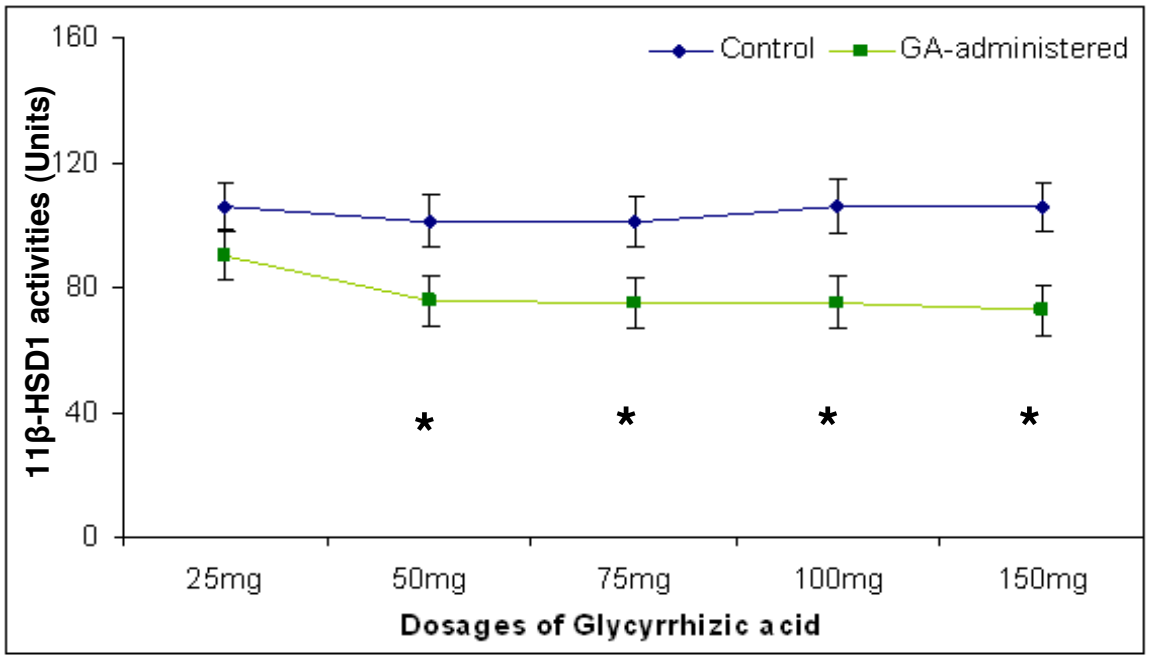

Figures 3.28: 11β-HSD1 activities in (a) abdominal muscle and (b) quadriceps femoris of rats administered with various dosages of glycyrrhizic acid (* indicate $P < 0.05$).

(a) Liver

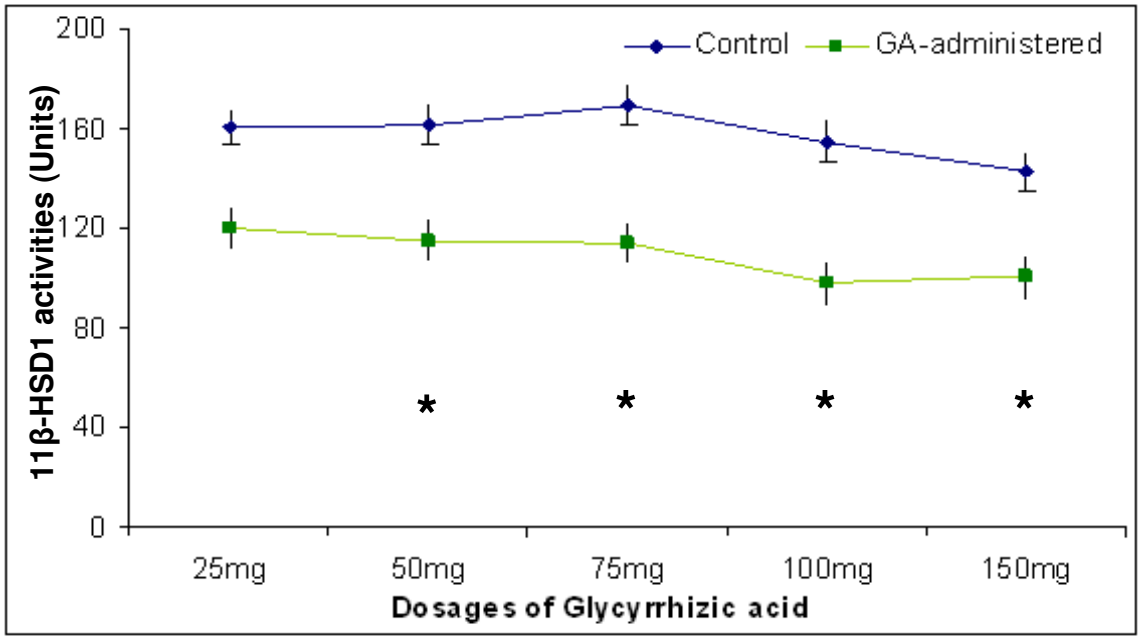

(b) Kidney

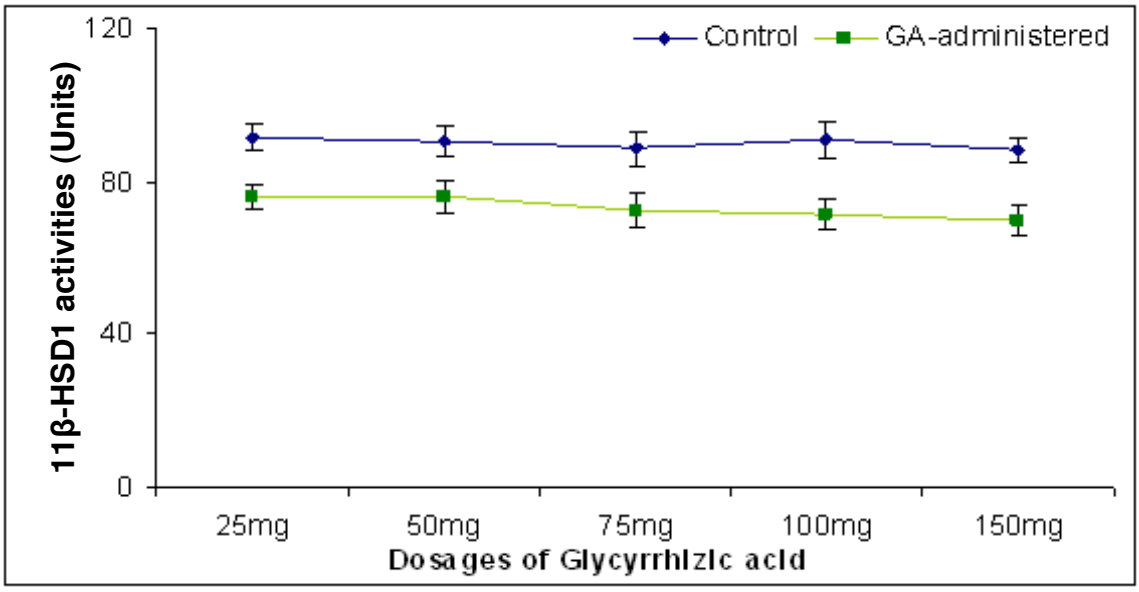

Figures 3.29: 11β-HSD1 activities in the (a) liver and (b) kidney of rats administered with various dosages of glycyrrhizic acid.

Reduction in 11β-HSD1 activites were noted in both tissues for all dosages of GA (* indicate $P < 0.05$).

Unlike for 11β-HSD1, the decrease in 11β-HSD2 activities in the visceral adipose tissues were only by a slightly larger amount (9.6% – 24.19%) when compared to the reduction in subcutaneous adipose tissues (4.8% – 18.71%) (Figure 3.30). The reduction in 11β-HSD2 activities was statistically significant in the visceral adipose tissues of rats given 100 and 150 mg/kg GA while for the subcutaneous adipose tissues, the decrease in activities was significant for rats administered with 75, 100 and 150 mg/kg GA.

Similar decreases in 11β-HSD2 activities in the abdominal muscle and quadriceps femoris following GA-administration were observed (Figure 3.31), as was previously noted for 11β-HSD1 activities. Likewise, 11β-HSD2 activities in the liver decreased by a larger amount (26.8% – 38.15%) when compared to the kidneys (6.2% – 14.2%) (Figure 3.32), mirroring the results obtained for 11β-HSD1 activities.

(a) Subcutaneous adipose tissue

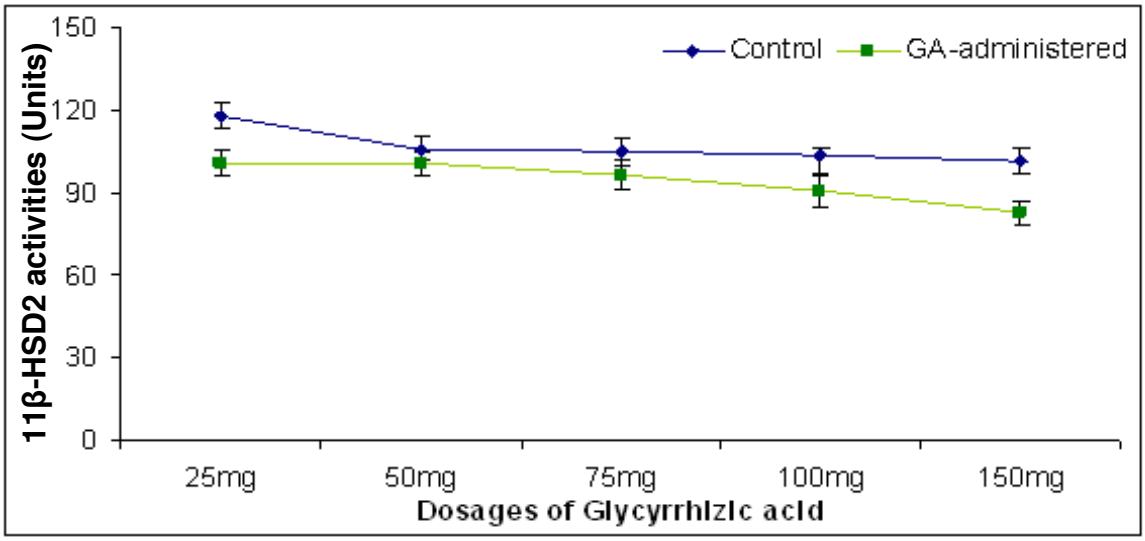

(b) Visceral adipose tissue

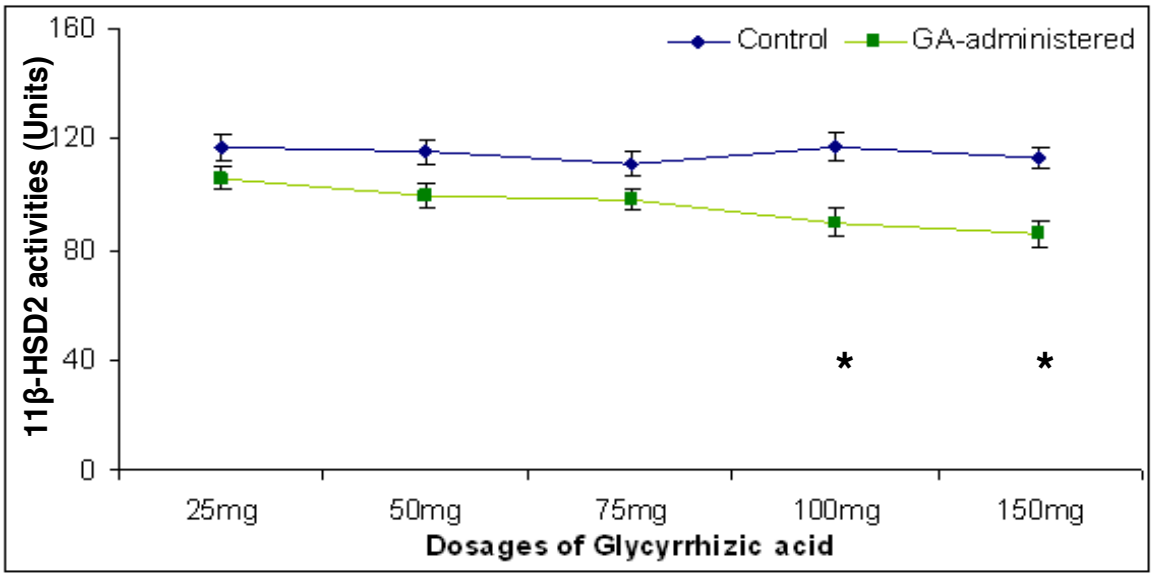

Figures 3.30: 11β-HSD2 activities in (a) subcutaneous and (b) visceral adipose tissues of rats administered with various dosages of glycyrrhizic acid.

In both types of adipose tissues, GA administration led to decreased 11β-HSD2 activities (* indicate $P < 0.05$).

(a) Abdominal muscle

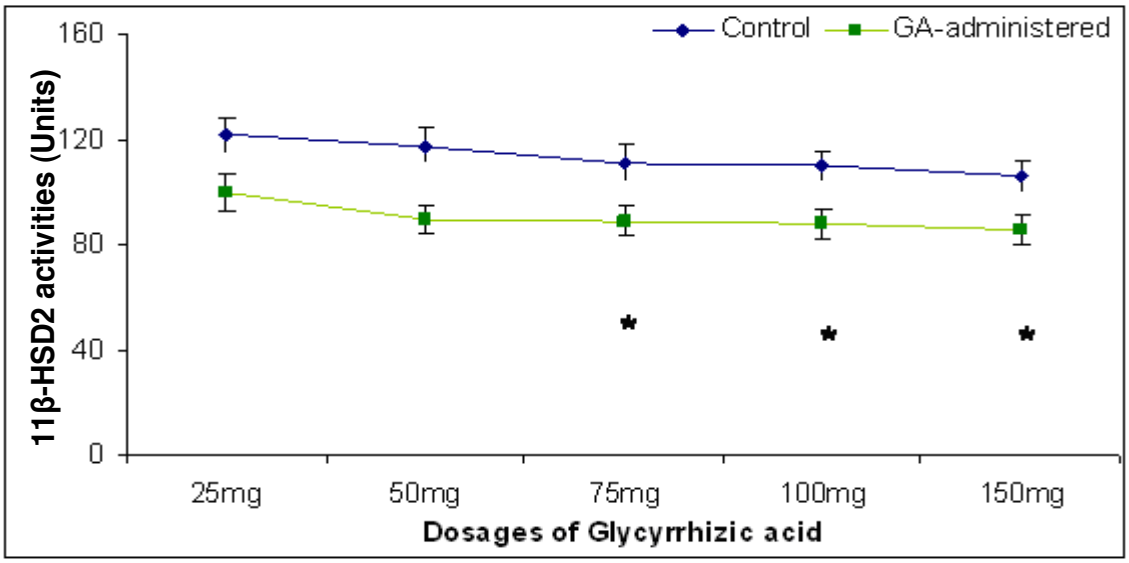

(b) Quadriceps femoris

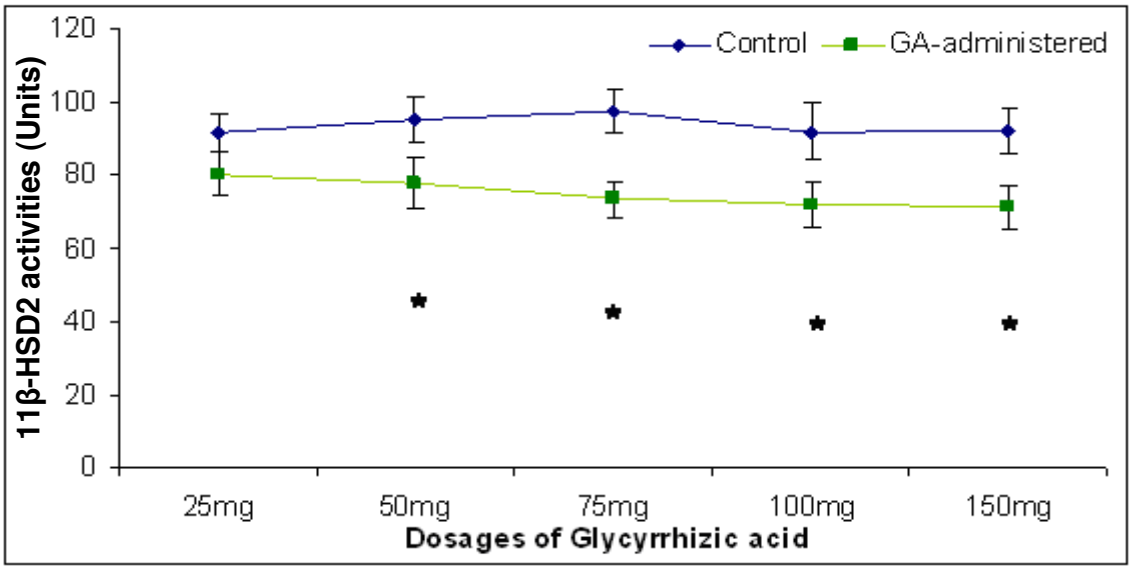

Figures 3.31: 11β-HSD2 activities in (a) abdominal muscle and (b) quadriceps femoris of rats administered with various dosages of glycyrrhizic acid.

Decreased 11β-HSD2 activities were observed for both tissues following GA administration (* indicate $P < 0.05$).

(a) Liver

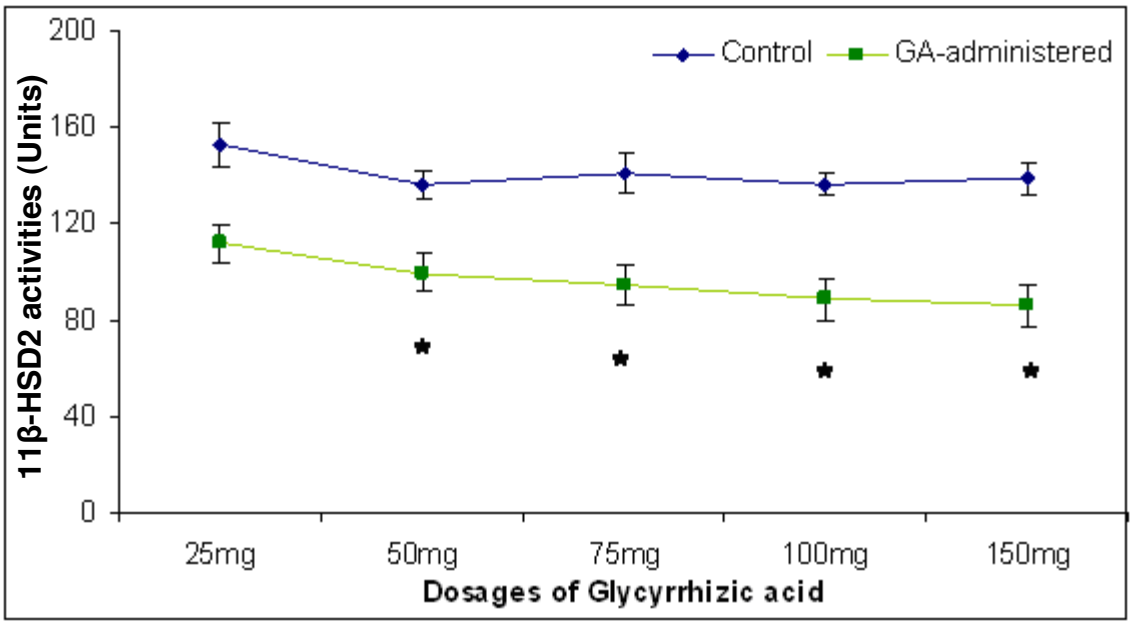

(b) Kidney

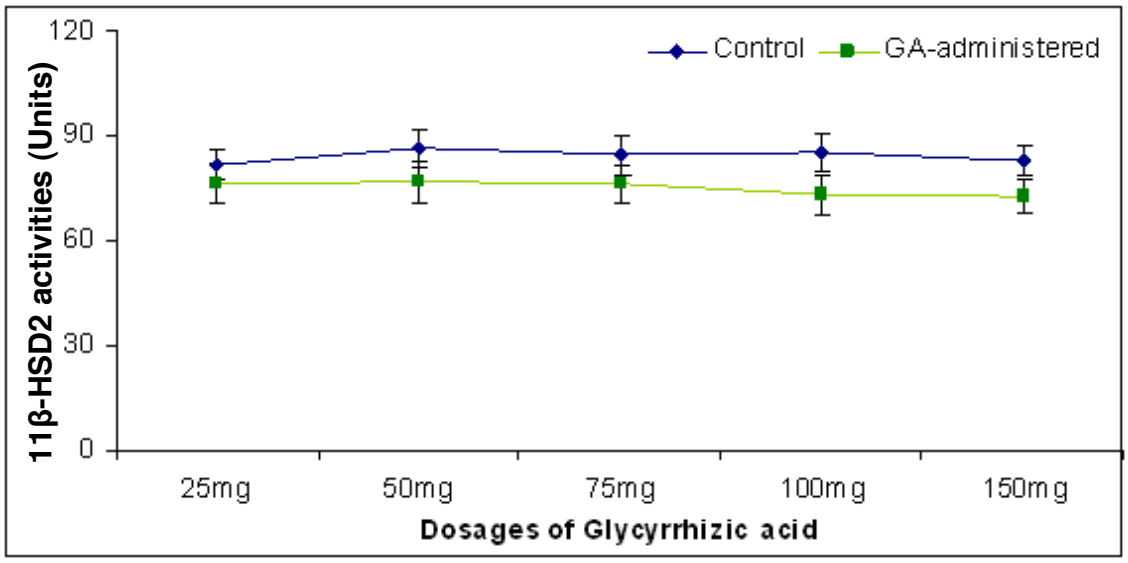

Figures 3.32: 11β-HSD2 activities in the (a) liver and (b) kidney of rats administered with various dosages of glycyrrhizic acid.

In both tissues, reduction in 11β-HSD2 activities was seen (* indicate $P < 0.05$).

Chapter 3

Results

(Part C)

3.3 Different treatment periods of orally-administered glycyrrhizic acid at 100 mg/kg

3.3.1 Treatment periods with dosage of 100 mg/kg of GA

The rats were given GA orally at 100 mg/kg for 12, 24 and 48 hours as well as one week duration. As there was no significant difference seen in rats given either 100 or 150 mg/kg of GA (see section 3.2), all subsequent work was conducted using 100 mg/kg GA.

3.3.2 Blood glucose, serum insulin and HOMA-IR

Treatment with GA led to significant decrease in the blood glucose levels of rats after 24 ($P = 0.02$), 48 hours ($P = 0.02$) and one week ($P = 0.01$) ($P < 0.05$). Blood glucose levels decreased by 23.7% within 12 hours of GA treatment and decreased further by 66.3% 48 hours after treatment, remaining at around 65% lower than the blood glucose levels of the control rats even after one week of treatment (Figure 3.33). Serum insulin levels were also lower in rats administered with GA. Median insulin levels decreased by 20.0% after 12 hours of GA treatment and was further reduced by 37.0% after 48 hours of treatment; nevertheless, the degree of decrease in serum insulin levels was not statistically significant (i.e., $P > 0.05$) (Figure 3.34). The HOMA-IR values were significantly reduced by 54.3% after 24 hours of GA treatment and remained at around 64% lower than the control rats after one week of GA administration (Figure 3.35).

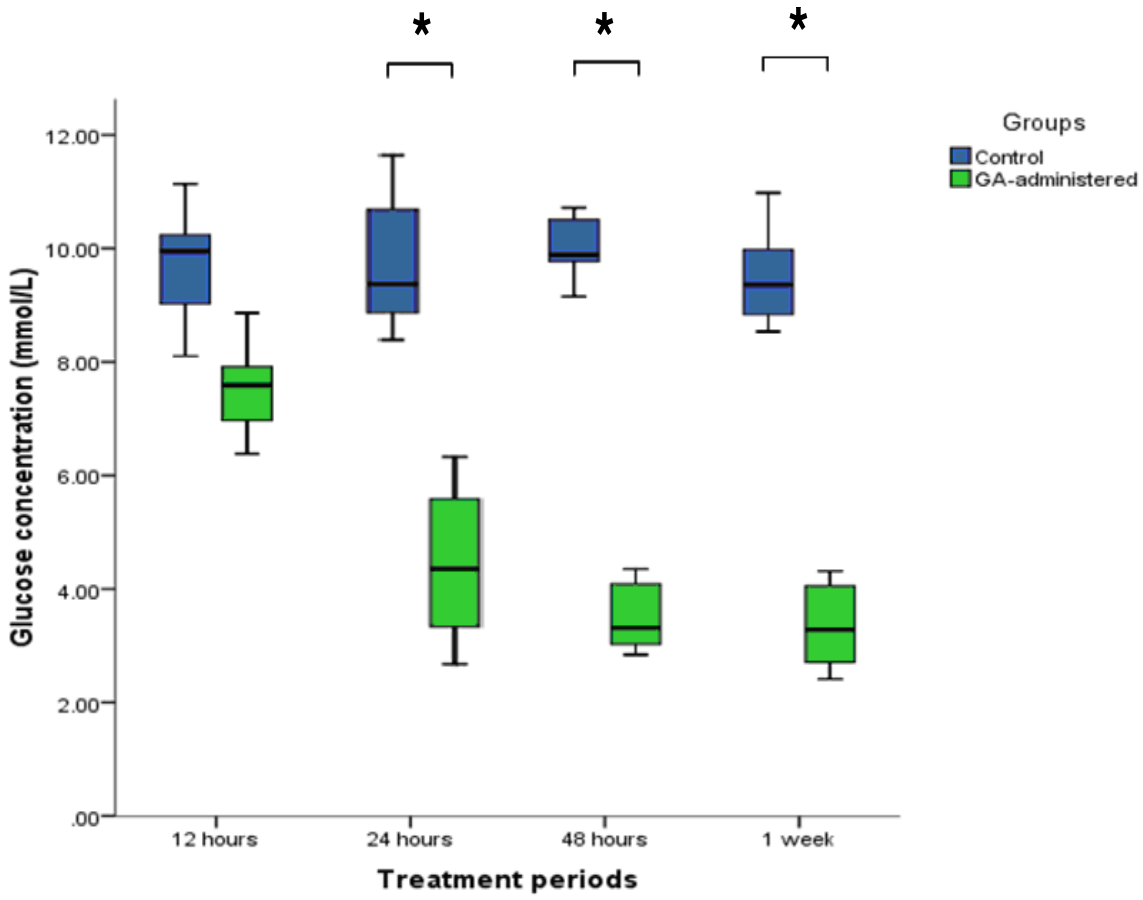

Figure 3.33: Blood glucose levels in GA-treated and control rats given GA for 12, 24 and 48 hours as well as one week.

Note the decrease in blood glucose levels for the GA-treated rats (* indicates $P < 0.05$).

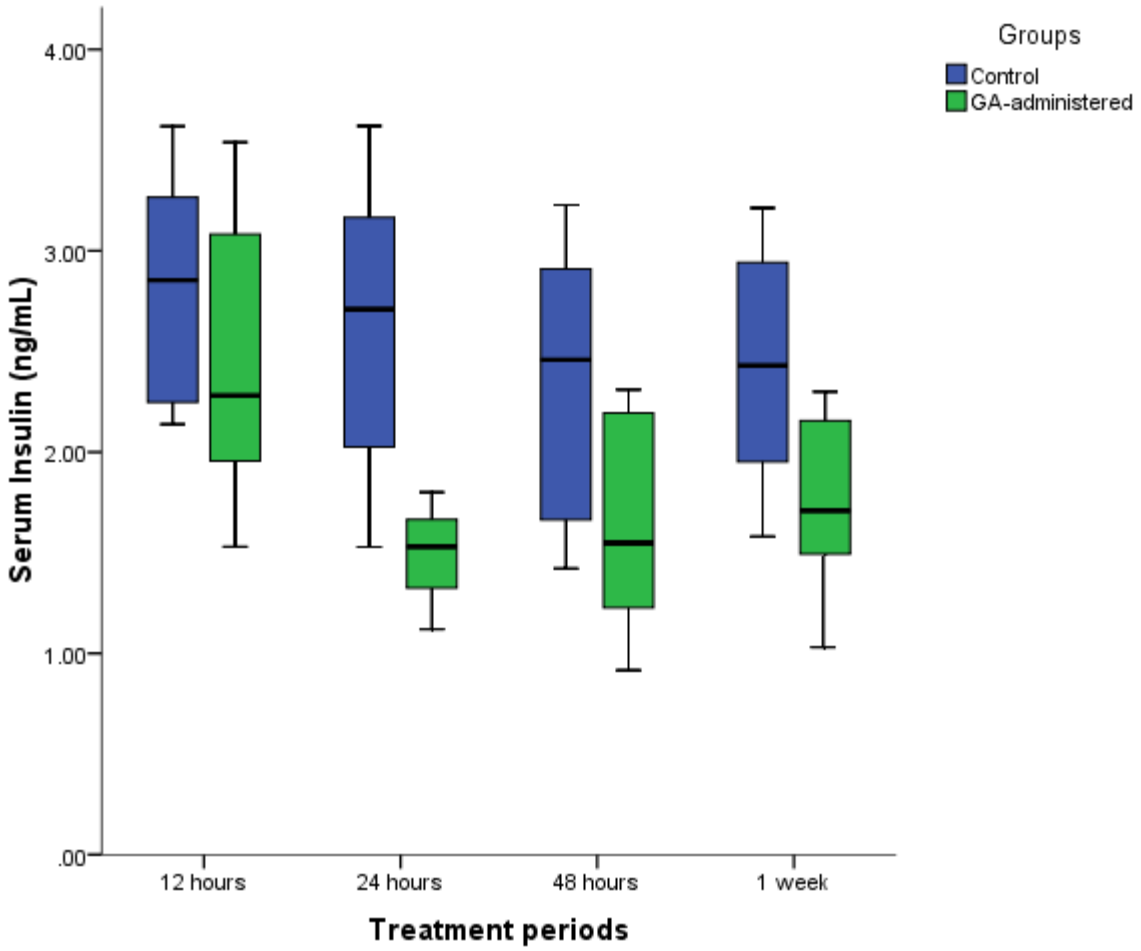

Figure 3.34: Serum insulin levels in GA-treated and control rats given GA for 12, 24 and 48 hours as well as one week.

Lower serum insulin levels were observed following GA treatment but the levels of decrease were not statistically significant ($P > 0.05$ for all treatment periods).

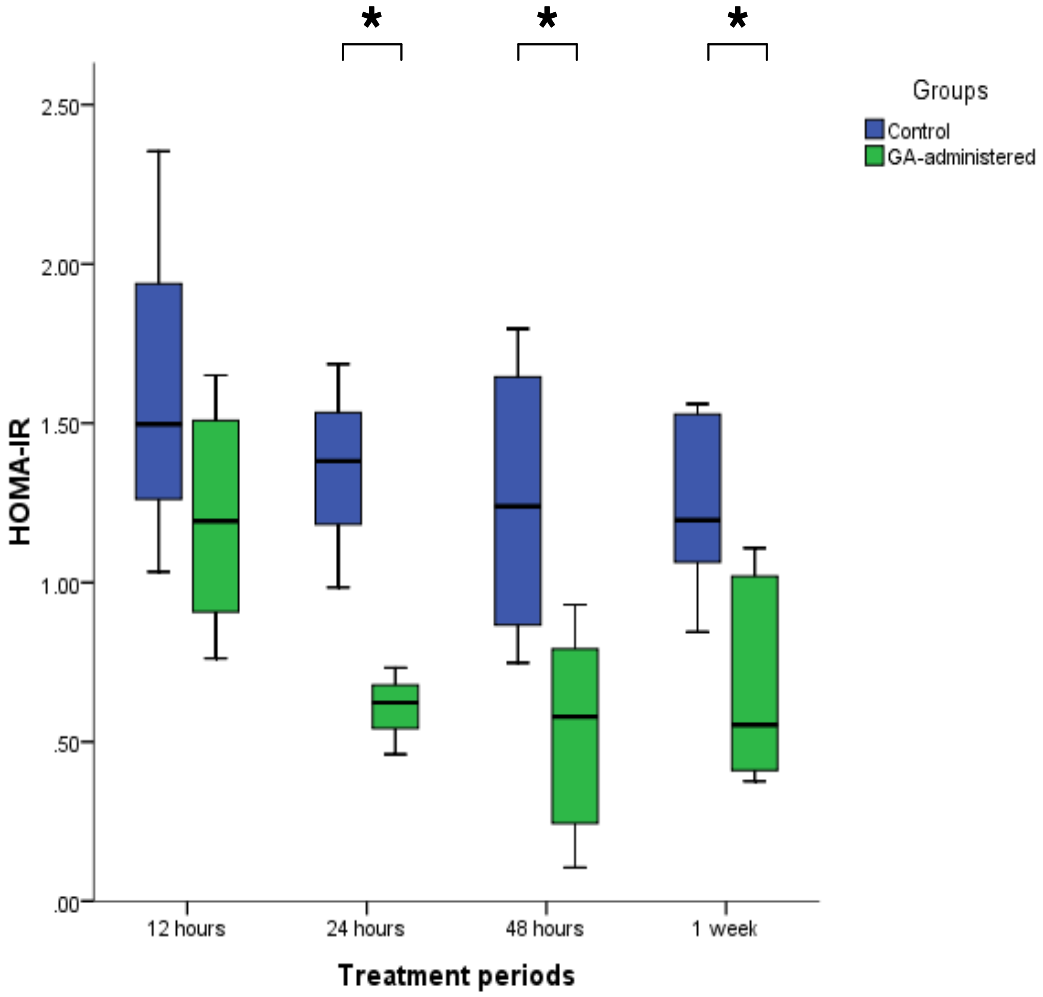

Figure 3.35: HOMA-IR in GA-treated and control rats given GA for 12, 24 and 48 hours as well as one week.

Marked decrease in the HOMA-IR values were observed following GA treatment (* indicates $P < 0.05$).

3.3.3 Serum lipid parameters

Consistent improvement in all lipid parameters was observed in the GA-administered rats relative to the control with the different treatment periods ($P > 0.05$) (Figure 3.36). Serum TAG, total cholesterol and LDL-cholesterol levels decreased with increasing time of GA treatment. Serum TAG reduced by 26.5% ($P = 0.12$) after 12 hours of GA treatment and remained at 35.2% ($P = 0.09$) lower than the control rats after one week of GA treatment. Total cholesterol decreased by 8.9% ($P = 0.16$) after 12 hours of GA treatment and was further reduced by 33.8% after one week of treatment. Similarly, mean serum LDL-cholesterol was reduced from 1.62% ($P = 0.11$) after 12 hours of treatment to 33.8% ($P = 0.08$) after one week of GA treatment. However, mean serum HDL-cholesterol increased by 3.3% ($P = 0.14$) after 12 hours of GA administration and increased further by 18.2% ($P = 0.10$) after 24 hours and 22.6% ($P = 0.09$) after one week of treatment.

3.3.4 **Total PPARγ expression**

3.3.4.1 Subcutaneous and visceral adipose tissues

GA treatment led to higher expression levels of total PPARγ in both the subcutaneous and visceral adipose tissues when compared to the control rats (Figure 3.37; Table 3.12). However, the visceral adipose tissues showed a larger increase in total PPARγ expression levels (more than 100-fold increase after 48 hours of GA treatment) when compared to the increase in the subcutaneous adipose tissues (about 40-fold after 48 hours and 80-fold after one week of treatment) which was statistically significant only for the one week treatment period ($P = 0.02$; $P < 0.05$). The increases in the visceral adipose tissues were statistically significant in rats administered with 100 mg/kg of GA for 24, 48 hours and one week ($P = 0.04$; $P < 0.05$).

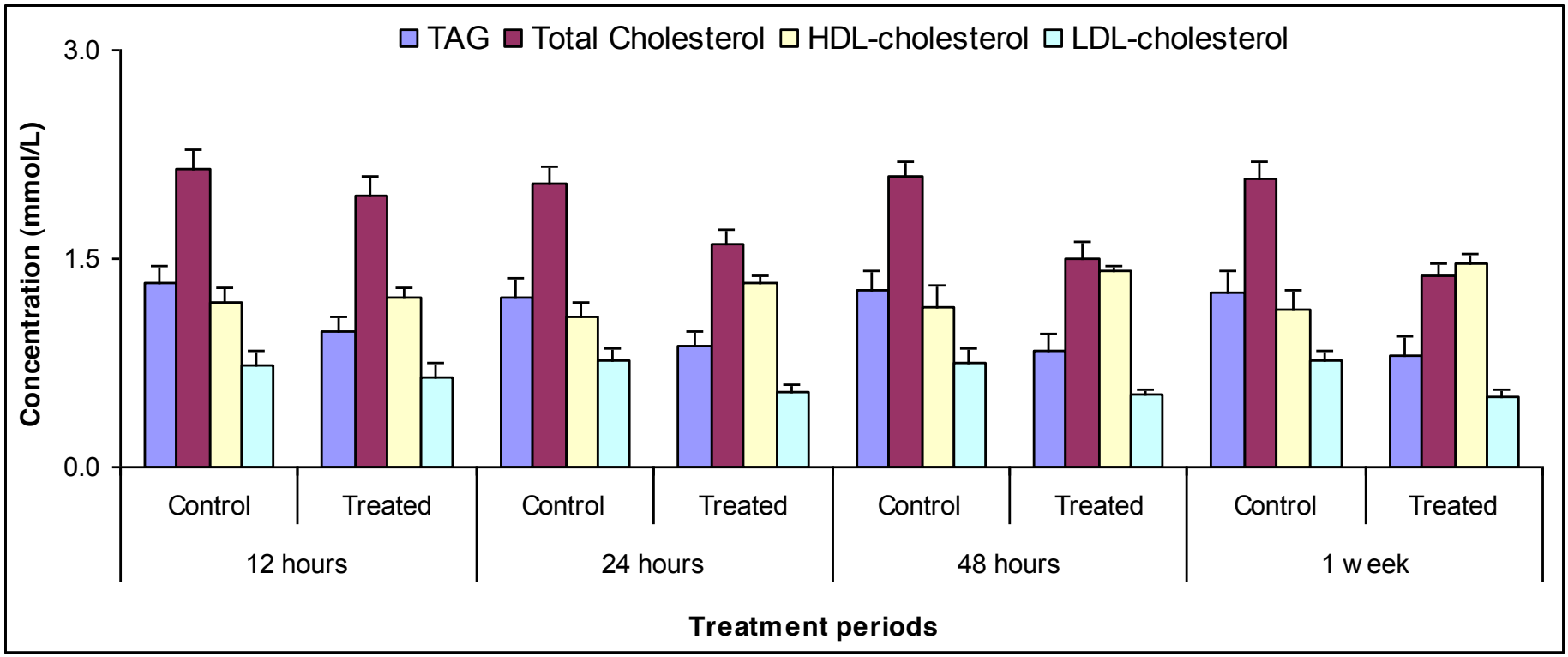

Figure 3.36: Mean serum TAG, total cholesterol, HDL-cholesterol and LDL-cholesterol of control and GA-administered rats with various treatment periods.

An overall improvement in the lipid profiles was observed with decrease in serum TAG, total cholesterol and LDL-cholesterol and increases in HDL-cholesterol levels following GA treatment ($P > 0.05$ for all parameters).

Table 3.12: Fold difference in total PPARγ expression in rats administered with 100 mg/kg GA for various treatment periods as indicated.

An increase in total PPARγ expression levels was observed in all tissues following GA-administration (* indicates $P < 0.05$).

Tissue	Fold-difference in total PPARγ expression levels			
	12 hours	24 hours	48 hours	1 week
ATS	0.7	35.9	38.7	79.9 *
ATV	16.8	78.5 *	102.6 *	108.8 *
MA	20.7	83.5 *	85.9 *	92.6 *
MT	31.2	108.1 *	112.6 *	116.9 *
L	35.4	53.5	58.1	56.7
K	9.4	11.2	17.9	19.7

Abbreviations: ATS, subcutaneous adipose tissue; ATV, visceral adipose tissue; MA, abdominal muscle; MT, quadriceps femoris muscle; L, liver; K, kidney.

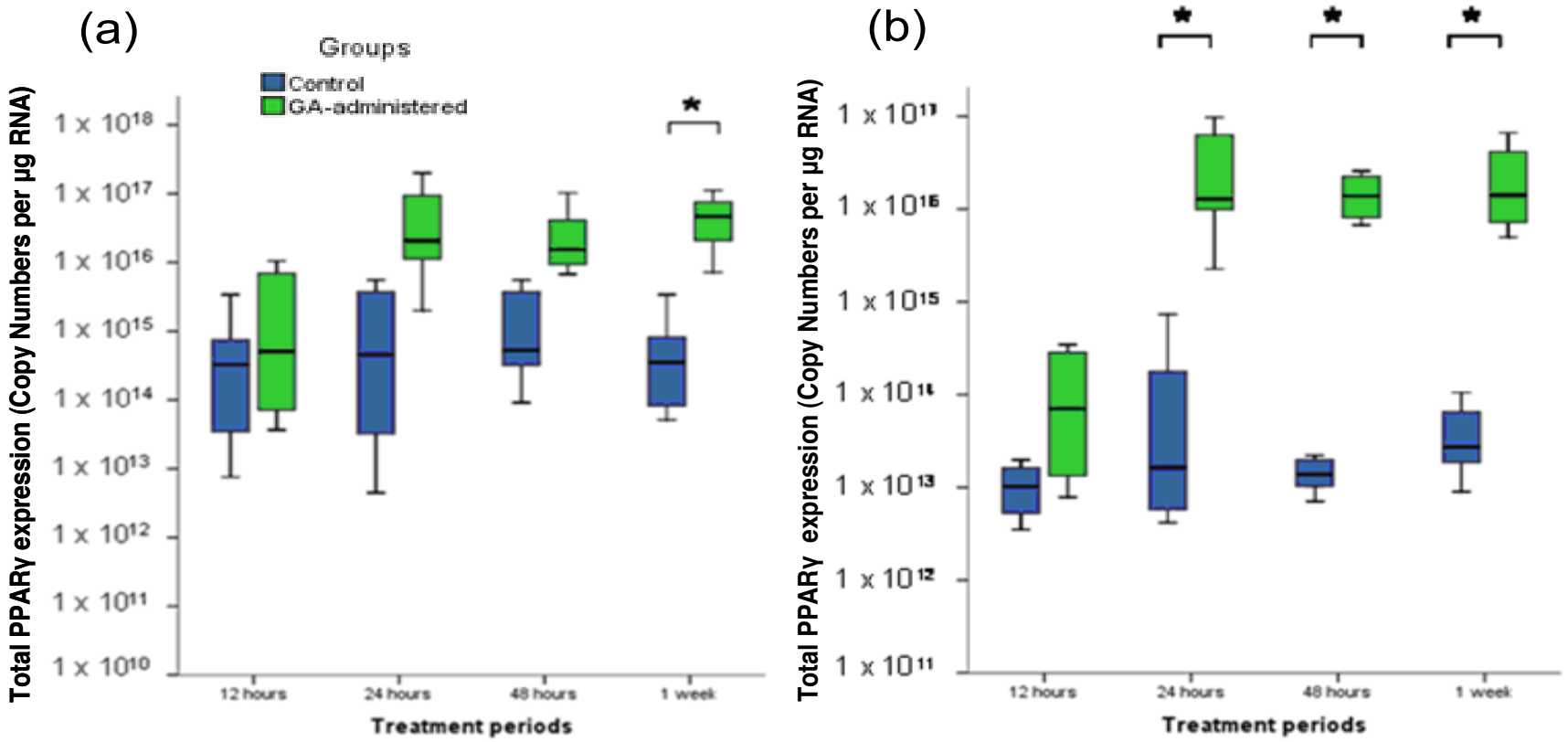

Figures 3.37: Total PPARγ expression levels in (a) subcutaneous and (b) visceral adipose tissues of rats administered with 100 mg/kg at various treatment periods.

Total PPARγ levels were higher for both tissues following GA treatment (* indicates $P < 0.05$).

3.3.4.2 Abdominal muscle and quadriceps femoris

Both abdominal muscle and quadriceps femoris showed increase in total PPARγ expression following GA administration with larger increase in the quadriceps femoris compared to the abdominal muscle (Figure 3.38). The quadriceps femoris showed more than 100-fold increase in total PPARγ expression levels after 24 hours of GA treatment while the abdominal muscle displayed more than 80-fold increase for the same treatment period. In both tissues, the increase in total PPARγ expression was statistically significant ($P < 0.05$) in rats treated with GA for 24 hours, 48 hours and one week.

3.3.4.3 Liver and kidney

GA treatment led to increased PPARγ expression in both the liver (Figure 3.39) and the kidneys (Figure 3.40) of rats. However, the increased expression levels were not statistically significant ($P < 0.05$).

3.3.5 **PPARγ1 expression**

3.3.5.1 Subcutaneous and visceral adipose tissues

Similar to total PPARγ, PPARγ1 also displayed higher expression levels in the subcutaneous and visceral adipose tissues compared to the control rats (Figures 3.41; Table 3.13). However, the increase in the subcutaneous adipose tissue at various treatment periods was statistically insignificant ($P > 0.05$) except for the one week treatment period ($P = 0.01$; $P < 0.05$). Significant increase in PPARγ expression levels in the visceral adipose tissue was noted for all time frames ($P = 0.04$-0.05; $P < 0.05$) except for the 12-hour treatment period.

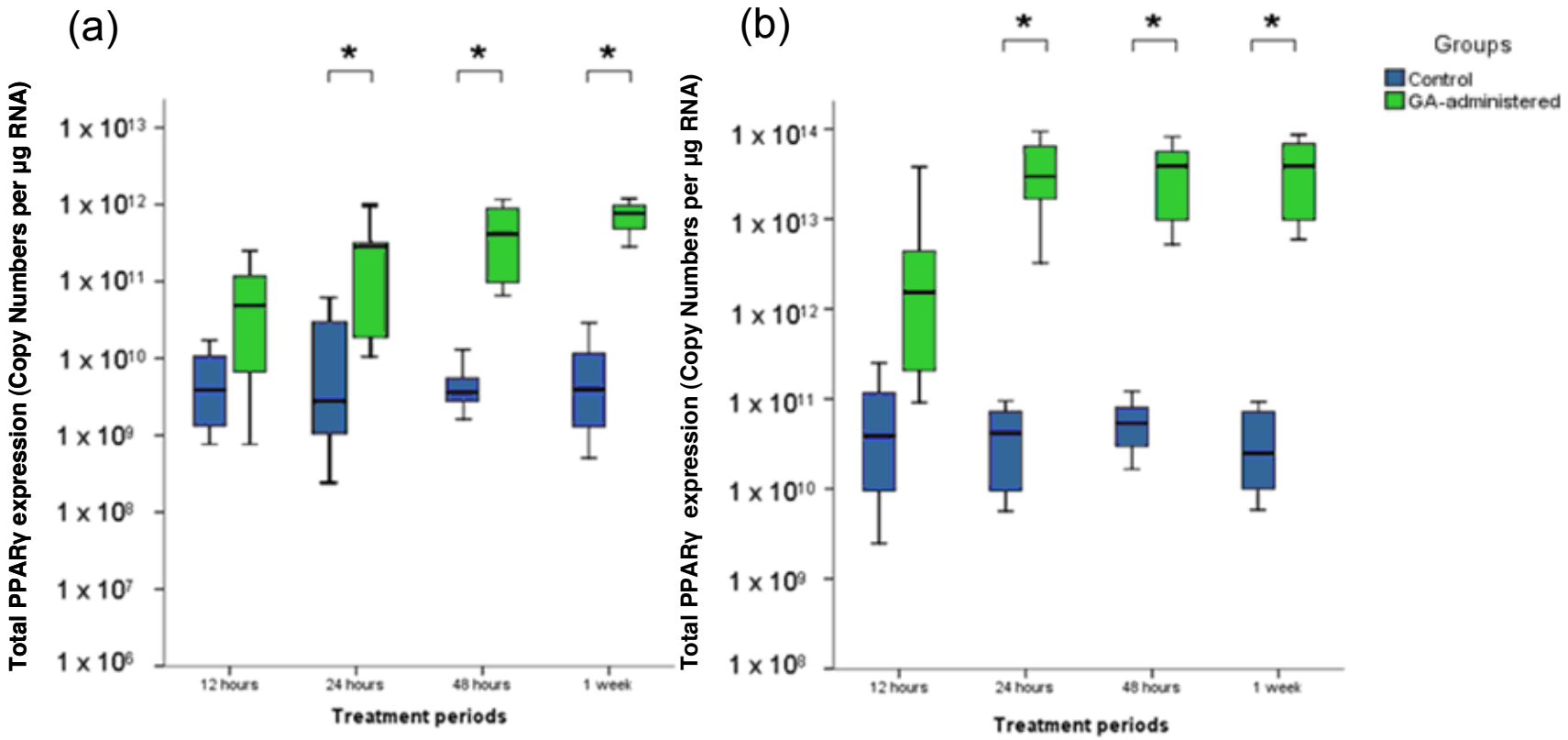

Figures 3.38: Total PPARγ expression levels in (a) abdominal muscle and (b) quadriceps femoris of rats administered with 100 mg/kg at various treatment periods.

Marked increase in PPARγ expression levels were noted in both tissues following GA-treatment (* indicates $P < 0.05$).

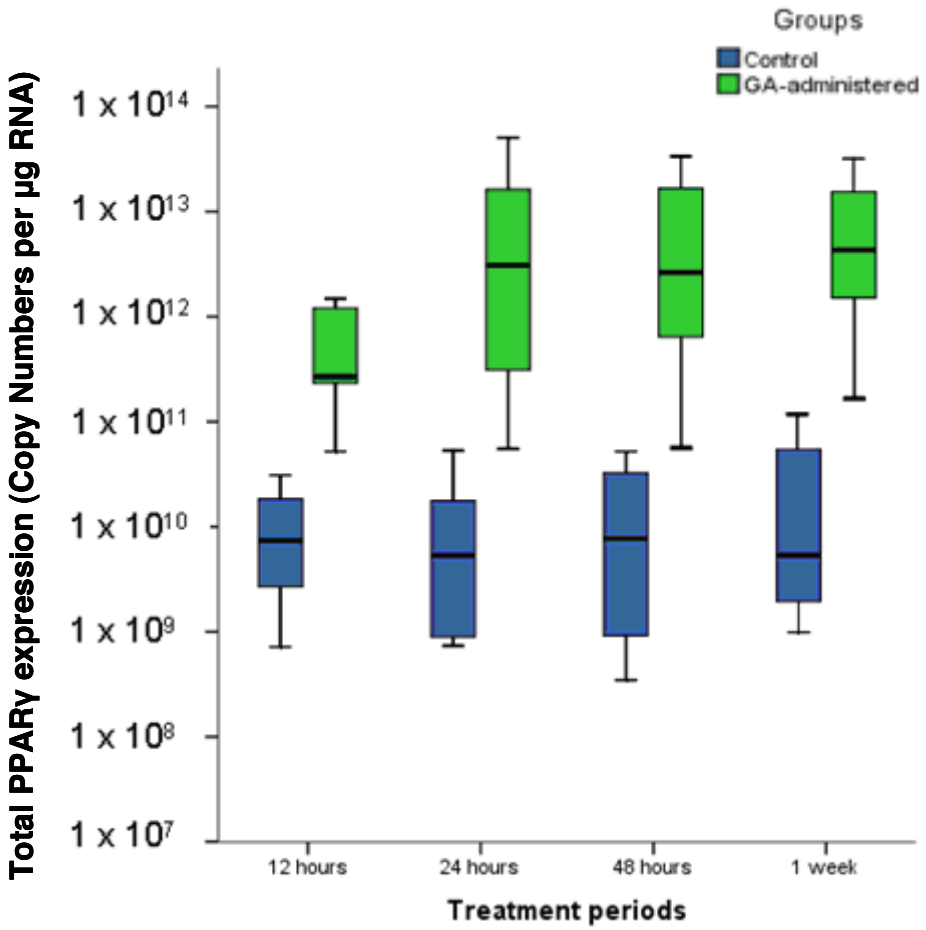

Figure 3.39: Total PPARγ expression levels in the liver of rats administered with 100 mg/kg GA at various treatment periods.

An increase in PPARγ expression levels was observed for all treatment periods although the increment was not statistically significant ($P > 0.05$).

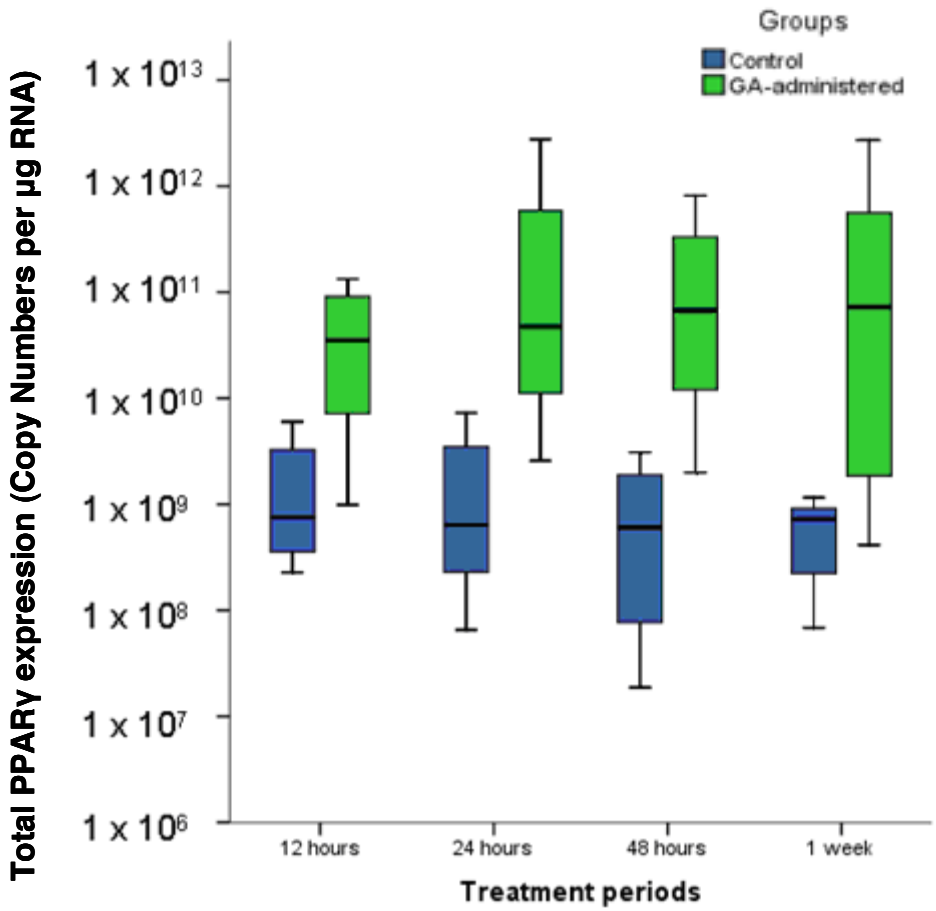

Figure 3.40: Total PPARγ expression levels in the kidneys of rats administered with 100 mg/kg GA at various treatment periods showing increase in PPARγ expression following GA treatment ($P > 0.05$ for all treatment periods).

Table 3.13: Fold difference in PPARγ1 expression in rats administered with 100 mg/kg GA over various treatment periods.

An increase in PPARγ1 expression levels was observed in all tissues following GA-administration (* indicates $P < 0.05$).

Tissue	Fold-difference in PPARγ1 expression levels			
	12 hours	24 hours	48 hours	1 week
ATS	15.8	17.4	26.8	59.8 *
ATV	15.2	52.0 *	66.9 *	77.5 *
MA	14.5	46.5 *	53.9 *	72.2 *
MT	18.6	58.5 *	102.2 *	127.3 *
L	16.7	16.9	22.4	58.1
K	27.8	28.5	19.9	17.8

Abbreviations: ATS, subcutaneous adipose tissue; ATV, visceral adipose tissue; MA, abdominal muscle; MT, quadriceps femoris muscle; L, liver; K, kidney.

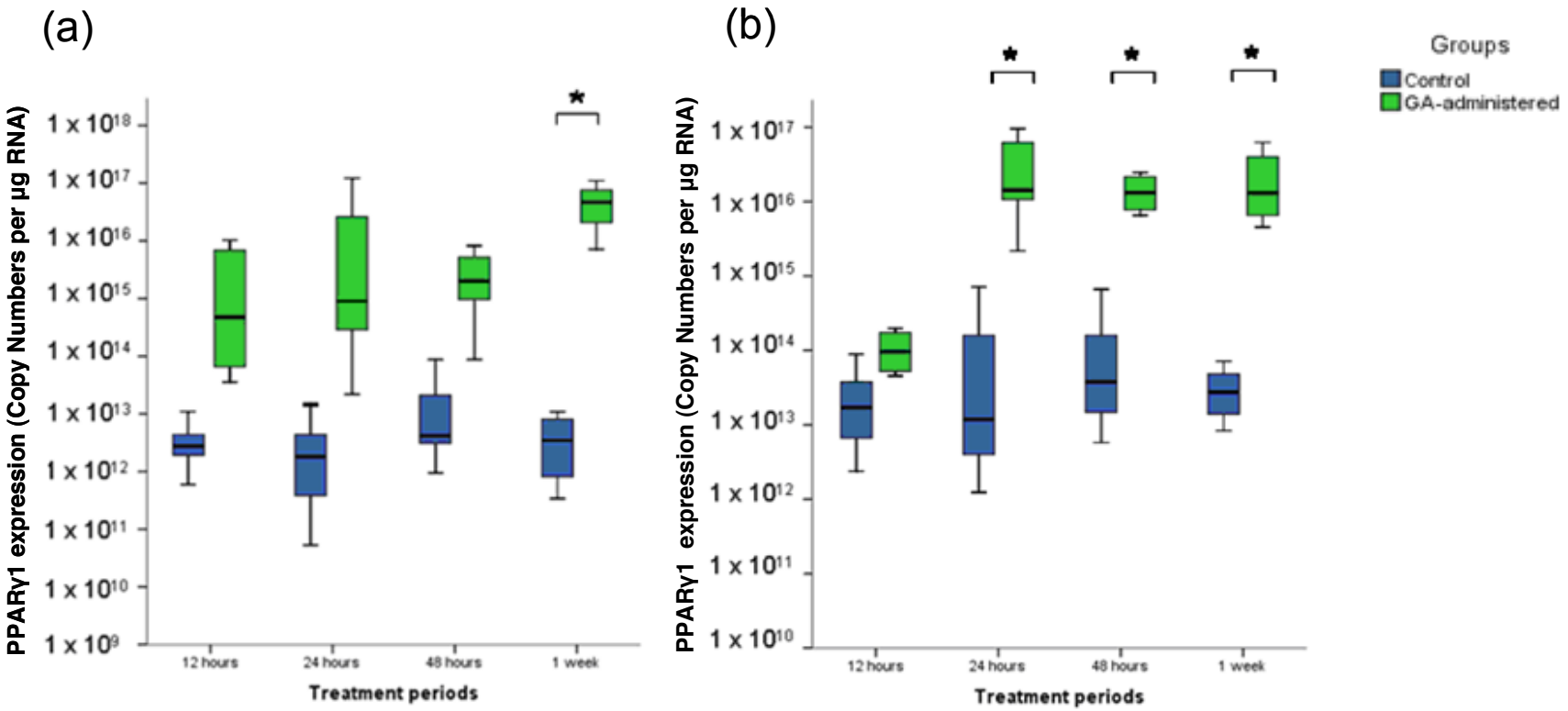

Figures 3.41: PPARγ1 expression levels in (a) subcutaneous and (b) visceral adipose tissues of rats administered with 100 mg/kg at various treatment periods.

Both tissues showed increased PPARγ1 expression levels (* indicates $P < 0.05$).

3.3.5.2 Abdominal muscle and quadriceps femoris

GA treatment also led to significant increase in PPARγ1 expression levels in both the abdominal muscle ($P = 0.03 – 0.04$) and quadriceps femoris ($P = 0.03 – 0.05$) except for the 12-hour treatment period (Figure 3.42).

3.3.5.3 Liver and kidney

The PPARγ1 expression levels in both the liver (Figure 3.43) and kidneys (Figure 3.44) were higher in the GA-administered rats compared to the control rats. However the increase in the expression levels in both these tissues at various treatment periods was statistically insignificant ($P > 0.05$).

3.3.6 **PPARγ2 expression**

3.3.6.1 Subcutaneous and visceral adipose tissues

Similar to total PPARγ and PPARγ1, higher expression of PPARγ2 was observed in the subcutaneous and visceral adipose tissues of rats following GA treatment (Figure 3.45; Table 3.14). The increase in PPARγ2 expression was more pronounced in the visceral adipose tissues (with a nearly 50-fold increase after 48 hours of GA treatment) as compared to the subcutaneous adipose tissues (about 15-fold increase after 48 hours) with a statistically significant increase for all time frames ($P = 0.03 – 0.04$; $P < 0.05$) except for the 12-hour treatment period.

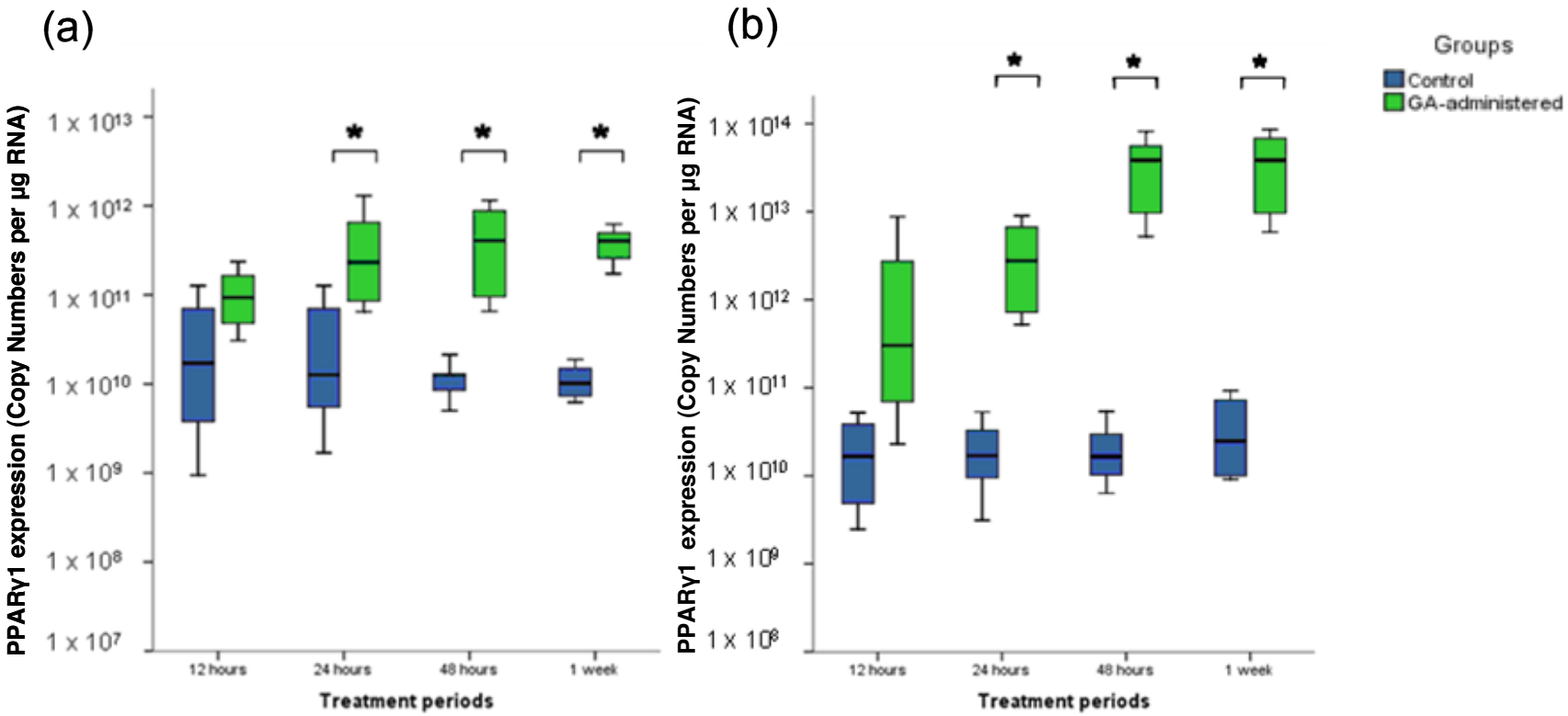

Figures 3.42: PPARγ1 expression levels in (a) abdominal muscle and (b) quadriceps femoris of rats administered with 100 mg/kg at various treatment periods.

Note the marked increase in PPARγ1 expression in both tissues for all the treatment periods (* indicates $P < 0.05$).

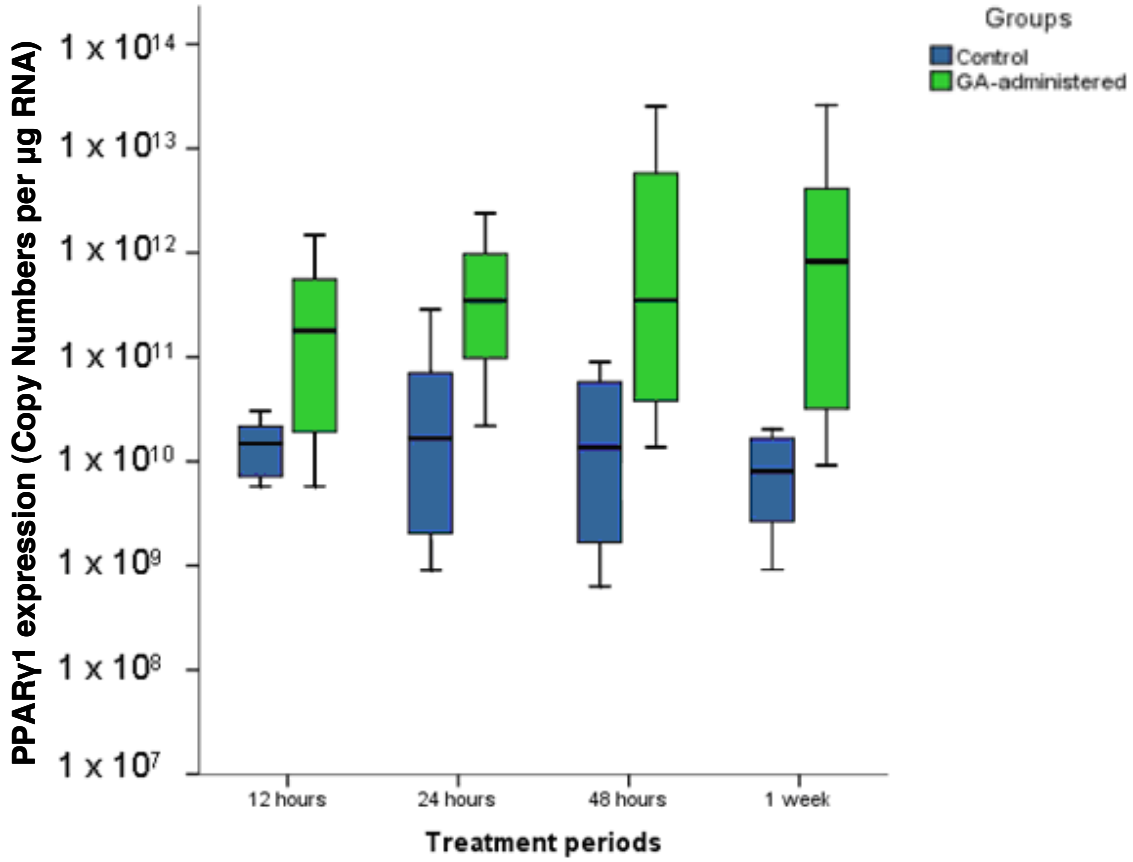

Figure 3.43: PPARγ1 expression levels in the liver of rats administered with 100 mg/kg GA at various treatment periods.

Increased PPARγ1 expression was observed for all treatment periods although the increases were not significant ($P > 0.05$).

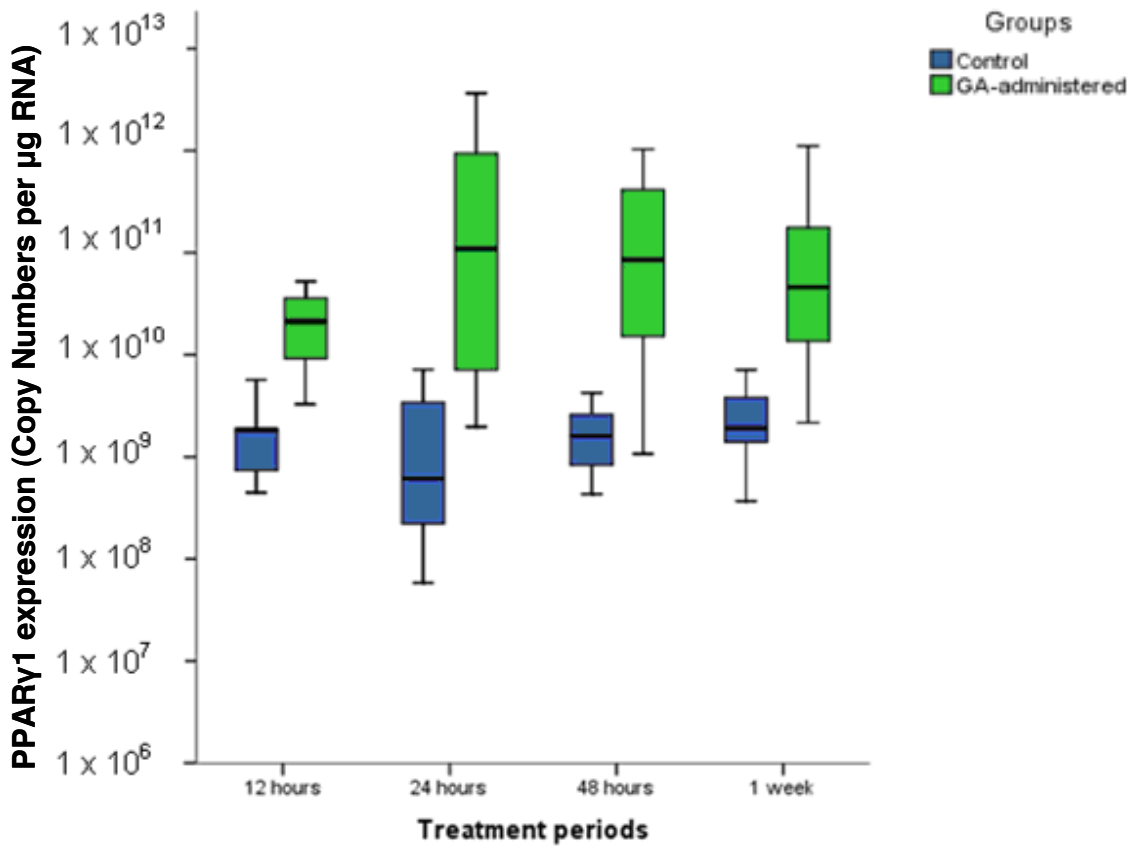

Figure 3.44: PPARγ1 expression levels in the kidney of rats administered with 100 mg/kg GA at various treatment periods.

Increased PPARγ1 expression was observed across all treatment periods ($P > 0.05$).

.

Table 3.14: Fold difference in PPARγ2 expression levels in rats administered with 100 mg/kg GA over various treatment periods. An increase in PPARγ2 expression levels was observed in all tissues following GA-administration (* indicates $P < 0.05$).

Tissue	Fold difference in PPARγ2 expression levels			
	12 hours	24 hours	48 hours	1 week
ATS	0.53	4.99	14.7	21.1 *
ATV	8.12	31.8 *	47.2 *	54.9 *
MA	18.9	37.4 *	46.8 *	62.1 *
MT	13.4	45.5 *	68.8 *	113.8 *
L	34.1	45.7	46.3	49.9
K	24.2	31.1	38.2	41.3

Abbreviations: ATS, subcutaneous adipose tissue; ATV, visceral adipose tissue; MA, abdominal muscle; MT, quadriceps femoris muscle; L, liver; K, kidney.

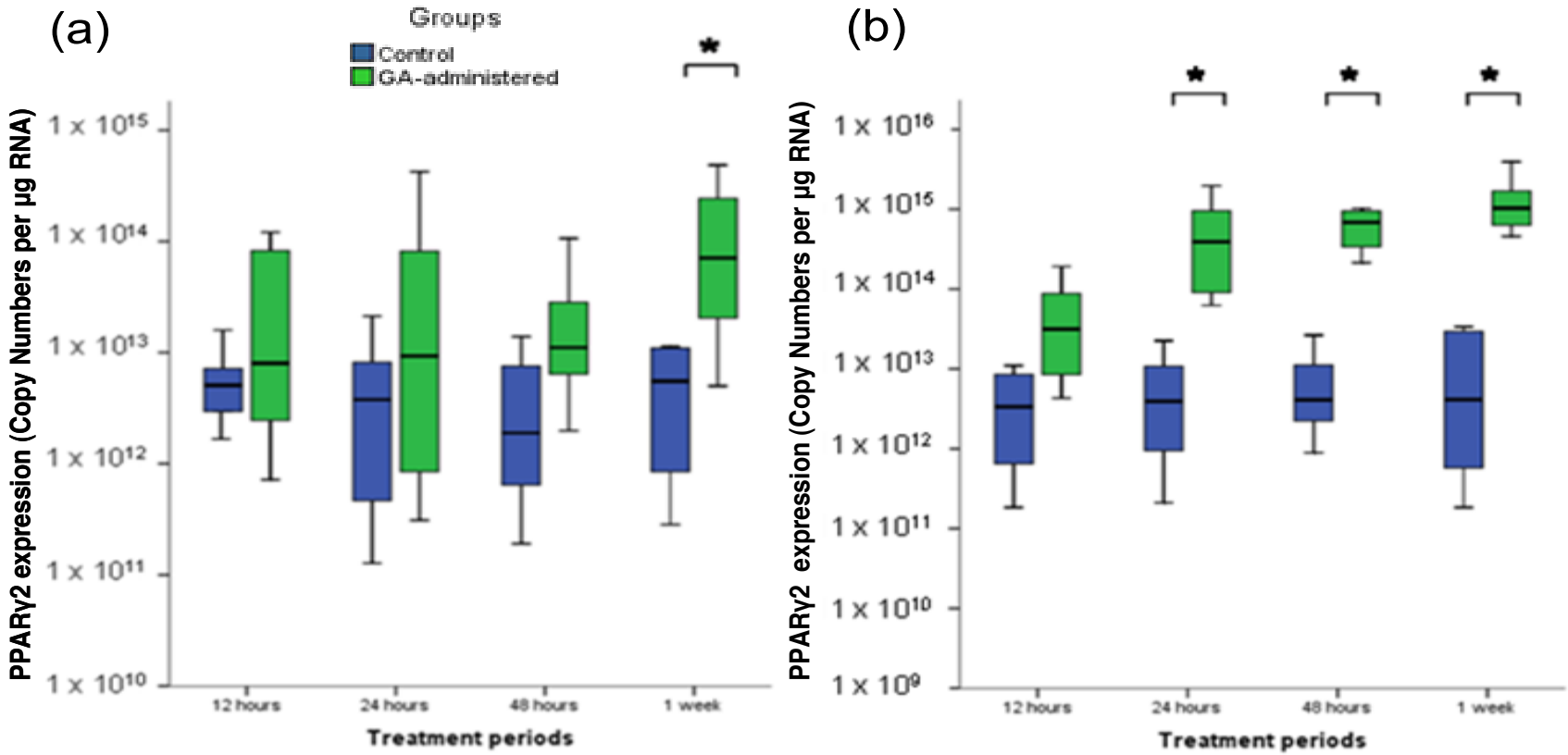

Figures 3.45: PPARγ2 expression levels in (a) subcutaneous and (b) visceral adipose tissues of rats administered with 100 mg/kg at various treatment periods.

A more significant increase in PPARγ2 expression was observed in the visceral adipose tissues as compared to the subcutaneous adipose tissues (* indicates $P < 0.05$).

3.3.6.3 Abdominal muscle and quadriceps femoris

Both abdominal muscle and the quadriceps femoris showed marked increase in PPARγ2 expression levels following GA administration (Figure 3.46) and the increased expression was statistically significant in all treatment periods except for the rats given GA for 12 hours. Quadriceps femoris showed a more than 100-fold increase in PPARγ2 levels after one week of treatment while the abdominal muscle displayed an approximately 80-fold increase.

3.3.6.4 Liver and kidney

The PPARγ2 expression levels in the liver and the kidney were higher in the GA-administered rats compared to the control rats (Figures 3.47 and 3.48). However the increase in the expression levels in both tissues was not statistically significant ($P > 0.05$).

3.3.7 Relative LPL expression in the various studied tissues

Relative LPL expression in all the tissues studied showed an increase with increasing time of GA treatment (Figure 3.49). In the subcutaneous adipose tissues, relative LPL expression increased by 6.7% ($P = 0.15$) following 12 hours of GA treatment and this increased further by 27% ($P = 0.10$), 34% ($P = 0.09$) and 51% ($P = 0.05$) after 24 hours, 48 hours and one week of GA treatment, respectively. A similar level of increase in LPL expression was also observed in the visceral adipose tissues with increments of 7.1% ($P = 0.10$) after 12 hours of treatment to 67% ($P = 0.04$) after one week of GA administration.

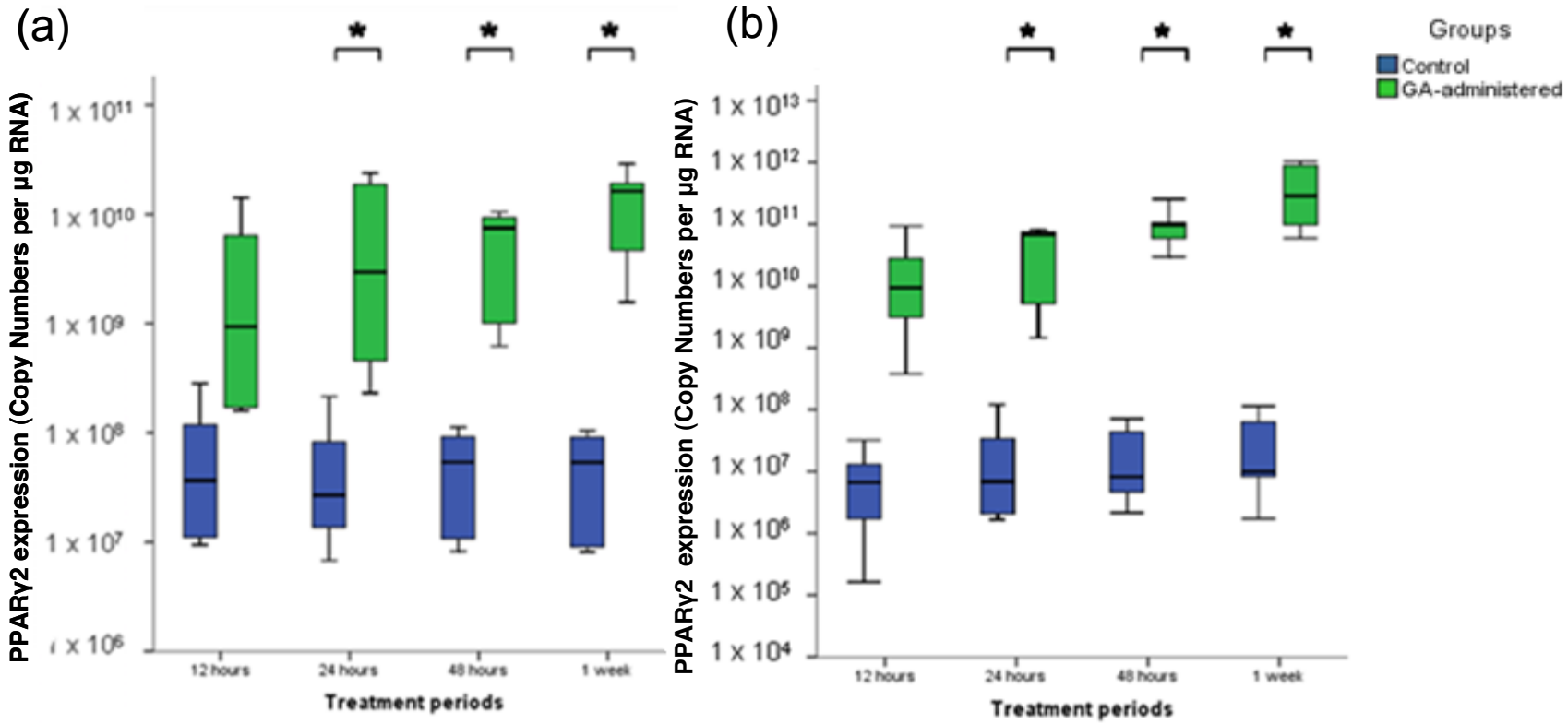

Figures 3.46: PPARγ2 expression levels in (a) abdominal muscle and (b) quadriceps femoris of rats administered with 100 mg/kg at various treatment periods.

Marked increase in PPARγ2 expression levels was observed for both tissues (* indicates $P < 0.05$).

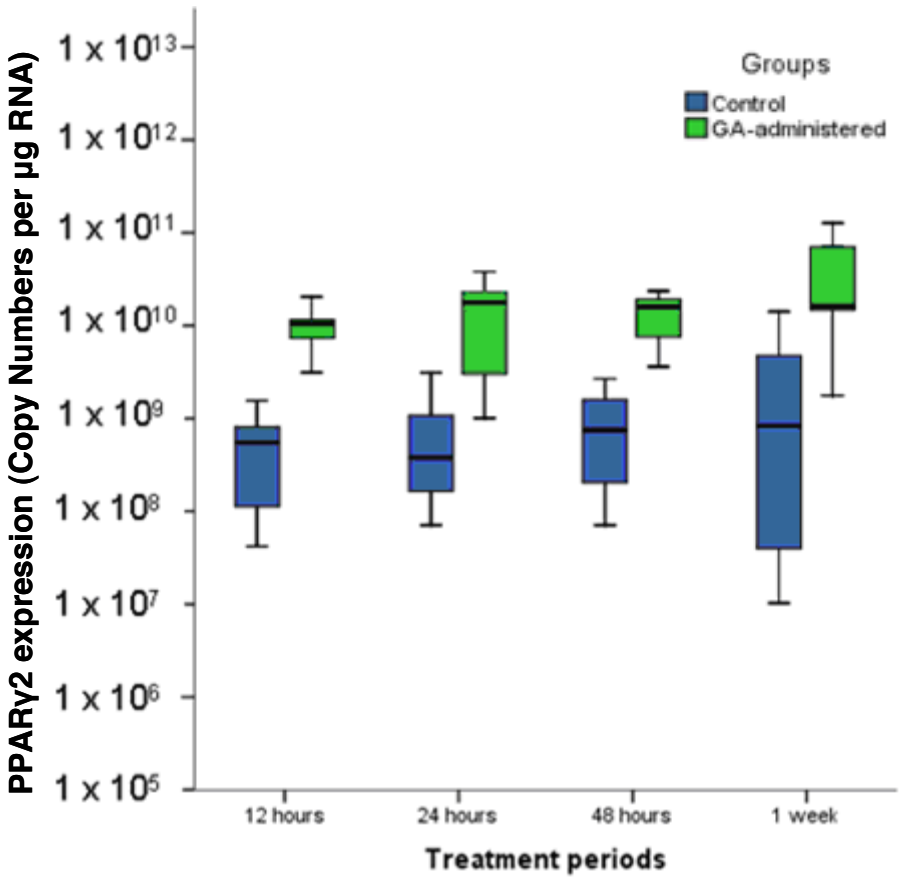

Figure 3.47: PPARγ2 expression levels in the liver of rats administered with 100 mg/kg GA at various treatment periods showing increase in expression levels after GA treatment ($P > 0.05$ for all treatment periods).

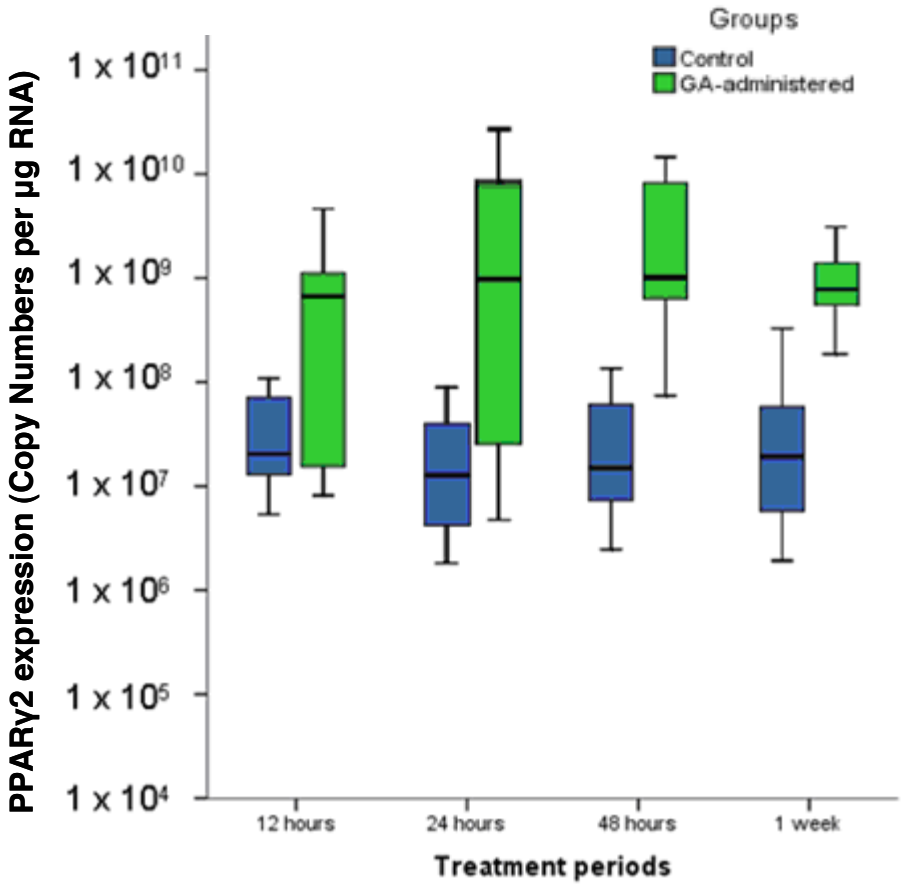

Figure 3.48: PPARγ2 expression levels in the kidney of rats administered with 100 mg/kg GA at various treatment periods.

GA treatment led to increase in PPARγ2 expression although $P > 0.05$ for all treatment periods.

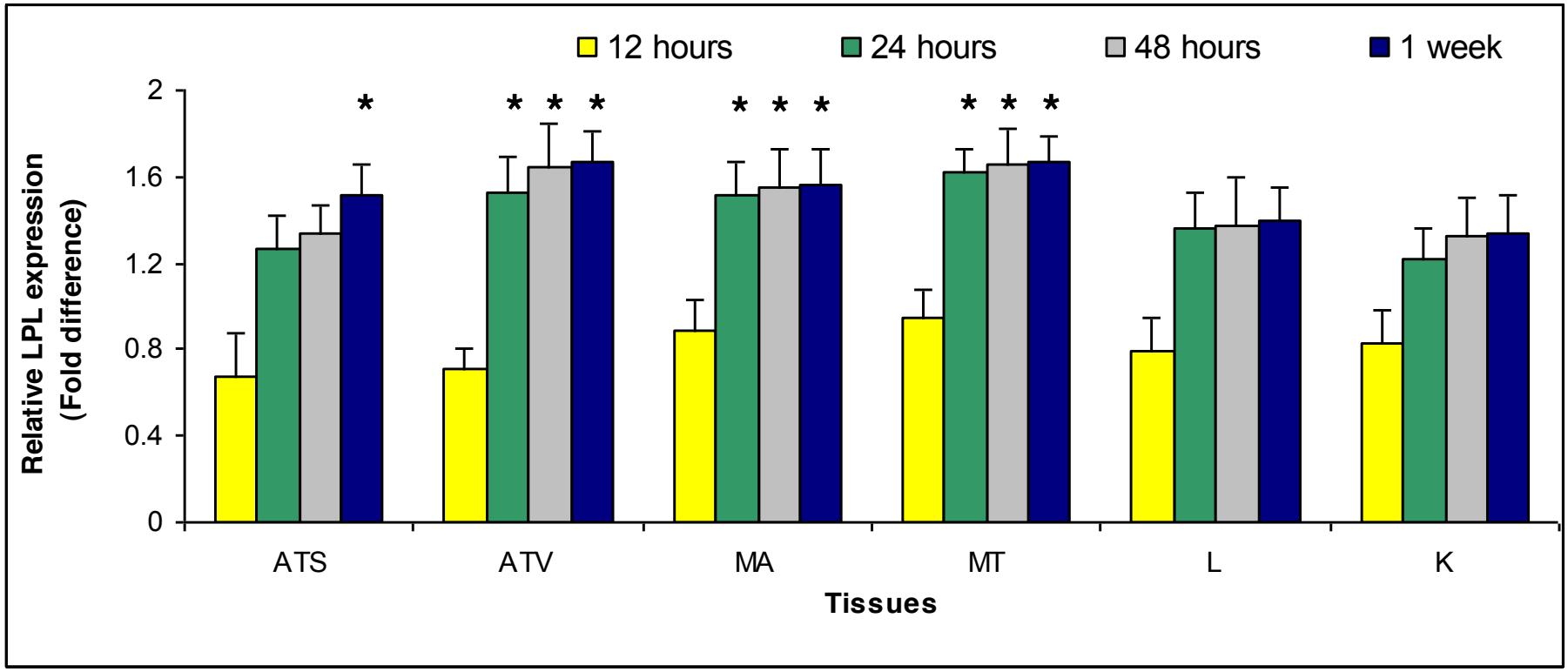

Figure 3.49: Relative expression (Fold difference) for LPL in various tissues in GA-administered rats at 100mg/kg in various treatment periods with β-actin as reference, GA-administered group as target and control group as calibrator (* indicates $P < 0.05$).

All tissues showed increased LPL expression levels following GA treatment. Abbreviations: ATS, subcutaneous adipose tissue; ATV, visceral adipose tissue; MA, abdominal muscle; MT, quadriceps femoris muscle; L, liver; K, kidney.

Both the abdominal muscle and quadriceps femoris also showed similar levels of increase in relative LPL expression. In the abdominal muscle, 12 hours of GA treatment led to a 8.9% ($P = 0.10$) increase in relative LPL expression and this further increased to 55% ($P = 0.05$) after 48 hours of GA treatment and maintained at 56% ($P = 0.04$) after one week of GA treatment. In the quadriceps femoris, relative LPL expression increased by 9.5% ($P = 0.11$) after 12 hours of GA treatment and peaked at 67% ($P = 0.04$) after one week of treatment.

Increased LPL expression was also observed in the liver and the kidneys albeit at a smaller level and not statistically significant. In both tissues, highest level of LPL expression was seen after one week of GA treatment with the liver showing a 40% ($P = 0.09$) increase and the kidneys, a 34% ($P = 0.09$) increase.

3.3.8 **11β**-HSD1 and 1**1β**-HSD2 activities

3.3.8.1 **11β**-HSD1 activities

A decrease in 11β-HSD1 activities was observed following GA treatment for all the tissues examined (i.e., subcutaneous and visceral adipose tissues, abdominal muscle, quadriceps femoris, liver and kidneys) and across all the different treatment periods (12, 24, 48 hours and one week) (Figures 3.50 – 3.52).

The decrease in 11β-HSD1 activities was more pronounced in the visceral adipose tissues when compared with the subcutaneous adipose tissues. (Figure 3.50) In the visceral adipose tissues, 11β-HSD1 activity decreased by 21.91% ($P = 0.10$) after 12 hours of GA treatment and decreased further by 40.0% ($P = 0.05$) and 41.12% ($P = 0.04$) after 48 hours and one week of GA treatment respectively. In contrast, for the subcutaneous adipose tissues, 11β-HSD1 activity decreased by only 5.70% ($P = 0.14$) after 12 hours of GA treatment and 10.05% ($P = 0.11$) after 48 hours treatment.

(a) Subcutaneous adipose tissue

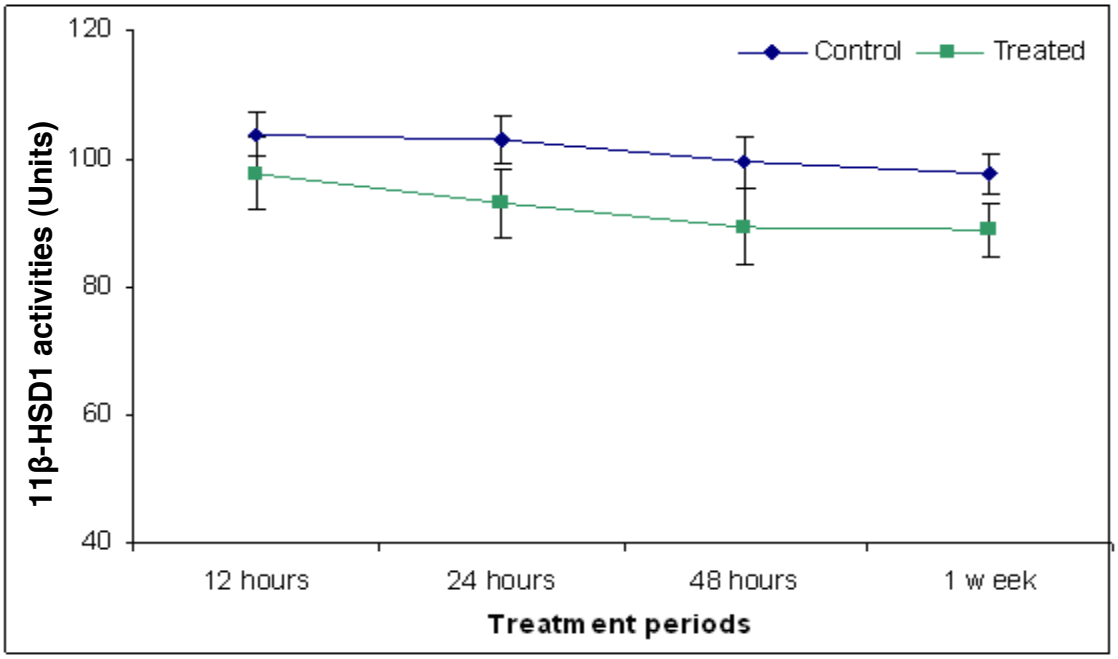

(b) Visceral adipose tissue

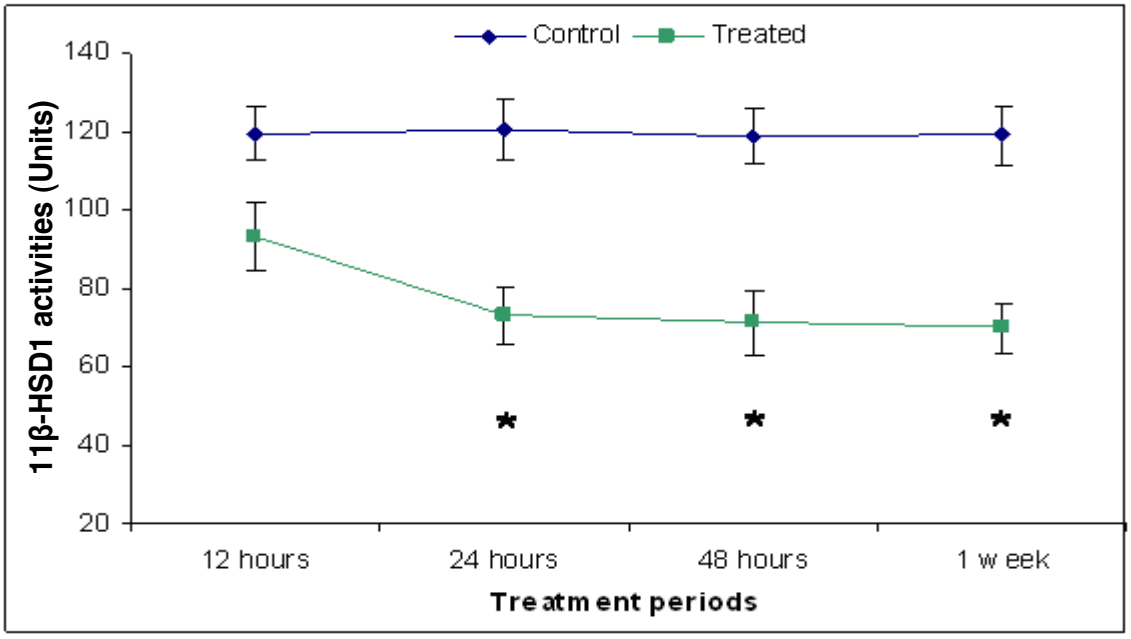

Figures 3.50: 11β-HSD1 activities in (a) subcutaneous and (b) visceral adipose tissues of rats administered with 100 mg/kg GA at various treatment periods (* indicates $P < 0.05$).

(a) Abdominal muscle

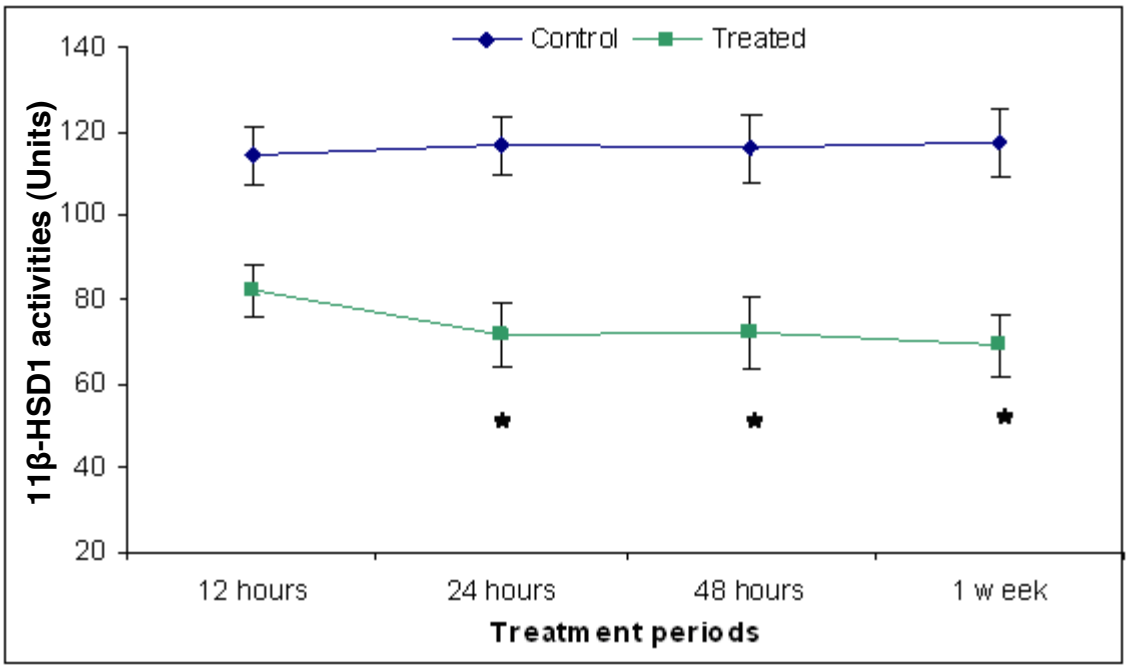

(b) Quadriceps femoris

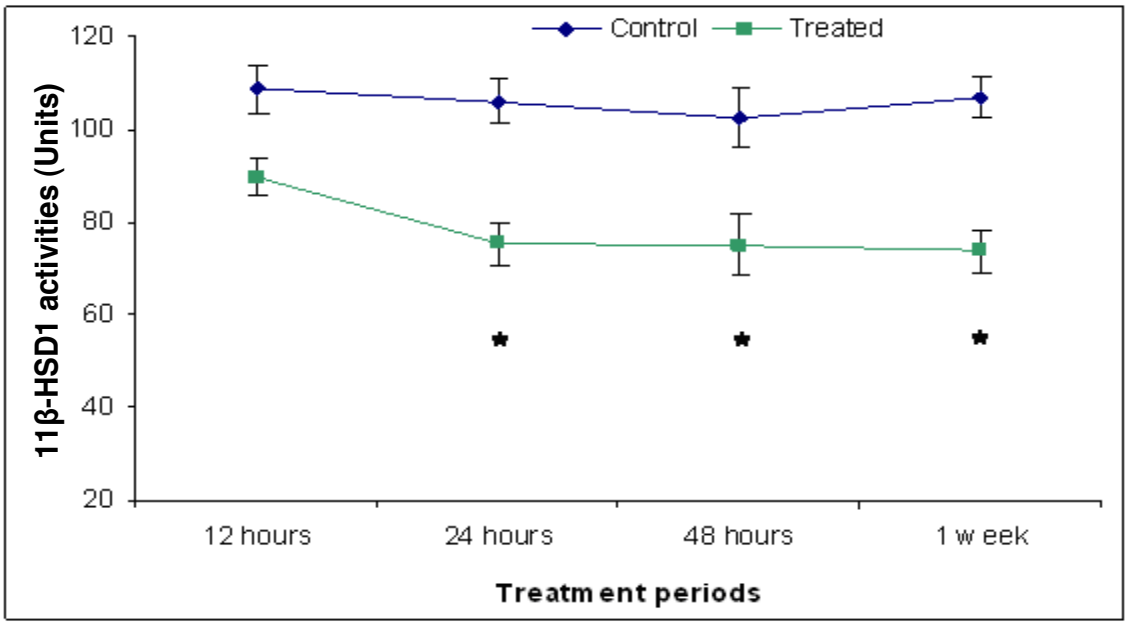

Figures 3.51: 11β-HSD1 activities in (a) abdominal muscle (b) quadriceps femoris of rats administered with 100 mg/kg GA at various treatment periods (* indicates $P < 0.05$).

(a) Liver

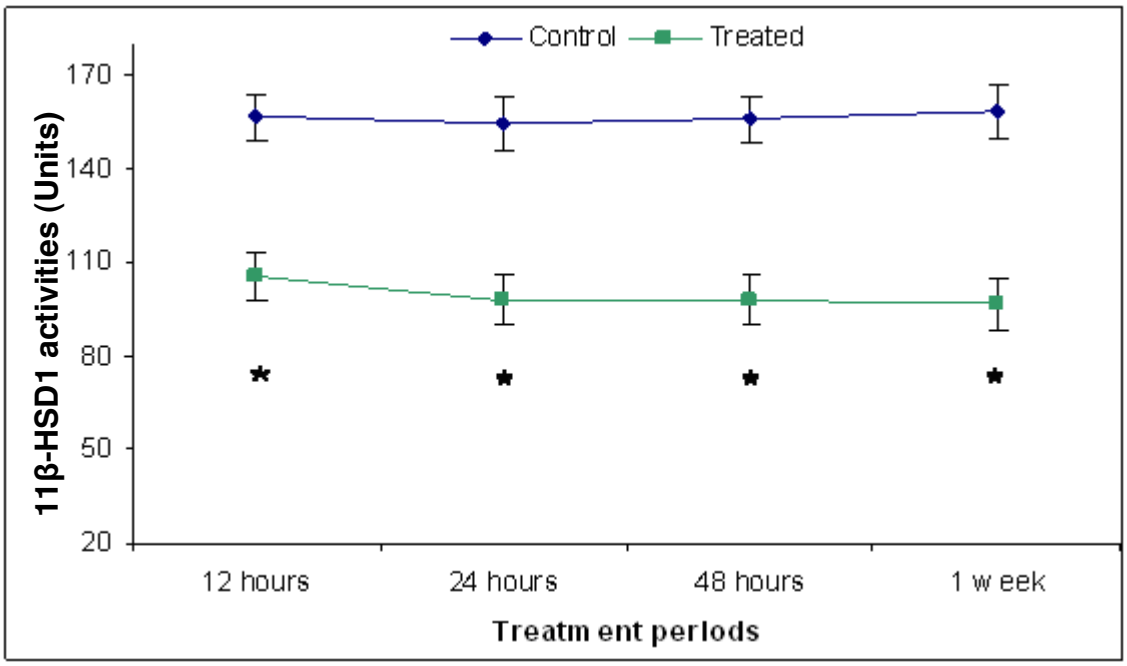

(b) Kidney

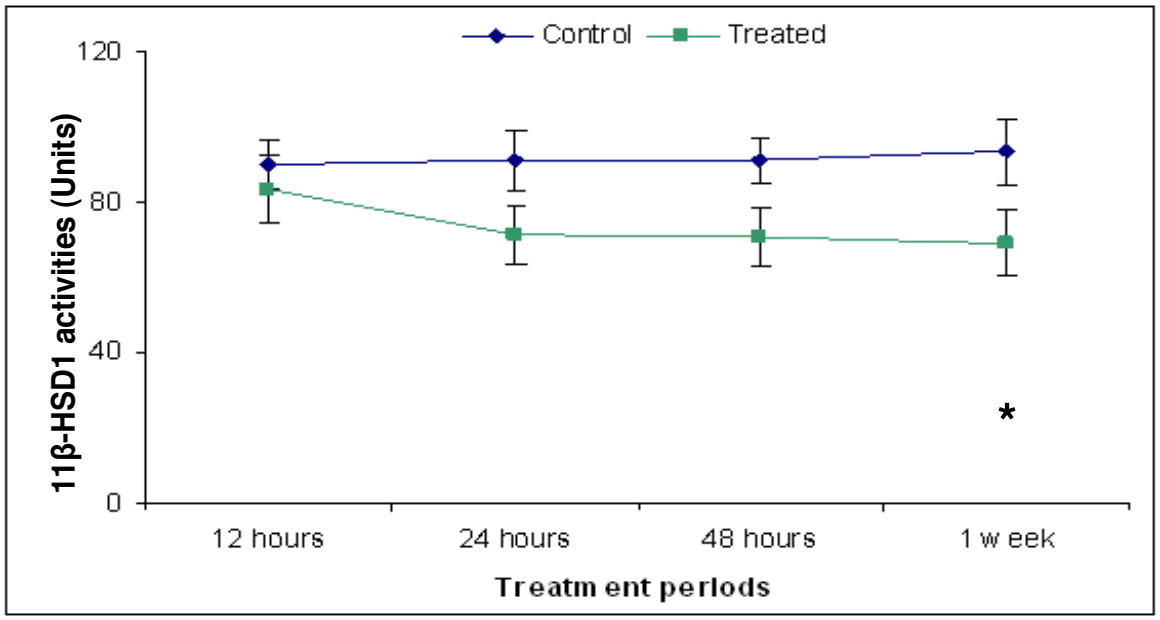

Figures 3.52: 11β-HSD1 activities in the (a) liver and (b) kidney of rats administered with 100 mg/kg GA at various treatment periods (* indicates $P < 0.05$).

Following one week of GA treatment, 11β-HSD1 activity decreased by only 8.9% ($P = 0.12$) in the subcutaneous adipose tissues.

The abdominal muscle had a slightly larger reduction in 11β-HSD1 activities following GA treatment when compared to the quadriceps femoris (Figure 3.51). After 12 hours of GA treatment, 11β-HSD1 activity in the abdominal muscle decreased by 28.09% ($P = 0.10$) whereas in the quadriceps femoris, the activity decreased by 17.54% ($P = 0.09$). Following one week of GA treatment, 11β-HSD1 activity in the abdominal muscle was lowered by 41.09% ($P = 0.04$) as compared to 30.84% ($P = 0.04$) reduction in the quadriceps femoris.

When comparing the liver and the kidneys, the liver had a much more significant decrease in 11β-HSD1 activity following GA treatment (Figure 3.52). After 12 hours of treatment, 11β-HSD1 activities were lowered by 32.59% ($P = 0.05$) in the liver whereas in the kidneys, the activities were reduced by only 7.29% ($P = 0.10$). Similarly, after 48 hours and one week of GA administration, 11β-HSD1 activities were down by 37.18% ($P = 0.04$) and 38.98% ($P = 0.04$) respectively in the liver, whereas in the kidneys, the activity levels were reduced by only 22.5% ($P = 0.07$) and 26.03% ($P = 0.05$), respectively.

3.3.8.2 **11β**-HSD2 activities

Similar to 11β-HSD1, reduction in 11β-HSD2 activities was observed in all the tissues examined across all the treatment periods. Interestingly, there was not such a marked decrease in 11β-HSD2 activities in the visceral adipose tissues when compared to the subcutaneous adipose tissues (Figure 3.53) as was noted for 11βHSD1. In the visceral adipose tissues, 11β-HSD2 activities decreased by 6.43% ($P = 0.10$) after 12 hours of GA treatment and decreased further by 25.28% ($P = 0.05$) after one week of treatment. In comparison, for the subcutaneous adipose tissues, 11β-HSD2 activities were reduced by 9.30% ($P = 0.12$) after 12 hours of GA treatment and 16.40% ($P = 0.05$) after one week of treatment.

There was also not much difference in the levels of decrease in 11β-HSD2 activities in the abdominal muscle compared with the quadriceps femoris (Figure 3.54) in contrast to the slightly larger decrease in 11β-HSD1 activity observed in the

abdominal muscle when compared with the quadriceps femoris. After 12 hours of GA treatment, 11β-HSD2 activities were lowered by 13.16% ($P = 0.11$) in the abdominal muscle and 9.24% ($P = 0.08$) in the quadriceps femoris. Following 48 hours of treatment, 11β-HSD2 activities dropped by 19.45% ($P = 0.05$) in the abdominal muscle while in the quadriceps femoris, the levels decreased by 25.85% ($P = 0.05$). After one week of GA treatment, the 11β-HSD2 activities were down by 21.61% ($P = 0.05$) in the abdominal muscle and 19.66% ($P = 0.05$) in the quadriceps femoris.

In contrast, the liver had a more pronounced decrease in 11β-HSD2 activities when compared to the kidneys (Figure 3.55), similar to what was observed for 11β-HSD1 activities. After 12 hours of GA treatment, 11β-HSD2 activities in the liver were lowered by 22.40% ($P = 0.05$) and this decreased further by 35.61% ($P = 0.03$) after 48 hours and 37.98% ($P = 0.02$) after one week of treatment. In the kidneys, 11β-HSD2 activities decreased by 13.65% ($P = 0.09$) after 12 hours of GA treatment and decreased by only 19.76% ($P = 0.05$) and 19.51% ($P = 0.05$) after 48 hours and one week of GA treatment respectively.

(a) Subcutaneous adipose tissue

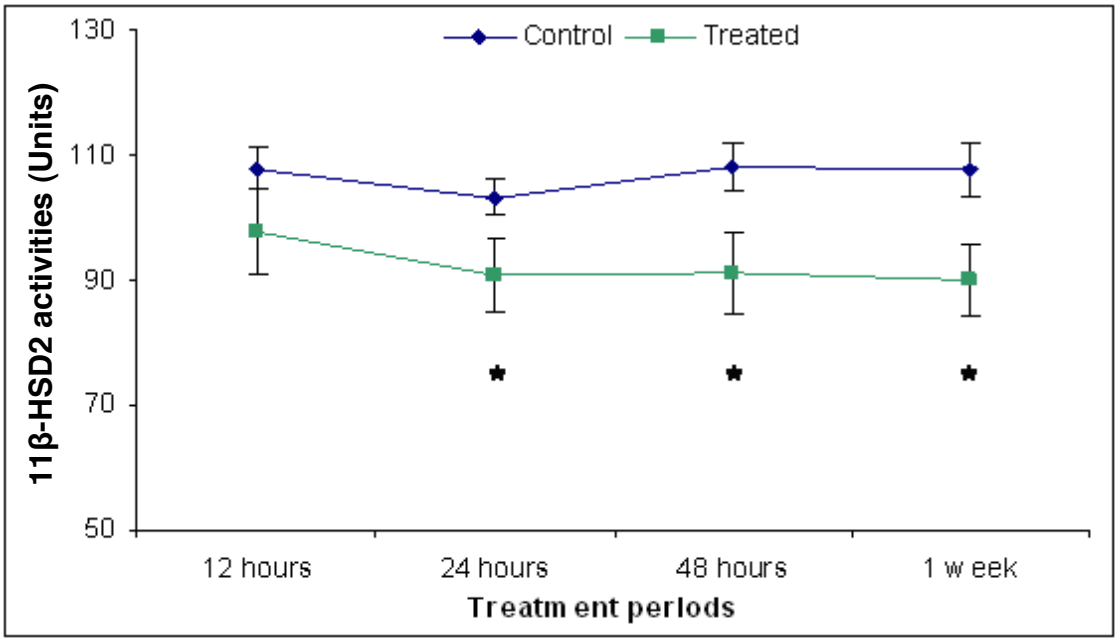

(b) Visceral adipose tissue

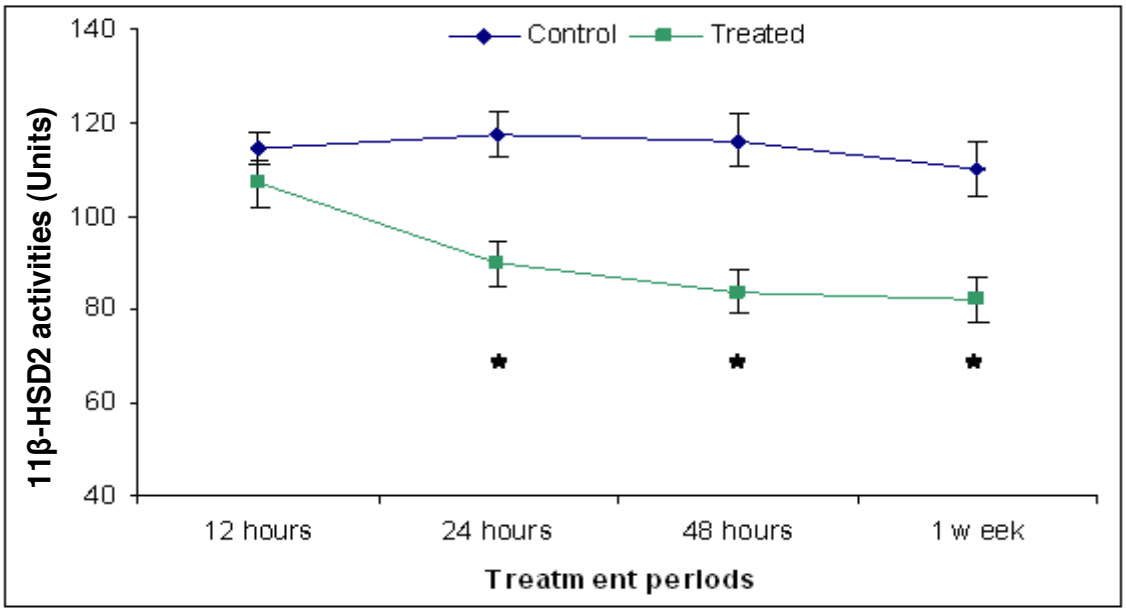

Figures 3.53: 11β-HSD2 activities in (a) subcutaneous and (b) visceral adipose tissues of rats administered with 100 mg/kg GA at various treatment periods (* indicates $P < 0.05$).

(a) Abdominal muscle

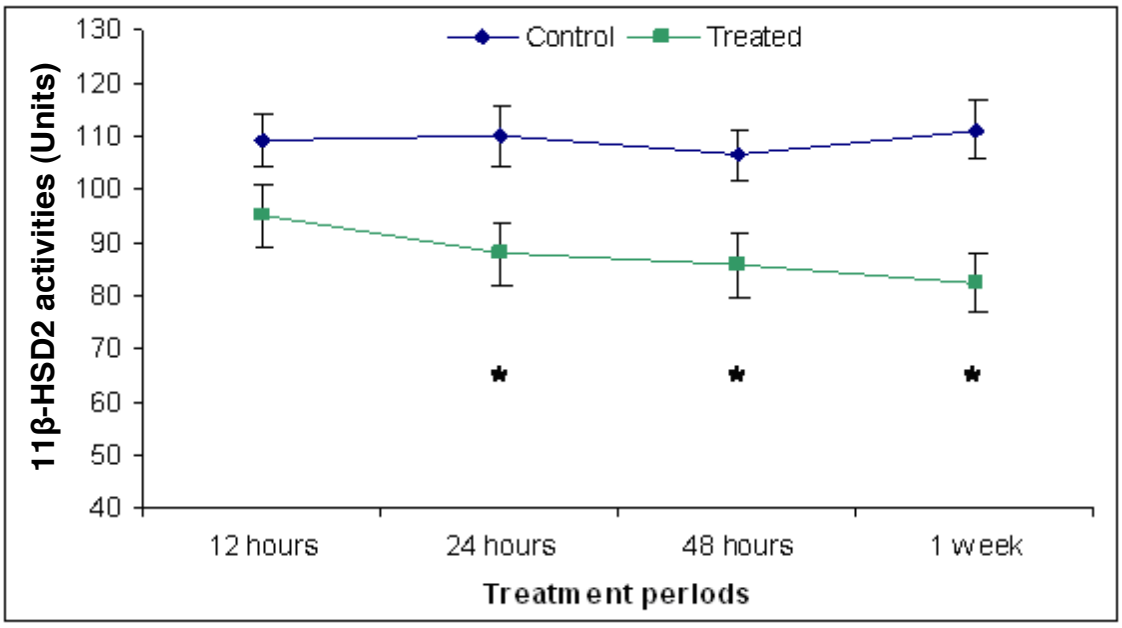

(b) Quadriceps femoris

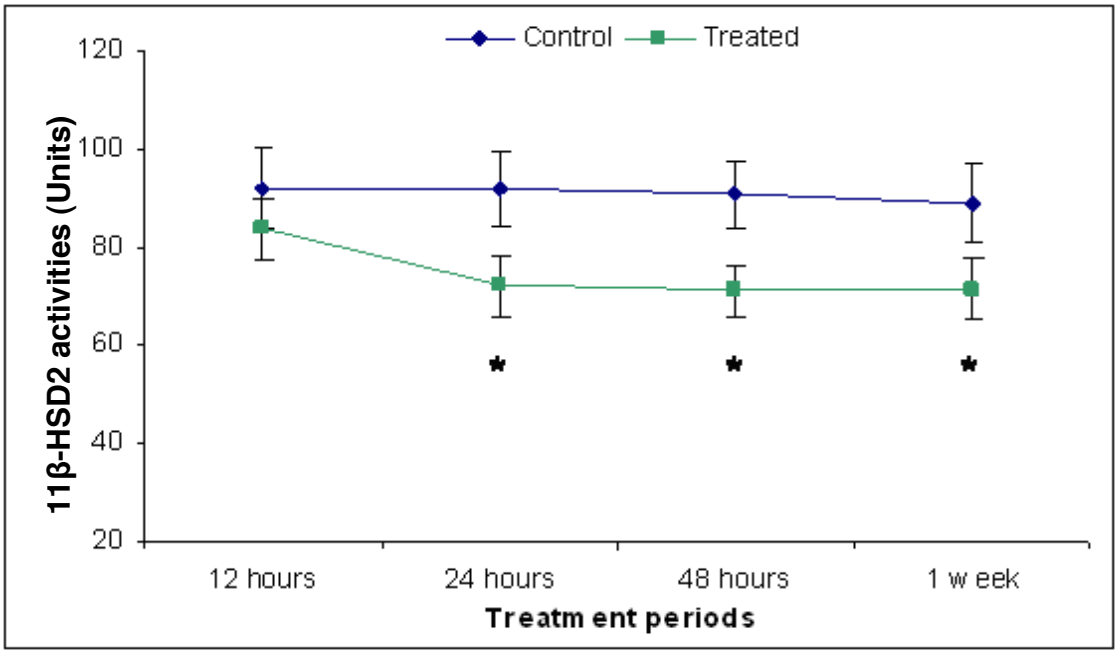

Figures 3.54: 11β-HSD2 activities in (a) abdominal muscle and (b) quadriceps femoris of rats administered with 100 mg/kg GA at various treatment periods (* indicates $P < 0.05$).

(a) Liver

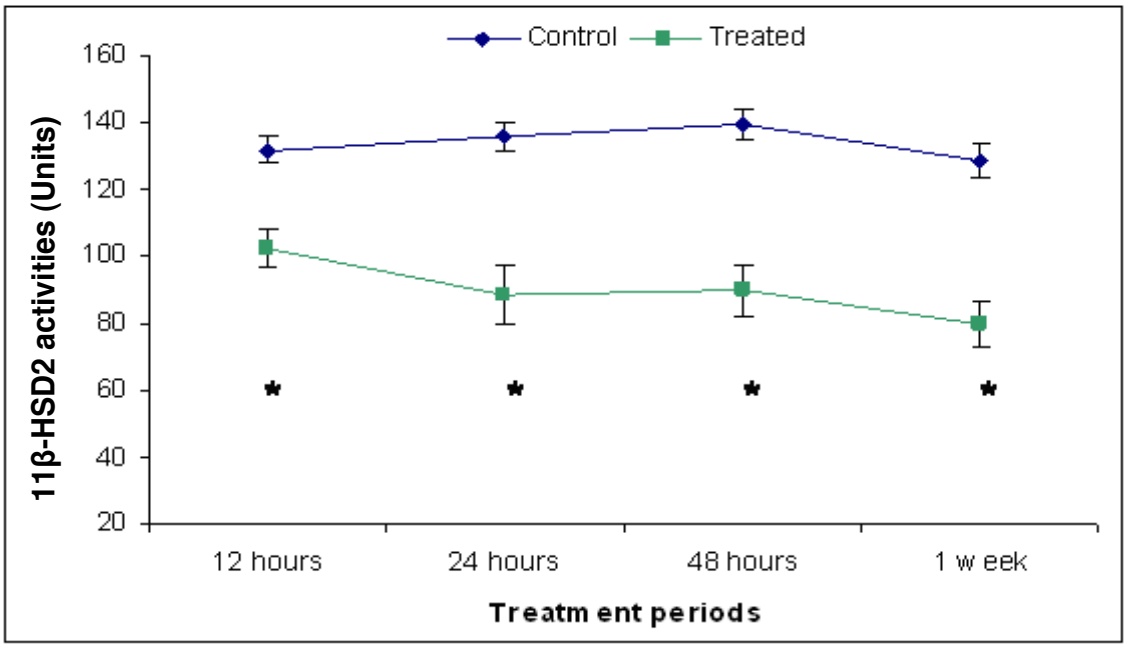

(b) Kidney

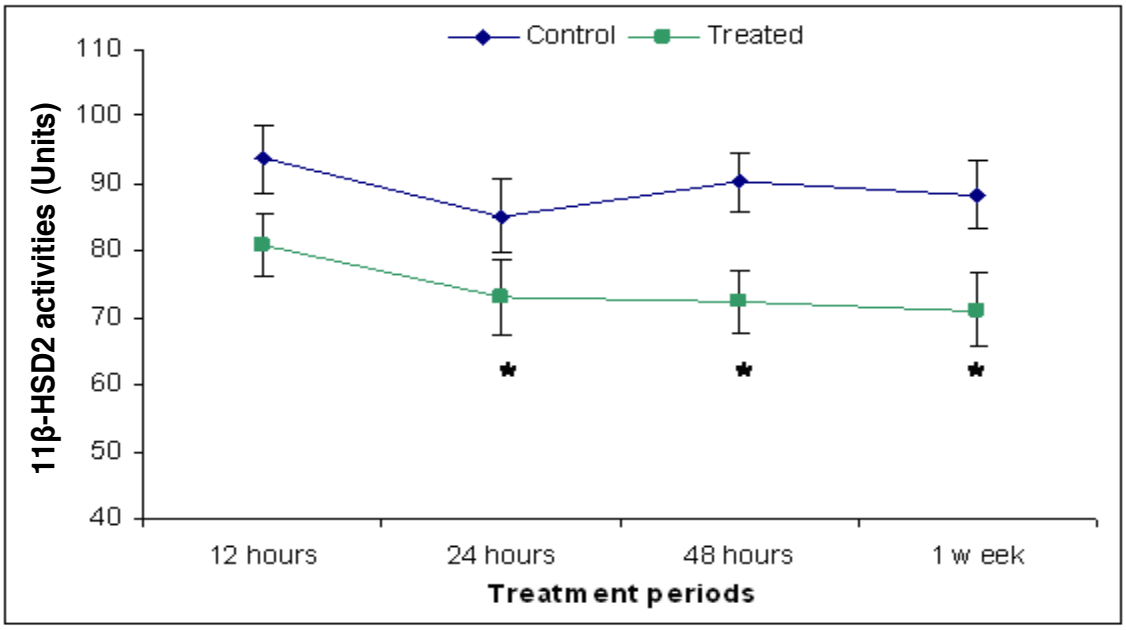

Figures 3.55: 11β-HSD2 activities in the (a) liver and (b) kidney of rats administered with 100 mg/kg GA at various treatment periods (* indicates $P < 0.05$).

Chapter 3

Results

(Part D)

3.4 Conditions shown to give optimal effects of glycyrrhizic acid in rats

Oral and intraperitoneal administrations of GA to the rats were done to determine the most effective route of administration for the compound by measuring the various parameters (i.e., blood glucose and serum insulin levels, lipid profile, expression levels of PPARγ1, PPARγ2 and LPL as well as 11β-HSD1 and 2 activities). No significant difference was seen (see section 3.1). Subsequently, GA was given to the rats orally. Dosages of 25, 50, 75, 100 and 150 mg/kg GA were used to determine the most effective concentration and 100 mg/kg of GA was found to be the optimum concentration as there no significant differences in the rats treated with either 100 or 150 mg/kg GA (see section 3.2). GA treatment was carried out for a period of 12, 24 and 48 hours as well as one week and it was found that one week of GA treatment yielded the optimal effect on the various parameters measured (see section 3.3). Thus, subsequent work was conducted with GA at 100 mg/kg for one week.

3.4.1 Rat tail-cuff pressure measurements

No significant difference ($P > 0.05$) between the tail-cuff pressure readings of both the control and rats treated with 100 mg/kg GA at days 0, 2, 4 and 6 was seen (Figure 3.56).

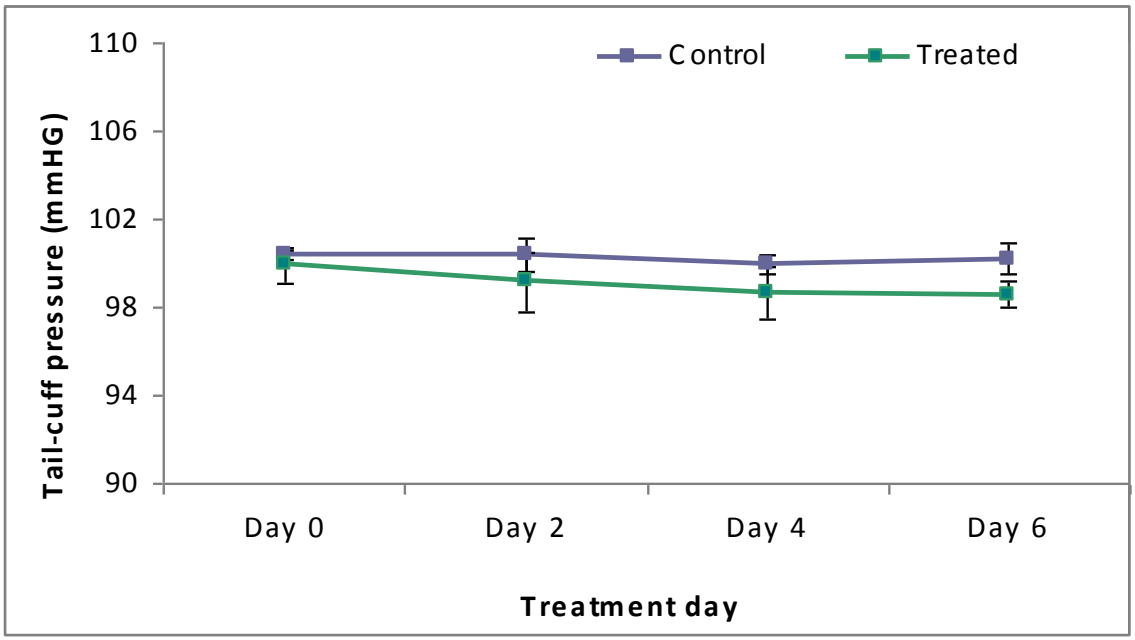

Figure 3.56: Mean tail-cuff pressure of the control and rats administered with 100mg/kg GA over a period of one week.

No significant difference ($P > 0.05$) in the tail-cuff pressure of the control and GA-treated rats was observed.

3.4.2 Summary of the parameters studied

In rats that were orally-administered with 100 mg/kg GA for one week, both blood glucose levels and HOMA-IR values were significantly decreased ($P < 0.05$) by about 65% while serum insulin levels were lowered by about 37% ($P > 0.05$). There were improvements in the lipid profile parameters with a decrease in serum TAG (by 35%), total cholesterol (34%) and LDL-cholesterol (34%) accompanied by an increase (by 22%) in HDL-cholesterol ($P > 0.05$).

Total PPARγ expression levels were significantly increased ($P < 0.05$) by more than 100-fold in the visceral adipose tissues and quadriceps femoris, approximately 80-fold in the subcutaneous adipose tissues and 90-fold in abdominal muscle. The quadriceps femoris also showed more than 100-fold increases in PPARγ1 and PPARγ2 expression levels after one week of GA treatment. LPL expression also showed increased levels with statistically significant increases in the subcutaneous and visceral adipose tissues (51% and 67%, respectively), as well as the abdominal muscle and quadriceps femoris (56% and 67% increases, respectively). 11β-HSD1 was significantly decreased in all studied tissues ($P < 0.05$) except for the subcutaneous adipose tissue while the 11β-HSD2 was significantly decreased in all the six tissues ($P < 0.05$)

Thus 100 mg/kg GA administration orally for one week gave optimum values in all parameters studied. The administration of 100 mg/kg GA for one week resulted in the most statistically significant improvements within the said treatment group as well as between the different treatment groups.

3.4.3 Histological analysis

3.4.3.1 Morphometric analysis of adipose tissues (visceral and subcutaneous)

The size of adipocytes has been implicated as a parameter for differentiation of adipocyte morphology (Bujalska *et al.*, 2007). Figure 3.57 shows tissue sections of adipose tissues in the control and GA-administered rats stained with H&E stain. Areas of roughly 100 adipocytes per tissue section per field view were viewed under 100 × magnifications.

The mean area of both the subcutaneous and visceral adipocytes decreased in the GA-administered group when compared to the control, with a larger reduction observed in the subcutaneous adipocytes. In the visceral adipose tissue, the mean adipocyte area in the control group was 389.37 ± 151.86 μm^2 while that of the GA-administered group was 369.05 ± 115.67 μm^2 (i.e., a reduction of 5.24 %; $P > 0.05$). In contrast, a reduction of 47.62% ($P > 0.05$) in the mean adipocyte area for the subcutaneous adipocytes was observed with the mean adipocyte area of 410.20 ± 150.48 μm^2 in the control group as compared to only 214.86 ± 110.09 μm^2 in the GA-administered group (Figure 3.57).

3.4.3.2 Liver Tissue

Photomicrographs of PAS stained liver slides viewed under 400× magnification (Figure 3.58) showed no structural difference between the control and GA-administered groups. However, a darker magenta colouration was observed in the GA-administered tissue compared to that of the control rats. This could be due to an increase in glycogen content (Kiernan, 1999) as blood glucose levels were significantly reduced.

Similar morphometric analysis of subcutaneous and visceral adipose tissues and liver were observed in rats treated with GA for different dosages and time frame. There

were no morphological differences observed in the abdominal muscle and kidney in rats administered with 100 mg/kg GA for one week (Figure 3.59). Absence of morphological differences was also observed in the abdominal muscle, quadriceps femoris and kidney of rats with the other studied dosages and treatment durations of GA administration.

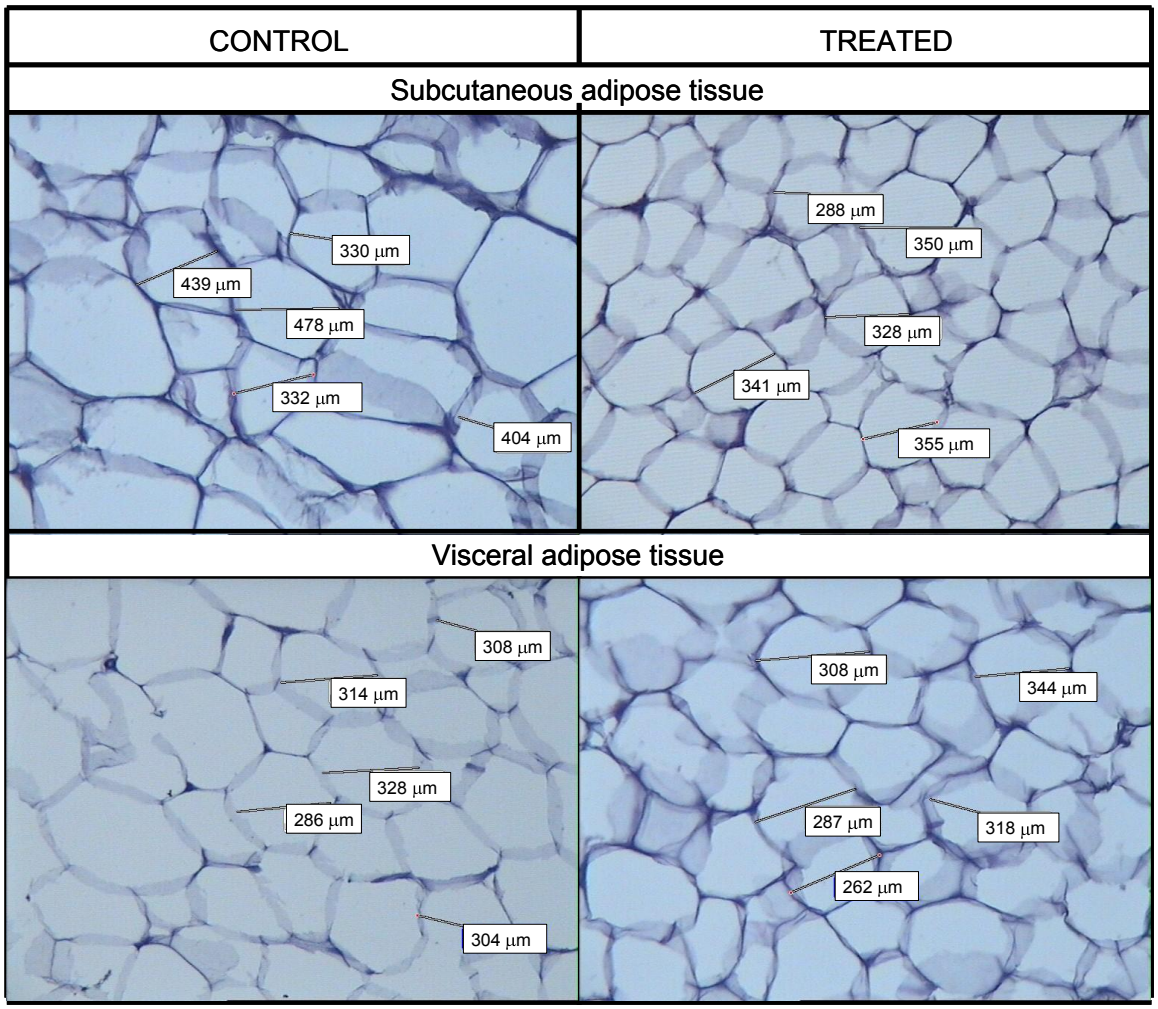

Figure 3.57: Mean area of adipocytes (μm^2) for the subcutaneous and visceral adipose tissues in the GA-treated rats compared with the control rats after one week of oral GA administration.

Note the larger reduction in mean adipocyte area for the subcutaneous adipose tissues as compared to the visceral adipose tissues ($P > 0.05$). Magnification: 400X.

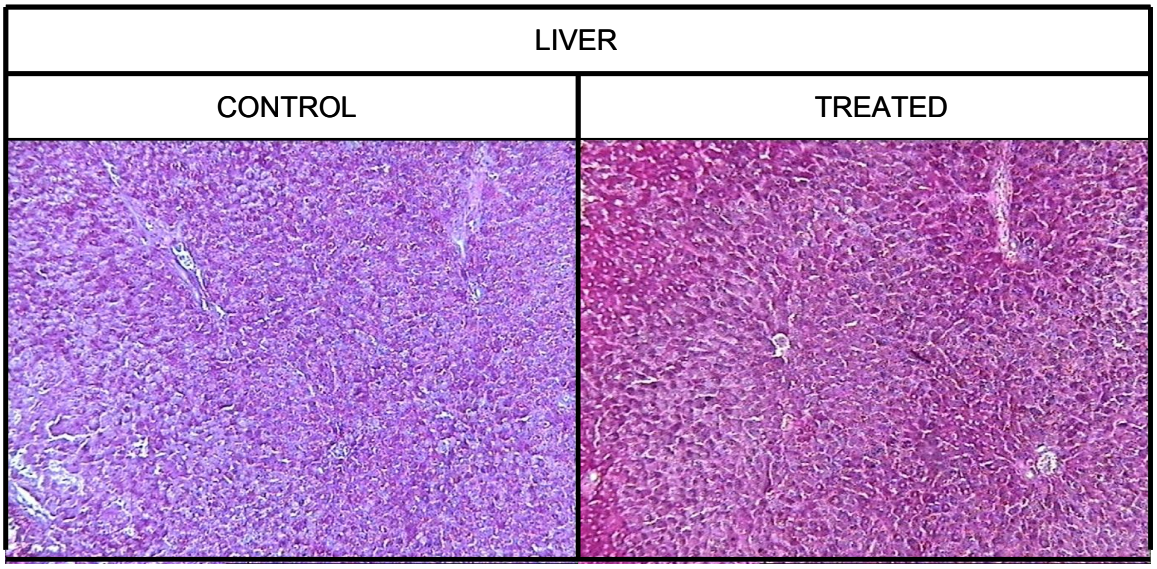

Figure 3.58: The liver tissue of GA-administered rats and control after one week of oral GA administration.

Note the intense magenta in the treated tissue. Magnification: 100X.

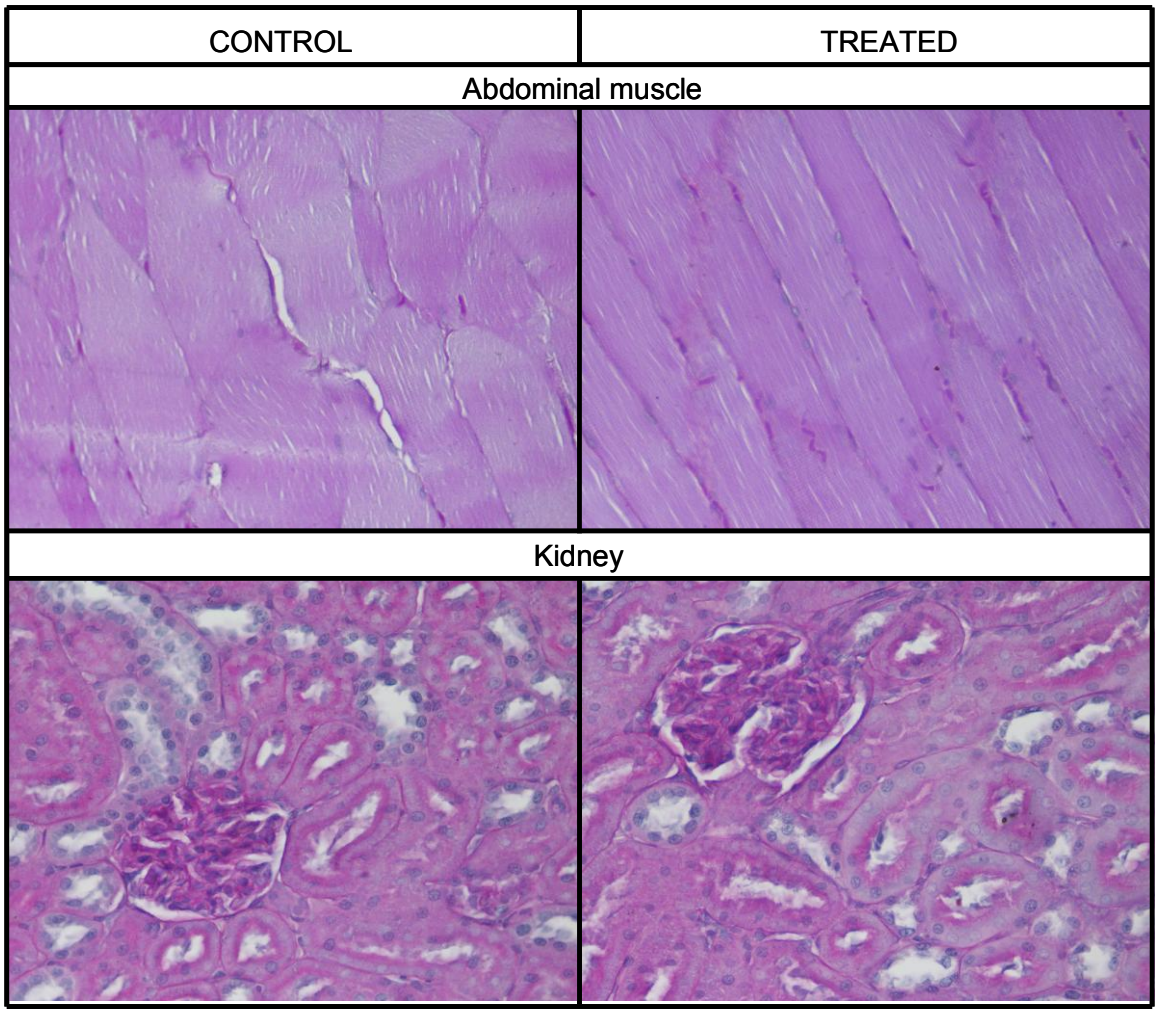

Figure 3.59: The abdominal muscle and kidney of GA-administered rats and control after one week of oral GA administration at 100 mg/kg.

There were no morphological differences observed. Magnification: 400X.

CHAPTER 4

Discussion

Chapter 4

DISCUSSION

Clinical definitions of the metabolic syndrome has been proposed by multiple organizations, with the latest being defined by the American Diabetes Association (ADA) in 2008, preceding the pioneer proposal by the World Health Organization (WHO) in 1998 (Balkau *et al.*, 2007; ADA, 2008). The criteria for the presence of metabolic syndrome are impaired fasting glucose, impaired glucose tolerance or insulin resistance (Hollander and Mechanick, 2008). Insulin is responsible for the regulation of plasma glucose levels by stimulating glucose uptake, metabolism and utilization in peripheral insulin-sensitive tissues (Guo and Tabrizchi, 2006; Wassink *et al.*, 2007). Insulin resistance depicts a state of decreased sensitivity of peripheral tissues towards insulin-stimulated glucose uptake or production leading to compensatory hyperinsulinaemia to maintain homeostasis which contributes towards insulin resistance (Shen, 2007). It also has a close association with genetic predisposition, aging and sedentary lifestyle (Zimmet *et al.*, 2001). Insulin resistance often co-exists with hypertension, dyslipidaemia, atherosclerosis, central obesity (Guo and Tabrizchi, 2006) and often proceeds to T2DM (Koh-Banaerjee *et al.*, 2004). Thus, the hallmark symptoms of the metabolic syndrome involve deviation from normal glucose metabolism, with elevated fasting glucose and insulin levels.

Since the 1940s, therapeutic agents have been used to treat T2DM. In spite of rave reviews regarding their insulin sensitizing capabilities, there are several drawbacks in their use as therapeutic drugs to improve insulin sensitivity (Jermendy, 2007; Rubenstrunk *et al.*, 2007). Thus, the solution would be the use of potential natural ligands which are being unearthed in view of replacing their synthetic counterparts. Glycyrrhizic acid is a natural constituent and active principle of licorice isolated from the dried root of *Glycyrrhiza glabra*. Knowledge of its medicinal properties and use of the plant has been recorded for over 4000 years (Stromer *et al.*, 1993; Ploeger *et al.*, 2001). It has been successfully proven to exhibit PPARγ-ligand binding activity through ligand binding assays (Kuroda *et al.*, 2003; Mae *et al.*,

2003).

Therefore, the effects of GA on PPARγ, 11β-HSD and LPL in relation to glucose and lipid profiles were studied as it has been implicated to improve the metabolic risk factors associated with diabetes mellitus and metabolic syndrome.

4.1 Effects of GA administration by two different routes, dosages and treatment periods

Part A:

Although there are different routes of administration for therapeutic agents, only two routes were evaluated in this study. The rats were subjected to GA administration via two routes: oral and intraperitoneal. Although previous studies have established that administration of GA orally resulted in low bioavailability, the results of the present study has proven that both routes of administration did not portray any significant differences in all the studied parameters (glucose and insulin levels, HOMA-IR, lipid profile, PPARγ and LPL expression as well as 11β-HSD1 and 2 activities).

Significant decrease in 11β-HSD1 and 2 activities were seen only in the liver of GA-administered rats via both routes of administration. This could be due to the influence of the first-pass effect where drugs were first exposed to the liver before reaching the vascular system (Gibaldi and Perrier, 1975). Inhibition of 11β-HSD1 and 2 activities could be seen earlier as GA was reported to be a competitive inhibitor towards these enzymes (Whorwood *et al.*, 1993; Tanahashi *et al.*, 2002) compared to the properties of PPARγ, a type of nuclear receptor which needs a few hours to a few days to demonstrate its cellular effect (Rang *et al.*, 2003).

An example of a parenteral administration method would be the intraperitoneal administration of GA. Advantages of the intraperitoneal administration method over the oral administration method includes rapid, extensive

and predictable delivery of the drug. This would ensure an effective dose of accurately administered drug with direct access to the bloodstream as well as the ability to be instantaneously stopped whenever necessary (Liska, 2004; Brunton *et al.*, 2006). However, there are also several disadvantages associated with the intraperitoneal administration of drugs. The absolute need for sterility, the pain involved in the injection process, the need for slow injection procedures, inability to administer large volumes of drugs and the occasional difficulty for patients to perform injection themselves in times when self-medication is necessary would be the main concerns regarding the suitability of the parenteral administration of drugs (Brunton *et al.*, 2006). Besides injectables costing more than other drug forms, the drug has got to be converted into a solution or a very fine suspension prior to administration (Liska, 2004).

Oral drug administration is widely used and is the most common route of administration (Brunton *et al.*, 2006). In addition to being a simple, safe, cheap and acceptable option to patients (Loh *et al.*, 1993), oral administration is also the most convenient and economical option (Brunton *et al.*, 2006). Several disadvantages of the oral route include the occasional interference of the drug action by food taken concurrently, destruction by digestive enzymes and irregularities in the absorption of drugs based on their physical properties (Brunton *et al.*, 2006).

Despite the poor bioavailability stemming from the degradative processes catalyzed by digestive enzymes in the stomach and poor absorption of drugs from the intestinal tract (Gibaldi and Perrier, 1975), oral administration was utilized for the remainder of the present study because it is a relatively easy method of administration compared to the intraperitoneal route and most importantly, it does not involve invasive procedures and does not cause pain to the rats. The use of oral administration for the remainder of the study was further justified by the absence of any significant differences in all the studied parameters between both the oral and intraperitoneal routes although in theory, the intraperitoneal route should produce a greater response.

Part B:

Upon the determination of the optimal route of GA administration, the effects of different dosages of GA on rats were studied. The dosages administered were 25, 50, 75, 100 and 150 mg/kg. Studies reported by Ishbrucker and Burdock (2006) and Ploeger *et al.* (2001) found that oral administration of GA would only be detectable in the plasma after doses exceeding 50 mg/kg. Ploeger *et al.* (2001) also further fortified the claim on the low oral bioavailability of GA, with plasma levels of GA only detectable after oral doses of 50 – 500 mg/kg. The 25 mg/kg dosage was chosen as it was reported that oral dosages below 25 mg/kg was expected to have no capacity-limited absorption of GA in both rats and humans (Ploeger *et al.*, 2001).

Based on the information, a baseline of 25 mg/kg of GA was orally-administered to the rats to determine the effects of GA on all the studied parameters. The results obtained from the oral administration of 25 mg/kg of GA supported the findings reported by Ishbrucker and Burdock (2006) and Ploeger *et al.* (2001), where there was no significant difference between the GA-administered rats and the control rats in all the studied parameters. The glucose and insulin levels, HOMA-IR, 11β-HSD 1 and 2 activities were reduced while the PPARγ and LPL expression were increased upon oral administration of 25 mg/kg GA, albeit the changes were insignificant.

Therefore, the oral administration of higher dosages of GA was done, with the dosages varying from 25, 50, 75, 100 to 150 mg/kg. Upon administration of the above dosages, a similar trend was observed in all the parameters determined, with the rats administered with both 100 mg/kg and 150 mg/kg of GA displaying the most significant changes in all the parameters. However, there was no significant difference in all the parameters between the rats fed with 100 and 150 mg/kg of GA. This could be due to the saturation of the plasma albumin carrier proteins involved in the binding of both GA and GE (Ploeger *et al.*, 2001). It has been reported that the binding of GA to plasma albumin and its subsequent absorption is saturable at doses of 25mg/kg and above in both rats and humans (Anderson, 2007). The administration of both 100 and 150 mg/kg of GA to the rats resulted in the most improvement in all the parameters.

Since the administration of both 100 and 150 mg/kg displayed no significant differences in all the tested parameters, 100 mg/kg of GA was use for the remainder of the study. The administration of 100 mg/kg of GA to the rats was not toxic as the LD_{50} for GA in rats was reported to be 610 mg/kg (Anderson, 2007).

Part C:

Experiments to establish the optimal GA treatment period were carried out after the optimal route of administration and dosage of GA were determined. The treatment duration evaluated was 12, 24, 48 hours and one week. The 12 hours treatment was chosen as GA has low oral bioavailability and remains in the plasma for over 8 hours (Anderson, 2007). Besides, the time taken for the GE to reach its maximum plasma levels upon oral administration of GA (10 – 480 mg/kg) ranged from 12 to 16 hours (Ploeger *et al.*, 2001). Taking into account both the factors mentioned, the 12-hour treatment was chosen as the starting point. The 24, 48 hours and one week treatment duration was performed to determine the effect of 100 mg/kg GA for longer treatment periods.

Upon completion of the study, it was observed that treatment of 100 mg/kg GA for one week gave the most changes in all the parameters, with more significant improvements compared to the 24- and 48-hour treatment. The results in this study was in concordance with that reported by Nwe *et al.* (2000), where administration of 80 - 100 mg/kg of GA for a duration of one week were found to lower the oxidative activity of 11β-HSD in the testis and liver of rats.

4.2 Blood glucose, serum insulin and HOMA-IR

The occurrence of disorders such as metabolic syndrome and T2DM are usually preceded by the presence of insulin resistance (Ko *et al.*, 2007). Insulin is responsible for the regulation of plasma glucose levels (Wassink *et al.*, 2007). A state of decreased sensitivity of peripheral tissues towards insulin-stimulated glucose

uptake or production leading to compensatory hyperinsulinaemia to maintain homeostasis, contributes towards insulin resistance (Shen, 2007). Hallmark symptoms of metabolic syndrome involve deviation from normal glucose metabolism, with elevated fasting glucose and insulin levels (Batsis *et al.*, 2007).

The rats treated with various dosages of GA and for different time periods displayed lower median blood glucose levels compared to the control (Figures 3.10 and 3.33). Glucose homeostasis was reported to occur within 2 hours after the last carbohydrate meal (Guyton and Hall, 2005). Therefore, in the present study, all the rats were subjected to 12-hr fasting blood glucose in order to represent the hepatic output via glycogenolysis.

Takii *et al.* (2001) and Francis *et al.* (2002) reported that the absence of hyperglycaemic conditions in the GA-administered rats could be attributable to the inhibition of active Na^+-glucose co-transport system in the small intestine, which in turn inhibits active glucose transport across the brush border. This system could be inhibited by the triterpene saponin structure of GA, which in turn negates the rapid and drastic postprandial blood glucose rise, ultimately leading to improved insulin sensitivity.

Although numerous studies have reported on the blood glucose lowering effect of GA, the exact regulatory mechanism has yet to be fully established. Based on studies done by Takii *et al.* (2001) and Nakagawa *et al.* (2004), normal and obese genetically diabetic KK-A^y mice given ethanolic extract of licorice roots displayed suppression of blood glucose levels, with the latter attributing the effect to activation of PPARγ.

Activation of PPARγ decreases blood glucose levels through the inhibition of glucagon gene transcription and secretion (Krätzner *et al.*, 2008). The action of glucagon opposes those of insulin, promoting glycogenolysis and gluconeogenesis, which ultimately enhances hepatic glucose output. PPARγ activation has been shown to inhibit the transcriptional activity of PAX6, a transcription factor pivotal to the α-cell-specific activation of the glucagon gene (Krätzner *et al.*, 2008). In a study reported by Kuroda *et al.* (2003), the administration of GA and TZDs to genetically

diabetic KK-A^y rats significantly decreased blood glucose levels, prompting the researchers to speculate that both GA and TZDs possessed a similar biological mechanism.

PPARγ activation in the adipose tissue has been shown to increase the expression of glucose transporter isotype 4 (GLUT4) and c-Cbl associating protein (CAP) which plays an important role in translocating GLUT4 to the cell surface (Wu *et al.*, 1998; Baumann *et al.*, 2000). The glucose transporters are glucose sensors for glucose stimulating insulin sensors (GSIS), where a decrease in the expression results in a decrease in glucose threshold for insulin secretion. Thus, the activation of PPARγ could lead to restoration of the glucose-sensing ability which activates GLUT 4 gene expression and leads to an increase in glucose uptake (Kim and Ahn, 2004).

The decrease in blood glucose could also be attributable to the inhibition of 11β-HSD. GA and GE are non-selective inhibitors of 11β-HSD activity (Ishbrucker and Burdock, 2006). Of particular interest is the inhibition of 11β-HSD 1 activity, which would lead to potential accumulation of peripheral glucocorticoids as 11β-HSD 1 is responsible for the interconversion of active glucocorticoids to their inactive 11-keto derivatives (Tomlinson *et al.*, 2004; Draper and Stewart, 2005). Thus, inhibition of 11β-HSD 1 has the potential of reducing blood glucose level through the prevention of insulin antagonism (Whorwood *et al.*, 2002).

Glucocorticoid (GC), a functional antagonist of insulin, is able to decrease insulin sensitivity in the liver and peripheral organs (Tomlinson and Stewart, 2007; Vegiopoulos and Verzig, 2007). GC is able to increase blood glucose by (1) increasing gluconeogenesis in the liver by increasing the rate-limiting enzymes phosphoenolpyruvate carboxykinase (PEPCK) and glucose-6-phosphatase (G6Pase), (2) increasing gluconeogenic substrate (amino acids and glycerol) by inducing proteolysis and lipolysis in the skeletal muscles and adipose tissues respectively, (3) decreasing insulin secretion from the pancreatic β-cells and (4) decreasing peripheral tissue glucose uptake through inhibition of insulin-stimulated glucose uptake by opposing the translocation of GLUT4 translocation to the cell surface membrane (decreases insulin sensitivity) (Dimitriadis *et al.*, 1997; Andrews *et al.*, 2003;

Cassuto *et al.*, 2005; Tomlinson and Stewart, 2007; Vegiopoulos and Verzig, 2007).

Both 11β-HSD1 inhibition and PPARγ agonism are associated with reduced expression of PEPCK and G6Pase (Alberts *et al.*, 2002; Kim and Ahn, 2004), the two rate-limiting enzymes of the gluconeogenesis pathway that is abnormally induced in T2DM patients (Vegiopoulos and Herzig, 2007). Alberts *et al.* (2002) reported that uncontrolled and accelerated gluconeogenesis contributes to at least 90% of the hepatic glucose output in T2DM patients and is therefore a significant contributor to hyperglycaemia.

Therefore, GA might have a glucose-lowering effect through increased PPARγ activation and inhibition of 11β-HSDs. This was supported by the results in this study as there was a significant decrease in the blood glucose levels as well as an increase in the glycogen storage in the liver as demonstrated by histological studies (Figure 3.58).

From the present study, it was observed that the serum insulin levels in the GA-administered rats were lower than those of the control rats. The decrease in the serum insulin levels could be attributed to the insulin sensitization properties due to the activation of PPARγ. Under a normoglycaemic state, circulatory insulin would oversee the suppression of hepatic glucose production and enhancement of glucose uptake by peripheral organs (Guo and Tabrizchi, 2006). Activation of PPARγ could have been responsible for the drop in the serum insulin levels in the GA-administered rats. Kim and Ahn (2004) has reported that PPARγ activation has the ability to restore both GLUT 2 and glucokinase (GK) expression which ultimately decreases insulin secretion and lowers serum insulin levels. This is because both the GLUT 2 transporter and the enzyme GK are components of the glucose-sensing apparatus of the β-cells whose expression are decreased in diabetes (Kim and Ahn, 2004). The pancreatic β-cells are able to sense the changes in blood glucose levels through GLUT2 and GK (Marty *et al.*, 2005) and therefore decreases the glucose-stimulated insulin secretion (GSIS) (Davani *et al.*, 2000; Swali *et al.*, 2008). The consequences of the enhanced glucose sensing apparatus include the restoration of normal β-cell function and protection against apoptosis, which ultimately allows for a reduction in insulin secretion (Kim and Ahn, 2004).

Results from this study concurred with the findings reported by Takii *et al.* (2001) and Jiang *et al.* (2002). Jiang *et al.* (2002) reported that oral administration of 30mg/kg of a PPARγ agonist to genetically obese Zucker (*fa*/*fa*) rats for seven days led to a reduction in insulin levels while Takii *et al.* (2001) fed GA to diabetic KK-A^y mice for seven weeks and reported a decrease in the serum insulin levels.

The decrease in serum insulin levels in the GA-administered rats may be due to (1) a decrease in blood glucose thus decreasing the pancreatic GSIS and (2) a decrease in compensatory insulin secretion due to an increase in the insulin sensitivity of the liver and peripheral tissues as a result of the inhibition of 11β-HSD1 (Guyton and Hall, 2005).

The use of TZDs has also been known to exert beneficial effects on the pancreatic β-cells, where its anti-hyperinsulinaemic actions interrupt the compensatory increase in insulin secretion during deterioration of insulin resistance states. In a study done by Buckingham *et al.* (1998), systemic clearance of insulin was not affected although administration of TZD to Zucker fatty rats caused a reduction in pre-proinsulin mRNA. Nevertheless, a reduction in demand for insulin is followed by a reduction in its synthesis, an indirect indication of improved insulin sensitivity. Thus, it could be proposed that the reduction in insulin levels in this study was due to an improvement in insulin sensitivity upon GA administration.

An increase in insulin sensitivity was observed as the activation of PPARγ promotes adipocyte differentiation and apoptosis in the subcutaneous and visceral adipose tissues respectively (Kota *et al.*, 2005; Guo and Tabrizchi, 2006). The presence of small and more insulin-sensitive adipocytes increases insulin sensitivity and thus decreases the amount of insulin secreted by the pancreatic β-cells (Kota *et al.*, 2005; Guo and Tabrizchi, 2006). In addition, the activation of PPARγ regulates the adipocyte hormone gene expressions to improve insulin sensitivity. Activation of PPARγ increases the adiponectin expression, which potentiates insulin sensitivity in the liver and skeletal muscles (Berger *et al.*, 2005) while a concurrent decrease in the production of leptin, resistin, tumour necrosis factor-α (TNF-α), interleukin-6 (IL-6) and 11β-HSD1 ameliorates the potential existence of insulin resistance (Rangwala

and Lazar, 2004). Thus, the activation of PPARγ would lead to enhanced insulin sensitivity.

Subsequently, with reduction in both blood glucose and serum insulin, the GA-administered rats developed a lower HOMA-IR, denoting higher insulin sensitivity compared to the control. The HOMA-IR is used for the assessment of insulin sensitivity, a higher value indicating lower insulin sensitivity (higher insulin resistance) and vice versa (Wallace *et al.*, 2004). Improvements in insulin sensitivity following GA administration are in agreement with studies reporting similar results, via 11β-HSD1 inhibition and PPARγ activation (Alberts *et al.*, 2003; Andrews *et al.*, 2003; Berthiaume *et al.*, 2004).

There was a significant decrease in the HOMA-IR index for the GA-administered rats compared to the control rats. By virtue of the ease in obtaining measurements of insulin resistance and its increasing frequency of use in studies, HOMA-IR is the preferred and reliable method of measuring insulin resistance (Miranda *et al.*, 2005). Since HOMA-IR is a yardstick for measurement of insulin resistance, the results indicated that the oral administration of 100 or 150 mg/kg GA for one week was sufficient to improve insulin sensitivity in rats.

4.3 Total PPARγ, PPARγ1 and PPARγ2 expression

4.3.1 Liver

Results from the present study indicated that the expression levels of total PPARγ, PPARγ1 and PPARγ2 were higher in the GA-administered rats compared to the control rats. The expression levels of PPARγ1 in rats of both groups were observed to be higher than those of PPARγ2. This is in agreement with the results reported by Guo and Tabrizchi (2006). Alternative promoter splicing is the determining factor for which type of PPARγ is synthesized and under normal physiological conditions, PPARγ1 was known to be the dominant type of PPARγ present in the liver. The presence of increased circulating fatty acids in obese mice was noted to induce specific activation of the PPARγ2 promoter to increase its

synthesis in the liver, a tissue with predominant PPARγ1 expression (Vidal-Puig *et al.*, 1996). However in this study, normal lean rats were used thus the higher expression levels of PPARγ1 were seen.

The importance of PPARγ has been highlighted by its role in adipocyte differentiation and insulin sensitization (Kota *et al.*, 2005) and is characterized by the adipose-specific expression of PPARγ2 (Rangwala and Lazar, 2004). Although the liver is an organ involved in glucose and lipid metabolism, only low levels of PPARγ (PPARγ1 and PPARγ2) were detected in the liver (Rangwala and Lazar, 2004). Low levels of PPARγ2 expression in the liver in this study were consistent with findings by Boelsterli and Bedoucha (2002) and Heikkinen *et al.* (2007). However, Boelsterli and Bedoucha (2002) reported that the up-regulation of PPARγ in the liver could be due to nutritional status and the presence of natural ligands.

Activation of PPARγ could likely be the cause of the increase in the total PPARγ, PPARγ1 and PPARγ2 expressions. Davies *et al.* (1999) has proven that hepatic total PPARγ mRNA and protein levels were up-regulated upon oral administration of an agonist, TZD to male Sprague Dawley rats. Although the exact mechanism involved in the activation of PPARγ in the liver remains unknown, it has been postulated that a circulating factor might be responsible for the stimulation of hepatic total PPARγ transcription during a state of increased energy availability (Chao *et al.*, 2000; Boelsterli and Bedoucha, 2002).

The up-regulation of hepatic total PPARγ would in turn activate several genes such as adipocyte fatty acid binding protein (aP2) and fatty acid translocase (FAT/CD36), previously present only in trace amounts in the liver of lean mice. Activation of aP2 in the liver prevents the detrimental effects of free fatty acids on cells and membranes while that of FAT/CD36 facilitates fatty acid transport, which ultimately lowers serum triacylglycerol levels and improves insulin sensitivity (Memon *et al.*, 2000).

Gavrilova *et al.* (2003) reported that PPARγ-knockout mice were found to display a delay in hepatic triacylglycerol uptake which ultimately leads to hyperlipidaemia, hyperglycaemia and hyperinsulinaemia. Murine models such as

ob/ob (leptin-deficient mice) and *db/db* mice (leptin receptor-deficient mice), have been shown to exhibit an up-regulation of hepatic PPARγ mRNA and protein expression levels (Chao *et al.*, 2000; Memon *et al.*, 2000; Bedoucha *et al.*, 2001; Boelsterli and Bedoucha, 2002).

4.3.2 Kidney

Dobrian (2006) and Guo and Tabrizchi (2006) reported that expression of PPARγ in the kidneys is low compared to those of the adipose tissues, complementing the fact that the kidney is not the main regulatory organ involved in lipid and glucose homeostasis. The results in our present study concur with the above work as the kidney of GA-administered rats displayed a lower PPARγ expression compared to the other tissues studied.

The PPARγ expression in the kidneys are constitutively expressed together with retinoid X receptor (RXR) in the inner medullary collecting ducts, glomeruli (Iglesias and Diez, 2006), proximal tubules, thick ascending limb of Henle's loop and renal microvascular endothelial cells in rats (Dobrian, 2006). The up-regulation of total PPARγ, PPARγ1 and PPARγ2 in the kidney, similar to those of the present study is postulated to bestow certain beneficial effects. The presence of PPARγ expression in the kidney suggests the potential regulation on renal sodium transport (Heikkinen *et al.*, 2007) and systemic fluid retention (Dobrian, 2006). Specific involvement of PPARγ in fluid metabolism was demonstrated in a murine model with collecting duct-specific ablation of PPARγ (Guan *et al.*, 2005; Zhang *et al.*, 2005). It was depicted that the activation of PPARγ by TZDs may potentially ameliorate elevated blood pressure in obesity-induced hypertension and renal injuries associated with obesity and insulin resistance in rats (Guan, 2004; Ruan *et al.*, 2008). Most importantly, the activation of PPARγ may render renoprotective effects on the kidneys through improved glucose metabolism (Chung *et al.*, 2005).

Although the activation of PPARγ potentiates renoprotection upon the kidneys; the exact mechanism remains unclear (Chung *et al.*, 2005). It has been widely reported that the renoprotective effects of PPARγ involves protection against diabetic nephropathy (Guan, 2004; Ruan *et al.*, 2008). Comparative studies done on

PPARγ agonists such as TZDs and other oral hypoglycaemic agents such as metformin and sulphonylurea exhibited similar glycaemic control but PPARγ agonists confer superior renal protection on type 2 diabetes models (Guan, 2004; Chung *et al.*, 2005; Ruan *et al.*, 2008). However, it has been found that the mechanism of renoprotection conferred by PPARγ activation is multifactorial and the roles of PPARγ in the kidney are governed by the location of PPARγ expression (Chung *et al.*, 2005).

Studies based on agonist activation of PPARγ by TZDs have proven the nephroprotective effect on the kidneys. Not only is the presence of microalbuminuria often associated with insulin resistance, it is also a predictive tool for future clinical proteinuria and increased risks of cardiovascular mortality (Buckingham *et al.*, 1998). It is also present in the World Health Organization clinical definition of metabolic syndrome in 1998 (Chew *et al.*, 2006). Thus, in the present study, the potential glycaemic control exerted by the kidneys could be due to the activation of PPARγ which could reduce the incidence of albuminuria through decreased excretion of urinary albumin as reported by Guan (2004) and Ruan *et al.* (2008).

Several other mechanisms could be implicated with the up-regulation of total PPARγ, PPARγ1 and PPARγ2 in the present study. In the glomerular mesangial cells, PPARγ activation suppresses the collagen I and fibronectin expression, thus displaying its anti-inflammatory and anti-fibrotic effects (Ricote *et al.*, 1998; Guytom *et al.*, 2001; Zheng *et al.*, 2002). Up-regulation of PPARγ expression in the kidneys has also been known to exert a vascular protective effect by attenuation of oxidative and nitrative stresses (Bagi *et al.*, 2004). Further vascular protective effects were observed through the reduction in the thickness of the common carotid artery (Sidhu *et al.*, 2004) by inhibition of smooth muscle proliferation (de Dios *et al.*, 2003).

The activation of PPARγ also leads to the inhibition of the renin-angiotensin system (RAS) in the kidney. This prevents the inflammatory processes associated with RAS activation (Chung *et al.*, 2005; Dobrian, 2006). Alleviation of RAS is also beneficial as angiotensin II is an important mediator in the pathogenesis of diabetic renal diseases. Activation of PPARγ also promotes anti-apoptotic effects (Chung *et*

al., 2005). Thus the role of GA as a potential agonist for PPARγ might render renoprotective effects in addition to its glycaemic control.

Such observations may possibly suggest additional role of GA against diabetic nephropathy besides its hypoglycaemic effects and improvement in insulin sensitivity (Mae *et al.*, 2003; Nakagawa *et al.*, 2004).

4.3.3 Skeletal muscles

Hevener *et al.* (2003) reported that PPARγ plays a crucial role in skeletal muscle insulin sensitivity and its agonistic action has an indirect effect on insulin action in the liver and adipose tissues. The expression levels of PPARγ in the muscles were low compared to those of adipose tissues (Henever, *et al.*, 2003), comprising only five to ten percent of the PPARγ expression in adipose tissues (Loviscach *et al.*, 2000). The results from our study is in agreement to those reported by Loviscach *et al.* (2000), where the expression levels of both abdominal and quadriceps femoris muscles were lower compared to adipose tissues. The expression levels of total PPARγ, PPARγ1 and PPARγ2 were significantly increased in the abdominal and quadriceps femoris muscle of GA-administered rats compared to the controls.

Muscles are pivotal tissues in glucose homeostasis and it is the primary organ for the insulin-stimulated glucose disposal, contributing to at least 70% of insulin-stimulated glucose disposal (Semple *et al.*, 2006). Due to the large relative mass of muscle in the body, a minute change in the PPARγ activity might result in significant metabolic effects (Heikkinen *et al.*, 2007). Thus, the increase in PPARγ expression in the GA-administered rats suggests possible up-regulation by GA. Increase in PPARγ expression correlates with enhanced insulin-stimulated glucose uptake into the muscles mediated by increased insulin-stimulated phosphatidylinositol-3-kinase (PI3K) activity and translocation of GLUT4 towards the cell membrane (Cha *et al.*, 2001; Semple *et al.*, 2006). Thus, the significant increase in total PPARγ expression of the quadriceps femoris muscle in the GA-administered rats were probably due to the enhancement in insulin-stimulated glucose uptake mechanisms. Guri *et al.* (2006)

reported that muscles are responsible for up to 80 percent of glucose uptake in the body and it seems likely that the significant reduction in blood glucose may be attributed to the muscle-specific glucose uptake through the GA-inducible PPARγ up-regulation pathways.

Heikkinen *et al.* (2007) reported that muscle-specific disruption of PPARγ based on a murine model, highlighted the importance of PPARγ in the skeletal muscle. The lack of PPARγ expression in the muscle tissues could result in the development of severe insulin resistance, which was characterized by postprandial hyperglycaemic and hyperinsulinaemic conditions accompanied by increased in white adipose tissues (Heikkinen *et al.*, 2007). Thus, this is the first direct evidence of the role of PPARγ in coordinating glucoregulatory responses in the skeletal muscles (Hevener *et al.*, 2003).

Although treated with TZDs, muscle-specific PPARγ-deficient mice displayed severe muscle insulin resistance which ultimately led to hyperinsulinaemia, glucose intolerance and hypertriglyceridaemia. This provided an indication that skeletal muscles are the direct targets of PPARγ activation and the absence of up-regulation in the skeletal muscles could lead to the failure to enhance insulin-mediated glucose uptake and insulin sensitivity (Heikkinen *et al.*, 2007).

In our present study, lipoprotein lipase (LPL) also displayed a significant fold difference in the abdominal muscle and quadriceps femoris when relative quantification of LPL was done. LPL was reported to be a downstream gene that is regulated by activation of PPARγ, where an increase in the expression of PPARγ would lead to an increase in the expression of LPL (Desvergne and Wahli, 1999). Thus, the increase in PPARγ expression in the present study was accompanied by a similar significant increase in LPL gene expression.

Based on histological studies on GA-administered rats by our research group, minimal lipid storage was observed in the skeletal muscles (unpublished results), thus indicating that the skeletal muscles are not the major targets of PPARγ activation. Muscle and adipose-specific GLUT4 inhibition could result in insulin resistance (Smith, 2002). Muscle GLUT4 depletion could lead to increased glucose

uptake by adipose tissue and ultimately cause an increase in adipose tissue mass (Smith, 2002). Semple and co-workers reported that more concrete studies on the enhancement of insulin-stimulated glucose uptake needs to be done as the muscle-specific roles of PPARγ still remains elusive due to the complex metabolic cross-talk between different insulin-sensitive organs (Semple *et al.*, 2006).

4.3.4 Adipose tissues

Up-regulation of total PPARγ, PPARγ1 and PPARγ2 expression levels in both the visceral and subcutaneous adipose tissues of GA-administered rats were seen. Adipose tissues of different anatomical locations have different physiological and biochemical properties (Rodriguez *et al.*, 2004). It was found that deposition of adipose tissues at different anatomical positions, particularly in the visceral region seems to portray positive corelation with the development of metabolic syndrome and T2DM (Montague *et al.*, 1998).

Camp *et al.* (2002) reported that the PPARγ expression is the highest in adipose tissues, regardless of the isoform, due to the importance of PPARγ in adipogenesis and adipocyte differentiation as well as insulin sensitization (Kota *et al.*, 2005). The results in the present study is in concordance to those reported by Camp *et al.* (2002), where the expression of both PPARγ isoforms were the highest in the adipose tissues. However, the PPARγ2 isoform has been implicated to be more important in adipogenesis as a 95% reduction of PPARγ2 expression in adipose tissues resulted in complete failure to perform adipogenesis. Camp *et al.* (2002) showed that when both PPARγ1 and PPARγ2 were exogenously delivered into deficient PPARγ cells, the over-expression of PPARγ1 had no effect while complete restoration of adipogenesis properties were observed with PPARγ2. The accumulation of fats in the visceral adipose tissue is directly proportional to risk of diabetes and cardiovascular complications compared to an increase in the subcutaneous adipose tissues (Boyko *et al.*, 2000; Cartwright *et al.*, 2007).

Thus, the up-regulation of PPARγ2 observed in the present study might have led to the stimulation of adipocyte differentiation of pre-adipocytes to form smaller but more insulin sensitive adipocytes (Guo and Tabrizchi, 2006). It was reported that an increase in the number of smaller and more insulin sensitive adipocytes by at least four fold could occur (Okuno *et al.*, 1998).

The activation of PPARγ could lead to the increase in the expression of genes which promote adipocyte differentiation like CCAAT/enhancer-binding proteins (C/EBPs) (Camp *et al.*, 2002) and sterol regulatory element binding protein 1 (SREBP-1) (Spiegelman and Flier, 1996). The development of smaller adipocytes is focused in the subcutaneous sites rather than the visceral region and this would increase the uptake of free fatty acids released from the hypertrophied adipocytes in the visceral region. Activation of PPARγ also regulates certain genes that are pivotal in lipid storage and metabolism such as phosphoenolphyruvate carboxykinase (PEPCK), LPL, acyl CoA synthase (ACS), fatty acid-binding-protein (aP2) and fatty acid transport protein-1 (FATP-1) to ultimately retain the mature adipocyte phenotype upon differentiation, through a positive feedback reaction (Fajas *et al.*, 1998; Auwerx, 1999). Increased expression of pre-adipocyte differentiation promoting genes in the subcutaneous adipose tissues could provoke the formation of insulin sensitive adipocytes which permits the increase of triacylglycerol storage in the subcutaneous adipose tissue (Gilde *et al.*, 2006). Based on the present histological analysis, the GA-administered rats displayed smaller adipocytes in the subcutaneous adipose tissues as opposed to those in the control group. Since the accumulation of free fatty acids in the visceral adipose tissues contribute to an increased risk of developing diabetes mellitus and metabolic syndrome, the repartitioning of fatty acids towards the subcutaneous adipose tissue caused by the apoptosis of mature adipocytes and stimulation of adipocyte differentiation confers a beneficial effect (Guo and Tabrizchi, 2006). GA induced PPARγ up-regulation proves to be beneficial in terms of decreasing fat storage in visceral adipose tissue (reducing visceral obesity) by redirecting the deposition towards the subcutaneous adipose tissues (Glide *et al.*, 2006) thereby decreasing the risk of developing T2DM and metabolic syndrome.

Although PPARγ2 is the main isoform of PPARγ involved in adipogenesis, the presence of PPARγ1 in adipocytes may indicate its involvement in adipogenesis as well. It has been postulated that PPARγ1 may function as a priming factor along with the C/EBPs or that it produces endogenous PPARγ ligands for the later stages of adipogenesis to sustain the expression of the mature adipocyte phenotype (Camp *et al.*, 2002).

Adipose tissues also function as an endocrine organ that secretes hormones and cytokines which would affect energy metabolism (Kota *et al.*, 2005). The up-regulation of PPARγ2 observed in our study could have caused the inhibition of pro-inflammatory adipokines such as interleukin-6 (IL-6) and tumour necrosis factor α (TNF-α). Both inflammatory mediators have been reported to cause insulin resistance by interfering with the normal signaling cascade of insulin receptors (Picard and Auwerx, 2002; Rangwala and Lazar, 2004; Kota *et al.*, 2005).

PPARγ2 activation could also down-regulate the expression of leptin and resistin. Leptin is responsible for the regulation of body weight through inhibition of feeding behavior (Camp *et al.*, 2002) while resistin causes insulin resistance (Guo and Tabrizchi, 2006). A hormone secreted by adipocytes, adiponectin, may be up-regulated by the activation of PPARγ and was noted to increase muscle fatty acid oxidation and improve insulin action to ameliorate insulin resistance (Camp *et al.*, 2002). Increased levels of adiponectin confer insulin sensitivity to skeletal muscles and liver as well. In the liver, adiponectin inhibits gluconeogenesis through a reduction in the both the PEPCK and glucose-6-phosphatase expression while increased fatty acid oxidation in the skeletal muscles enable enhanced glucose uptake (Gilde *et al.*, 2006; Waki and Tontonoz, 2006). Up-regulation of PPARγ also causes an increase in GLUT4 and c-Cbl associating protein (CAP), both pivotal for the translocation of GLUT4 to the cell surface for enhanced glucose uptake (Camp *et al.*, 2002; Guo and Tabrizchi, 2006). Thus, the up-regulation of PPARγ2 expression observed in the present study could have improved insulin sensitivity through the regulation of adipokine (increase adiponectin secretion) and adipose tissue inflammatory mediators (down regulation of TNF-α and IL-6).

Histological analysis showed a decrease in adipocyte sizes in the visceral adipose tissues in the present study, thereby suggesting potential repartitioning of free fatty acids from visceral adipose tissues to subcutaneous adipose tissues induced by PPARγ activation. However, repartitioning of free fatty acids causes obesity, which is a risk factor itself for the development of metabolic syndrome and diabetes mellitus. It has been proven that visceral fat is more lipolytic and thus increases the efficiency in the delivery of free fatty acids to organs such as the liver and skeletal muscle which would then lead to insulin resistance. However, increased subcutaneous adipose tissue has less detrimental effects as the smaller and more insulin sensitive adipocytes would reduce the circulatory free fatty acids and prevent accumulation in the muscle, liver and pancreatic islets (Camp *et al.*, 2002). Thus, the repartitioning of adipose tissues observed in our study might not have detrimental effects as the HOMA-IR showed that there was improvement in insulin sensitivity.

4.4 LPL expression in the studied tissues

Insulin resistance plays a pivotal role in metabolic syndrome leading to hyperinsulinaemia, hyperglycaemia, lipid and lipoprotein dysregulation (dyslipidaemia and visceral obesity) (Fulop *et al.*, 2006). LPL, which is a key regulator of lipoprotein metabolism, has been reported by Pollare *et al.* (1991) and Kern (1997) to be reduced in both the adipose tissues and muscles in the presence of IR.

Kageyama *et al.* (2003) reported that insulin is associated with the biosynthesis of LPL, where the insulin-signaling pathway will activate both the PPARα and PPARγ. Both genes will then bind to the PPRE at the LPL gene promoter to up-regulate the LPL gene expression (Hanyu *et al.*, 2004). It was demonstrated that plasma LPL activity reflects the whole-body insulin sensitivity and was negatively correlated with HOMA-IR. This was supported by the results from this study which were in agreement with the observations mentioned above, where higher insulin sensitivity (lower HOMA-IR) in the GA-administered rats could develop concomitantly with an increase in tissue LPL expression.

Mead and co-workers (2002) reported that changes in the LPL expression are mediated predominantly through the action of hormones, such as insulin, glucocorticoid and adrenaline. Regulators of LPL mRNA expression such as insulin and glucose increase the mRNA expression and its activity in pre-adipocytes while glucocorticoids, IL-6 and TNF-α have LPL-decreasing effects (Mead *et al.*, 2002). However, this was not observed in our study as the insulin level was decreased concomitantly with an increase in tissue LPL-expression. Therefore, it could be that LPL gene expression was strongly up-regulated by the activation of PPARγ.

LPL is a downstream gene that is regulated by the activation of PPARγ, where an increase in the expression of PPARγ would lead to an increase in the expression of LPL (Desvergne and Wahli, 1999). Thus, the increase in PPARγ expression in this study was accompanied by a similar significant increase in LPL gene expression. LPL is a key enzyme in the metabolism of triacylglycerol-rich lipoproteins and plays the role of a gatekeeper in energy metabolism by controlling the generation of fatty acids. In adipose tissues, the increase in LPL production could enhance the clearance of plasma triacylglycerol and provide the pre-adipocytes with additional fatty acids, which can further stimulate the transactivation capacity of PPAR (Schoonjans *et al.*, 1996).

Variation in fat cell sizes and LPL activity among different anatomical fat depots have been documented (Fried *et al.*, 1993). It was found that obese subjects will have lower LPL activity at the omental depot (visceral depot) compared to the subcutaneous fat cells. Thus, the lower LPL expression in the omental adipose tissue may be a general feature of overall insulin resistance (Fried *et al.*, 1993). Our results with lean rats support the findings by Fried and co-workers (1993) where the LPL expression in the visceral depots were found to be higher compared to the subcutaneous depots.

Boden and Shulman (2002) reported that over-expression of LPL in the muscle and liver could lead to increase in intra-tissue TAG content and such increase in lipid accumulation in peripheral tissues have been linked to impairment of insulin signaling and IR. The present study was not in concordance with Boden and Shulman's findings, as the insulin sensitivity and LPL expression both increased in

the GA-administered rats. Such disagreement could be due to the presence of leptin sensitivity in the experimental subjects. Muoio and Newgard (2006) reported that in the leptin resistant state, the LPL-generated free fatty acid activates PPARγ, thus leading to up-regulation of the lipogenic enzymes like the acetyl-CoA carboxylase (ACC) and fatty acid synthase (FAS) that could lead to ectopic TAG accumulation (Unger and Orci, 2001). However, in the leptin sensitive state, LPL-generated free fatty acid would activate PPARα instead. This could then lead to an increase in transcription of genes of FA oxidation such as mitochondrial carnitine palmitoyltransferase-I (mCPT-I) and acyl-CoA oxidase (ACO). These enzymes could promote the compensatory oxidation of the surplus free fatty acid, with the unneeded energy dissipated as heat (Unger and Orci, 2001). Therefore, it could be postulated that the experimental rats used were leptin sensitive as there was an increase in tissue LPL expression coupled with a decrease in tissue lipid accumulation (unpublished data).

LPL expression has been found in the kidney and was shown to hydrolyze TAG in circulating lipoproteins. However, no significant changes were seen in the activity or the amount of detectable LPL in the kidney although treated with acute insulin (Tavangar *et al.*, 1992). Our present study was in concordance with those reported by Tavangar *et al.* (1992) as there were no significant differences in the kidney of the GA-administered rats compared to the control.

4.5 Modulation of serum lipid

In the present study, increase in tissue LPL expression was consistent with the improvement of serum lipid parameters in the GA-administered rats. A reduction in serum TAG, total cholesterol and LDL-cholesterol together with an elevation in HDL-cholesterol was observed (Figures 3.13 and 3.36).

The decrease in TAG in GA-administered rats may be attributed to the action of GA which causes an increase in its tissue uptake. Berthiaume *et al.* (2007) had demonstrated that inhibition of 11β-hydroxysteroid dehydrogenase 1 could reduce hepatic very-low-density lipoprotein (VLDL) which may have increased the hepatic

free fatty acid oxidation due to the induced expression of fat-catabolizing enzymes (Morton *et al.*, 2001). Hepatic VLDL secretion is regulated by the amount of lipids available for the assembly of VLDL (Berthiaume *et al.*, 2007). Thus, this could have caused the reduction in TAG as it is required to boost the VLDL secretion.

Increased LPL action on plasma lipoproteins would lead to an accelerated conversion of VLDL to IDL and LDL particles (Lefebvre *et al.*, 1997). However, this was not observed in the present study. The decrease in LDL-cholesterol in GA-administered rats may be due the decreased levels of VLDL since LDL is a derivative of VLDL (Lefebvre *et al.*, 1997). Elevation of HDL-cholesterol in GA-administered rats may be due to the increased apo A-I production since the rate of HDL synthesis is dependent on the production of apo A-I (Kolovou *et al.*, 2005). Apo-A-I is the major protein of HDL that is subjected to accelerate catabolism in individuals with metabolic syndrome (Kolovou *et al.*, 2005). Morton and co-workers (2001) along with Staels and co-workers (1998) have reported that apo A-I mRNA was significantly elevated in the 11β-HSD1 knock-out mice as well as after the activation of PPARα. The rate of HDL synthesis is dependent on the production of apo A-I (Dullens *et al.*, 2007). Therefore this could be postulated as the HDL-increasing mechanism of GA.

Dullens and co-workers (2007) also reported that increase in apo A-I production could be a suitable target for the treatment of dyslipidaemia together with the current treatments (e.g. fibrates) of lowering serum LDL-cholesterol. Increasing HDL-cholesterol can also serve as an alternative way for dyslipidaemia treatment. Dyslipidaemia is often characterized by a normal range or only mildly-raised LDL-cholesterol. However, the underlying abnormality was found to be the predominance of the more atherogenic small, dense LDL rather than the less atherogenic large, buoyant LDL particles (Kolovou *et al.*, 2005). It was demonstrated that a greater increase of LDL and VLDL may cause a greater decrease in HDL as there is a reciprocal relationship between the concentration of VLDL and HDL (Kolovou *et al.*, 2005). Many studies have shown that small, dense LDL particles have pro-atherogenic properties such as (i) reduced LDL receptor-mediated clearance (ii) increase arterial wall retention and (iii) increased susceptibility to oxidation (Kolovou *et al.*, 2005).

Thus, the beneficial act of HDL in atheroprotective mechanism is brought about through its ability to counteract LDL oxidation, which is the major initiating event that promotes the development of atherosclerosis. Therefore, pharmacological interventions now focus on raising the HDL-cholesterol levels as a therapeutic target in combating dyslipidaemia (Mayers *et al.*, 2003; Chapman *et al.*, 2004; Drexel, 2006).

The increased LPL expression by GA in this study may be pivotal in the amelioration of lipid parameters especially in dyslipidaemic subjects. This is because in the dyslipidaemic state, induced LPL expression may contribute to the increased clearance of such lipoproteins to reduce serum TAG. Besides, the formation of small, dense LDL and reduction in HDL in the dyslipidaemic subjects are attributed to CETP-mediated lipid exchange between both lipoprotein particles and TAG-enriched VLDL particles. This exchange was discovered by Tan and co-workers (1999) to be substrate driven rather than enzyme driven. Thus, an elevated catabolism of TAG-enriched VLDL by LPL may serve to positively re-modulate HDL and LDL profiles in dyslipidaemic subjects. Hence this mechanism could be responsible for the benefits of increased LPL expression in those following pharmacological intervention.

4.6 **11β**-HSD1 and 2 activities

The GA dosages used in the present study have significant inhibitory effects on 11β-HSD1 and 2. The effects of GA and its derivative, GE are diffuse and widespread in the body. It was reported that GE is a more potent inhibitor of 11β-HSD1 and 11β-HSD2 (Li *et al.*, 1997).

4.6.1 Adipose tissues

Adipose tissue is the largest energy store in the body and has an important function in maintaining energy balance by controlled synthesis and breakdown of

lipids. Besides being an energy storage organ, the adipose tissue is an endocrine organ, especially the visceral adipose tissue, as it has more active endocrine activities compared to the subcutaneous adipose tissue (Ronti *et al.*, 2006). Adipose tissue can be divided into the stromal tissue fraction (the pre-adipocytes), where 11β-HSD2 predominates and the adipocytes fraction, where only 11β-HSD1 is expressed and oxoreductase activities detected (Fain *et al.*, 2008).

In the present study, the 11β-HSD1 activities were higher compared to 11β-HSD2 activities in both the subcutaneous and visceral depots. This is in agreement with a report by Bujalska *et al.* (2002) who demonstrated that 11β-HSD2 activities were extremely low or negligible in the adipose tissues compared to the 11β-HSD1 activities.

Glucocorticoid (GC) increases the expression of the hormone-sensitive lipase and decreases the expression of PEPCK (Vegiopoulos and Verzig, 2007). This increases the rate of lipolysis and decreases the availability of glycerol for re-esterification of free fatty acids. As a result, the pouring of glycerol and free fatty acids from the adipose tissues into the blood stream increases. The inhibition of 11β-HSD1 in the adipose tissues suppresses lipolysis, thus decreasing the supply of gluconeogenic substrate to the liver and the release of free fatty acids into the blood circulation (Savage *et al.*, 2007). Inhibition of 11β-HSD1 in the adipose tissue is able to suppress gluconeogenesis by decreasing the substrate availability and preventing the release of free fatty acid which could induce insulin resistance. Masuzaki and co-workers (2001) reported that decreased 11β-HSD1 activity in knockout 11β-HSD1 mice showed resistance against induced obesity and its metabolic consequences while Paterson and co-workers (2005) reported that adipocyte-specific over-expression of 11β-HSD1 could promote the development of visceral obesity and metabolic syndrome in transgenic rodents. Berger *et al.* (2001) and Laplante *et al.* (2003) reported that PPARγ agonist has a potential in down-regulating the expression of 11β-HSD1 (Wake *et al.*, 2007) activity in both adipose depots (Morton *et al.*, 2004).

Adipose tissues, especially the visceral adipose tissue, are an active endocrine organ which secretes pro-inflammatory cytokines and adipokines such as TNF-α, IL-

6 and resistin. This could increase insulin resistance in the liver and skeletal muscle. Decreased 11β-HSD1 has been shown to decrease the secretion of the pro-inflammatory cytokines and adipokines by the visceral depot. Thus, this helps to improve insulin sensitivity in the liver and skeletal muscles (Draper and Stewart, 2005; Ronti *et al.*, 2006).

A switch in the 11β-HSD1 activity from dehydrogenase reaction to oxoreductase reaction is required for the differentiation of pre-adipocytes to adipocytes (Bujalska *et al.*, 2002). An inhibition of 11β-HSD1 oxoreductase reaction in both the subcutaneous and visceral depot differentiation leads to hypertrophy of the adipocytes, thus decreasing the development of obesity (Bujalska *et al.*, 2008).

The higher 11β-HSD2 activity in the visceral adipose tissue was in agreement with the findings of Milagro *et al.* (2007). According to Lee *et al.* (2008), the 11β-HSD2 was detected in pre-adipocytes but not in the adipocytes. 11β-HSD2 converts the active GC to inactive GC which is required for the stimulation of the pre-adipocyte proliferation. 11β-HSD2 in the pre-adipocytes converts the highly protein-bound active GC into negligible protein-bound inactive GC, which then provides the substrate to 11β-HSD1 in the adipocytes in a paracrine manner. Conversion of inactive GC to active GC by 11β-HSD1 in the adipocytes exposes the adipocytes to the active GC (Lee *et al.*, 2008). Exposure of adipocytes to active GC could result in a dose-dependent increase in 11β-HSD1 level and activity which further amplifies the local generation of active GC (Bujalska *et al.*, 1999). Therefore, a decrease in the 11β-HSD2 activities in the subcutaneous and visceral depots was able to prevent obesity by (i) decreasing the proliferation of pre-adipocytes and (ii) decreasing the supply of inactive GC to 11β-HSD1 to adipocytes by a paracrine manner, thus decreasing the exposure of active GC in the adipocytes.

In the present study, both the 11β-HSD1 and 11β-HSD2 activities were higher in the subcutaneous adipose tissue. This could indicate a higher proliferation of pre-adipocytes and a higher differentiation of adipocytes in the subcutaneous compared to the visceral depots after GA treatment (Liu *et al.*, 2008). The presence of more pre-adipocytes and increased differentiation of adipocytes in the subcutaneous depot (Mussig *et al.*, 2008) may indicate a redistribution of free fatty

acids from the visceral to the subcutaneous depot and therefore could prevent visceral adiposity. The present study further supports the work done by Mussig and co-workers (2008) as there was an increase in the number of small size adipocytes in the subcutaneous depots (Figure 3.58).

Bujalska *et al.* (1999) reported that cortisol (corticosterone)-mediated 11β-HSD1 up-regulation in adipose stromal cell cultures was inhibited by co-incubation with GE. This is in agreement with results from this study which showed a significant decrease in 11β-HSD1 activities in both subcutaneous and visceral depots.

4.6.2 Skeletal muscles

Abdominal muscle and quadriceps femoris, both of which are skeletal muscles are target tissues of GC and insulin. The balance between the actions of GC and insulin determines the turnover rate of the muscle proteins. These muscles are major sites of peripheral insulin resistance and glucose disposal (Vegiopoulos and Verzig, 2007). Skeletal muscle accounts for the majority of insulin-induced glucose uptake, utilization and storage in mammals and is a prime target for GC-induced IR via alteration through post-GR effects either on downstream insulin signaling or glucose utilization (Qi and Rodrigues, 2006).

Both 11β-HSD1 and 11β-HSD2 activities were shown to be anatomical specific. The 11β-HSD1 and 2 activities were lower in the quadriceps femoris compared to the abdominal muscle. Lower 11β-HSD1 activities in the quadriceps femoris is supported by the genomic study by Gomez-Sanchez *et al.* (2008), who showed that relative expression of 11β-HSD1 gene in thigh muscle was lower than that of the abdominal muscle. The 11β-HSD2 activities were comparable but lower than the 11β-HSD1 activities in abdominal muscle. This might be a protective mechanism to prevent excessive activation of GR by increasing the turnover rate of active GC since 11β-HSD2 has been reported to have a protective effect on skeletal muscles (Jang *et al.*, 2007).

Results from this study showed higher levels of 11β-HSD1 activities in the quadriceps femoris compared to the abdominal muscle. This may be due to the higher physical activities undertaken by the quadriceps femoris and thus has higher metabolic capabilities compared to the abdominal muscle (Stump *et al.*, 2006). The low levels of 11β-HSD2 activity in the quadriceps femoris could be due to a decrease in the turnover rate of the active GC in order to compensate for the low 11β-HSD1 activities in the quadriceps femoris compared to the abdominal muscle (Stump *et al.*, 2006).

Levels of 11β-HSD1 activities were higher than 11β-HSD2 in the abdominal and quadriceps femoris muscles. This is agreeable with current reports of higher expressions of 11β-HSD1 compared to 11β-HSD2 in the muscle (Edwards *et al.*, 1988; Draper and Stewart, 2005; Jang *et al.*, 2007). However, Jang and co-workers (2007) demonstrated a poor correlation of 11β-HSD1 and 2 expressions with their respective activities. This, suggests the presence of site-specific post-translational factors such as (i) availability of co-factors (NADP and NADPH), (ii) close functionality of microsomal hexose-6-phosphate dehydrogenase and glucose-6-phosphatase which affect enzyme kinetics (Walker *et al.*, 2007) and (iii) expressions of GC receptors (Whorwood *et al.*, 2002).

Elevated 11β-HSD1 activity increases active GC levels in the skeletal muscles. This will suppress the insulin signalling pathway by decreasing insulin receptor autophosphorylation and insulin receptor substrate-1 (IRS-1) expression and phosphorylation (Vegiopoulos and Verzig, 2007). GCs also decrease insulin-stimulated glycogen synthesis by preventing dephosphorylation (and hence preventing activation) of glycogen synthase (Ruzzin *et al.*, 2005). GCs also prevent GLUT4 translocation to the cell surface membrane, thus decreasing the uptake of blood glucose. Last but not least, GC also prevents amino acids uptake into the skeletal muscles, proteolysis and inhibits protein synthesis in skeletal muscles, thus increasing the substrate for gluconeogenesis in the liver (Vegiopoulos and Verzig, 2007).

The inhibition of 11β-HSD1 activities which decreases intracellular active GC levels in the skeletal muscles by GA and GE will prevent hyperglycaemia by

increasing insulin sensitivity of the skeletal muscles and decreasing the effects of GC on glucose and protein metabolism (Vegiopoulos and Verzig, 2007). Furthermore, inhibition of 11β-HSD1 has been proven to increase uptake of free fatty acids and β-oxidation by increasing the expression of mitochondrial carnitine palmitoyltransferase 1 and acyl-CoA oxidase. Therefore, this can prevent the development of dyslipidaemia and FFA-induced insulin resistance (Berthiaume *et al.*, 2007).

Although other potential mechanisms may contribute towards reducing insulin signaling and action in skeletal muscles (Stump *et al.*, 2006), decreased 11β-HSD1 activities in muscles may contribute to the observed improvement in insulin sensitivity (Whorwood *et al.*, 2002; Berthiaume *et al.*, 2007).

4.6.3 Liver

The liver had the highest 11β-HSD1 activity amongst the six tissues that were examined, not only in the GA-administered rats but in the control rats as well. 11β-HSD1 is highly expressed in metabolically active tissues and act predominantly as an oxo-reductase *in vivo* that regenerates active corticosterone (cortisol in humans) (Tomlinson *et al.*, 2004). The liver is also a GC-targeted organ whereby GC will stimulate gluconeogenesis during stress. Therefore the presence of 11β-HSD1 is essential for potentiating the effects of GC. The liver is also an important site for detoxification of foreign compounds and 11β-HSD1 is involved in the phase I biotransformation of various foreign substances from xenobiotics, drugs, insecticides to carcinogens where it reduces the carbonyl groups to highly reactive hydroxyl group in these compounds for glucuronyl or sulphate conjugation (Tomlinson *et al.*, 2004).

11β-HSD2 activities were detected in the liver in both the control and GA-administered rats. However, the GA-administered rats displayed lower 11β-HSD2 activities in the present study. The presence of 11β-HSD2 activities might be due to the high density of blood vessels in the liver since epithelial cells of the blood vessel contain moderate amounts of 11β-HSD2 (Gong *et al.*, 2008).

The presence of high 11β-HSD1 activities in the liver is deleterious. Liu *et al.* (2005) reported that increased 11β-HSD1 expression in the hepatocytes contributes to the development of phenotypes seen in the db/db mice, a diabetic rodent model. Furthermore, Paterson *et al.* (2004) reported that an increased hepatic 11β-HSD1 expression levels in apoE-HSD1 transgenic mice model has been shown to develop insulin resistance, hyperglycaemia, fatty liver and dyslipidaemia. Therefore, the inhibition of 11β-HSD1 by GA in the liver is able to prevent the development of insulin resistance, hyperglycaemia, fatty liver and dyslipidaemia. This was also supported by a research done by Shimoyama and co-workers (2003), where a significant dose-dependent inhibition of hepatic 11β-HSD1 activity with similar dose of GA (100 and 200 mg/kg *p.o.*) was seen.

Increased 11β-HSD1 enables GC to be more available to the hepatocytes. As mentioned above, GC increases hepatic gluconeogenesis and this is due to the induction of PEPCK and G6Pase where GC-GR complex up-regulates the transcription of these genes by binding to the glucocorticoid regulatory unit (GRU) (Cassuto *et al.*, 2005). Cassuto and co-workers (2005) also demonstrated that an increase in active GC by 11β-HSD1 in the hepatocytes in cell cultures could increase its binding to GR and therefore increases the expression of PEPCK and G6Pase genes. The high expression of PEPCK caused by high levels of GCs is one of the key factors in hyperglycaemia and insulin resistance leading to diabetes mellitus (Valera *et al.*, 1994; Sun *et al.*, 2002). Thus, an inhibition of 11β-HSD1 by GA decreases the active GC available for the GR binding and thereby decreasing the expression of PEPCK and G6Pase genes. This was further supported by recent data from our research group which showed decreased PEPCK and G6Pase activities in GA-administered rats (unpublished data).

GC also increases the activity of fatty acid synthase and acetyl-CoA carboxylase which then lead to dyslipidaemia by increasing the very-low-density lipoprotein (VLDL) production and secretion as well as TAG synthesis. Furthermore, GC decreases β-oxidation of the free fatty acids by interfering with the activity of acyl-CoA dehydrogenase, subsequently leading to TAG accumulation in the liver (fatty liver) (Nuotio-Antar *et al.*, 2007). The inhibition of 11β-HSD1 by GA may decrease the active GC levels in the hepatocytes which could then prevent the

development of fatty liver (Nuotio-Antar *et al.*, 2007). Berthiaume *et al.* (2007) showed that 11β-HSD1 inhibition increased the partitioning of TAG towards oxidative tissues. Inhibition of 11β-HSD1 also decreases the secretion of VLDL and TAG production and their accumulation in the liver (Berthiaume *et al.*, 2007).

Therefore, inhibition of 11β-HSD1 prevents dyslipidaemia and fatty liver development by (i) decreasing activities of fatty acid synthase and acetyl-CoA carboxylase (therefore preventing accumulation of TAG in the liver) (ii) decreasing free fatty acids delivery from the visceral depot by the suppression of lipolysis after inhibition of 11β-HSD1 by GA and (iii) decreasing VLDL secretion from the liver into the blood circulation (Mai *et al.*, 2005).

Decreased 11β-HSD1 activities could increase hepatic glucose uptake by increasing translocation of GLUT2 to the cell surface membrane of hepatocytes (Vegiopoulos and Verzig, 2007). Therefore, 11β-HSD1 inhibition by GA in the normal male Sprague Dawley rats could lead to the removal of excess glucose in the blood circulation when the blood glucose was higher than the basal blood glucose level. This shows that GA may have a fine-tuning effect on blood glucose levels.

4.6.4 Kidney

11β-HSD1 activity was detected in this current study and this was expected as low levels of gluconeogenesis can occur in the kidney when the rats encounter stress (Elliot and Elliot, 2005). The present study shows that 11β-HSD2 activities were higher than 11βHSD1 which further supports the role of 11β-HSD2 in the kidney. 11β-HSD2 activities were observed in the kidney and this may be due to the function of the kidney as a MC-targeted organ. Draper and Stewart (2005) reported that the presence of 11β-HSD2 in the kidney is essential for protecting the MR from non-specific binding of active GC.

11β-HSD2 activities in the kidney has been demonstrated to increase in severe obesity and negatively associated with insulin sensitivity in humans (Mussig *et al.*, 2008) and in the obese Zucker rats compared to the lean Zucker rats (Livingstone *et al.*, 2000). 11β-HSD2 in the kidney converts the active GC to

inactive GC. The inactive GC has low binding affinity towards the corticosteroid-binding globulin and albumin while active GC binds tightly to these proteins with a very small fraction of active GC existing in the free form (the biologically active form). In addition, inactive GC levels do not show diurnal variations while active GC does (Tomlinson *et al.*, 2004). Thus, the circulating inactive GC acts as a rapid substrate pool which could be activated by 11β-HSD1 in the adipose tissues and the liver especially when the active GC levels are low. This will then allow 11β-HSD1 to maintain or even increase the active GC levels in the adipose tissues and liver.

An increased 11β-HSD2 activity in the kidney intensifies the supply of direct substrate to the 11β-HSD1 and increases 11β-HSD1 activities (Livingstone *et al.*, 2000; Mussig *et al.*, 2008) further inducing insulin resistance in the liver and lipolysis in the adipose tissues, especially the visceral depot. Furthermore, the free fatty acids released into the hepatic portal vein and transported to the liver could also induce hepatic insulin resistance (Mai *et al.*, 2005). Consequently, the increase in the 11β-HSD2 activities in kidney induces hepatic insulin resistance and adipose tissue lipolysis by increasing the inactive GC as the substrate for 11β-HSD1 to produce active GC in the adipose tissues and the liver when the active GC in the blood circulation is low. Thus, the inhibition of renal 11β-HSD2 by GA could be beneficial as it can prevent hepatic insulin resistance and reduce lipolysis in the adipose tissues (Mussig *et al.*, 2008).

4.7 Histological analysis

4.7.1 Adipose tissue

Based on Figure 3.57, the size of adipocytes in the subcutaneous adipose tissue exhibited a decrease but there was an increase in the number of adipocytes. The increase in the number of small adipocytes could be a result of adipocyte differentiation. Okuno *et al.* (1998) showed that the size of adipocytes became smaller after administration of troglitazone to Zucker fatty rats leading them to conclude that the reduction was due to TNF-α or leptin as a result of PPARγ activation.

A number of genes involved in fat metabolism such as lipoprotein lipase, acyl-CoA synthase, uncoupling protein and fatty acid binding protein was shown to have peroxisome proliferator responsive element (PPRE) in their promoter region. Therefore, it was postulated that the anti-diabetic effects of TZD is mostly due to the lipid remodeling effect of PPAR activation (Okuno *et al.*, 1998). Small adipocytes are more sensitive to insulin and they can take in more glucose due to the high surface area. Upon insulin stimulation, small adipocytes were proven to oxidize more glucose compared to large adipocytes. Therefore, the increased number of small adipocytes in subcutaneous tissue of GA-administered rats can actually decrease blood glucose levels (Okuno *et al.*, 1998). Insulin has anti-lipolytic actions and small adipocytes appeared to be more sensitive to this action. Hence, small adipocytes secrete less free fatty acid compared to those hypertrophied adipocytes. Besides, small adipocytes secrete less tumor necrosis factor α (TNF-α) compared to large adipocytes (Mori *et al.*, 1999). Cell culture studies showed that TNF-α inhibit autophosphorylation of insulin receptor and interferes with the phosphorylation of insulin receptor substrate-1 (Gokhan *et al.*, 1994; Sell *et al.*, 2006). Therefore, the increase in the number of small adipocytes improves insulin resistance.

In the visceral adipose tissue, the size of adipocytes in GA-administered rats appeared to be similar to the control rats. This was consistent with the studies done by Mori and co-workers (1999), who showed that the differentiation of pre-adipocytes into adipocytes only occurred in the subcutaneous adipose tissue. However, the adipocytes in the visceral depots of GA-administered rats appeared to be irregular shaped. The irregular shaped cells could most likely be caused by apoptosis. It is an important process to maintain tissue homeostasis by ensuring the proliferation rate of tissues is equaled to the rates of cell death (Thompson, 1995). Apoptosis of adipocytes regulates adipose tissue distribution and as a preventive measure in avoiding the over-spill of fatty acid into other organs (Delle-Fera *et al.*, 2000).

Visceral adipose tissue has different functions and metabolism compared to subcutaneous adipose tissue. From the endocrinology perspective, the visceral depot is more active compared to the subcutaneous (Rosen and Spiegelman, 2006). Thus it has been identified as one of the factors of metabolic syndrome (Hanson *et al.*,

2002). McCarty (2001) discovered that the visceral adipocytes are insensitive to insulin, an entity that plays a pivotal role in anti-lipolytic actions and promotes re-esterification of fatty acids. McCarty (2001) also reported that visceral depots are more prone to undergo lipolysis compared to the subcutaneous. Therefore this will lead to the free fatty acid being released by the visceral depot to enter the portal circulation. When the supply of fatty acid is overwhelming, it will be stored in the liver and muscle. The increased intramuscular triacylglycerol levels and high triacylglycerol levels in liver will cause impairment in insulin sensitivity (McCarty, 2001).

On the other hand, subcutaneous adipose tissue is highly sensitive to insulin action. Under normal conditions, subcutaneous adipose tissue will not release fatty acids into the circulation. But under conditions where fuel is needed, subcutaneous adipose tissue will release free fatty acids as an energy fuel source which is unlikely to be re-stored in other parts of the body. In other words, the fat stored in the subcutaneous depot is not pathogenic while fat stored in the visceral depot is pathogenic (McCarty, 2001).

The lipolysis occurred in the visceral adipose tissue might be due to the inhibition of 11β-HSD 1. Although both adipose tissues have 11β-HSD1, the visceral adipose tissues have higher amount compared to the subcutaneous adipose tissues (Armanini *et al.*, 2005). Previous study by Hansen and co-workers (2006) showed that over-expression of 11β-HSD1 in mice caused visceral obesity by increasing the levels of corticosterone. In our study, 11β-HSD1 activity in rats given GA was lower than the control rats in the visceral depot, supporting the presence of lipolysis reported by McCarty (2001), where inhibition of 11β-HSD1 by GA prevented the occurrence of visceral obesity.

As glycyrrhizic acid inhibits 11β-HSDs, visceral obesity can also be inhibited. This is mainly due to the inhibition of 11β-HSD1 which reduces the availability of cortisol. Cortisol (active GC) causes accumulation of triacylglycerols in adipocytes and the differentiation of pre-adipocytes into adipocytes (Armanini *et al.*, 2005). Therefore, in the visceral depots the size of adipocytes remained the same. indicating no differentiation of adipocytes occurred (Figure 3.57). Milagro and co-

workers (2007) reported that 11β-HSD2 is involved in the regulation of adipocytes in the subcutaneous tissue. They found that 11β-HSD2 synthesis was up-regulated in the subcutaneous adipose tissue of high fat-fed animals leading to the prediction that the up-regulation is able to diminish the action of glucocorticoid, hence decreasing lipid depot in this tissue (Milagro *et al.*, 2007). GA was long known to inhibit both 11β-HSD type 1 and 2 (Ploeger *et al.*, 2001). Therefore, the inhibition of 11β-HSD2 by GA could possibly improve lipid deposition in the subcutaneous tissue. The deposition of lipid in the subcutaneous adipose tissue has "lipid stealing" effect where it protects other organs from harmful effects of free fatty acids (Davies *et al.*, 2001). Hence, this further supports that GA could improve insulin sensitivity through the inhibition of 11β-HSD2.

In addition, PPARγ activation by GA in the adipose tissue may be responsible for the smaller adipocytes seen in the GA-administered rats. PPARγ stimulates the differentiation of pre-adipocytes in the adipose tissues, thus generating smaller adipocytes that are more insulin-sensitive than the larger adipocytes and are more efficient in storing lipids (Bogacka *et al.*, 2004; Ronti *et al.*, 2006). This occurrence is known as the adipose tissue remodeling system as it accounts for the lipid-steal hypothesis, where smaller adipocytes generally take up circulating free fatty acids more easily, thus reducing the flux of free fatty acid to the liver and muscles. The beneficial effect of this process reverses the incidence of IR and was reported to be responsible for the insulin-sensitizing effects of TZDs (Bragt and Popeijus, 2008). Berthiaume *et al.* (2004) and Bogacka *et al.* (2004) reported that PPARγ predominantly triggers adipocyte differentiation in the subcutaneous adipose tissue rather than in the visceral adipose. Thus, it favors the diversion of lipid from the visceral depot to the subcutaneous depot. This will lead to an increase in the subcutaneous accumulation and a decrease or unchanged size of the visceral adipose tissue (Berthiaume *et al.*, 2004; Bogacka *et al.*, 2004).

4.7.2 Liver

The liver is one of the most important organs in the body which is involved in metabolism, detoxification of foreign substances and storage of vitamins and

minerals. It is one of the major target organs of insulin. The involvement of the liver in carbohydrate metabolism is particularly important in the control of blood glucose levels. Liver buffers blood glucose by storing glucose as glycogen when the blood glucose levels are high. When there is a need for glucose, the liver releases glucose from its glycogen storage through glycogenolysis. When the glycogen stores are depleted, the liver converts glucogenic amino acids and glycerol to glucose by gluconeogenesis (Marieb, 1998). The histological staining of the liver from both the control and GA-administered rats demonstrated normal morphology. This indicates that glycyrrhizic acid did not cause any adverse effects such as inflammation in the liver. However, the GA-administered rats showed darker magenta color compared to the control rats (Figure 3.58), which are indicative of higher polysaccharide and carbohydrate contents (Kiernan, 1999).

GA improves insulin sensitivity of the liver and hence increases glucose uptake into hepatocytes for storage. These changes in glucose homeostasis are affected by GA through the activation of PPARγ and the PPARγ activator has been demonstrated to downregulate genes involved in gluconeogenesis such as pyruvate carboxylase, phosphoenolpyruvate carboxykinase (PEPCK) and glucose-6-phosphatase (Way *et al.*, 2001). Under normal physiological conditions, both glucokinase and glucose transporter 2 (GLUT2) act as the glucose sensing apparatus in the liver. Activation of PPARγ leads to up-regulation of GLUT2 and glucokinase expression. GLUT2 helps in the uptake of glucose into the liver while glucokinase traps the glucose by phopshorylation. These will eventually lead to glycogen synthesis in the liver (Kim and Ahn, 2004).

4.8 PPARγ activation and 11β-HSD inhibition on blood pressure

Despite its shortcomings, the tail-cuff method for measuring systolic blood pressure (SBP) in rats is still very useful, especially when the screening of large populations of animals and/or the follow-up of SBP over long time periods are involved (Fritz and Rinaldi, 2007). The blood pressure measurements obtained using the tail-cuff method did not show much variation over the treatment period of one

week. However, Stormer *et al.* (1993) reported that chronic administration of 0.5 g GA to humans has been associated with the development of pseudoaldosteronism and this includes symptoms such as electrolyte imbalance (hypernatraemia and hypokalaemia) and increased blood pressure in rats. Administration of 0.5 g of GA to humans daily for 3 to 10 days resulted in similar symptoms (Stormer *et al.*, 1993). Such effects were due to the non-selective nature of GA that inhibits not only 11β-HSD1 but also 11β-HSD2. Therefore, following the administration of GA, glucocorticoid activation of the mineralocorticoid receptor (MR) could result in mediation of physiological mineralocorticoid actions such as sodium reabsorption and potassium excretion which are associated with increased blood pressure resulting from renal sodium retention (Ferrari and Krozowski, 2000). However in our study, not much variation was noted in the blood pressure. This could be due to the length of exposure and dosages of GA used, which were shorter than those reported by Stormer and workers (1993).

Guan (2004) reported that PPARγ could be involved in the regulation of blood pressure in both diabetic animal models and human patients. Although not much variation in blood pressure was reported, there was a slight decrease in blood pressure in the GA-administered rats. Here, we postulate that there are two mechanisms involved in blood pressure regulation by PPARγ; a direct and an indirect mechanism. The direct mechanism is associated with the PPARγ action on the vasculature and kidney tubule while the secondary mechanism involves the enhancement of insulin sensitivity rendered by the agonist activation of PPARγ (Dobrian, 2006). Normal Sprague Dawley rats fed 47 and 94 mg/kg of TZD was found by Song *et al.* (2004) to display a decrease in blood pressure after 3 days and the treatment using the lower dosage actually resulted in a lower blood pressure compared to the higher dose. The increase in blood pressure of spontaneously hypertensive rats was also suppressed upon oral administration of 300 mg/kg body weight ethanolic licorice extract for four weeks (Mae *et al.*, 2003).

Although the direct regulation of blood pressure control has been reported by researchers, the exact mechanism has not been elucidated. However, a breakthrough was discovered as both the endothelial and smooth muscle cells were identified as key cells involved in the amelioration of blood pressure (Dobrian, 2006). The up-

regulation of PPARγ in the present study may have caused the inhibition of vasoconstrictors such as endothelin-1 (Iglarz *et al.*, 2003) and stimulation of vasodilators such as nitric oxide (NO) in endothelial cells leading to decreased blood pressure (Ryan *et al.*, 2004). Down-regulation of the AT1 receptor upon PPARγ activation reduces vascular contractility in the smooth muscle cells also lead to lower blood pressure (Takeda *et al.*, 2000). The normal function of the AT1 receptor increases sodium and water retention, thus leading to a sustained bout of hypertension (Dobrian, 2006).

Hypertension in obesity arises from increased sodium reabsorption in the renal proximal tubule due to an increased renal sympathetic and renin-angiotensin system (RAS) activation (Dobrian, 2006). Although the blood pressure results in the present study did not show much variation over the treatment duration, the regulation of the blood pressure in the rats could be attributed to the activation of PPARγ. Angiotensin II increases during hypertension (Dobrian, 2006) but activation of PPARγ relieves the rise of angiotensin II by downregulating the angiotensin II receptor 1, thus leading to inhibition of the RAS (Ruan *et al.*, 2008).

Besides the RAS, leptin has also been shown to cause hypertension. A study by Rahmouni *et al.* (2005) showed that hyperleptinaemia caused by diet-induced obesity in mice resulted in increased renal sympathetic activity and increased blood pressure. Activation of PPARγ has been shown to inhibit the production of leptin through binding on the promoter region of the leptin gene (De Vos *et al.*, 1995). Dobrian (2006) on the other hand postulated that the mechanism of blood pressure reduction could be due to a reduction in leptin production upon PPARγ activation, which ultimately has a direct tubular effect. The above was supported by findings of our research group where leptin concentration in GA-administered rats was no different compared to the control groups (unpublished results).

It has been reported that the inhibition of 11β-HSD2 in the kidney can cause hypertension, hypokalaemia and hypernatraemia (Stromer *et al.*, 1993). However, it was not observed in the present study as the administration of GA to Sprague Dawley rats leads to increased expression of renal medulla cyclooxygenase type 2 (COX-2) due to 11β-HSD 2 inhibition (Yao *et al.*, 2005). This will cause an increase

in the prostaglandin levels which have natriuretic and diuretic effects and lead to prevention of hypertensive state in rats (Yao *et al.*, 2005).

4.9 GA as PPARγ agonist

Concern has been raised over the suitability of TZDs as anti-diabetic drugs as they have the potential to cause edema, cardiovascular complications and weight gain in spite of their effectiveness in alleviating blood glucose levels (Shearer and Billin, 2007). Thus, researchers are looking for natural substitutes for TZDs in view of retaining the same levels of efficacy but with reduced side effects. To date, polyunsaturated fatty acids have been reported to possess non-specific PPARγ ligand-binding activity and flavanoids, isoprenols and triterpene acids are the most recent compounds to exhibit such characteristics (Kuroda *et al.*, 2003; Mae *et al.*, 2003). Both researches performed ligand binding assays on ethanolic root extracts of licorice and detected ligand-binding activity.

Diabetic KK-A^y mice fed with approximately 100 to 300 mg/kg body weight ethanolic extract of licorice for four weeks resulted in a decrease in blood glucose and serum insulin levels while diet-induced obese C57BL mice displayed a reduction in the weight of the visceral adipose tissues upon similar treatment (Mae *et al.*, 2003). Studies done by Takii *et al.* (2001) and Kuroda *et al.* (2003) reported a decrease in blood glucose levels upon feeding of 4.1g/kg diet and 100mg/kg body weight GA to genetically diabetic KK-A^y mice for 7 weeks and 4 days respectively while Takii *et al.* (2001) showed a significant decrease in serum insulin levels as well. A different study involving obese diabetic KK-A^y mice fed with licorice extract for four weeks displayed a reduction in blood glucose levels and weight of abdominal fat (Nakagawa *et al.*, 2004). Our results showed that GA may be a potential natural ligand to mediate PPARγ activation, thus resulting in the amelioration of blood glucose and serum insulin levels.

4.10 Postulated effects of GA

Glycyrrhizic acid has been shown to have PPARγ-ligand binding activity using ligand binding assays (Kuroda *et al.*, 2003; Mae *et al.*, 2003). From the present study, the expression of PPARγ2 was tissue specific, with the highest expression observed in the subcutaneous adipose tissue while the lowest was seen in the kidney. Both the visceral and subcutaneous adipose tissues displayed the highest expression thus substantiating its importance in adipogenesis and adipocyte remodeling. Increased total PPARγ, PPARγ1 and PPARγ2 expression levels in the liver and skeletal muscles may indicate an increase in circulatory glucose uptake by increasing the translocation of glucose transporters to the cell membrane thus enhancing the circulatory glucose uptake. The PPARγ expression levels were the lowest in the kidney, which plays an important role in the regulation of electrolyte concentration and blood pressure. The up-regulation of total PPARγ, PPARγ1 and PPARγ2 expression levels coupled with a significant decrease in blood glucose and non-significant decrease in serum insulin levels as well as a significant increase of HOMA-IR indicates improvement in insulin sensitivity due likely to ligand-binding activation of PPARγ. For instance, in the adipose tissues, agonist action of GA on PPARγ2 alters the expression of adipokines (Fulop *et al.*, 2006; Waki and Tontonoz 2006) which stimulate (i) apoptosis of mature adipocytes and pre-adipocytes differentiations (Delle-Fera *et al.*, 2000) and (ii) net influx of free fatty acids into adipocytes. In the muscle tissues, agonist effect of GA on PPARγ2 up-regulates GLUT4 and glucose kinase which in turn facilitate (i) the influx of glucose into skeletal muscle tissues and (ii) increase glycogen synthesis (Semple *et al.*, 2006). Similarly in the liver tissues, agonist action of GA on PPARγ2 has been associated with up-regulation of GLUT2 which increases hepatic glucose influx and glycogen synthesis.

Up-regulation of total PPARγ, PPARγ1 and PPARγ2 expression levels upon GA administration in all six tissues had been coupled with the inhibition of 11β-HSD1 enzyme activity and an increase in the downstream LPL gene expression levels (Desvergne and Wahli, 1999). Decreased 11β-HSD1 enzyme activity improves insulin sensitivity through a reduction in hepatic gluconeogenesis and

improved glucose uptake into peripheral organs (Dimitriadis *et al.*, 1997) while the increase in LPL gene expression increases the storage of free fatty acids (Desvergne and Wahli, 1999). Thus, the activation of PPARγ due to GA administration has been postulated to improve insulin sensitivity in concert with a decrease in 11β-HSD1 enzyme activity and an increase in LPL gene expression.

The insulin sensitizing effects of GA was based on the lowering of active GC by 11β-HSD1, where the GC is a functional antagonist to insulin. Inhibition of 11β-HSD1 is able to decrease the blood glucose levels by (i) increasing glucose uptake in the liver, skeletal muscles and adipose tissues via increasing translocation of glucose transporters to the cell surface membrane, (ii) decreasing hepatic gluconeogenesis and (iii) decreasing supply of gluconeogenic substrate by preventing proteolysis and lipolysis in the skeletal muscles and adipose tissues (Vegiopoulous and Verzig, 2007; Savage *et al.*, 2007).

Decrease in 11β-HSD1 activities also decreases insulin resistance by decreasing lipolysis and hence preventing FFA-induced insulin resistance in the liver and peripheral tissues. Furthermore, a decrease in lipolysis (especially in the visceral depot) will prevent excessive secretion of VLDL and hence dyslipidaemia, thereby decreasing transport of free fatty acids to the liver. Furthermore, repartitioning of triacylglycerol from the visceral to the subcutaneous depot could help in preventing visceral obesity by altering the relative 11β-HSD1 and 11β-HSD2 activities in the subcutaneous and visceral adipose tissues.

The combined effects of GA on PPARγ, 11β-HSD, LPL, insulin sensitizing properties, improved lipid profile and the regulation of blood pressure are summarized in Figure 4.1.

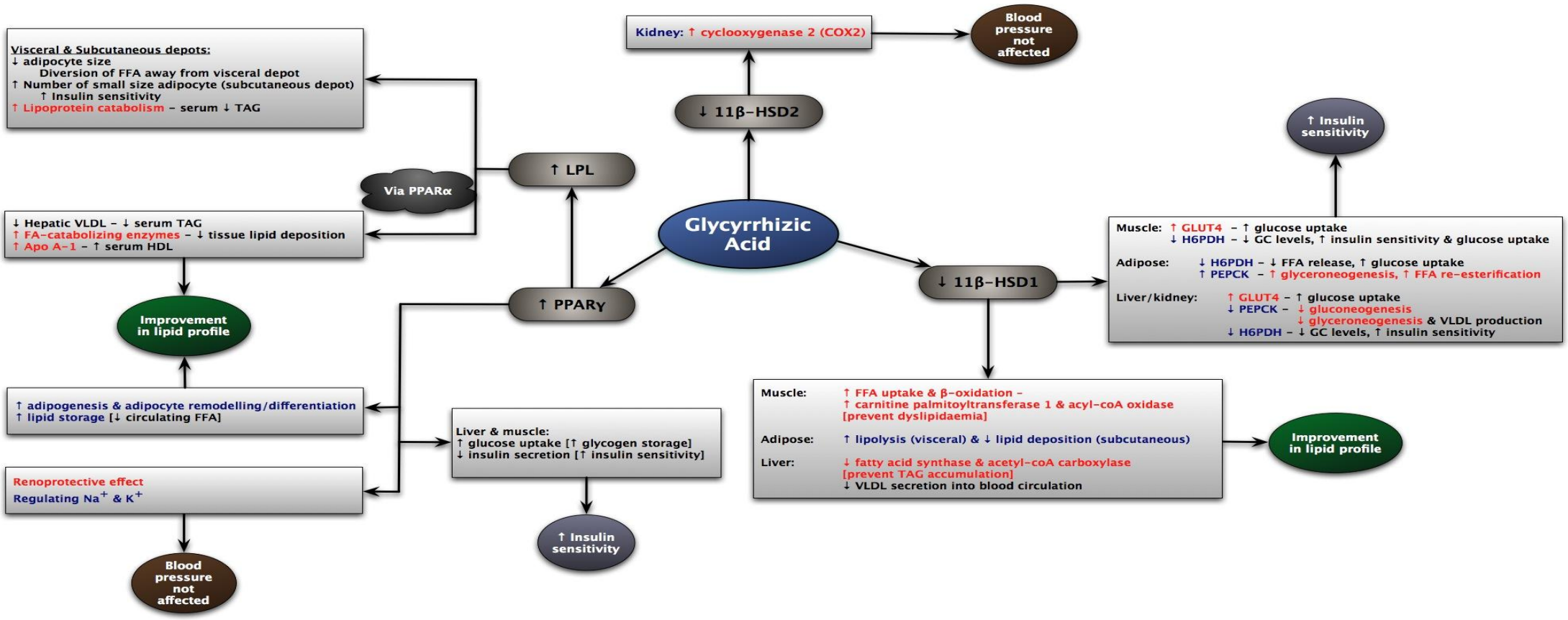

Figure 4.1: Postulated mechanisms of GA action.

Note: Black font – Data from this study; Blue font – Data obtained from other studies done by our research group; Red font – Information obtained from publications. Abbreviations: FFA, Free fatty acid; TAG, Triacylglycerol; VLDL, Veryl-low-density lipoprotein; HDL, High density lipoprotein; Na^+, Sodium; K^+, Potassium; GLUT4, Glucose transporter 4; H6PDH, Hexose-6—phosphate dehydrogenase; PEPCK, Phosphoenolpyruvate carboxykinase; GC, Glucocorticoid; PPARγ, Peroxisome proliferator activated receptor gamma; LPL, Lipoprotein lipase; 11β-HSD, 11β-hydroxysteroid dehydrogenase.

Chapter 5

Conclusion

CONCLUSION

The results of this study showed that the most effective route of GA administration was the oral route as there were no significant differences seen between the oral and intraperitoneal routes in the various parameters studied (i.e., blood glucose and serum insulin levels, lipid profile, expression levels of PPARγ1, PPARγ2 and LPL as well as 11β-HSD1 and 2 activities). Thus, all subsequent work was performed using oral administration. Although the administration of 100 and 150 mg/kg of GA was found to be the optimum concentration among the different dosages studied (25, 50, 75, 100 and 150 mg/kg), there were no significant differences between the rats administered with either 100 mg/kg or 150 mg/kg of GA. Thus, 100 mg/kg GA was chosen as the optimum dosage for subsequent work as the lower dosage could produce a similar effect as that of the higher dosage. One week of GA administration yielded optimal effects on the various parameters measured when various time lines of 12, 24, 48 hours and one week were studied.

Blood glucose and HOMA-IR were significantly decreased in rats orally-administered with 100 mg/kg GA for 1 week ($P < 0.05$) while serum insulin displayed a non-significant decrease ($P < 0.05$). The decrease in blood glucose levels could account for the decrease in serum insulin levels. Thus, a reduction in the demand for insulin will cause a reduction in its synthesis, which indirectly signifies an improvement in insulin sensitivity.

There were improvements in the lipid profile with a decrease in serum TAG, total cholesterol and LDL-cholesterol accompanied by an increase in HDL-cholesterol ($P > 0.05$). The increase in tissue LPL expression correlates with the improvement in lipid parameters in the GA-administered rats.

Increase in PPARγ expression could have increased the aP2 gene activation in the liver, which in turn increased fatty acid transportation, thereby leading to a decrease in TAG levels and an improvement in insulin sensitivity. The inhibition of 11β-hydroxysteroid dehydrogenase 1 (11β-HSD1) could reduce hepatic very-low density lipoprotein (VLDL) levels, which in turn increases the oxidation of hepatic free fatty acid. This could cause the reduction in TAG as it is required to boost the VLDL secretion. The decrease in LDL-cholesterol in GA-administered rats may be due to the lowered levels of VLDL since LDL is a derivative of VLDL. Elevation of HDL-cholesterol in GA-administered rats may be due to the increased apo A-I production since the rate of HDL synthesis is dependent on the production of apo A-I

Total PPARγ, PPARγ1 and PPARγ2 expressions were significantly increased in the subcutaneous and visceral adipose tissues, abdominal muscle and quadriceps femoris ($P < 0.05$) while a non-significant increase was observed in the liver and the kidney ($P > 0.05$). Similar to the expression of PPARγ, the LPL expression was also significantly increased in the subcutaneous and visceral adipose tissues, abdominal muscle and quadriceps femoris ($P < 0.05$) while a non-significant increase was observed in the liver and the kidney ($P > 0.05$). Increase in expression levels of total PPARγ, PPARγ1 and PPARγ2 in all the tissues were representative of their functions as regulators of glucose homeostasis and lipid metabolism. Up-regulation of PPARγ expression in the liver and skeletal muscles enhances glucose uptake through the up-regulation of GLUT2 and GLUT4 respectively while the up-regulation of PPARγ in adipose tissues (i) increases adipogenesis, (ii) promotes apoptosis of mature, lipid-filled adipocytes and (iii) regulates the hormones and adipokines secreted in view of increasing insulin sensitivity. However, expression levels of total PPARγ, PPARγ1 and PPARγ2 were the lowest in the kidneys, which has only a small contribution towards glucose homeostasis. Nevertheless, the low expression levels of PPARγ in the kidneys were pivotal towards regulation of sodium exchange and blood pressure.

11β-HSD1 was significantly decreased in all the studied tissues ($P < 0.05$) except for the subcutaneous adipose tissue while the 11β-HSD2 was significantly

decreased in all the six tissues ($P < 0.05$). The decrease in the 11β-HSD1 and 11β-HSD2 activities may have lowered the active glucocorticoids in metabolically active tissues (eg: skeletal muscle), which in turn increased the translocation of the glucose transporter isotype 4 and 2 (GLUT-4 and GLUT-2) to facilitate the removal of glucose from the blood. This was supported by our data as there was a significant decrease in the blood glucose levels as well as an increase in glycogen storage in the liver, as demonstrated by histological studies on the liver and other tissues.

Overall, this study has proven its importance by demonstrating the interlinking roles of PPARγ, 11β-HSD and LPL in reducing blood glucose and HOMA-IR and improving the lipid profile in rats. Studies on these parameters have not been reported before and thus this study highlighted the combined importance of PPARγ, LPL and 11β-HSD in combating the risk factors of metabolic syndrome. Effects of GA on these factors have also not been reported before and the present study demonstrated that it could play a role in modulating the expression of these parameters.

FUTURE WORK

Not much work has been done on the exact mechanism of the activation of PPARγ by GA. The use of GA as a natural replacement for TZDs, α-glucosidase inhibitors, sulfonylureas and biguanides in treating diabetes mellitus is slowly enticing researchers towards developing a natural substitute with fewer side effects.

In order to confirm the postulation that GA could lead to the activation of PPARγ, transactivation assays could be performed using transfected cells carrying a PPRE-containing reporter construct. Examples of cell lines previously used were the NIH 3T3 and CV-1 fibroblast cells (Wang *et al.*, 2000; Sato *et al.*, 2002).

The use of rat models with metabolic syndrome risk factors (obese and diabetic rats such as Zucker diabetic fatty rats) would be highly advocated compared to just prolonging the treatment duration at the current dose with wild type rats. This is to ensure that the effects of GA could be more prominently observed in the former. Examples of these are illustrated, where (i) the hypoglycaemic effects of inhibition of 11β-HSD1 by GA may only be mediated when there is excessive, but not basal glucose levels and (ii) the lower HOMA-IR, that is indicative of improved insulin sensitivity would be more meaningful in the insulin resistant state, rather than in an already insulin sensitive wild type rat.

In order to verify that β-oxidation was induced in the GA-administered group, investigation could be carried out on (i) the increase in the expression of genes coding for enzymes of β-oxidation such as skeletal muscle isotype of carnitine palmitoyltransferase I (mCPT-I) and acyl-CoA oxidase (ACO) and (ii) a decreased respiratory quotient compared to the control.

REFERENCES

Alberti, K.G.M.M. and Zimmet, P.Z. (1998) Definition, diagnosis and classification of diabetes mellitus and its complications. *Diabetic Medicine*, 15: 539-553.

Alberti, K.G.M.M., Zimmet, P. and Shaw, J. (2005) The metabolic syndrome- a new worldwide definition. *The Lancet*, 366: 1059-1062.

Alberts, P., Engblom, L., Edling, N., Forsgren, M., Klingstrom, G., Larsson, C., Ronquist-Nii, Y., Ohman, B. and Abrahmsen, L. (2002) Selective inhibition of 11β-hydroxysteroid dehydrogenase type 1 decreases blood glucose concentrations in hyperglycaemic mice. *Diabetologia*, 45: 1528-1532.

Alberts, P., Nilsson, C., Selen, G., Engblom, L.O., Edling, N.H., Norling, S., Klingstrom, G., Larsson, C., Forsgren, M., Ashkzari, M., Nilsson, C.E., Fiedler, M., Berqvist, E., Eva, B.B. and Abrahmsen, L.B. (2003) Selective inhibition of 11β-hydroxysteroid dehydrogeanse type 1 improves hepatic insulin sensitivity in hyperglycemic mice strains. *Endocrinology*, 144: 4755-4762.

Altschul, S.F., Gish, W., Miller, W., Myers, E.W. and Lipman, D.J. (1990) Basic local alignment tool. *Journal of Molecular Biology*, 215: 403-410.

American Diabetes Association (2002) Report of the expert committee on the diagnosis and classification of diabetes mellitus. *Diabetes Care*, 25(Suppl. 1): S5 – S20.

American Diabetes Association (2008) Standards of medical care in Diabetes-2008. *Diabetes Care*; 31(Supp1): S12-S54.

Ameshima, S., Golpon, H., Cool, C.D., Chan, D., Vandivier, R.W., Gardai, S.J., Wick, M., Nemenoff, R.A., Geraci, M.W. and Voelkel, N.F. (2003) Peroxisome proliferator-activated receptor gamma (PPARγ) expression is decreased in pulmonary hypertension and affects endothelial cell growth. *Circulation Research*, 92: 1162-1169.

Anderson, F.A. (2007) Final report on the safety assessment of glycyrrhetinic acid, potassium glycyrrhetinate, disodium succinoyl glycyrrhetinate, glyceryl glyrrhetinate, glycyrrhetinyl stearate, stearyl glycyrrhetinate, glycyrrhizic acid, ammonium glycyrrhizate, dipotassium glycyrrhizate, disodium glycyrrhizate, trisodium glycyrrhizate, methyl glycyrrhizate and Potassium glycyrrhizinate. *International Journal of Toxicology*, 26(S2): 79 – 112.

Andrews, R.C., Rooyackers, O. and Walker, B.R. (2003) Effects of the 11ß-hydroxysteroid dehydrogenase inhibitor carbenoxolone on insulin sensitivity in men with type 2 diabetes. *The Journal of Clinical Endocrinology & Metabolism*, 88: 285 – 291.

Applied Biosystems (2004) *Guide to performing relative quantitation of gene expression using real-time quantitative PCR*. Roche Molecular Systems, Inc and F. Hoffmann-La Roche Ltd, USA. Pp. 1-60.

Armanini, D., Nacamulli, D., Francini_pesenti, F., Battagin, G., Ragazzi, E. And Fiore, C. (2005) Glycyrrhetinic acid, the active principle of licorice can reduce the thickness of subcutaneous thigh fat through topical application. *Steroids*, 70: 538-542.

Auwerx, J. (1999) PPARγ, the ultimate thrifty gene. *Diabetologia*, 42: 1033-1049.

Babu, A. and Fogelfeld, L. (2006) Metabolic syndrome and prediabetes. *Diabetes Mellitus*, 52: 55 – 144.

Bagi, Z., Koller, A. and Kaley, G. (2004) PPAR gamma activation, by reducing oxidative stress, increases bioavailability in coronary arterioles of mice with type 2 diabetes. *American Journal of Physiology - Heart and Circulatory Physiology*, 286: 742-748.

Bagry, H.S., Raghavendran, S. and Carli, F. (2008) Metabolic syndrome and insulin resistance. *Anesthesiology*, 108: 506-523.

Balkau, B., Valensi, P., Eschwege, E. and Slama, G. (2007) A review of the metabolic syndrome. *Diabetes & Metabolism*, 33: 405-413.

Baltina, L.A. (2003) Chemical modification of glycyrrhizic acid as a route to new bioactive compounds for medicine. *Current Medical Chemistry*, 10: 155-171.

Batsis, J.A., Nieto-Martinez, R.E. and Lopez-Jiminez, F. (2007) Metabolic syndrome: from global epidemiology to individualized medicine. *Clinical Pharmacology & Therapeutics*, 82(5): 509-524.

Baumann, C.A., Chokshi, N., Saltiel, A.R. and Ribon, V. (2000) Cloning and characterization of a functional peroxisome proliferator activator receptor-gamma responsive element in the promoter of the CAP gene. *The Journal of Biological Chemistry*, 275(13): 9131-9135.

Bedoucha, M., Atzpodien, E. and Boelsterli, U.A. (2001) Diabetic KK-A^y mice exhibit increased hepatic PPARγ1 gene expression and develop hepatic steatosis upon chronic treatment with antidiabetic thiazolidinediones. *Journal of Hepatology,* 35: 17-23.

Berger, J., Tanen, M., Elbrecht, A., Hermanowski-Vosatka, A., Moller, D. E., Wright, S. D. and Thieringer, R. (2001) Peroxisome proliferator-activated receptor-γ ligands inhibit adipocyte 11β-hydroxysteroid dehydrogenase type 1 expression and activity. *The Journal of Biological Chemistry*, 276(16): 12629-12635.

Berger, J.P., Akiyama, T.E. and Meinke, P.T. (2005) PPARs: Therapeutic targets for metabolic disease. *Trends in Pharmacological Sciences*, 26(5): 244-251.

Berthiaume, M., Sell, H., Lalonde, J., Gélinas, Y., Tchernof, A., Richard, D. and Deshaies, Y. (2004) Actions of PPARγ agonism on adipose tissue remodeling, insulin sensitivity and lipemia in absence of glucocorticoids. *American Journal of Physiology: Regulatory, Integrative and Comparative Physiology*, 287: 1116-1123.

Berthiaume, M., Laplante, M., Tchernot, A. and Deshaies, Y. (2007) Metabolic action of peroxisome proliferator-activated receptor γ agonism in rats with exogenous hypercorticosteronemia. *International Journal of Obesity*, 31: 1660 – 1670.

Björntorp, P. and Rosmond, R. (2000) Obesity and cortisol. *Nutrition*, 16: 924 – 936.

Boden, G. and Shulman, G.I. (2002) Free fatty acids in obesity and type 2 diabetes: defining their role in the development of insulin resistance and β-cell dysfunction. *European Journal of Clinical Investigation*, 32(3): 14-23.

Boelsterli, U. A. and Bedoucha, M. (2002) Toxicological consequences of altered peroxisome proliferator-activated receptor γ (PPARγ) expression in the liver: insights from models of obesity and type 2 diabetes. *Biochemical Pharmacology*, 63: 1-10.

Bogacka, I., Xie, H., Bray, G.A., Smith, S.R. (2004) The effect of pioglitazone on peroxisome proliferator-activated receptor-γ target genes related to lipid storage *in vivo*. *Diabetes Care*, 27(7): 1660-1667.

Boyko, E.J., Fujimoto, W.Y., Leonetti, D.L. and Newell-Morris, L. (2000) Visceral adiposity and risk of type 2 diabetes: A prospective study among Japanese Americans. *Diabetes Care*, 23: 465-471.

Bragt, M.C.E. and Popeijus, H.E. (2008) Peroxisome proliferator-activated receptors and the metabolic syndrome. *Physiology & Behaviour*, 94(2): 187-197.

Braun, J.E.A. and Severson, D.L. (1992) Regulation of the synthesis, processing and translocation of lipoprotein lipase. *Biochemical Journal*, 287: 337 – 347.

Brown, J. D. and Plutzky, J. (2007) Peroxisome proliferator activated receptors as transcriptional nodal points and therapeutic targets. *Circulation*, 518-533.

Brown, R.J. and Rader, D.J. (2007) Lipases as modulators of atherosclerosis in murine models. *Current Drug Targets*, 8: 1307 – 1319.

Brunton, L.L., Lazo, J.S. and Parker, K.L. (2006) *The pharmacological basis of therapeutics*. McGraw-Hill Medical Publishing Division, USA; 11th Edition. Pp. 4 – 7.

Buckingham, R.E., Al-Barazanji, K.A., Toseland, N., Slaughter, M., Connor, S.C., West, A., Bond, B., Turner, N.C. and Clapham, J.C. (1998) Peroxisome proliferator-activated receptor-γ agonist, rosiglitazone, protects against nephropathy and pancreatic islet abnormalities in Zucker fatty rats. *Diabetes*, 47: 1326-1334.

Bujalska, I.J., Kumar, S., Hewison, M. and Stewart, P.M. (1999) Differentiation of adipose stromal cells: The roles of glucocorticoids and 11β-hydroxysteroid dehydrogenase. *Endocrinology*, 140: 3188 – 3196.

Bujalska, I.J., Walker, E.A., Hewison, M. and Stewart, P.M. (2002) A switch in dehydrogenase to reductase activity of 11β-hydroxysteroid dehydrogenase type 1 upon differentiation of human omental adipose stromal cells. *The Journal of Clinical Endocrinology & Metabolism*, 87: 1205 – 1210.

Bujalska, I.J., Durrani, O.M., Abbott, J., Oniyimba, C.U., Khosla, P., Moosavi, A.H., Reuser, T.T.Q., Stewart, P.M., Tomlinson, J.W., Walker, E.A. and Rauz, S. (2007) Characterisation of 11β-hydroxysteroid dehydrogenase 1 in human orbital adipose tissue: a comparison with subcutaneous and omental fat. *Journal of Endocrinology*, 192: 279 – 288.

Bujalska, I.J., Gathercole, L.L., Tomlinson, J.W., Darimont, C., Ermolieff, J., Fanjul, A. N., Rejto, P.A. and Stewart P.M. (2008) A novel selective 11beta-hydroxysteroid dehydrogenase type 1 inhibitor prevents human adipogenesis. *Journal of Endocrinology* 197: 297-307.

Camp, H.S., Ren, D. and Leff, T. (2002) Adipogenesis and fat-cell function in obesity and diabetes. *Trends in Molecular Medicine*, 8(9): 442-447.

Campbell, M.J. and Machin, D. (2002) *Medical Statistics: A commonsense approach*, 3rd Edition. John Wiley. Pp. 169-170.

Cartwright, M.J., Tchkonia, T. and Kirkland, J.L. (2007) Aging in adipocytes: potential impact of inherent, depot-specific mechanisms. *Experimental Gerontology*, 42: 463-471.

Carr, D.B., Utzschneider, K.M., Hull, R.L., Kodama, K., Retzlaff, B.M., Brunzell, J.D., Shofer, J.B., Fish, B.E., Knopp, R.H. and Kahn, S.E. (2004) Intra-abdominal fat is a major determinant of the National Cholesterol Education Program Adult Treatment Panel III criteria for the metabolic syndrome. *Diabetes*, 53: 2087 – 2094.

Cassuto, H., Kochan, K., Chakravarty, K., Cohen, H., Blum, B., Olswang, Y., Hakimi, P., Xu, C., Massillon, D., Hanson, R.W. and Reshef, L. (2005) Glucocorticoids regulate transcription of the gene for phosphoenolpyruvate carboxykinase in the liver via an extended glucocorticoid regulatory unit. *Journal of Biological Chemistry*, 280(40): 33873-33884.

Cha, B.S., Ciaraldi, T.P., Carter, L., Nikoulina, S.E., Mudaliar, S., Mukherjee, R., Paterniti Jr., J.R. and Henry, R.R. (2001) Peroxisome proliferator-activated receptor (PPAR) γ and retinoid X receptor (RXR) agonists have complimentary effects on glucose and lipid metabolism in human skeletal muscle. *Diabetologia,* 44: 444-452.

Chao, L., Marcus-Samuels, B., Mason, M.M., Moitra, J., Vinson, C., Arioglu, E., Gavrilova, O. and Reitman, M.L. (2000) Adipose tissue is required for the antidiabetic, but not for the hypolipidemic effect of thiazolidinediones. *Journal of Clinical Investigation*, 106: 1221-1228.

Chapman, M., Assmann, G., Fruchart, J., Shepherd, J., Sirtori, C. (2004) Raising high-density lipoprotein cholesterol with reduction of cardiovascular risk: the role of nicotinic acid - a position paper developed by the European Consensus Panel on HDL-C. *Current Medical Research Opinion*, 20(8):1253-68.

Chew, G.T., Gan, S.K. and Watts, G.F. (2006) Revisiting the metabolic syndrome. *Medical Journal of Australia*, 185(8): 445-449.

Chung, B.H., Lim, S.W., Ahn, K.O., Sugawara, A., Ito, S., Choi, B.S., Kim, Y.S., Bang, B.K. and Yang, C.W. (2005) Protective effect of peroxisome proliferator-activated receptor gamma agonist on diabetic and non-diabetic renal diseases. *Nephrology*, 10: 40-43.

Cockram, C.S. (2000) The epidemiology of diabetes mellitus in the Asia-Pacific region. *Hong Kong Medical Journal*, 6: 43-52.

Cummings, D.E. and Schwartz, M.W. (2003) Genetics and pathophysiology of human obesity. *Annual Review of Medicine*, 54: 453-471.

Dahlman, I. and Arner, P. (2007) Obesity and polymorphisms in genes regulating human adipose tissue. *International Journal of Obesity*, 31: 1629-1641.

Davani, B., Khan, A., Hult, M., Martensson, E., Okret, S., Efendic, S. Jornvall, H. and Oppermann, U.C.T. (2000) Type 1 11 beta-hydroxysteroid dehydrogenase mediates glucocorticoid activation and insulin release in pancreatic islets. *Journal of Biological Chemistry*, 275: 34841-34844.

Davies, G.F., Khandelwal, R.L. and Roesler, W.J. (1999) Troglitazone induces expression of PPARγ in liver. *Molecular Cell Biology Research Communications*, 2: 202-208.

Davies, P.J.A., Berry, S.A., Shipley, G.I., Eckel, R.H., Hennuyer, N., Crombie, D.I., Ogilvie, K.M., Peinado-onsurbe, J., Fievet, C., Leibowitz, M.D., Heyman, R.A. and Auwerx, J. (2001) Metabolic effects of rexinoids: tissue-specific regulation of lipoprotein lipase activity. *Molecular Pharmacology*, 59: 170-176.

de Dios, S.T., Bruemmer, D., Dilley, R.J., Ivey, M.E., Jennings, G.L., Law, R.E. and Little, P.J. (2003) Inhibitory activity of clinical thiazolidinedione peroxisome proliferator activating receptor-gamma ligands toward internal mammary artery, radial artery and saphenous vein smooth muscle cell proliferation. *Circulation*, 107: 2548-2550.

Della-Fella, M.A., Qian, H. And Baile, C.A. (2000) Adipocyte apoptosis in the regulation of body fat mass by leptin. *Diabetes, Obesity and Metabolism*, 3: 299-310.

Desvergne, B. and Wahli, W. (1999) Peroxisome proliferator-activated receptors: nuclear control of metabolism. *Endocrine Reviews*, 20(5): 649-688.

De Vos, P., Lefebvre, A,, Miller, S.G., Guerre-Milli, M., Wong, K., Saladin, R., Hamann, L.G., Staels, B., Briggs, M.R. and Auwerx, J. (1996) Thiazolidinediones repress *ob* gene expression in rodents via activation of peroxisome proliferator-activated receptor γ. *Journal of Clinical Investigation*, 98(4): 1004-1009.

Dimitriadis, G., Leighton, B., Parry-Billings, M., Sasson, S., Young, M., Krause, U., Bevan, S., Piva, T., Wegener, G. and Newsholme, E.A. (1997) Effects of glucocorticoid excess on the sensitivity of glucose transport and metabolism to insulin in rat skeletal muscle. *Biochemistry Journal*, 321: 707 – 712.

Dluby, R.G., Lawrence, J.E. and Williams, G.H. (2003) *Endocrine Hypertension. In 'Williams Textbook of Endocrinology'*, 10th edition. Elsevier Saunders, Philadelphia.

Dobrian, A.D. (2006) The complex role of PPARγ in renal dysfunction in obesity: managing a Janus-faced receptor. *Vascular Pharmacology*, 45: 36-45.

Draper, N., Walker, E.A., Bujalska, I.J., Tomlinson, J.W., Chadler, S.M., Arlt, W., Lavery, G.G., Bedendo, O., Ray, D.W., Laing, I., Malunowicz, E., White, P.C., Hewison, M., Mason, P.J., Connell, J.M., Shackleton, C.H. and Stewart, P.M. (2003) Mutations in the genes encoding 11β-hydroxysteroid dehydrogenase type 1 and hexose-6-phosphate dehydrogenase interact to cause cortisone reductase deficiency. *Natural Genetics*, 34: 434 – 439.

Draper, N. and Stewart, P.M. (2005) 11β-hydroxysteroid dehydrogenase and the pre-receptor regulation of corticosteroid hormone action. *Journal of Endocrinology*, 186: 251 – 271.

Drexel, H. (2006) Reducing risk by raising HDL-cholesterol: the evidence. *European Heart Journal Supplements*, 8(Suppl F): F23-F29.

Dubuquoy, L., Dharancy, S., Nutten, S., Pettersson, S., Auwerx, J. and Desreumaux, P. (2002) Role of peroxisome proliferator-activated receptor γ and retinoid X receptor heterodimer in hepatogastroenterological diseases. *Lancet*, 360: 1410-1418.

Dugi, K.A., Dichek, H.L., Talley, G.D., Brewer Jr., H.B. and Santamarina-Fojo, S. (1992) Human lipoprotein lipase: The loop covering the catalytic site is essential for interaction with lipid substrate. *The Journal of Biological Chemistry*, 267(35): 25086 – 25091.

Dullens, S.P.J., Plat, J. and Mensink, R.P. (2007) Increasing apo A-I production as a target for CHD rich reduction. *Nutrition, Metabolism & Cardiovascular Diseases*, 17: 616-628.

Eckel, R.H., Grundy, S.M. and Zimmet, P.Z. (2005) The metabolic syndrome. *Lancet*, 365: 1415-1428.

Edwards, C.R.W., Burt, D., Mcintyre, M.A., De Kloet, E.R., Stewart, P.M., Brett, L., Sutanto, W.S. and Monder, C. (1988) Localization of 11-beta-hydroxysteroid dehydrogenase tissue specific protector of the mineralocorticoid receptor. *Lancet*, 2: 986 – 989.

Elliot, W.H. and Elliot, D.C. (2005) *Biochemistry and Molecular Biology*. Oxford University Press: Oxford. 3rd Edition.

Evans, R.M. (1988) The steroid and thyroid hormone receptor superfamily. *Science*, 240: 889 – 895.

Evans, R.M., Barish, G.D. and Wang, Y. (2004) PPARs and the complex journey to obesity. *Nature Medicine*, 10(4): 1-7.

Fain, J.N., Buehrer, B., Bahouth, S.W., Tichansky, D.S. and Madan, A.K. (2008) Comparison of messenger RNA distribution for 60 proteins in fat cells vs the nonfat cells of human omental adipose tissue. *Metabolism Clinical and Experimental*, 57: 1005-1015.

Fajas, L., Fruchart, J.C. and Auwerx, J. (1998) Transcriptional control in adipogenesis. *Current Opinion in Cell Biology*, 10: 165-173.

Fernyhough, M.E., Okine, E., Hausman, G., Vierck, J.L. and Dodson, M.V. (2007) PPARγ and GLUT-4 expression as developmental regulators/markers for preadipocyte differentiation into an adipocyte. *Domestic Animal Endocrinology*, 33: 367-378.

Ferrari, P. and Krozowski, Z. (2000) Role of the 11β-hydroxysteroid dehydrogenase type 2 in blood pressure regulation. *Kidney International*, 57: 1374-1381.

Francis, G., Kerem, Z., Makkar, H.P.S. and Becker, K. (2002) The biological action of saponins in animal systems: A review. *British Journal of Nutrition*, 88: 587-605.

Fried, S.K., Russell, C.D., Grauso, N.L. and Brolin, R.E. (1993) Lipoprotein lipase regulation by insulin and glucocorticoid in subcutaneous and omental adipose tissues of obese women and men. *Journal of Clinical Investigation*, 92: 2191-2198.

Friedewald, W.T., Levy, R.I., Fredrickson, D.S. (1972) Estimation of the concentration of LDL-cholesterol in plasma without use of the preparative ultracentrifuge. *Clinical Chemistry*. 18: 499-502.

Fritz, M. and Rinaldi, G. (2007) Influence of nitric oxide-mediated vasodilation on the blood pressure measured with the tail-cuff method in the rat. *Journal of Biomedical Science*, 14: 757-765.

Fujimoto, W.Y. (2000) The importance of insulin resistance in the pathogenesis of type 2 diabetes mellitus. *The American Journal of Medicine*, 108(6A): 9-14.

Fulop, T., Tessier, D. and Carpentier, A. (2006) The metabolic syndrome. *Pathologie Biologie*, 54: 375-386.

Gavrilova, O., Haluzik, M., Matsusue, K., Cutson, J. J., Johnson, L., Dietz, K. R., Nicol, C. J., Vinson, C., Gonzalez, F. J. and Reitman, M. L. (2003) Liver peroxisome proliferator-activated receptor γ contributes to hepatic steatosis, triglyceride clearance and regulation of body fat mass. *The Journal of Biological Chemistry*, 278(36): 34268-34276.

Gilbaldi, M. and Perrier, D. (1975) Route of administration and drug disposition. *Drug Metabolism Review*, 3(1): 185-199.

Gilde, A.J., Fruchart, J.C. and Staels, B. (2006) Peroxisome proliferators-activated receptors at the crossroads of obesity, diabetes and cardiovascular disease. *Journal of the American College of Cardiology*, 48: A24-A32.

Gokhan, S.H., Murray, D.L., Choy, L.N. and Spiegelman, B.M. (1994) Tumor necrosis

factor α inhibits signaling from the insulin receptor. *Procedings of the National Academy of Sciences on the United States of America*, 91: 4854-4858.

Gomez-Sanchez, E.P., Romero, D.G., de Rodriguez, A.F., Warden, M.P., Krozowski, Z. and Gomez-Sanchez, C.E. (2008) Hexose-6-phosphate dehydrogenase and 11β-hydroxysteroid dehydrogenase -1 tissue distribution in the rat. *Endocrinology*, 149(2): 525-533.

Gong, R., Morris, D.J. and Brem, A.S. (2008). Variable expression of 11β-hydroxysteroid dehydrogenase (11β-HSD) isoforms in vascular endothelial cells. *Steroids* 73: 1187-1196.

Groop, L.C. (1999) Insulin resistance: The fundamental trigger of type 2 diabetes. *Diabetes, Obesity and Metabolism*, 1(Supp. 1):S1-S7.

Grundy, S.M., Cleeman, J.I., Daniels, S.R., Donato, K.A., Eckel, R.H., Franklin, B.A., Gordon, D.J., Krauss, R.M., Savage, P.J., Smith, Jr. S.C., Spertus, J.A. and Costa, F. (2005) Diagnosis and management of the metabolic syndrome. *Circulation*, 112: 2735-2752.

Guan, Y. (2004) Peroxisome proliferator-activated receptor family and its relationship to renal complications of the metabolic syndrome. *Journal of the American Society of Nephrology*, 15: 2801-2815.

Guan, Y., Hao, C., Cha, D.R., Rao, R., Lu, W., Kohan, D.E., Magnuson, M.A., Redha, R., Zhang, Y. and Breyer, M.D. (2005) Thiasolidinediones expand body fluid volume through PPRgamma stimulation of ENaC-mediated renal salt absorption. *Nature Medicine*, 11: 861-866.

Guo, L. and Tabrizchi, R. (2006) Peroxisome proliferator-activated receptor gamma as a drug target in the pathogenesis of insulin resistance. *Pharmacology & Therapeutics*, 111: 145-173.

Guri, A.J., Hontecillas, R. And Bassaganya-Riera, J. (2006) Peroxisome proliferators-activated receptors bridging metabolic syndrome with molecular nutrition. *Clinical Nutrition*, 25: 871-885.

Gurnell, M. (2005) Peroxisome proliferator-activated receptor γ and the regulation of adipocyte function: Lessons from human genetic studies. *Clinical Endocrinology & Metabolism*, 19(4): 501-523.

Guytom, K., Bond, R., Reilly, C., Gilkeson, G., Halushka, P. and Cook, J. (2001) Differential effects of 15-deoxy-delta (12,14)-prostaglandin J2 and a peroxisome proliferator-activated receptor gamma agonist on macrophage activation. *Journal of Leukocyte Biology*, 69: 631-638.

Guyton, A.C. and Hall, J.E. (2005) *Dietary balances; regulation of feeding; obesity and starvation; vitamins and minerals. In 'Textbook of Medical Physiology'*, Elsevier Saunders, Philadelphia.11th Edition.

Hansen, E., Hajri, T. and Abumrad, N.N. (2006) Is all fat the same? The role of fat in the pathogenesis of the metabolic syndrome and type 2 diabetes mellitus. *Surgery*, 139: 711-716.

Hanson, R.I., Imperatore, G., Bernett, P.H. and Knowler, W.C. (2002) Components of the "Metabolic Syndrome" and incidence of type 2 diabetes. *Diabetes*, 51: 3120-3127.

Hanyu, O., Miida, T., Obayashi, K., Ikarashi, T., Soda, S., Kaneko, S., Hirayama, S., Suzuki, K., Nakamura, Y., Yamatani, K. and Aizawa, Y. (2004) Lipoprotein lipase (LPL) mass is preheparin serum reflects insulin sensitivity. *Atherosclerosis*, 174: 385-390.

Harris, M.I. (1995) Epidemiologic studies on the pathogenesis of Non-Insulin-Dependent Diabetes Mellitus (NIDDM). *Clinical and Investigative Medicine*, 18(4): 231-239.

Hauner, H., Entenmann, G., Wabitisch, M., Gaillard, D., Ailhaud, G., Negrel, R. and Pfeiffer, E.F. (1989) Promoting effects of glucocorticoids on the differentiation of

human adipocytes precursor cells cultured in a chemically defined medium. *Journal of Clinical Investigation*, 84: 1663 – 1670.

Heikkinen, S., Auwerx, J. and Argmann, C.A. (2007) PPARγ in human and mouse physiology. *Biochimica et Biophysica Acta*, 1771: 999-1013.

Hevener, A.L., He, W., Barak, Y., Le, J., Gandyopadhyay, G., Olson, P., Wilkes, J., Evan, R.E and Olefsky, J. (2003) Muscle-specific PPARg deletion causes insulin resistance. *Nature Medicine*, 9(12): 1491-1497.

Hollander, J.M. and Mechanick, J.I. (2008) Complementary and alternative medicine and the management of the metabolic syndrome. *Journal of American Dietetic Association*, 108: 495-509.

Hollenberg, S.M., Weinberger, C., Ong, E.S., Cerelli, G., Oro, A., Lebo, R., Thompson, E.B., Rosenfeld, M.G. and Evans, R.M. (1985) Primary structure and expression of a functional human glucocorticoid receptor cDNA. *Natur*e, 318: 635-641.

Houseknecht, K.L., Cole, B.M. and Steele, P.J. (2002) Peroxisome proliferator-activated receptor gamma (PPARγ) and its ligands: A review. *Domestic Animal Endocrinology*, 22: 1-23.

Iglarz, M., Touyz, R.M., Amiri, F., Lavoie, M., Diep, Q.N. and Schiffrin, E.L. (2003) Effect of peroxisome proliferator-activated receptor-α and –γ activators on vascular remodeling in endothelin-dependent hypertension. *Arteriosclerosis, Thrombosis and Vascular Biology*, 23: 45-51.

Iglesias, P. and Diez, J.J. (2006) Peroxisome proliferator-activated receptor gamma agonist in renal disease. *European Journal of Endocrinology*, 154: 613-612.

Isbrucker, R.A. and Burdock, G.A. (2006) Risk and safety assessment on the consumption of Licorice root (Glycyrrhiza sp.), its extract and powder as a food ingredient, with emphasis on the pharmacology and toxicology of Glycyrrhizin. *Regulatory Toxicology and Pharmacology*, 46: 167-192.

Jang, C., Obeyesekere, V.R., Diley, R.J., Krozowski, Z., Inder, W.J. and Alford, F.P. (2007). Altered activity of 11β-hydroxysteroid dehydrogenase types 1 and 2 in skeletal muscle confers metabolic protection in subjects with type 2 diabetes. *The Journal of clinical endocrinology and metabolism*, 92(8): 2314-3320.

Jiang, G., Dallas-Yang, Q., Li, Z., Szalkowski, D., Liu, F., Shen, X., Wu, M., Zhou, G., Doebber, T., Berger, J., Moller, D. E. and Zhang, B. B. (2002) Potentiation of insulin signaling in tissues of Zucker obese rats after acute and long-term treatment with PPAR agonists. *Diabetes*, 51: 2412-2419.

Jermendy, G. (2007) PPARγ agonists – antidiabetic drugs with a potential role in the treatment of diseases other than diabetes. *Diabetes Research and Clinical Practice*, 78: 29-39.

Kageyama, H., Hirano, T., Okada, K., Ebara, T., Kageyama, A., Murakami, T., Shioda, S. and Adachi, M. (2003) Lipoprotein lipase mRNA in white adipose tissue but not in skeletal muscle is increase by pioglitazone through PPARγ. *Biochemical and Biophysical Research Communications*, 305: 22 – 27.

Kern, C.D., Francone, O.L. and Stevens, K.A. (2006) Differential regulation of the cynomolgus, human and rat acyl-CoA oxidase promoters by PPARα. *Gene*, 380: 84-94.

Kiernan, J.A. (1999) Carbohydrate Histochemistry. In *Histological & Histochemical Methods: Theory & Practice.* Butterworth Heinemann, Oxford. 3rd Edition. Pp.213-242.

Kim, H. and Ahn, Y. (2004) Role of peroxisome proliferator-activated receptor-γ in the glucose-sensing apparatus of liver and β-cells. *Diabetes*, 53(1): S60-S65.

Ko, B-S., Jang, J.S., Hong, S.M., Sung, S.R., Lee, J.E., Lee, M.Y., Jeon, W.K and Park. S. (2007) Changes in components, Glycyrrhizic and Glycyrrhetinic Acid in raw *Glycyrrhiza uralensis* Fisch, modify insulin sensitizing and insulinotropic actions. *Bioscience, Biotechnology and Biochemistry*, 71(6): 1452-1461.

Koh-Banerjee, P., Wang, Y., Hu, F.B., Spiegelman, D., Willet, W.C. and Rimn, E.B. (2004) Changes in body weight and body fat distribution as risk factors for clinical diabetes in US men. *American Journal of Epridemiology*, 159(12): 1150-1159.

Kolovou, G.D., Anagnostopoulou, K.K. and Cokkinos, D.V. (2005) Pathophysiology of dyslipidaemia in the metabolic syndrome. *Postgraduate Medical Journal*, 81: 358 – 366.

Konrad, D., Rudich, A. and Schoenle, E.J. (2007) Improved glucose tolerance in mice receiving intraperitoneal transplantation of normal fat tissue. *Diabetologia,* 50: 833-839.

Korc, M. (2003) Diabetes mellitus in the era of proteomics. *Molecular & Cellular Proteomics*, 399-404.

Kota, B.P., Huang, T.H. and Roufogalis, B.D. (2005) An overview on biological mechanisms of PPARs. *Pharmacological Research*, 51: 85-94.

Krätzner, R., Fröhlich, F., Lepler, K., Schröder, M., Röher, K., Dickel, C., Tzvetkov, M. V., Quentin, T., Oetjen, E. and Knepel, W. (2008) A peroxisome proliferator-activated receptor γ - retinoid X receptor heterodimer physically interacts with the transcriptional activator PAX6 to inhibit glucagon gene transcription. *Molecular Pharmacology*, 73: 509-517.

Krauss, R.M. (2004) Lipids and lipoproteins in patients with type 2 diabetes: *Diabetes Care*, 27(6): 1496 – 1504.

Krozowski, K. and Funder, J.W. (1983) Renal mineralocorticoid receptors and hippocampal corticosterone binding species have identical intrinsic steroid specificity. *Proceedings National Academy of Science U.S.A.*, 80: 6056 – 6060.

Krozowski, K., Li, K.X.Z., Koyaman, K., Smith, R.E., Obeyesekere, V.R., Stein-Oakley, A., Sasano, H., Coulter, C., Cole, T. and Sheppard, K.E. (1999) The type I and II 11β-hydroxysteroid dehydrogenase enzymes. *Journal of Steroid Biochemistry and Molecular Biology*, 69: 391 – 401.

Kuroda, M., Mimaki, Y., Sashida, Y., Mae, T., Kishida, H., Nishuyama, T., Tsukagawa, M., Konishi, E., Takahashi, K., Kawada, T., Nakagawa, K. and Kitahara, M. (2003) Phenolics with PPAR-γ ligand binding activity obtained from Licorice (Glycyrrhiza uralensis Roots) and ameliorative effects of Glycyrin on genetically diabetic KK-A^y Mice. *Bioorganic & Medicinal Chemistry Letters*, 13: 4267-4272.

Lann, D. and LeRoith, D. (2007) Insulin resistance as the underlying cause for the metabolic syndrome. *Medical Clinics of North America*, 91: 1063 – 1077.

Laplante, M., Sell, H., MacNaul, K.L., Richard, D., Berger, J.P. and Deshaies, Y. (2003) PPAR-γ activation mediates adipose depot-specific effects on gene expression and lipoprotein lipase activity: mechanisms for modulation of postprandial lipemia and differential adipose accretion. *Diabetes*, 52: 291 – 299.

Lavery, G.G., Hauton, D., Hewitt, K.N., Brice, S.M., Sherlock, M., Walker, E.A. and Stewart, P.M. (2007) Hypoglycemia with enhanced hepatic glycogen synthesis in recombinant mice lacking hexose-6-phosphate dehydrogenase. *Endocrinology*, 148: 6100 – 6106.

Lee, C., Lee, S., Shin, S. G. and Hwang, S. (2008) Real-time PCR determination of rRNA gene copy number: Absolute and relative quantification assays with Escherichia coli. *Applied Microbiology and Biotechnology*, 78: 371-376.

Lefebvre, A.M., Peinado-Onsurbe, J., Leitersdorf, I., Briggs, M.R., Paterniti, J.R., Fruchart, J. C., Fievet, C., Auwerx, J. and Staels, B. (1997) Regulations of lipoprotein metabolism by thizolidinediones occurs through a distinct but complementary mechanism relative to fibrates. *Arteriosclerosism Thrombosis and Vascular Biology*, 17: 1756-1764.

Li, A.C. and Glass, C.K. (2004) PPAR- and LXR-dependent pathways controlling lipid metabolism and the development of atherosclerosis. *Journal of Lipid Research*, 45: 2161-2173.

Li, K.X.Z., Obeyesekere, V.R., Krozowski, Z.S. and Ferrari, P. (1997) Oxoreductase and dehydrogenase activities of the human and rat 11ß-hydroxysteroid dehydrogenase type 2 enzyme. *Endocrinology*, 138: 2948 – 2952.

Liska, M.K. (2004) *Drugs and the human body with implications for society*. Pearson Prentice Hall, New Jersey. 7th Edition. Pp. 97 – 98.

Liu, Y.J., Nakagawa, Y., Wang, Y., Sakurai, R., Tripathi, P.V., Lutfy, K. and Friedman, T.C. (2005) Increased glucocorticoid receptor and 11β-hydroxysteroid dehydrogenase type 1 expression in hepatocytes may contribute to the phenotype of type 2 diabetes in db/db mice. *Diabetes*, 54: 32 – 40.

Liu, Y., Nakagawa, Y., Wang, Y., Liu, L., Du, H., Wang, W., Ren, X., Lutfy, K. and Friedman, T. C. (2008). Reduction of hepatic glucocorticoid receptor and hexose-6-phosphate dehydrogenase expression ameliorates diet-induced obesity and insulin resistance in mice. *Journal of Molecular Endocrinology*, 41: 53-64.

Livingstone, D.E.W., Jones, G.C., Smith, K. and Jamieson, P.M. (2000) Understanding the role of glucocorticoids in obesity: tissue-specific alterations of corticosterone metabolism in obese Zucker rats. *Endocrinology*, 141: 560-563.

Livingstone, D.E.W. and Walker, B.R. (2003) Is 11β-Hydroxysteroid dehydrogenase type 1 a therapeutic target? Effects of carbenoxolone in lean and obese Zucker rats. *The Journal of Pharmacology and Experimental Therapeutics*, 305(1): 167 – 172.

Loh, C.S., MacRobert, A.J., Bedwekk, J., Regula, J., Krasner, N. and Brown, S.G. (1993) Oral versus intravenous administration of 5-aminolaevulinic acid for photodynamic therapy. *British Journal of Cancer*; 68(1): 41-51.

Loviscach, M., Rehman, N., Carter, L., Mudaliar, S., Mohadeen, P., Ciaraldi, T.P., Veerkamp, J.H. and Henry, R.R. (2000) Distribution of peroxisome proliferator-activated receptors (PPARs) in human skeletal muscle and adipose tissue: Relation to insulin action. *Diabetologia*, 43: 304-311.

Mae, T., Kishida, H., Nishiyama, T., Tsukagawa, M., Konishi, E., Kuroda, M., Mimaki, Y., Sashida, Y., Takahashi, K., Kawada, T., Nakagawa, K. and Kitahara, M. (2003) A Licorice ethanolic extract with peroxisome proliferator-activated receptor-γ ligand-binding activity affects diabetes in KK-Ay mice, abdominal obesity in diet-induced obese C57BL mice and hypertension in spontaneously hypertensive rats. *The Journal of Nutrition*, 133: 3369-3377.

Mahler, R.J. and Adler, M.L. (1999) Type 2 diabetes mellitus: Update on diagnosis, pathophysiology and teatment. *The Journal of Clinical Endocrinology & Metabolism*, 84(4): 1165-1171.

Mai, K., Kullmann, V., Bobbert, T., Maser-Gluth, C., Mohlig, M., Bahr, V., Pfeiffer, A. F. H., Spranger, J. and Diederich, S. (2005) In vivo activity of 11β-hydroxysteroid dehydrogenase type 1 and free fatty acid-induced insulin resistance. *Clinical Endocrinology*, 63: 442-449.

Marieb, E.N. (1998) *The endocrine system: In human anatomy & physiology.,* Benjamin/Cummings Science Publishing, California. 4th edition. Pp. 586-620.

Marty, N., Dallaporta, M. Foretz, M. Emery, M., Tarussio, D., Bady, U., Binnert, C., Beermann, F. and Thorens (2005) Regulation of glucagon secretion by glucose transporter type 2 (GLUT2) and astrocyte-dependent glucose sensors. *The Journal of Clinical Investigation*, 115: 3545-3553.

Mastura, I., Zanariah, H., Fatanah, I., Idzwan, M.F., Wan Shaariah, M.Y., Jamaiyah, H., Geeta, A. (2008) An audit of diabetes control and management (ADCM). *Medical Journal of Malaysia*, 63(Supplement C): 76-77.

Masuzaki, H., Paterson, J., Shinyama, H., Morton, N.M., Mullins, J.J., Seckl, J.R. and Flier, J.S. (2001) A transgenic model of visceral obesity and the metabolic syndrome. *Science,* 294: 2166 – 2170.

Matthews, C.K., van Holde, K.E. and Ahern, K.G. (2000) *Lipid metabolism I: Fatty Acids, Triacylglycerols and Lipoproteins. In 'Biochemistry'*. Addison-Wesley Publishing Company: San Francisco. 3rd Edition. Pp. 632.

Mayers, C.D., Molly, C., Carr, M.D., Park S. and Brunzell, J.D. (2003) Varying cost and free nicotinic acid content in over-the-counter niacin preparations for dyslipidemia. *Annals of Internal Medicine*, 139(12); 996-1002.

McCarty, M.F. (2001) Modulation of adipocyte lipoprotein lipase expression as a strategy for preventing or treating visceral obesity. *Medical Hypotheses*, 57: 192-200.

Mead, J.R., Irvine, S.A. and Ramji, D.P. (2002) Lipoprotein lipase: Structure, function, regulation and role in disease. *Journal of Molecular Medicine*, 80: 753 – 769.

Memon, R. A., Tecott, L. H., Nonogaki, K., Beigneux, A., Moser, A. H., Grunfeld, C. and Feingold, K. R. (2000) Up-regulation of peroxisome proliferator-activated receptors (PPAR-α) and PPAR-γ messenger ribonucleic acid expression in the liver in murine obesity: Troglitazone induces expression of PPAR-γ-responsive adipose tissue-specific genes in the liver of obese diabetic mice. *Endocrinology*, 141(11): 4021-4031.

Milagro, F.I., Campión, J. and Martínez, A. (2007) 11β-hydroxysteroid dehydrogenase type 2 expression in white adipose tissue is strongly correlated with adiposity. J*ournal of Steroid Biochemistry & Molecular Biology*, 104: 81 – 84.

Miller, W.L. and Chrousos, G.P. (2001) *The Adrenal Cortex. In 'Endocrinology and Metabolism'*. McGraw-Hill, New York. 4th edition.

Milnar, B., Marc, J., Janez, A. and Pfeifer, M. (2007) Molecular mechanisms of insulin resistance and associated diseases. *Clinica Chimica Acta*, 375: 20-35.

Miranda, P.J., DeFronzo, R.A., Califf, R.M. and Guyton, J.R. (2005) Metabolic syndrome: Definition, pathophysiology and mechanisms. *American Heart Journal*, 33-45.

Misra, A. and Khurana, L. (2008) Obesity and the metabolic syndrome in developing coutries. *Journal of Clinical Endocrinology and Metabolsim*, 93(11): S9-S30.

Moller, D.E. and Kaufman, K.D. (2005) Metabolic syndrome: A clinical and molecular perspective. *Annual Reviews of Medicine*, 56: 45 – 62.

Montague, C.T., Prins, J.B., Sanders, L., Zhang, J.L. Sewter, C.P., Digby, J., Byme, C.D. and O'Rahilly, S. (1998) Depot-related gene expression in human subcutaneous and omental adipocytes. *Diabetes*, 47; 1384-1391.

Mori, Y., Murakawa, Y., Okada, K., Horikoshi, H., Yokoyama, J., Tajima, N. and Ikeda, Y. (1999) Effects of troglitazone on body fat distribution in type 2 diabetic patients. *Diabetes Care*, 22: 908-912.

Morton, M.M., Holmes, M.C., Fievet, C., Staels, B., Tailleux, A., Mullins, J.J. and Seckl, J.R. (2001) Improved lipid and lipoprotein profile, hepatic insulin sensitivity and glucose tolerance in 11β-hydroxysteroid dehydrogenase type 1 null mice. *The Journal of Biological Chemistry*, 276(44): 41293-41300.

Morton, N.M., Ramage, L. and Seckl, J.R. (2004) Down-regulation of adipose 11β-hydroxysteroid dehydrogenase type 1 by high-fat feeding in mice: a potential adaptive mechanism counteracting metabolic disease. *Endocrinology*, 145, 2707 – 2712.

Mukherjee, M. (2003) Human digestive and metabolic lipases – a brief review. *Journal of Moleculare Catalysis B: Enzymatic*, 22: 369 – 401.

Muoio, D.M. and Newgard, C.B. (2006) Obesity-related derangements in metabolic regulation. *Annual Review of Biochemistry*, 75: 367-401.

Mussig, K., Remer, T., Haupt, A., Gallwitz, B., Fritsche, A., Häring, H.U. and Maser-Gluth, C. (2008) 11β-hydroxysteroid dehydrogenase 2 activity is elevated in severe obesity and negatively associated with insulin sensitivity. *Obesity*, 16(6): 1256-1260.

Nakagawa, K., Kishida, H., Arai, N., Nishiyama, T., Mae, T. (2004) Licorice flavonoids suppress abdominal fat accumulation and increase in blood glucose level in obese diabetic KK-A^y mice. *Biological and Pharmacological Bulletin*, 27: 1775-1778.

Nestel, P., Lyu, R., Low, L.P., Sheu, W.H., Nitiyanant, W., Saito, I. and Tan, C.E. (2007) Metabolic syndrome: Recent prevalence in East and Southeast Asian populations. *Asia Pacific Journal of Clinical Nutrition*, 16(2): 362-367.

Ng, I.E.H. (2008) *11β-Hydroxysteroid Dehydrogenase Levels in Rats on Combination of Normal and High Fat Diet and Given Glycyrrhizic Acid*. Honours Thesis, Monash University.

Nolan, T., Hands, R.E. and Bustin, S.A. (2006) Quantification of mRNA using real-time PCR. *Nature*, 1(13), 1559 – 1582.

Nuotio-Antar, A.M., Hachey, D.L. and Hasty, A.H. (2007) Carbenoxolone treatement attenuates symptoms of metabolic syndrome and atherogenesis in obese, hyperlipidemic mice. *American Journal of Physiology – Endocrinology and Metabolism*, 293: E1517 – E1528.

Nwe, K.H.H., Hamid, A., Morat, P.B. and Khalid, B.A.K. (2000) Differential regulation of the oxidative 11β-hydroxysteroid dehydrogenase activity in testis and liver. *Steroids*, 65, 40 – 45.

Okuno, A., Tamemoto, H., Tobe, K., Ueki, K., Mori, Y., Iwamoto, K., Umesono, K., Akanuma, Y., Fujiwara, T., Horikoshi, H., Yazaki, Y. and Kadowaki, T. (1998) Troglitazone increases the number of small adipocytes without the change of white adipose tissue mass in obese Zucker rats. *Journal of Clinical Investigation*, 101(6): 1354-1361.

Okutucu, B., Dınçer, A., Habib, Ö. and Zıhnıoglu, F. (2007) Comparison of five methods for determination of total plasma protein concentration. *Journal of Biochemical and Biophysical Methods*, 70: 709 – 711.

Ostenson, C.G. (2001) The pathophysiology of type 2 diabetes mellitus: An overview. *Acta Physiologica Scandinavica*, 171: 241-247.

Pácha, J., Mikšik, I., Lisá, V. and Pohlová, I. (1997) Hormonal regulation of intestinal 11β-hydroxysteroid dehydrogenase. *Life Sciences*, 61: 2391 – 2396.

Paterson, J.M., Morton, N.M., Fievet, C., Kenyon, C.J., Holmes, M.C., Staels, B., Seckl, J.R. and Mullins, J.J. (2004) Metabolic syndrome without obesity: hepatic overexpression of 11β-hydroxysteroid dehydrogenase type 1 in transgenic mice. *Proceedings of the National Academy of Science of United States of America*, 101(18): 7088-7093.

Paterson, J.M., Seckl, J.R. and Mullins, J.J. (2005) Genetic manipulation of 11β-hydroxysteroid dehydrogenases in mice. *The American Journal of Physiology - Regulatory, Integrative and Comparative Physiology*, 289: R642 – R652.

Permutt, M.A., Wasson, J. and Cox, N. (2005) Genetic epidemiology of diabetes. *The Journal of Clinical Investigation*, 115(6): 1431-1439.

Picard, F. and Auwerx, J. (2002) PPAR and glucose homeostasis. *Annual Review of Nutrition*, 22: 167-197.

Pillarisetti, S. and Saxena, U. (2003) Lipoprotein lipase as a therapeutic target for dyslipidemia. *Frontiers in Bioscience*, 8: d238 – 241.

Plaffl, M.W., Horgan, G.W. and Dempfle, L. (2002) Relative expression software tool (REST©) for group-wise comparison and statistical analysis of relative expression results in real-time PCR. *Nucleic Acid Research*, 30 (9): 1 – 10.

Ploeger, B.A., Meulenbelt, J. and DeJongh, J. (2000) Physiologically based pharmacokinetic modelling of glycyrrhizic acid, A compound subject to presystemic metabolism and enterohepatic cycling. *Toxicology and Applied Pharmacology*, 162: 177-188.

Ploeger, B., Mensinga, T., Sips, A., Seinen, W., Meulenbelt, J. and DeJongh, J. (2001) The pharmacokinetics of glycyrrhizic acid evaluated by physiologically based pharmacokinetic modelling. *Drug Metabolism Reviews*, 33(2): 125-147.

Pollare, T., Vessby, B. and Lithell, H. (1991) Lipoprotein lipase activity in the skeletal muscle is related to insulin sensitivity. *Arteriosclerosis, Thrombosis and Vascular Biology*, 11: 1192-1203.

Preiss-Landi, K., Zimmermann, R., Hammerle, G. And Zechner, R. (2002) Lipoprotein lipase: The regulation of tissue specific expression and its role in lipid and energy metabolism. *Current Opinion of Lipidology*, 13(5): 471 – 481.

Qi, D. and Rodrigues, B. (2006) Glucocorticoids produce whole body insulin resistance with changes in cardiac metabolism. *American Journal of Physiology, Endocrinology and Metabolism,* 292: E654 – E667.

Qiagen (2006) Appendix B: Storage, quantitation and determination of quality of total RNA. In: *RNeasy® Mini Handbook*, QIAGEN: USA, pp. 65-67.

Rahmouni, K., Morgan, D.A., Morgan, G.A., Mark, A.L. and Haynes, W.G. (2005) Role of selective leptin resistance in diet-induced obesity hypertension. *Diabetes*, 54: 2012-2018.

Rang, H.P., Dale, M.M., Ritter, J.M. and Moore, P.K. (2003) *Pharmacology: Absorption and distribution of drugs.* Churchill Livingstone, Edinburg (UK); 5th Edition: 98 – 100.

Rangwala, S.M. and Lazar, M.A. (2004) Peroxisome proliferator-activated receptor γ in diabetes and metabolism. *Trends in Pharmacological Sciences*, 25(6): 331-336.

Richter, B., Bandeira-Echtler, E., Bergerhoff, K., Clar, C. and Ebrahim, S.H. (2007) Rosiglitazone for type 2 diabetes mellitus. *Cochrane Database of Systematic Reviews*, Issue 3. Art. No.: CD006063. DOI: 10.1002/14651858.CD006063.pub2.

Ricote, M., Li, A.C., Wilson, T.M., Kelly, C.J. and Glass, C.K. (1998) The peroxisome proliferator-activated receptor-gamma in a negative regulator of macrophage activation. *Nature*, 391: 79-82.

Ricote, M. and Glass, C.K. (2007) PPARs and molecular mechanisms of transrepression. *Biochimica et Biophysica Acta*, 1771: 926-935.

Rodriguez, E., Ribot, J., Rodriguez, A.M. and Palou, A. (2004) PPARγ2 expression in response to cafeteria diet: gender- and depot-specific effects. *Obesity Research*, 9: 1455-1463.

Ronti T, Lupattelli G and Mannarino E (2006) The endocrine function of adipose tissue: an update. *Clinical Endocrinology*, 64: 355 – 365.

Rosen, E.D. and Spiegelman, B.M. (2006) Adipocytes as regulators of energy balance and glucose homeostasis. *Nature*, 444: 847-854.

Rosmond, R., Radulovic, V., Holm, G. (2006) A brief update of glucocorticoid receptor variants and obesity risk. *Annals of the New York Academy of Sciences*, 1083: 153-164.

Ruan, X., Zheng, F. and Guan, Y. (2008) PPARs and the kidney in metabolic syndrome. *American Journal of Physiology Renal Physiology*, 294: 1032-1047.

Rubenstrunk, A., Hanf, R., Hum, D.W., Fruchart, J. and Staels, B. (2007) Safety issues and prospects for future generations of PPAR modulators. *Biochimica et Biophysica Acta*, 1771: 1065-1081.

Ruzzin, J., Wagman, A.S. and Jensen, J. (2005) Glucocorticoid-induced insulin resistance in skeletal muscles: defects in insulin signalling and the effects of a selective glycogen synthase kinase-3 inhibitor. *Diabetologia*, 48: 2119-2130.

Ryan, M.J., Didion, S.P., Mathur, S., Faraci, F.M. and Sigmund, C.D. (2004) PPAR agonist rosiglitazone improves vascular function and lowers blood pressure in hypertensive transgenic mice. *Hypertension*, 43: 661-666.

Saltiel, A.R. (2001) New perspectives into the molecular pathogenesis and treatment of type 2 diabetes. *Cell*, 104: 517-529.

Santamarina-Fojo, S. and Brewer Jr., H.B. (1994) Lipoprotein lipase: Structure, function and mechanism of action. *International Journal of Clinical & Laboratory Research*, 24: 143 – 147.

Savage, D.B., Petersen, K.F. and Shulman, G.I. (2007) Disordered lipid metabolism and the pathogenesis of insulin resistance. *Physiology Review*, 87: 507-520.

Schoonjans, K., Peinado-Onsurbe, J., Lefebvre, A.M., Heyman, R.A., Briggs, M., Deeb, S., Staels, B. and Auwerx, J. (1996) PPARα and PPARγ activators direct a distinct tissue-specific transcriptional response via a PPRE in the lipoprotein lipase gene. *The European Molecular Biology Organization Journal*, 15(19): 5336-5348.

Seckl, J.R. (1997) 11 beta-hydroxysteroid dehydrogenase in the brain: A novel regulator of glucocorticoid action? *Frontiers in Neuroendocrinology*, 18: 49-99.

Sell, H., Dietze-Schroeder, D. and Eckel, J. (2006) The adipocytes-myocyte axis in insulin resistance. *Trends in Endocrionology and Metabolism*, 17: 416-422.

Semple, R.K., Chatterjee, V.K.K. and Rahilly, S.O. (2006) PPARγ and human metabolic disease. *Journal of Clinical Investigation*, 116: 581-589.

Shearer, B.G. and Billin, A.N. (2007) The next generation of PPAR drugs: Do we have the tools to find them? *Biochimica et Biophysica Acta*, 1771: 1082-1093.

Shen, G.X. (2007) Lipid disorders in diabetes mellitus and current management. *Current Pharmaceutical Analysis*, 3: 17-24.

Shimoyama Y, Hirabyashi K, Matsumoto H, Sato T, Shibata S and Inoue H (2003) Effects of glycyrrhetinic acid derivatives on hepatic and renal 11β-hydroxysteroid dehydrogenase activities in rats. *Journal of Pharmacy and Pharmacology*, 55: 811 – 817.

Sidhu, J.S., Kaposzta, Z., Markus, H.S. and Kaski, J.C. (2004) Effect of rosiglitazone on common carotid intima-media thickness progression in coronary artery disease patients without diabetes mellitus. *Atherosclerosis, Thrombosis and Vascular Biology*, 24: 930-934.

Smith, U. (2002) Impaired ('Diabetic') insulin signaling and action occur in fat cells long before glucose intolerance – Is insulin resistance initiated in the adipose tissue? *International Journal of Obesity*, 26: 897-904.

Smith, S.A. (2003) Central role of the adipocyte in the insulin-sensitizing and cardiovascular risk modifying actions of thiazolidinediones. *Biochimie*, 85: 1219-1230.

Song, J., Knepper, M.A., Hu, X., Verbalis, J.G. and Ecelbarger, C.A. (2004) Rosiglitazone activates renal sodium- and water-reabsorptive pathways and lowers blood pressure in normal rats. *The Journal of Pharmacology and Experimental Therapeutics*, 308: 426-433.

Spiegelman, B.M. and Flier, J.S. (1996) Adipogenesis and obesity: Rounding out the big picture. *Cell*, 87: 377-389.

Staels, B., Dallongeville, J., Auwerx, J., Schoojans, K., Leitersdorf, E. And Fruchart, J.C. (1998) Mechanisms of action of fibrates on lipid and lipoprotein metabolism. *Circulation*, 98: 2088-2093.

Stormer, F.C., Reistad, R. and Alexander, J. (1993) Glycyrrhizic acid in liquorice – evaluation of health hazard. *Food and Chemical Toxicology*, 31(4): 303-312.

Stump, C.S., Henriksen, E.J., Wei, Y. and Sowers J.R. (2006) The metabolic syndrome: role of skeletal muscle metabolism. *Annals of Medicine*, 38: 389-402.

Sun, Y., Liu, S., Ferguson, S., Wang, L.Q., Klepcyk, P., Yun, J.S. and Friedman, J.E. (2002) Phosphoenolpyruvate carboxykinase overexpression selectively attenuates insulin signaling and hepatic insulin sensitivity in transgenic mice. *Journal of Biological Chemistry*, 277: 233001-23307.

Swali, A., Walker, E.A., Lavery, G.G., Tomlinson, J.W. and Stewart, P.M. (2008) 11β-hydroxysteroid dehydrogenase type 1 regulates insulin and glucagon secretion in pancreatic islets. *Diabetologia,* 51(11): 2003-2011.

Takii, H., Kometani, T., Nishimura, T., Nakae, T., Okada, S. and Fushiki, T. (2001) Antidiabetic effect of Glycyrrhizin in genetically diabetic KK-A^y mice. *Biological and Pharmaceutical Bulletin*, 24(5): 484-487.

Takeda, S., Ishihara, K., Wakui, Y., Amagaya, S., Maruno, M., Akao, T. and Kobashi, K. (1996) Bioavailability study of glycyrrhetic acid after oral administration of Glycyrrhizin in rats; relevance to the intestinal bacterial hydrolysis. *Journal of Pharmacy and Pharmacology*, 48, 902 – 905.

Takeda, K., Ichiki, T., Tokunou, T., Funakoshi, Y., Iino, N., Hirano, K., Kanaide, H. and Takeshita, A. (2000) Peroxisome proliferator-activated receptor activators downregulate angiotensin II type 1 receptor in vascular smooth muscle cells. *Circulation*, 102: 1834-1839.

Tan, K.C.B., Shiu, S.W.M. and Chu, B.Y.M. (1999) Roles of hepatic lipase and cholesteryl ester transfer protein in determining low density lipoprotein subfraction distribution in Chinese patients with non-insulin-dependent diabetes mellitus. *Atherosclerosis*, 145: 273-278.

Tan, H.H. and Lim, S.C. (2001) Latent Autoimmune Diabetes in Adults (LADA): A case series. *Singapore Medical Journal*, 42(11): 513 – 516.

Tan, C.E., Ma, S., Wai, D., Chew, S.K. and Tai, E.S. (2004) Can we apply the National Cholesterol Education Program Adult Treatment Panel definition of the metabolic syndrome to Asians? *Diabetes Care*; 27(5): 1182 – 1186.

Tanahashi, T., Mune, T., Morita, H., Tanahashi, H., Isomura, Y., Suwa, T., Daido, H., Gomez-Sanchez, C.E. and Yasuda, K. (2002) Glycyrrhizic acid suppresses type 2 11β-hydroxysteroid dehydrogenase expression in vivo. *Journal of Steroid Biochemistry and Molecular Biology*, 80, 441 – 447.

Tavangar, K., Murata, Y., Pedersen, M.E., Goers, J.F., Hoffman, A.R. and Kraemer, F. (1992) Regulation of lipoprotein lipase in the diabetic rat. *Journal of Clinical Investigation*, 90: 1672-1678.

Thompson, C.B. (1995) Apoptosis in the pathogenesis and treatment of disease. *Science*, 267 (5203): 1456-1462.

Tiu, K.M. (2008) *Molecular cloning and expression of peroxisome proliferator-activated receptor gamma 2 (PPARγ2) in glycyrrhizic acid (GA) treated and non-treated Rats.* Honours Thesis, Monash University.

Tomlinson, J.W., Walker, E.A., Bujalska, I.J., Draper, N., Lavery, G.G., Cooper, M.S., Hewison, M. and Stewart, P.M. (2004) 11β-hydroxysteroid dehydrogenase type 1: A tissue-specific regulator of glucocorticoid response. *Endocrine Reviews*, 25: 831 – 866.

Tomlinson, J.W. and Stewart, P.M. (2007) Modulation of glucocorticoid action and the treatment of type-2 diabetes. *Clinical Endocrinology and Metabolism*, 21(4): 607-619.

Tsutsumi, K. (2003) Lipoprotein lipase and artherosclerosis. *Current Vascular Pharmacology*, 1: 11 – 17.

Unger, R.H. and Orci, I. (2001) Diseases of liporegulation: new perspective on obesity and related disorders. *FASEB Journal*, 15: 312-321.

Vaerman, J.L., Saussoy, P. and Ingargiola, I. (2004) Evaluation of real-time PCR data. *Journal of Biological Regulators and Homeostatic Agents*, 18: 212 – 214.

Valera, A., Pujol, A., Pelegrin, M. and Bosch, F. (1994) Transgenic mice overexpressing phosphoenolpyruvate carboxykinase develop non-insulin-dependent diabetes mellitus. *Proceedings in National Academy of Science U. S. A.*, 91: 9151-9154.

van Tilbeurgh, H., Roussel, A., Laouel, J.M. and Cambillau, C. (1994) Lipoprotein lipase- Molecular model based on the pancreatic lipase X-ray structure: Consequences for heparin binding and catalysis. *The Journal of Biological Chemistry*, 269(6): 4626 – 4633.

van Zwieten, P.A and Mancia, G. (2006) Background and treatment of metabolic syndrome: A therapeutic challenge. *Seminars in Cardiothoracic and Vascular Anesthesia*, 10(3): 206-214.

Vegiopoulos, A. and Verzig, S. (2007) Glucocorticoids, metabolism and metabolic diseases. *Molecular and Cellular Endocrinology*, 275: 43-61.

Vidal-Puig, A., Jimenez-Linan, M., Lowell, B.B., Hamann, A., Hu, E., Spiegelman, B., Flier, J.S. and Moller, D.E. (1996) Regulation of PPARγ gene expression by nutrition and obsity in rodents. *Journal of Clinical Investigation*, 97(11): 2553-2561.

Wake, D.J., Strand, M., Rask, E., Westerbacka, J., Livingstone, D.E.W., Soderberg, S., Andrew, R., Yki-Jarvinen, H., Olsson, T. and Walker, B.R. (2007) Intra-adipose sex steroid metabolism and body fat distribution in idiopathic human obesity. *Clinical Endocrinology,* 66: 440 – 446.

Waki, H. and Tontonoz, P. (2006) Endocrine function of adipose tissue. *Annual Review of Pathology: Mechanisms of Disease*, 2: 31-56.

Walker, E.A., Ahmed, A., Lavery, G.G., Tomlinson, J.W., Kim, S.Y., Cooper, M.S., Ride, J.P., Hughes, B.A., Shackleton, C.H.L., McKiernan, P., Elias, E., Chou, J.Y. and Stewart, P.M. (2007) 11β-hydroxysteroid dehydrogenase type 1 regulation by intracellular glucose 6-phosphate provides evidence for a novel link between glucose metabolism and hypothalamo-pituitary-adrenal axis Function. *The Journal of Biological Chemistry*, 82: 27030 – 27036.

Wallace, T.M., Levy, J.C. and Matthews, D.R. (2004) Use and abuse of HOMA modelling. *Diabetes Care*, 27(6): 1487-1495.

Wang, Z., Nishioka, M., Kurosaki, Y., Nakayama, T. and Kimura, T. (1995) Gastrointestinal absorption characteristics of Glycyrrhizin from glycyrrhiza extract. *Biological and Pharmaceutical Bulletin*, 18: 1238 – 1241.

Wassink, A.M.J., Olijhoek, J.K. and Visseren, F.L.J. (2007) The metabolic syndrome: Metabolic changes with vascular consequences. *European Journal of Clinical Investigation*, 37: 8-17.

Way, J.M., Harrington, W.W., Brown, K.K., Gottschalk, W.K., Sundseth, S.S., Mansfield, T.A., Ramachandran, R.K., Willson, T.M. and Kliewer, S.A. (2001) Comprehensive messenger ribonucleic acid profiling reveals that peroxisome proliferators-activated receptor γ activation has coorfinate effects on gene expression in multiple insulin-sensitive tissues. *Endocrinology*, 142: 1269-1277.

Whorwood, C.B., Sheppard, M.C. and Stewart, P.M. (1993) Licorice inhibits 11β-hydroxysteroid dehydrogenase messenger ribonucleic acid levels and potentiates glucocorticoid hormone action. *Endocrinology*, 132, 2287 – 2292.

Whorwood, C.B., Donovan, S.J., Flanagan, D., Phillips, D.I. and Byrne, C.D. (2002) Increased glucocorticoid receptor expression in human skeletal muscle cells may contribute to the pathogenesis of the metabolic syndrome. *Diabetes*, 51, 1066–1075.

Wong, H., Davis, R.C., Thuren, T., Goers, J.W., Nikazy, J., Waite, M. and Schotz, M.C. (1994) Lipoprotein lipase domain function. *The Journal of Biological Chemistry*, 269(14): 13019 – 10323.

Wong, H. and Schotz, M.C. (2002) The lipase gene family. *Journal of Lipid Research*, 43: 993 – 999.

Wu, Z., Xie, Y., Morrison, R.F., Bucher, N.L. and Farmer, S.R. (1998) PPARgamma induces the insulin-dependent glucose transporter GLUT4 in the absence of C/EBPalpha during the conversion of 3T3 fibroblasts into adipocytes. *Journal of Clinical Invesitgation*, 101(1): 22-32.

Yao, B., Harris, R.C. and Zhang, M.Z. (2005). Interactions between 11β-hydroxysteroid dehydrogenase and COX-2 in kidney. *American Journal of Physiology Regulatory, Integrative and Comparative Physiology,* 288: 1767-1773.

Zhang, Y., Repa, J.Y., Gauthier, K. and Mangelsdorf, D.J. (2001) Regulation of lipoprotein lipase by the oxysterol receptors, LXRα and LXRβ. *The Journal of Biological Chemistry*, 276(46): 43018 – 43024.

Zhang, H., Zhang, A., Kohan, D.E., Nelson, R.D., Gonzalez, F.J. and Yang, T. (2005) Collecting duct-specific deletion of peroxisome proliferator-activated receptor gamma blocks thiazolidinediones-induced fluid retention. *Proceedings of the National Academy of Sciences*, 102: 9406-9411.

Zheng, F., Fornono, A. and Elliot, S.J. (2002) Upregulation of type 1 collagen by TGF-beta in mesangial cells is blocked by PPAR gamma activation. *American Journal of Physiology Renal Physiology*, 282: 639-648.

Zimmet, P., Alberti, K.G.M.M. and Shaw, J. (2001) Global and society implications of the diabetes epidemic. *Nature*, 414: 782-787.

APPENDIX 1

Equation for calculation of sample size

$$m = (z_\alpha + z_{2\beta})^2 [\pi_1 (1 - \pi_1) + \pi_2 (1 - \pi_2)] / \delta^2$$

$(z_\alpha + z_{2\beta})^2$ = ordinates for the normal distribution

when power = 80%, $(z_\alpha + z_{2\beta})^2 = 7.849$

power = 90%, $(z_\alpha + z_{2\beta})^2 = 10.507$

π_1 = proportion in the control group

= 0.05

π_2 = proportion in the treated group

= 0.00

δ = difference in means

$= \pi_2 - \pi_1$

α = significance level (taken to be 5%)

(Campbell and Machin, 2002)

APPENDIX 2

Table A.2.1: Volume of respective reagents used for the preparation of glucose standards

Standard Glucose (10 mmol/L)/ µL	Protein Precipitate /mL	Final Volume/ mL	Final glucose concentration/ mmol/L
100	5.9	6.0	5
200	5.8	6.0	10
300	5.7	6.0	15
400	5.6	6.0	20

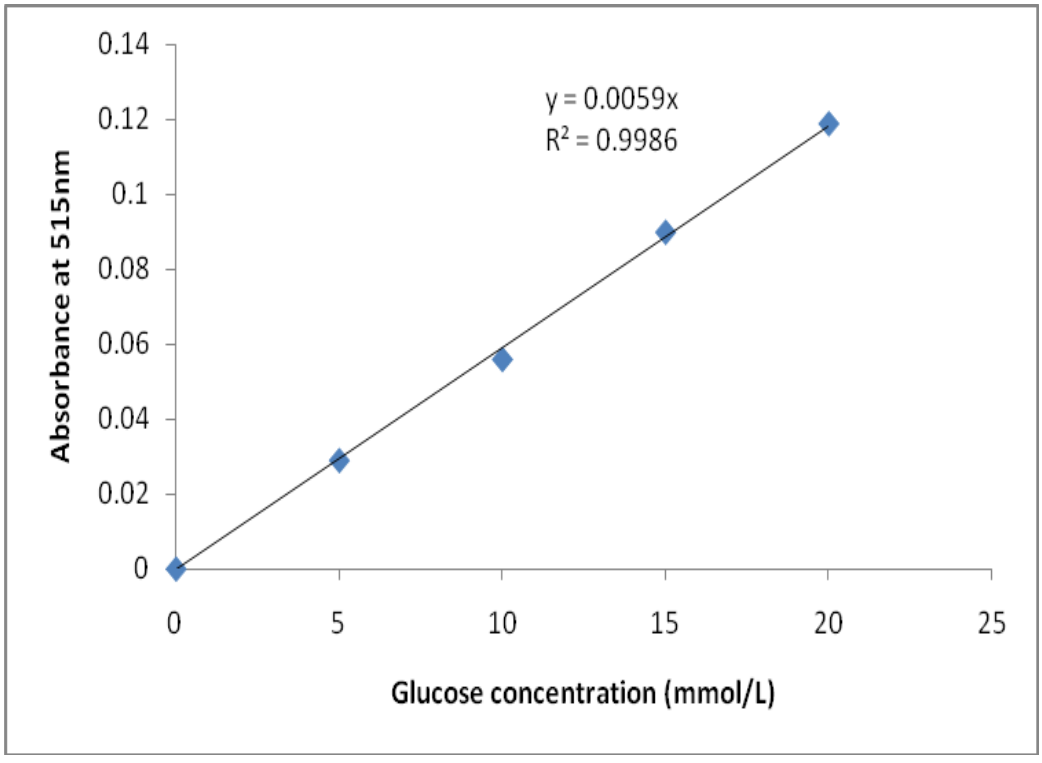

Figure A2.1: Representative standard curve of glucose standards ranging from 5 to 20 mmol/L.

Table A2.2: Volume of respective reagents used for the preparation of insulin standards

Concentration of insulin standards/ ng/mL	Volume of standard **added/ µL**	Final insulin concentration/ ng/mL
0.2	10	0.2
0.5	10	0.5
1.0	10	1.0
2.0	10	2.0
5.0	10	5.0
10.0	10	10.0

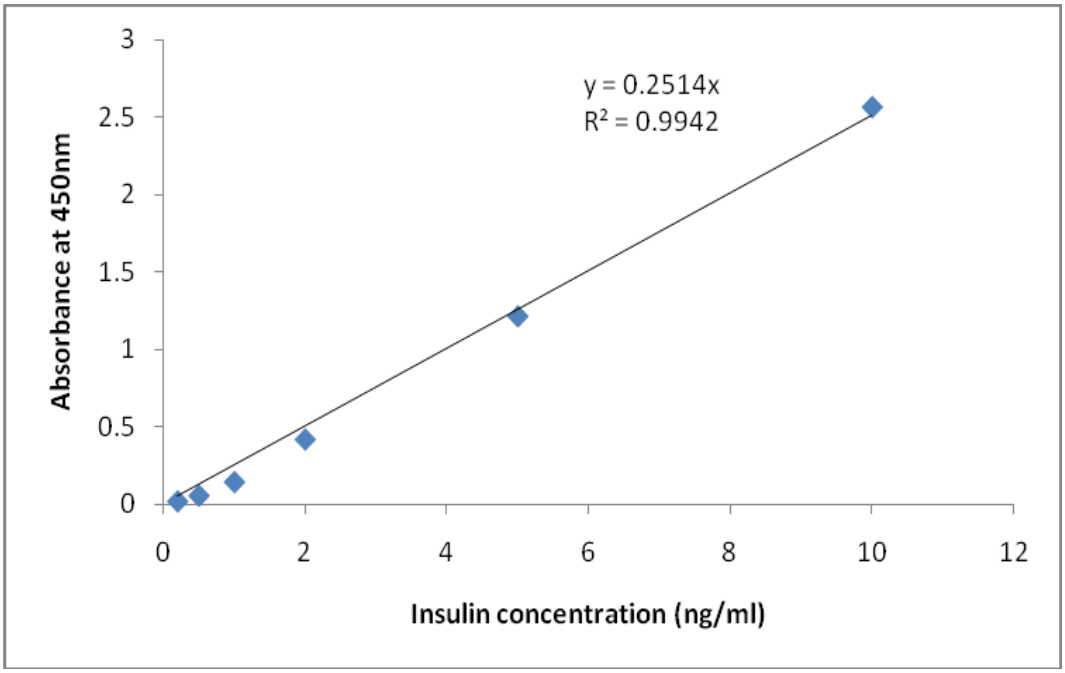

Figure A2.2: Representative standard curve of insulin standards ranging from 0.2 to 10 ng/mL.

Table A.2.3: Volume of respective reagents used for the preparation of TAG standards

Standard TAG (3.39 mmol/L)/ µL	Distilled water /µL	Final Volume/ µL	Final TAG concentration/ mmol/L
2.2	12.8	15.0	0.50
4.4	10.6	15.0	1.00
8.8	6.2	15.0	2.00
13.2	1.8	15.0	3.00

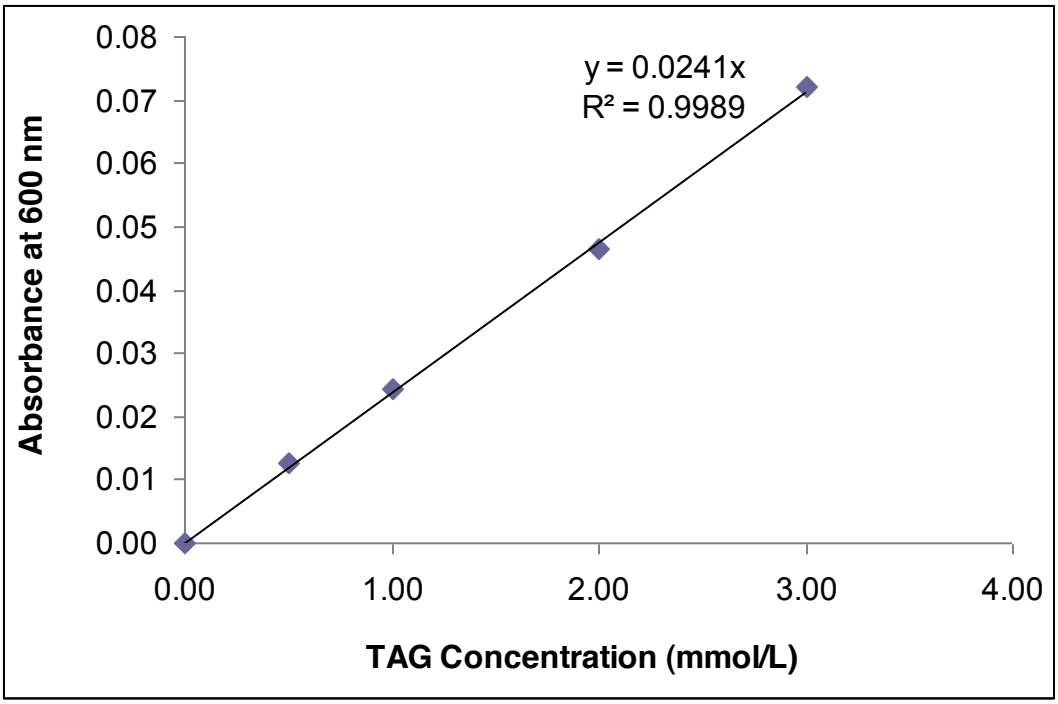

Figure A2.3: Representative standard curve of TAG standards ranging from 0.50 to 3.00 mmol/L.

Table A.2.4: Volume of respective reagents used for the preparation of cholesterol standards

Standard cholesterol (5.17 mmol/L)/ µL	Distilled water /µL	Final Volume/ µL	Final cholesterol concentration/ mg/dL
1.9	8.1	10.0	1.00
3.9	6.1	10.0	2.00
5.8	4.2	10.0	3.00
7.7	2.5	10.0	4.00
9.7	0.3	10.0	5.00

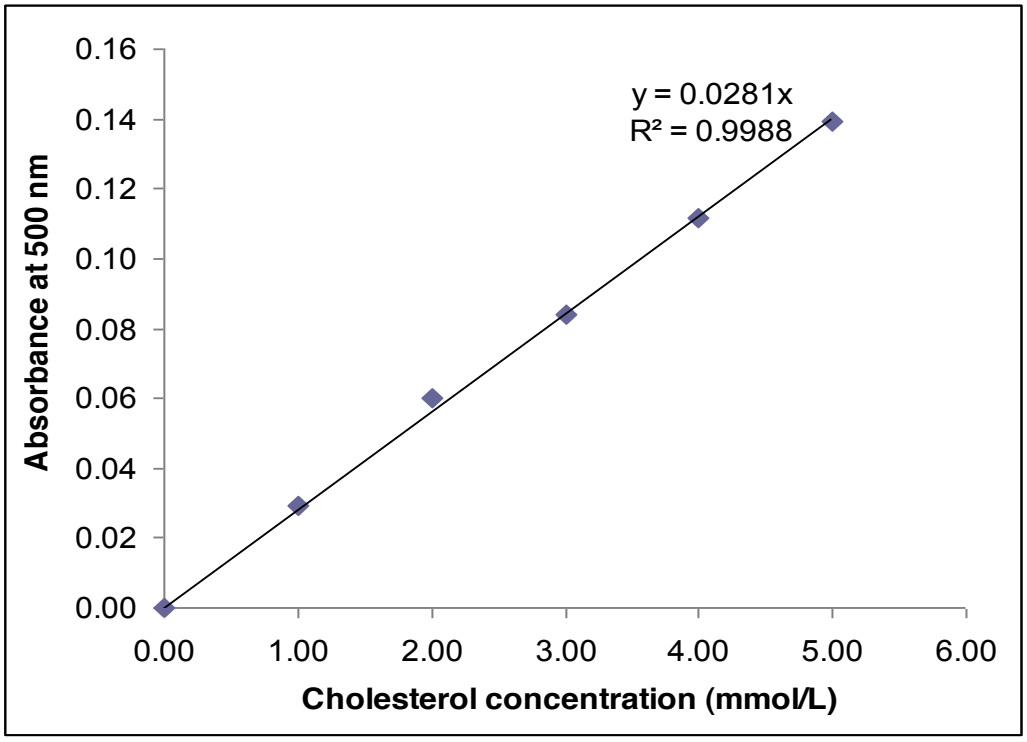

Figure A2.4: Representative standard curve of cholesterol standards ranging from 1.00 to 5.00 mmol/L.

Table A2.5: Volume of respective reagents used for the preparation of HDL-cholesterol standards

Standard HDL-cholesterol **(5.17 mmol/L)/ µL**	Distilled water **/µL**	**Final Volume/ µL**	Final HDL-cholesterol concentration/ mg/dL
4.7	30.3	35.0	0.20
9.5	25.5	35.0	0.40
18.9	16.1	35.0	0.80
28.4	6.6	35.0	1.20
33.1	1.9	35.0	1.40

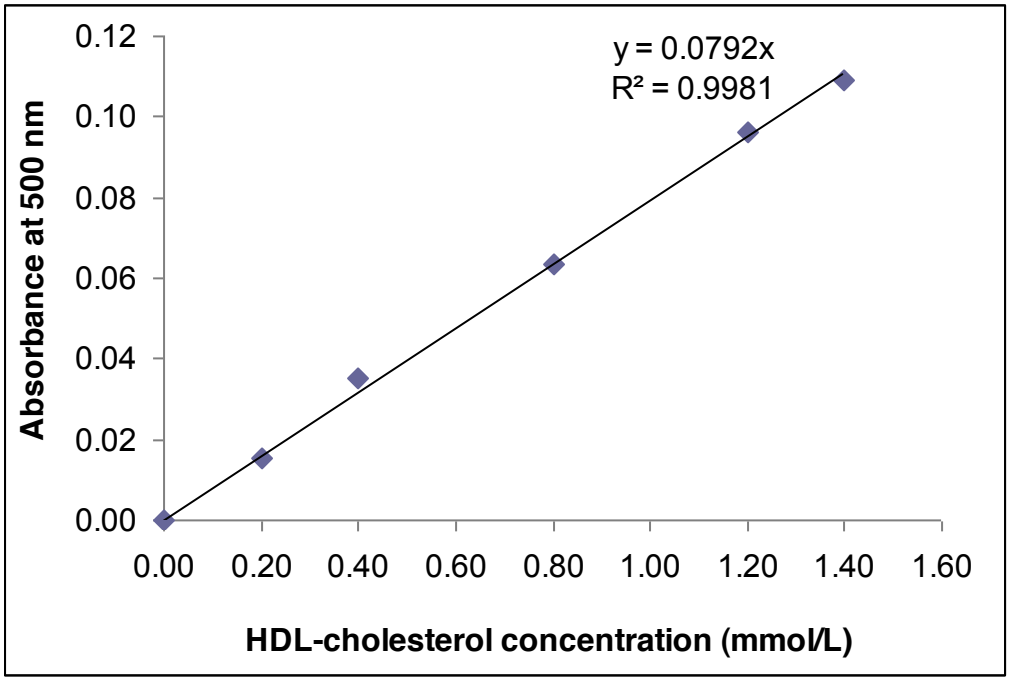

Figure A2.5: Representative standard curve of HDL-cholesterol standards ranging from 0.20 to 1.40 mmol/L.

APPENDIX 3

Protocol for total mRNA extraction from liver and kidney (Qiagen, USA)

30mg of liver and kidney tissues mentioned in Section 2.1.6.2 were snap frozen in liquid nitrogen and ground to fine powder under liquid nitrogen using a mortar and pestle. The suspension was transferred to an RNase-free, liquid-nitrogen-cooled microcentrifuge tube and the liquid nitrogen was allowed to evaporate. Then, 600µl of buffer RLT (as per manufacturer) was added into each tube. The solution was mixed to ensure homogenous mixing prior to the transfer of the lysate into a Qiashredder spin column placed in a 2ml collection tube. The lysate was centrifuged at 16,000 x g for 2 minutes to homogenize the tissue. The supernatant was transferred to a new microcentrifuge tube. 600µl of 70% ethanol was added and mixed immediately. 700µl of the mixture was transferred into an RNeasy spin column placed in a 2ml collection tube. The column was centrifuged at 10,000 x g for 15 seconds and the resulting flow-through was discarded. The same centrifugation conditions were used for the remainder of the lysate.

Next, 700µl of buffer RW1 (as per manufacturer) was added into the RNeasy spin column and centrifuged at 10,000 x g for 15 seconds to wash the column membrane. The flow-through was again discarded and the spin column was transferred to another clean 2ml-collection tube. 500µl of buffer RPE (as per manufacturer) was added into the spin column and centrifuged at 10,000 x g for 15 seconds. The flow-through was discarded. The step was repeated with the same conditions except centrifugation duration was increased to two minutes instead of 15 seconds. The spin column was transferred to a new 2ml-collection tube and was centrifuged at 16,000 x g for one minute. The spin column was again transferred to a new 2ml-collection tube and 30µl of RNase-free water was added directly to the membrane. The spin column was centrifuged at 10,000 x g for one minute to elute the bound mRNA.

APPENDIX 4

Protocol for total mRNA extraction from abdominal and quadriceps femoris muscles (Qiagen, USA)

30mg of abdominal and quadriceps femoris muscles mentioned in Section 2.1.6.2 were snap frozen in liquid nitrogen and ground to fine powder under liquid nitrogen using a mortar and pestle. The suspension was transferred to an RNase-free, liquid-nitrogen-cooled microcentrifuge tube and the liquid nitrogen was allowed to evaporate. Then, 300µl of buffer RLT was added into each tube. The solution was vortex to ensure homogenous mixing prior to the transfer of the lysate into a Qiashredder spin column placed in a 2ml-collection tube. The lysate was centrifuged at 16,000 x g for 2 minutes. 590µl of distilled water and 10µl of 20mg/mL Proteinase K solution were added to the flow-through (eluent) and mixed thoroughly. The column was incubated at 55^{O}C for 10 minutes in a water bath prior to centrifugation at 10,000 x g for three minutes. The supernatant was transferred into a new microcentrifuge tube and 450µl of 95% ethanol was added. The solution was mixed well and 700µl of the mixture was transferred into an RNeasy spin column placed in a 2ml collection tube. The column was centrifuged at 10,000 x g for 15 seconds and the flow-through was discarded. The same centrifugation conditions were used for the rest of the lysate.

Next, 350µl of buffer RW1 (as per manufacturer) was added into the RNeasy spin column and centrifuged at 10,000 x g for 15 seconds to wash the column membrane. The flow-through was again discarded and the spin column was transferred to another clean 2ml-collection tube. 500µl of buffer RPE (as per manufacturer) were added into the spin column and centrifuged at 10,000 x g for 15 seconds. The flow-through was discarded. The step was repeated under the same conditions except centrifugation duration was increased to two minutes instead of 15 seconds. The spin column was transferred to a new 2ml collection tube and was centrifuged at 16,000 x g

for one minute. The spin column was again transferred to a new 2ml collection tube and 30µl of RNase-free water was added directly to the membrane. The spin column was centrifuged at 10,000 x g for one minute to elute the bound mRNA.

APPENDIX 5

Protocol for total mRNA extraction from subcutaneous and visceral adipose tissues (Qiagen, USA)

100mg of subcutaneous and visceral adipose tissue were cut into tiny pieces and placed into a 2ml-microcentrifuge tube. 1ml of QIAzol Lysis Reagent (as per manufacturer) and 20 stainless steel beads with diameters of approximately 5mm were immediately added into the microcentrifuge tube. The tissue was homogenized by vortexing for two minutes. The homogenate was transferred into a new 2ml-microcentrifuge tube and placed at room temperature (25°C) for 5 minutes to ensure dissociation of nucleoprotein complexes. Then, 200µl of chloroform were added and the mixture was vortexed for 15 seconds before incubation at room temperature for 3 minutes. Then, the tube was centrifuged at 4ºC and 12,000 x g for 15 minutes. The upper aqueous phase was transferred to a new collection tube. 600µl of 70% ethanol were added and mixed thoroughly by vortexing. 700µl of the mixture were transferred to an RNeasy spin column placed in a 2ml-collection tube and centrifuged at 10,000 x g for 15 seconds. The flow-through was discarded. The same centrifugation conditions were repeated for the rest of the mixture.

Next, 700µl of buffer RW1 (as per manufacturer) was added into the RNeasy spin column and centrifuged at 10,000 x g for 15 seconds to wash the column membrane. The flow-through was again discarded and the spin column was transferred

to another clean 2ml collection tube. 500µl of buffer RPE (as per manufacturer) was added into the spin column and centrifuged at 10,000 x g for 15 seconds. The flow-through was discarded. The step was repeated with the same conditions except centrifugation duration was increased to two minutes instead of 15 seconds. The spin column was transferred to a new 2ml-collection tube and centrifuged at 16,000 x g for one minute. The spin column was again transferred to a new 2ml-collection tube and 30µl of RNase-free water was added directly to the membrane. The spin column was centrifuged at 10,000 x g for one minute to elute the bound mRNA.

APPENDIX 6

Table A6.1: Reaction mixture for RNase-free DNase treatment

Reaction mixture	1X reaction mixture	Final concentration
Extracted RNA (1µg)	4µl	0.5µg/1µl
RQ1 RNase-free DNase 10X reaction buffer	1µl	1X
RQ1 RNase-free DNase (1U/µg RNA)	5µl	5 units
Total	10µl	-

APPENDIX 7

Table A7.1: Reaction mixture for cDNA synthesis

Reaction mixture	1X reaction mixture	Final concentration
10X Buffer Reverse Transcriptase	2µl	1X
dNTP Mix (5mM each dNTP)	2µl	0.5mM each dNTP
Oligo-dT primer (10µM)	1µl	1mM
RNase inhibitor (10U/µl)	1µl	10 units
Omniscript Reverse Transcriptase	1µl	4 units
RNase-free water	1µl	-
RNA template	1µl	1µg
Total	10µl	-

APPENDIX 8

Table A8.1: Characteristics of primers and probes for total PPARγ, PPARγ2, LPL and BAC amplification (Sigma, USA)

Primer/Probe	**Sequence (5'→3')**	Length (bp)	T_m(^{0}C)	Amplicon size (bp)
PPARγ2 forward primer	TATGCTGTTATGGGTGAAACTC	22	64	91
PPARγ2 reverse primer	CTTGTGAAGTGCTCATAGGC	20	62	
PPARγ2 LNA probe	(6-Fam)CCTCCTGTTGACCCAGAGC(BHQ1)	18	91	
Total PPARγ forward primer	CCCTGGCAAAGCATTTGTAT	20	58	100
Total PPARγ reverse primer	GGTGATTTGTCTGTTGTCTTTCC	23	66	
Total PPARγ LNA probe	(6-Fam)TCCTTCCCGCTGACCA(BHQ1)	16	84	
LPL forward primer	CAGCAAGGCATACAGGTG	18	58	143
LPL reverse primer	CGAGTCTTCAGGTACATCTTAC	22	60	
LPL LNA probe	(6-Fam)TTCTCTTGGCTCTGACC(BHQ1)	17	88	
BAC forward primer	GTATGGGTCAGAAGGACTCC	20	62	80
BAC reverse primer	GTTCAATGGGGTACTTCAGG	20	60	
BAC LNA probe	(TET)CCTCTCTTGCTCTGGGC(BHQ1)	17	90	

Figure A8.1: *Rattus norvegicus* peroxisome proliferator-activated receptor gamma (Pparg) mRNA (1518bp) [NCBI Accession Number: NM_013124.2].

```
1    ATGGGTGAAA CTCTGGGAGA TCCTCCTGTT GACCCAGAGC ATGGTGCCTT CGCTGATGCA
61   CTGCCTATGA GCACTTCACA AGAAATTACC ATGGTTGACA CAGAGATGCC ATTCTGGCCC
121  ACCAACTTCG GAATCAGCTC TGTGGACCTC TCTGTGATGG ATGACCACTC CCATTCCTTT
181  GACATCAAAC CCTTTACCAC GGTTGATTTC TCCAGCATTT CTGCTCCACA CTATGAAGAC
241  ATCCCGTTCA CAAGAGCTGA CCCAATGGTT GCTGATTACA AATATGACCT GAAGCTCCAA
301  GAATACCAAA GTGCGATCAA AGTAGAGCCT GCGTCCCCGC CTTATTATTC TGAAAAAACC
361  CAACTCTACA ACAGGCCACA TGAAGAGCCT TCAAACTCCC TCATGGCCAT CGAGTGCCGA
                                      TOTAL PPAR cloning(F)
                                        ------------------->
421  GTCTGTGGGG ATAAAGCATC AGGCTTCCAC TATGGAGTCC ATGCTTGTGA AGGATGCAAG
481  GGTTTTTTCC GAAGAACCAT CCGATTGAAG CTTATTTATG ATAGGTGTGA TCTTAACTGT
541  CGGATCCACA AAAAGAGTAG AAATAAATGT CAGTACTGTC GGTTTCAGAA GTGCCTTGCT
601  GTGGGGATGT CTCACAATGC CATCAGGTTT GGGCGAATGC CACAGGCCGA GAAGGAGAAG
661  CTGTTGGCGG AGATCTCCAG TGATATCGAC CAGCTGAACC CAGAGTCTGC TGATCTGCGA
       TOTAL PPAR (F)
      --------------------->
721  GCCCTGGCAA AGCATTTGTA TGACTCATAC ATAAAGTCCT TCCCGCTGAC CAAGCCAAG
                                          <-----------------
                                      TOTAL PPAR LNA PROBE
781  GCGAGGGCGA TCTTGACAGG AAAGACAACA GACAAATCAC CATTTGTCAT CTACGACATG
                        <-------------------------
                                 TOTAL PPAR (R)
841  AATTCCTTAA TGATGGGAGA AGACAAAATC AAGTTCAAAC ATATCACCCC CCTGCAGGAG
901  CAGAGCAAAG AGGTGGCCAT CCGCATTTTT CAAGGGTGCC AGTTTCGATC CGTGGAAGCT
                               <----------------------
                            TOTAL PPAR cloning(R)
961  GTGCAAGAGA TCACAGAGTA TGCCAAAAAT ATCCCTGGTT TCATTAACCT TGACTTGAAT
1021 GACCAAGTGA CTCTGCTCAA GTATGGTGTC CATGAGATCA TCTACACCAT GCTGGCCTCC
1081 CTGATGAATA AAGATGGAGT CCTCATATCA GAGGGACAAG GATTCATGAC CAGGGAGTTC
1141 CTCAAAAGCC TGCGGAAGCC CTTTGGTGAC TTTATGGAGC CTAAGTTTGA GTTTGCTGTG
1201 AAGTTCAATG CACTGGAATT AGATGACAGT GACTTGGCCA TATTTATAGC TGTCATTATT
1261 CTCAGTGGAG ACCGCCCAGG CTTGCTGAAC GTGAAGCCCA TCGAGGACAT CCAAGACAAC
1321 CTGCTGCAGG CCCTGGAACT CCAGCTGAAG CTGAACCACC CGGAGTCCTC CCAGCTGTTC
1381 GCCAAGGTGC TCCAGAAGAT GACAGACCTC AGGCAGATTG TCACAGAGCA CGTGCAGCTA
1441 CTGCATGTGA TCAAGAAGAC GGAGACAGAT ATGAGCCTTC ACCCTCTGCT CCAGGAGATC
1501 TACAAGGACT TGTATTAG
```

Figure A8.2: *Rattus norvegicus* peroxisome proliferator-activated receptor gamma 2 (Pparg2) mRNA (1785bp) [NCBI Accession Number: AF156666].

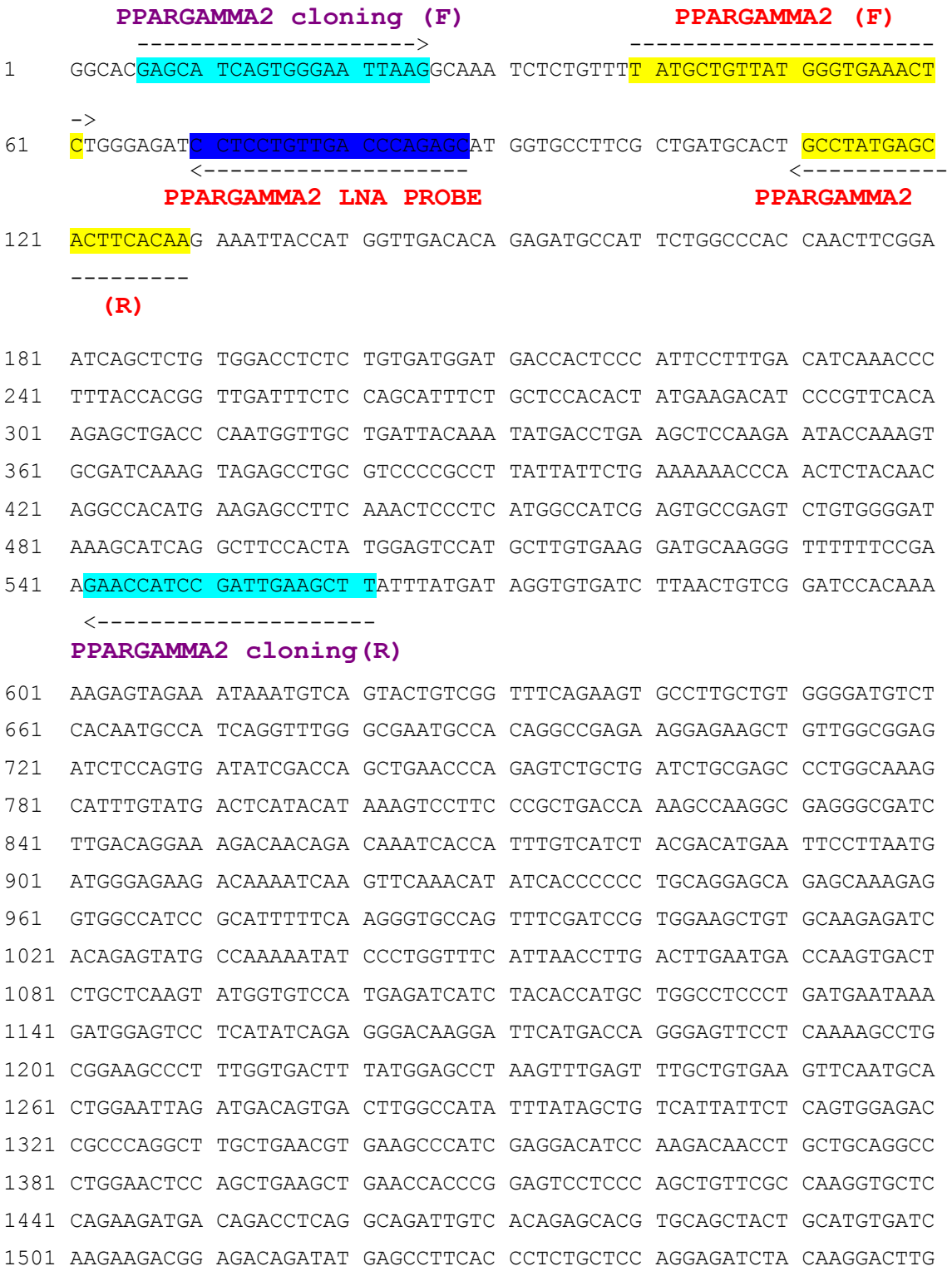

1561 TATTAGCAGA AAAGTCCCAG TCGCTGACAA AGTGTTCCTT CTATCGATTG CACTATTATT
1621 TTGAGGGAAA AAAATCTGAC ACCTAAGAAA TTTACTGTGA AAAAAGCATT TAAAAACAAA
1681 AAGTTTTAGA ACATGATCTA TTTTATGCAT ATTGTTTATA AAGATACATT TACAATTTAC
1741 TTTTAATATT AAAAATTACC ACACTAAAAA AAAAAAAAAA AAAAA

Figure A8.3: *Rattus norvegicus* lipoprotein lipase mRNA (3055bp) [NCBI Accession Number: BC081836].

```
1    CTCCTCCAAG AAATTCTGCC CCTTGTAGCT GTTCTGCCCT CCCCTTTAAA GGTTGACTTG
61   CCCCGCGGCG CTCCACCGCG CTCTAGTCCT CTGACGCCTC CGGCTCAACC CTTTGCAACG
121  CGGATCCCCG CCCGCCTGAC TGCCCGCGCA GCGCAGTTCC AGCAGCAAAG CAGAAGGGCG
181  CGCCCGGAGA TGGAGAGCAA AGCCCTGCTC CTGGTGGCCC TGGGAGTTTG GCTCCAGAGT
241  TTGACCGCCT TCCGCGGAGG GGTGGCCGCA GCAGACGGGG GAAGAGATTT CTCAGACATC
301  GAAAGTAAAT TTGCCCTAAG GACCCCTGAA GACACAGCTG AGGACACTTG TCATCTGATT
361  CCTGGATTAG CAGACTCTGT GTCTAACTGC CACTTCAACC ACAGCAGCAA AACCTTTGTG
421  GTGATCCATG GATGGACGGT GACAGGAATG TATGAGAGTT GGGTGCCCAA ACTTGTGGCT
481  GCCCTATACA AAAGAGAACC TGACTCCAAT GTCATTGTAG TAGACTGGTT GTATCGGGCC
541  CAGCAACATT ATCCAGTGTC TGCCGGCTAT ACCAAGCTGG TGGGAAATGA TGTGGCCAGG
601  TTCATCAACT GGTTGGAGGA AGAATTTAAC TACCCCCTAG ACAATGTCCA CCTCTTAGGG
661  TACAGTCTTG GAGCCCATGC TGCTGGCGTG GCAGGAAGTC TGACCAACAA GAAGGTCAAT
721  AGAATTACTG GCTTGGATCC AGCTGGGCCT AACTTTGAGT ATGCAGAAGC CCCTAGTCGC
781  CTTTCTCCTG ATGATGCGGA TTTCGTAGAT GTCTTACACA CATTTACCAG GGGGTCGCCT
841  GGTCGAAGTA TTGGGATCCA GAAACCAGTA GGGCATGTTG ATATTTATCC CAATGGAGGC
901  ACTTTCCAGC CAGGATGCAA CATTGGAGAA GCCATTCGTG TAATTGCAGA GAAGGGGCTT
961  GGAGATGTGG ACCAGCTGGT GAAGTGCTCG CACGAGCGCT CCATCCATCT CTTCATTGAC
                                    LPL (F)
                                 ----------------->
1021 TCCCTGCTGA ATGAAGAAAA CCCCAGCAAG GCATACAGGT GCAATTCCAA GGAGGCATTT
1081 GAGAAAGGGC TCTGCCTGAG TTGCAGAAAG AATCGCTGTA ACAACGTGGG CTATGAGATC
1141 AACAAGGTCA GAGCCAAGAG AAGCAGTAAG ATGTACCTGA AGACTCGCTC TCAGATGCCC
         <-----------------    <-----------------------
           LPL LNA PROBE            LPL (R)
1201 TACAAAGTAT TCCATTACCA AGTCAAGATT CACTTTTCTG GAACTGAGAA TGACAAGCAA
1261 AACAACCAGG CCTTCGAGAT TTCTCTGTAT GGCACAGTGG CTGAAAGTGA GAACATTCCC
1321 TTCACCCTGC CGGAGGTCGC CACAAATAAA ACCTACTCCT TCTTGATTTA CACGGAGGTG
1381 GACATCGGGG AATTGCTGAT GATGAAGCTT AAGTGGAAGA ACGACTCCTA CTTCCGCTGG
1441 TCAGACTGGT GGAGCAGTCC CAGCTTTGTC ATCGAGAAGA TCCGAGTGAA AGCCGGAGAG
1501 ACTCAGAAAA AGGTCATCTT CTGTGCCAGG GAGAAAGTTT CTCATCTGCA GAAAGGAAAG
1561 GACGCTGCAG TGTTTGTGAA ATGCCATGAC AAGTCTCTGA AGAAGTCGGG CTGACACTGG
1621 ACAAACCAAC AAGAGAAGAA AGCATCTGAG TTCTTTGAAG ACCGAAGAAA ATGAAGTAAA
1681 TTTTATTTAA AAAAAATACC CTTGTTTGGG TGTTTGAAAG TGGATTTTCC TGAGTATTAA
1741 TCCCAGCTAT ATCTTGTTAG TTAAATAGAA GACAGTGTCA AATATTAAAA GGTGGCTAAC
1801 ACAACGTGAG GAACCTAATG GCCGATAGCA TGTCCTCCAG CATCAGAAGA CAGCAGAGAG
```

1861 GAGAAGCATG CCATCTTATA TCCCTTAAGA AGGAATCATT TGTTCCCAAC CATACAAGAC
1921 TCCTTCATGT GACCCATTTG GTCATGGTCT AAAATTAGTA AGGGCCTCTT ATTTTCATTA
1981 GATCTCTGAG GTTTTAAATT GAGACCTTCT CAAAGTTCTC TTGAAGTCTA ATATAGACAA
2041 CATTTTTTTG TGCTGTGAGT CAGATCCATT TCTTTAGCAG TTGAAACAGC TGGCCATTGT
2101 AACTAGTTCT TTTACCATCA GGATATAGCA CCCCTACCAA ATAAAATAAA TAAATAAAGT
2161 GACCAGGGAC ATGTGACTTT GCAAAAGCAA TGGAAGACGT GGCTCGTGGA TTCCTGACCC
2221 TTAGTCCCAC CACAACGAAG TACAAGTCAG TAGAGGTACA AAACCTAGAC TGAGTAATTC
2281 TTAGTAGACT TCAAGTTTTA TGGCTTAATT CCTCTGTCTT TTAAAAACGT GTCACATATT
2341 ATAACATTAT TCTCTAGACA GATGTTGAAA TGAGCTTGTG ATTCAGGTGA CATATGAATT
2401 GAGCTGAGAG AAAATAATGC CCTGGCTGAT TTTATTTCTC TGTTTTGCTT TCTTGAGAAA
2461 AGGAATACTT GTCCCACTCC GTATCTGAGC CTGACCAAGA ACTAAACTAT GTACTTCAGG
2521 CTTACCTTGA ACTCTCAACC ATCCTGCCTT GGCTTCCTGA GTGCTGGGAG CTTGATAACC
2581 ATAATTTTAT TATCAGATTT TTCTTAGTCA TTTTCACCAA TAGAACACAT TCAATGCCCA
2641 ATCGTTAGCA TTTCGTTTGA GACTCATCTT GACCGTACCT CTGTCACACG TCTAACACAT
2701 CACATTAATT TCTAGTTTAG AAGTGATCAA GTTCAAATTC TGCACTGCGC AAAGTACAAG
2761 TTTTAGAGCA GGACCATTTT TTTTTACCAC GTAAAAGTCG AAATTACTAG GAAATGTGTA
2821 TATCGATGCT TGTACACTGT TGCGTGCAAA GTGAGGAGCC TTCTATTGTG ATAGCCATAG
2881 ACAGTACCAG GCTCGTTGCC GCTCTTTTGT TTTACTATAA AAAAATCAAT AATGAAGAAT
2941 TATTTATGAA CAAGATCTCA TATGTTCAGA TTGCTTTTAC TATTCATCAA TATAAAATGT
3001 TAAAAAAAAA TAAAACAAGT TCTATCTCAG AAAAAAAAAA AAAAAAAAAA AAAAA

Figure A8.4: *Rattus norvegicus* β-actin mRNA (1296bp) [NCBI Accession Number: BC063166].

```
1    GGGGTCGAGT CCGCGTCCAC CCGCGAGTAC AACCTTCTTG CAGCTCCTCC GTCGCCGGTC
61   CACACCCGCC ACCAGTTCGC CATGGATGAC GATATCGCTG CGCTCGTCGT CGACAACGGC
121  TCCGGCATGT GCAAGGCCGG CTTCGCGGGC GACGATGCTC CCCGGGCCGT CTTCCCCTCC
                                                  BAC (F)
                                                ---------------------->
181  ATCGTGGGCC GCCCTAGGCA CCAGGGTGTG ATGGTGGGTA TGGGTCAGAA GGACTCCTAC
241  GTGGGCGACG AGGCCCAGAG CAAGAGAGGC ATCCTGACCC TGAAGTACCC CATTGAACAC
                <-----------------      ---------------------->
                  BAC LNA PROBE              BAC (R)
301  GGCATTGTCA CCAACTGGGA CGATATGGAG AAGATTTGGC ACCACACTTT CTACAATGAG
361  CTGCGTGTGG CCCCTGAGGA GCACCCTGTG CTGCTCACCG AGGCCCCTCT GAACCCTAAG
421  GCCAACCGTG AAAAGATGAC CCAGATCATG TTTGAGACCT TCAACACCCC AGCCATGTAC
481  GTAGCCATCC AGGCTGTGTT GTCCCTGTAT GCCTCTGGTC GTACCACTGG CATTGTGATG
541  GACTCCGGAG ACGGGGTCAC CCACACTGTG CCCATCTATG AGGGTTACGC GCTCCCTCAT
601  GCCATCCTGC GTCTGGACCT GGCTGGCCGG GACCTGACAG ACTACCTCAT GAAGATCCTG
661  ACCGAGCGTG GCTACAGCTT CACCACCACA GCTGAGAGGG AAATCGTGCG TGACATTAAA
721  GAGAAGCTGT GCTATGTTGC CCTAGACTTC GAGCAAGAGA TGGCCACTGC CGCATCCTCT
781  TCCTCCCTGG AGAAGAGCTA TGAGCTGCCT GACGGTCAGG TCATCACTAT CGGCAATGAG
841  CGGTTCCGAT GCCCCGAGGC TCTCTTCCAG CCTTCCTTCC TGGGTATGGA ATCCTGTGGC
901  ATCCATGAAA CTACATTCAA TTCCATCATG AAGTGTGACG TTGACATCCG TAAAGACCTC
961  TATGCCAACA CAGTGCTGTC TGGTGGCACC ACCATGTACC CAGGCATTGC TGACAGGATG
1021 CAGAAGGAGA TTACTGCCCT GGCTCCTAGC ACCATGAAGA TCAAGATCAT TGCTCCTCCT
1081 GAGCGCAAGT ACTCTGTGTG GATTGGTGGC TCTATCCTGG CCTCACTGTC CACCTTCCAG
1141 CAGATGTGGA TCAGCAAGCA GGAGTACGAT GAGTCCGGCC CCTCCATCGT GCACCGCAAA
1201 TGCTTCTAGG CGGACTGTTA CTGAGCTGCG TTTTACACCC TTTCTTTGAC AAAACCTAAC
1261 TTGCGCAAAA AAAAAAAAAA AAAAAAAAAA AAAAAA
```

APPENDIX 9

Table A9.1: Optimized reaction mixtures for total PPARγ, PPARγ2, LPL and BAC qRT-PCR

Reaction mixture	1X reaction mixture	Final concentration
Jumpstart™ Taq Ready Mix™	12.5µl	1X
Forward primer (30µM)	0.25µl	0.3µM
Reverse primer (30µM)	0.25µl	0.3µM
LNA Dual-labeled Fluorogenic Probe	0.25µl	0.3µM
RNase-free water	10.75µl	-
cDNA template	1µl	0.1µl
Total	25µl	-

APPENDIX 10

Standard Curve Construction for Quantification of total **PPARγ and PPARγ2 Expression**

10.1 Total RNA extraction

Total RNA extracted from male *Rattus norvegicus* tissues was used as a template for PCR amplification of total PPARγ and PPARγ2 using two-step RT PCR procedure for cloning into the pDrive vector. Spectrophotometric analysis of extracted RNA in 10mM TrisCl, pH 7.5 revealed good purity characterized by an average A_{260}/A_{280} ratio of 1.92 ± 0.03 and 2.01 ± 0.05 respectively. Electrophoretic analysis with 1.2% agarose gel showed good RNA integrity (Figure A10.1). Extracted RNA from different tissues showed good integrity; as seen by the relative intactness of the 28S rRNA (4700bp) and 18S rRNA (1900bp) bands.

10.2 PCR optimization and amplification

Several annealing temperatures were tested to obtain the optimum temperature for the amplification of the total PPARγ and PPARγ2. A general trend of increasing annealing temperature with reduced amount of amplicon was observed. Accumulation of non-specific amplifications products was not observed at lower temperature (Figure A10.2 a and b).

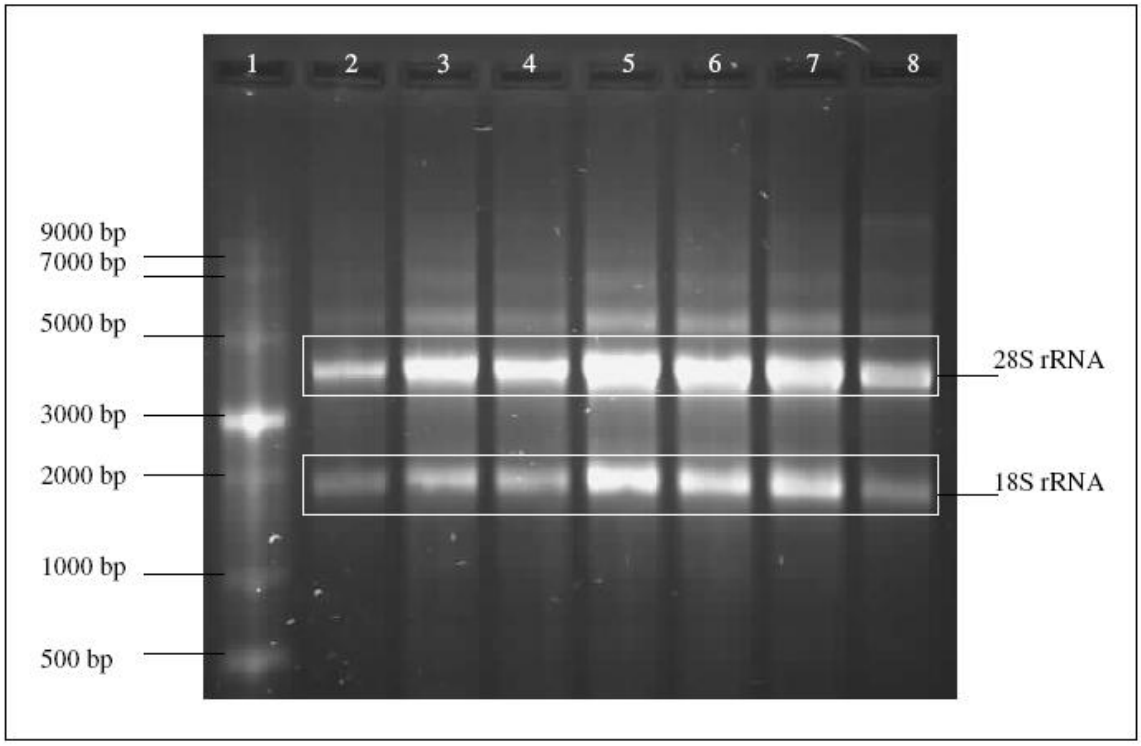

Figure A10.1: Gel image of total RNA extracted from rat tissues separated by gel electrophoresis.

Lane 1: ssRNA Ladder (Qiagen), Lane 2: Liver tissues, Lane 3 and 4: Kidney tissues, Lane 5: Abdominal muscle, Lane 6: Quadriceps femoris muscle, Lane 7: Visceral adipose tissue, Lane 8: Subcutaneous adipose tissues.

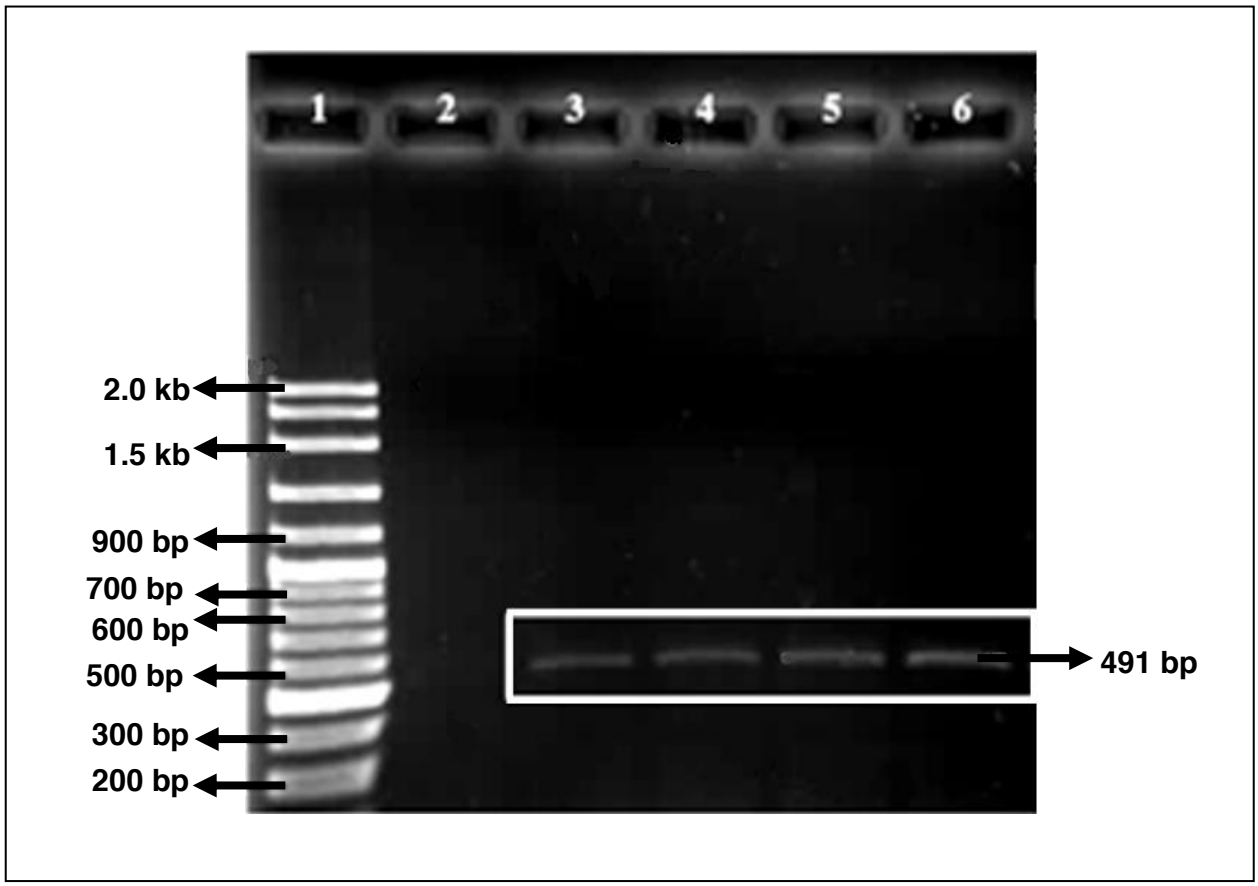

Figure A10.2a: Agarose gel electrophoresis of PCR annealing temperature optimization of total PPARγ.

Lane 1: Hyperladder IV (Bioline), Lane 2: 64.1°C, Lane 3: 61.6°C, Lane 4: 57.7°C, Lane 5: 55.8°C

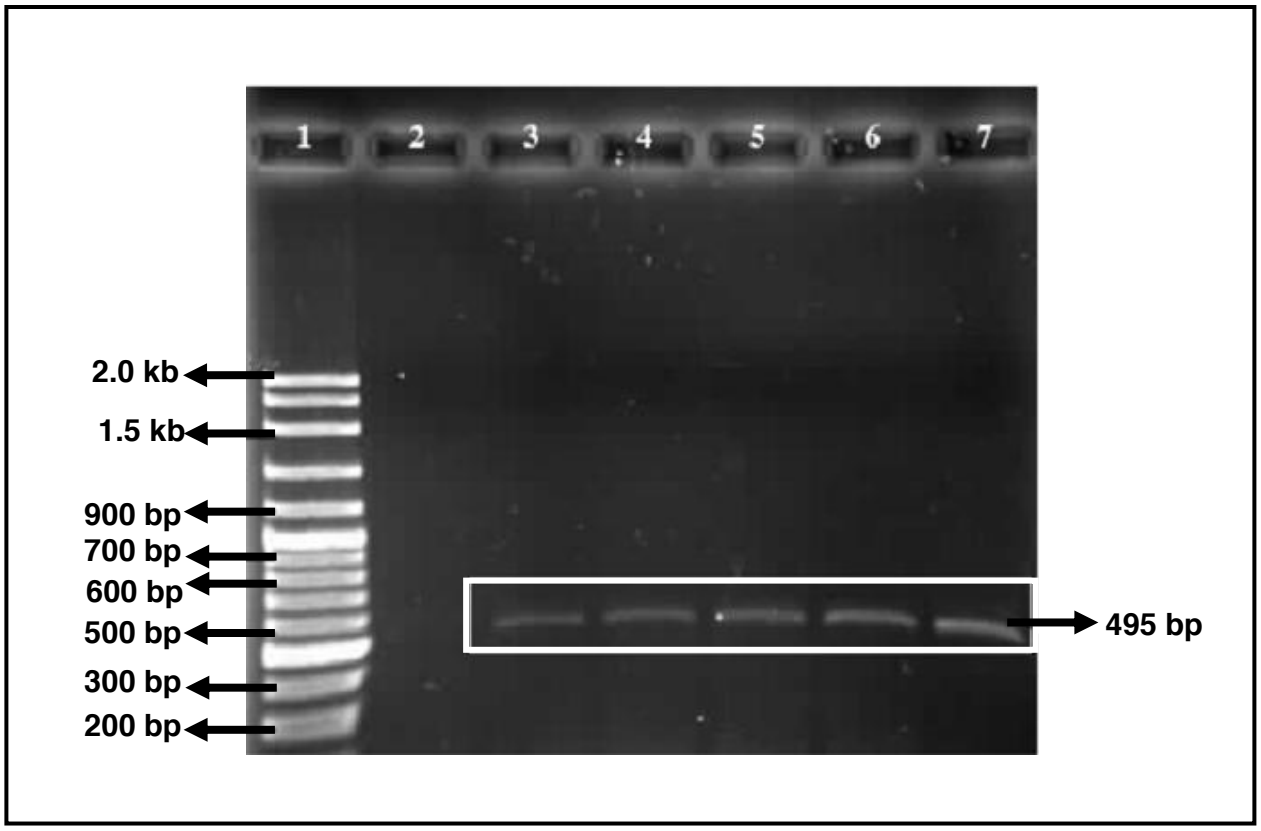

Figure A10.2b: Agarose gel electrophoresis of PCR annealing temperature optimization of PPARγ2.

Lane 1: Hyperladder IV (Bioline), Lane 2: 64.0°C, Lane 3: 62.1°C, Lane 4: 60.4°C, Lane 5: 58.8°C, Lane 6: 56.9°C, Lane 7: 55.0°C

10.3 Cloning and transformation of total PPARγ and PPARγ2

A series of competent cells with molar ratio of vector to PCR-amplified total PPARγ and PPARγ2 inserts specifically at 1:2, 1:5 and 1:10 ligation mixture was prepared, with the 1:10 ratio producing the highest transformation efficiency of 5 x 10^7 cfu/μg DNA.

Positive control was included by cloning a non-recombinant pDrive plasmid into QIAGEN EZ Competent Cells. Inclusion of the positive control allowed validation of the competency of the host cells as well as the functionality of ampicillin, IPTG and X-Gal.

10.4 Selection of transformants

Screening of clones was performed based on the IPTG X-Gal induction method (Figure A10.3). Following the transformant screening, 18 recombinant clones designated as W1 to W18 and 2 non-recombinant clones was included as negative control designated as B1 and B2 were cultured in LB Broth before subjected to plasmid extraction.

10.5 Purification of plasmid from transformants

Plasmids were extracted from transformants grown for 16 hours in LB Broth supplemented with ampicillin. The extracted plasmids were subjected to gel electrophoresis. High intensity of extracted plasmid bands was observed (Figure A10.4).

Like other uncut plasmids, extracted pDrive plasmid (3.85kb) when analysed in agarose gel showed at least two topologically-different DNA forms corresponding to the

supercoiled forms and open-circular (nicked) forms. Supercoiled pDrive plasmid exhibited the fastest migration rate while the open-circular plasmid DNA migrated slower.

10.6 Restriction digestion of recombinant pDrive plasmid by EcoRI

The multiple cloning site of pDrive plasmid resides within flanking EcoRI digestion sites. Restriction digestion with EcoRI was performed on the extracted plasmid to screen the transformants for recombinant clones. Following restriction analysis of EcoRI-digested plasmid via agarose electrophoresis, recombinant clones were identified from a single band of 506bp of total PPARγ and 510bp of PPARγ2 fragments (Figure A10.5a and b). The presence of these bands indicated that the insert of interest had been successfully cloned into the pDrive plasmid.

In contrast, non-recombinant plasmid isolated from blue forming colony in IPTG X-Gal selection (negative control) subjected to restriction digestion with EcoRI had no total PPARγ and PPARγ2 fragment inserts.

10.7 Plasmid sequencing

Sequencing of recombinant pDrive plasmid was performed to verify the identity of insertion as total PPARγ and PPARγ2. When the sequences obtained were subjected to nucleotide sequence similarity search using BLASTN (Altschul *et al.*, 1990), the identity of the inserts in the recombinant pDrive plasmid was confirmed to be total PPARγ and PPARγ2 respectively (Figure A10.6a and b).

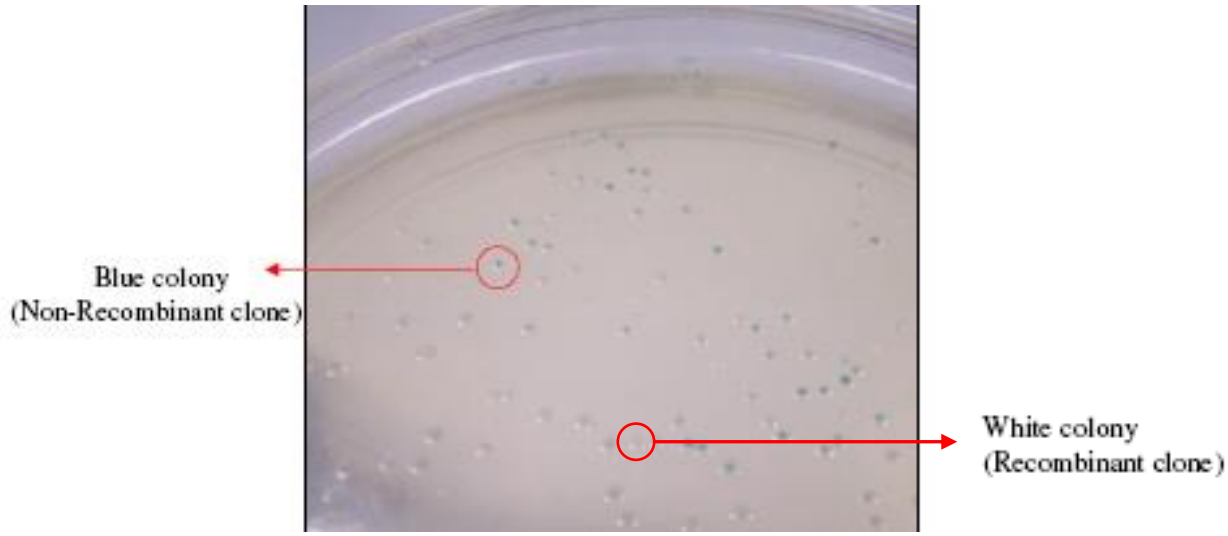

Figure A10.3: Recombinant clone screening based on blue-white X-Gal IPTG selection.

Blue colonies are transformed cells containing non-recombinant pDrive plasmid whereas transformed cells possessing recombinant pDrive plasmid had white colonial morphology.

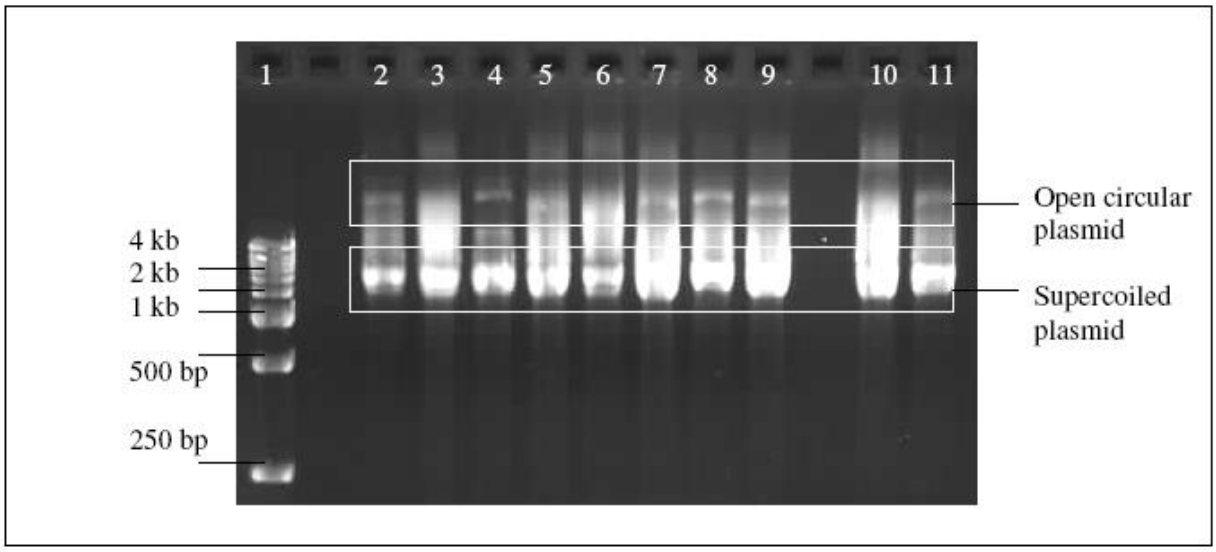

Figure A10.4: Agarose gel electrophoresis of plasmids extracted from cultured transformants.

Lane 1: 1kb DNA Ladder, Lane 2: W1 plasmid, Lane 3: W2 plasmid, Lane 4: W3 plasmid, Lane 5: W4 plasmid, Lane 6: W5 plasmid, Lane 7: W6 plasmid, Lane 8: W7 plasmid, Lane 9: W8 plasmid, Lane 10: B1 plasmid and Lane 11: B2 plasmid.

10.8 Absolute quantification of total **PPARγ, PPARγ1 and PPARγ2 expression**

10.8.1 Construction of standard curve for total PPARγ

The construction of the total PPARγ standard curve was performed using plasmids containing the total PPARγ insert as the template. The plasmids were subjected to spectrophotometric quantification prior to serial dilution of the plasmid. The plasmid with a starting template concentration of 3.61×10^{11} copy numbers per μg of mRNA were subjected to a series of dilutions to concentrations of 3.61×10^{9}, 3.61×10^{7}, 3.61×10^{5} and 3.61×10^{3} copy numbers per μg of mRNA. The standard curve was represented as log copy number against C_t values (Figure A10.7).

10.8.2 Construction of standard curve for PPARγ2

A similar procedure to that in Section 3.3.3.1 was adhered to for the construction of the PPARγ2 standard curve. The only difference would be use of plasmids containing the PPARγ2 inserts in place of the plasmids containing total PPARγ inserts and a starting template concentration of 1.07×10^{11} copy numbers per μg of mRNA. The plasmids were then subjected to a series of dilutions to concentrations of 1.07×10^{9}, 1.07×10^{7}, 1.07×10^{5} and 1.07×10^{3} copy numbers per μg of mRNA. The standard curve was also represented as log copy number against C_t values (Figure A10.8).

10.8.3 Electrophoretic detection of PPARγ and LPL real-time PCR (qRT-PCR) products

The products derived from qRT-PCR amplification of PPARγ, LPL and β-actin (BAC) was subjected to electrophoresis on a 4% (w/v) agarose gel. The expected

amplicon size for total PPARγ, PPARγ2, LPL and BAC is 100bp, 91bp, 144bp and 80bp respectively. The presence of single bands in accordance to the expected amplicon sizes after amplification indicated the successful amplification of the amplicons. Figures A10.9, 10.10, 10.11 and 10.12 represent the amplicons of total PPARγ, PPARγ2, LPL and BAC respectively.

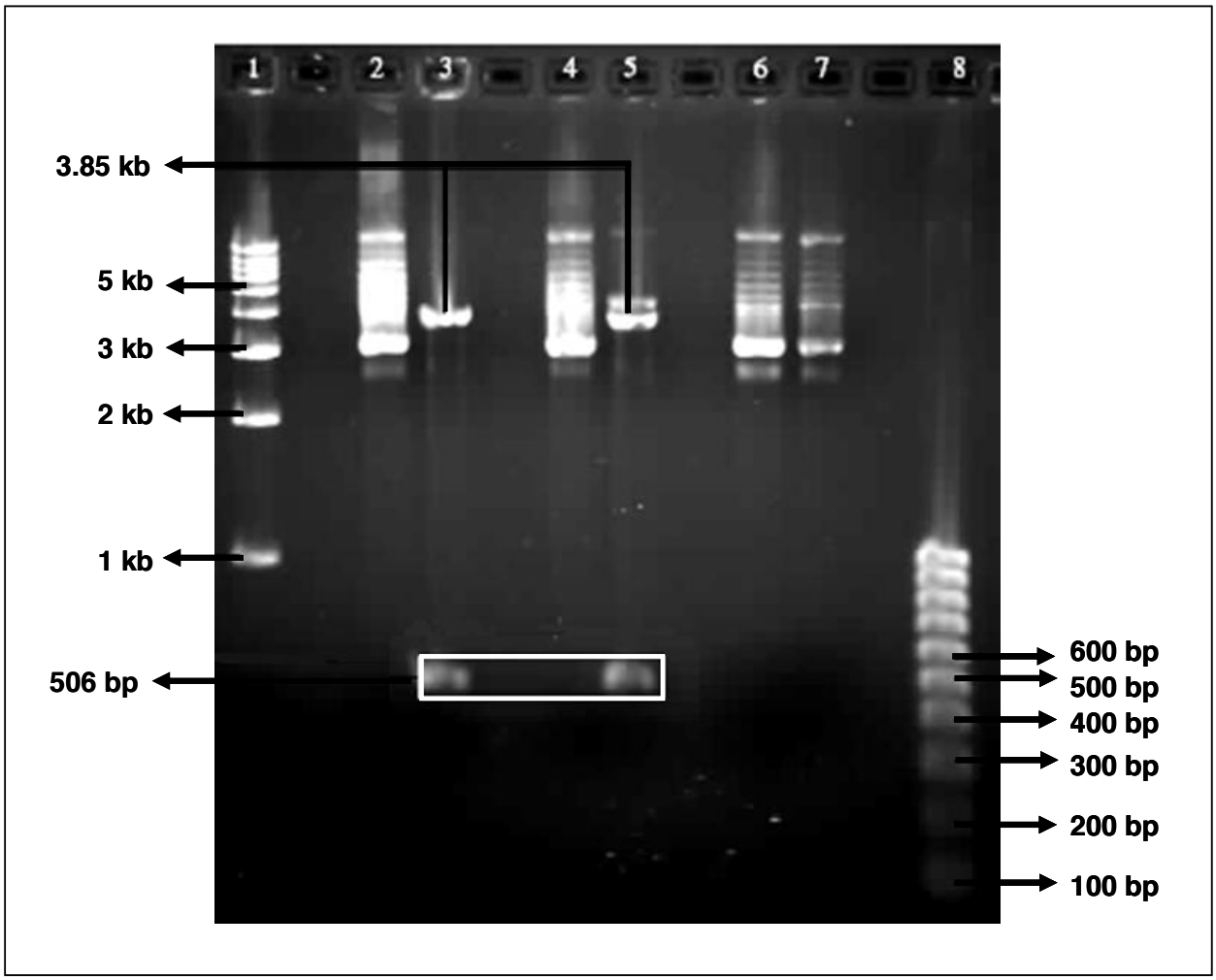

Figure A10.5a: Restriction analysis of pDrive recombinant clone with EcoRI.

Lane 1: 1 kb Ladder, Lane 2: uncut pDrive plasmid, Lane 3: EcoRI digested pDrive plasmid with two bands of 3.85 kb (pDrive vector) and 506 bp (total PPARγ fragment), Lane 4: uncut pDrive plasmid, Lane 5: EcoRI digested pDrive plasmid with two bands of 3.85 kb (pDrive vector) and 506 bp (total PPARγ fragment), Lane 6: uncut pDirve plasmid (negative control), Lane 7: EcoRI digested pDrive plasmid (negative control), Lane 8: 100 bp Ladder.

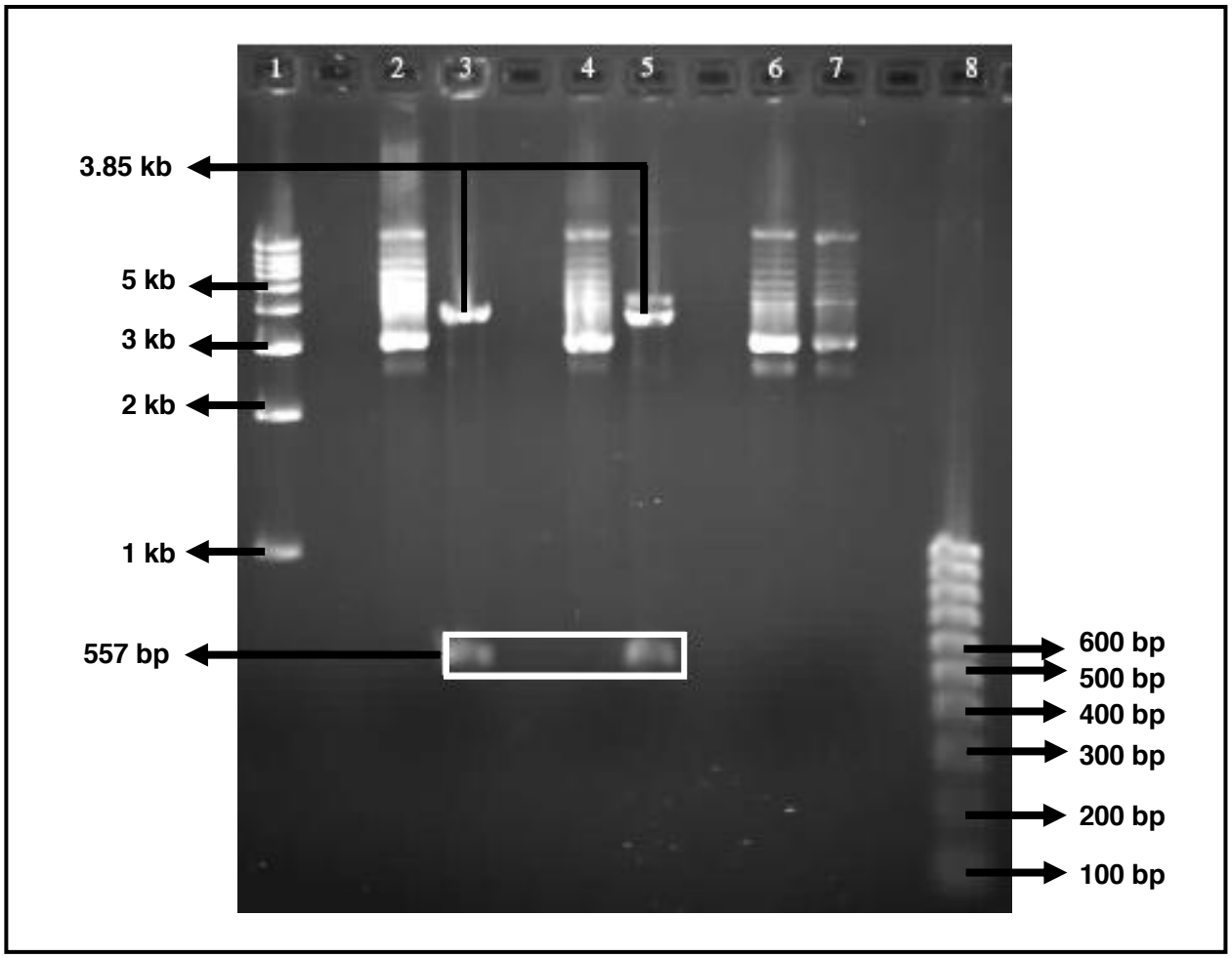

Figure A10.5b: Restriction analysis of pDrive recombinant clone with EcoRI.

Lane 1: 1 kb Ladder, Lane 2: uncut pDrive plasmid, Lane 3: EcoRI digested pDrive plasmid with two bands of 3.85 kb (pDrive vector) and 557 bp (PPARγ2 fragment), Lane 4: uncut pDrive plasmid, Lane 5: EcoRI digested pDrive plasmid with two bands of 3.85 kb (pDrive vector) and 557 bp (PPARγ2 fragment), Lane 6: uncut pDirve plasmid (negative control), Lane 7: EcoRI digested pDrive plasmid (negative control), Lane 8: 100 bp Ladder.

ref|NM_013124.3| Rattus norvegicus peroxisome proliferator-activated receptor gamma (Pparg), transcript variant 1, mRNA
Length=1805

GENE ID: 25664 Pparg | peroxisome proliferator-activated receptor gamma [Rattus norvegicus] (Over 100 PubMed links)

Score = 907 bits (491), Expect = 0.0
Identities = 491/491 (100%), Gaps = 0/491 (0%)
Strand=Plus/Plus

```
Query  1     TGGAGTCCATGCTTGTGAAGGATGCAAGGGTTTTTTCCGAAGAACCATCCGATTGAAGCT  60
             ||||||||||||||||||||||||||||||||||||||||||||||||||||||||||||
Sbjct  539   TGGAGTCCATGCTTGTGAAGGATGCAAGGGTTTTTTCCGAAGAACCATCCGATTGAAGCT  598

Query  61    TATTTATGATAGGTGTGATCTTAACTGTCGGATCCACAAAAAGAGTAGAAATAAATGTCA  120
             ||||||||||||||||||||||||||||||||||||||||||||||||||||||||||||
Sbjct  599   TATTTATGATAGGTGTGATCTTAACTGTCGGATCCACAAAAAGAGTAGAAATAAATGTCA  658

Query  121   GTACTGTCGGTTTCAGAAGTGCCTTGCTGTGGGGATGTCTCACAATGCCATCAGGTTTGG  180
             ||||||||||||||||||||||||||||||||||||||||||||||||||||||||||||
Sbjct  659   GTACTGTCGGTTTCAGAAGTGCCTTGCTGTGGGGATGTCTCACAATGCCATCAGGTTTGG  718

Query  181   GCGAATGCCACAGGCCGAGAAGGAGAAGCTGTTGGCGGAGATCTCCAGTGATATCGACCA  240
             ||||||||||||||||||||||||||||||||||||||||||||||||||||||||||||
Sbjct  719   GCGAATGCCACAGGCCGAGAAGGAGAAGCTGTTGGCGGAGATCTCCAGTGATATCGACCA  778

Query  241   GCTGAACCCAGAGTCTGCTGATCTGCGAGCCCTGGCAAAGCATTTGTATGACTCATACAT  300
             ||||||||||||||||||||||||||||||||||||||||||||||||||||||||||||
Sbjct  779   GCTGAACCCAGAGTCTGCTGATCTGCGAGCCCTGGCAAAGCATTTGTATGACTCATACAT  838

Query  301   AAAGTCCTTCCCGCTGACCAAAGCCAAGGCGAGGGCGATCTTGACAGGAAAGACAACAGA  360
             ||||||||||||||||||||||||||||||||||||||||||||||||||||||||||||
Sbjct  839   AAAGTCCTTCCCGCTGACCAAAGCCAAGGCGAGGGCGATCTTGACAGGAAAGACAACAGA  898

Query  361   CAAATCACCATTTGTCATCTACGACATGAATTCCTTAATGATGGGAGAAGACAAAATCAA  420
             ||||||||||||||||||||||||||||||||||||||||||||||||||||||||||||
Sbjct  899   CAAATCACCATTTGTCATCTACGACATGAATTCCTTAATGATGGGAGAAGACAAAATCAA  958

Query  421   GTTCAAACATATCACCCCCCTGCAGGAGCAGAGCAAAGAGGTGGCCATCCGCATTTTTCA  480
             ||||||||||||||||||||||||||||||||||||||||||||||||||||||||||||
Sbjct  959   GTTCAAACATATCACCCCCCTGCAGGAGCAGAGCAAAGAGGTGGCCATCCGCATTTTTCA
1018

Query  481   AGGGTGCCAGT  491
             ||||||||||
Sbjct  1019  AGGGTGCCAGT  1029
```

Figure A10.6a: Comparison of sequencing result of nucleotide sequences from recombinant clones with mRNA sequence of total PPARγ using BLASTN.

BLASTN results revealed 100% similarity between sequencing results with total PPARγ mRNA sequence.

>gb|AF156666.1|AF156666 Rattus norvegicus peroxisome proliferator-activated receptor gamma 2 (PPARgamma2) mRNA, complete cds
Length=1785

GENE ID: 25664 Pparg | peroxisome proliferator-activated receptor gamma
[Rattus norvegicus] (Over 100 PubMed links)

Score = 1029 bits (557), Expect = 0.0
Identities = 557/557 (100%), Gaps = 0/557 (0%)
Strand=Plus/Plus

```
Query  1    CGAGCATCAGTGGGAATTAAGGCAAATCTCTGTTTTATGCTGTTATGGGTGAAACTCTGG  60
            ||||||||||||||||||||||||||||||||||||||||||||||||||||||||||||
Sbjct  5    CGAGCATCAGTGGGAATTAAGGCAAATCTCTGTTTTATGCTGTTATGGGTGAAACTCTGG  64

Query  61   GAGATCCTCCTGTTGACCCAGAGCATGGTGCCTTCGCTGATGCACTGCCTATGAGCACTT  120
            ||||||||||||||||||||||||||||||||||||||||||||||||||||||||||||
Sbjct  65   GAGATCCTCCTGTTGACCCAGAGCATGGTGCCTTCGCTGATGCACTGCCTATGAGCACTT  124

Query  121  CACAAGAAATTACCATGGTTGACACAGAGATGCCATTCTGGCCCACCAACTTCGGAATCA  180
            ||||||||||||||||||||||||||||||||||||||||||||||||||||||||||||
Sbjct  125  CACAAGAAATTACCATGGTTGACACAGAGATGCCATTCTGGCCCACCAACTTCGGAATCA  184

Query  181  GCTCTGTGGACCTCTCTGTGATGGATGACCACTCCCATTCCTTTGACATCAAACCCTTTA  240
            ||||||||||||||||||||||||||||||||||||||||||||||||||||||||||||
Sbjct  185  GCTCTGTGGACCTCTCTGTGATGGATGACCACTCCCATTCCTTTGACATCAAACCCTTTA  244

Query  241  CCACGGTTGATTTCTCCAGCATTTCTGCTCCACACTATGAAGACATCCCGTTCACAAGAG  300
            ||||||||||||||||||||||||||||||||||||||||||||||||||||||||||||
Sbjct  245  CCACGGTTGATTTCTCCAGCATTTCTGCTCCACACTATGAAGACATCCCGTTCACAAGAG  304

Query  301  CTGACCCAATGGTTGCTGATTACAAATATGACCTGAAGCTCCAAGAATACCAAAGTGCGA  360
            ||||||||||||||||||||||||||||||||||||||||||||||||||||||||||||
Sbjct  305  CTGACCCAATGGTTGCTGATTACAAATATGACCTGAAGCTCCAAGAATACCAAAGTGCGA  364

Query  361  TCAAAGTAGAGCCTGCGTCCCCGCCTTATTATTCTGAAAAAACCCAACTCTACAACAGGC  420
            ||||||||||||||||||||||||||||||||||||||||||||||||||||||||||||
Sbjct  365  TCAAAGTAGAGCCTGCGTCCCCGCCTTATTATTCTGAAAAAACCCAACTCTACAACAGGC  424

Query  421  CACATGAAGAGCCTTCAAACTCCCTCATGGCCATCGAGTGCCGAGTCTGTGGGGATAAAG  480
            ||||||||||||||||||||||||||||||||||||||||||||||||||||||||||||
Sbjct  425  CACATGAAGAGCCTTCAAACTCCCTCATGGCCATCGAGTGCCGAGTCTGTGGGGATAAAG  484

Query  481  CATCAGGCTTCCACTATGGAGTCCATGCTTGTGAAGGATGCAAGGGTTTTTTCCGAAGAA  540
            ||||||||||||||||||||||||||||||||||||||||||||||||||||||||||||
Sbjct  485  CATCAGGCTTCCACTATGGAGTCCATGCTTGTGAAGGATGCAAGGGTTTTTTCCGAAGAA  544

Query  541  CCATCCGATTGAAGCTT  557
            |||||||||||||||||
Sbjct  545  CCATCCGATTGAAGCTT  561
```

Figure A10.6b: Comparison of sequencing result of nucleotide sequences from recombinant clones with mRNA sequence of PPARγ2 using BLASTN.

BLASTN results revealed 100% similarity between sequencing results with PPARγ2 mRNA sequence.

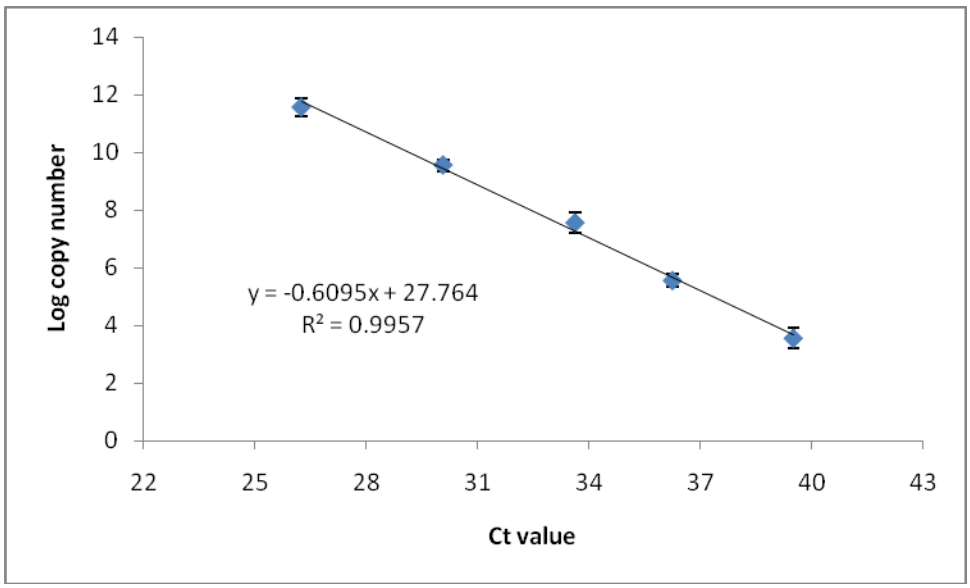

Figure A10.7: Standard curve of log copy number against C_t value for quantification of total PPARγ.

Construction of the standard curve was based on the average results of 3 replicates.

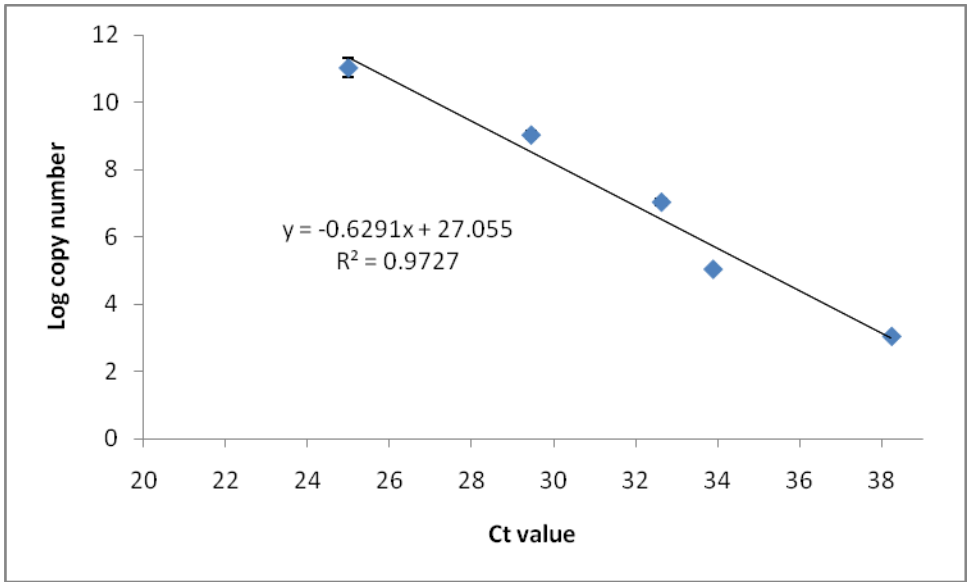

Figure A10.8: Standard curve of log copy number against C_t value for quantification of PPARγ2.

Construction of the standard curve was based on the average results of 3 replicates.

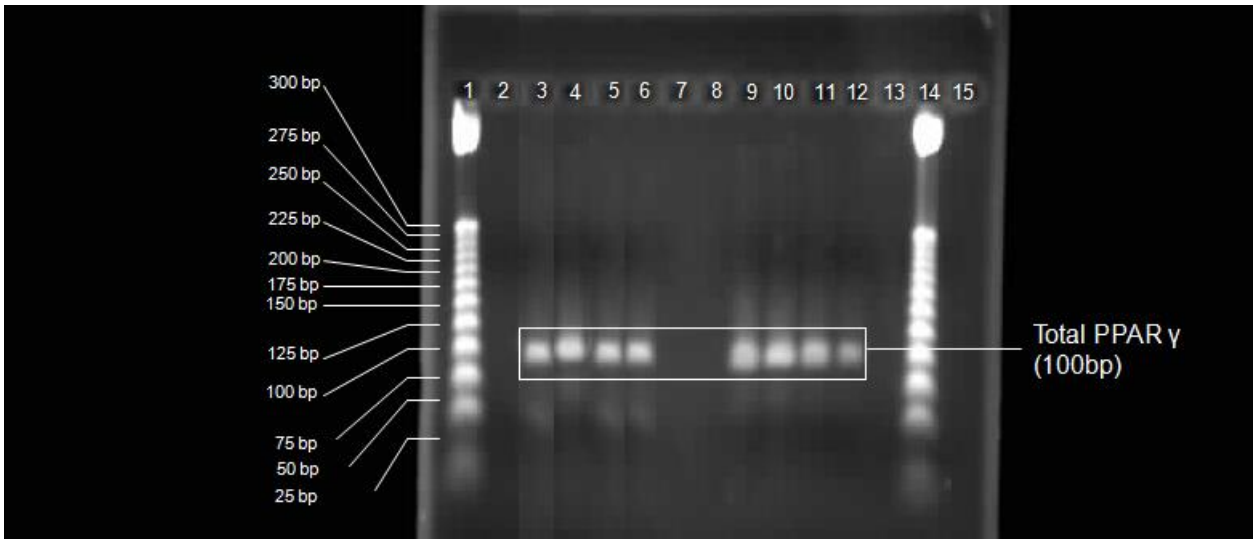

Figure A10.9: The 4% agarose gel image of total PPARγ amplicons obtained after real time PCR of various tissues.

The total PPARγ amplicon bands were approximately at 100 bp, which coincide with its expected amplicon size.

Lanes 1 and 14: 25 bp DNA step ladder, Lane 3: total PPARγ amplicon from control subcutaneous adipose tissue, Lane 4: total PPARγ amplicon from control visceral adipose tissue, Lane 5: total PPARγ amplicon from control liver tissue, Lane 6: total PPARγ amplicon from control kidney tissue, Lanes 7 and 8: non-template control from total PPARγ amplification, Lane 9: total PPARγ amplicon from treated subcutaneous adipose tissue, Lane 10: total PPARγ amplicon from treated visceral adipose tissue, Lane 11: total PPARγ amplicon from treated liver tissue, Lane 12: total PPARγ amplicon from treated kidney tissue.

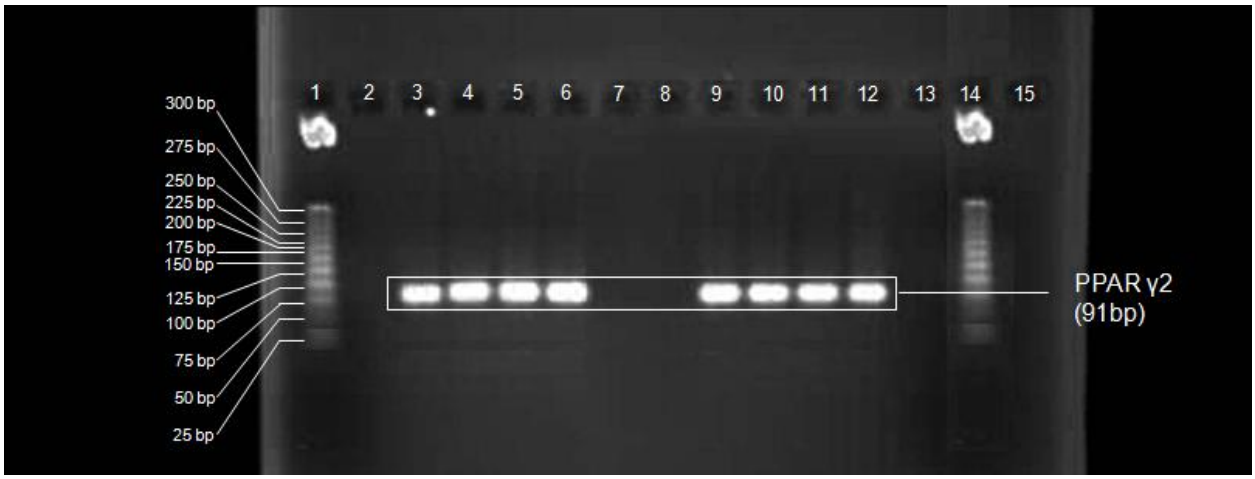

Figure A10.10: The 4% agarose gel image of PPARγ2 amplicons obtained after real time PCR of various tissues.

The PPARγ2 bands were approximately at 91 bp, which coincide with its expected amplicon size.

Lanes 1 and 14: 25 bp DNA step ladder, Lane 3: PPARγ2 amplicon from control subcutaneous adipose tissue, Lane 4: PPARγ2 amplicon from control visceral adipose tissue, Lane 5: PPARγ2 amplicon from control liver tissue, Lane 6: PPARγ2 amplicon from control kidney tissue, Lanes 7 and 8: non-template control from PPARγ2 amplification, Lane 9: PPARγ2 amplicon from treated subcutaneous adipose tissue, Lane 10: PPARγ2 amplicon from treated visceral adipose tissue, Lane 11: PPARγ2 amplicon from treated liver tissue, Lane 12: PPARγ2 amplicon from treated kidney tissue.

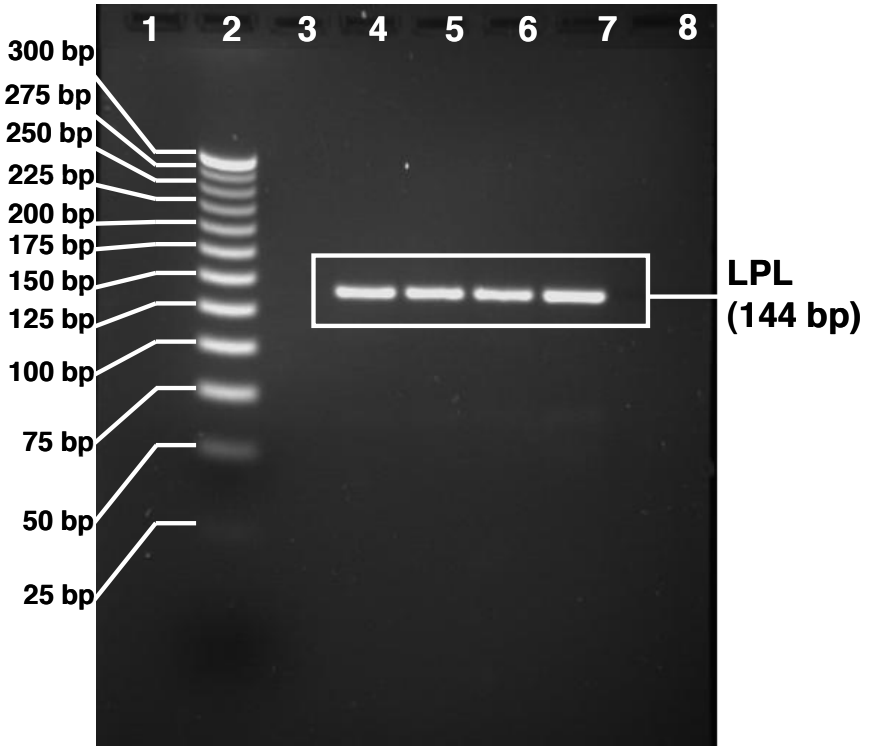

Figure A10.11: The 4% agarose gel image of LPL amplicons obtained after real time PCR of various tissues.

The LPL bands were approximately at 144 bp, which coincide with its expected amplicon size.

Lane 2: 25bp DNA step ladder, Lane 3: non-template control from LPL amplification, Lane 4: LPL amplicon from control visceral adipose tissue, Lane 5: LPL amplicon from control liver tissue, Lane 6: LPL amplicon from control kidney tissue, Lane 7: LPL amplicon from treated subcutaneous adipose tissue, Lane 8: non-template control from LPL amplification.

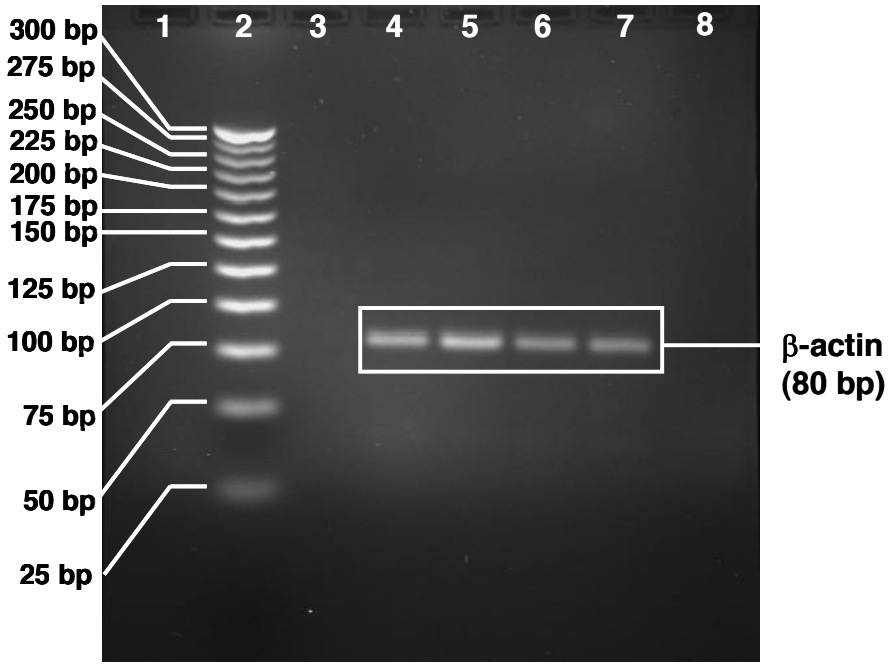

Figure A10.11: The 4% agarose gel image of β-actin amplicons obtained after real time PCR of various tissues.

The β-actin bands were approximately at 80 bp, which coincide with its expected amplicon size.

Lane 2: 25bp DNA step ladder, Lane 3: non-template control from β-actin amplification, Lane 4: β-actin amplicon from control visceral adipose tissue, Lane 5: β-actin amplicon from control liver tissue, Lane 6: β-actin amplicon from control kidney tissue, Lane 7: β-actin amplicon from treated subcutaneous adipose tissue, Lane 8: non-template control from β-actin amplification.

APPENDIX 11

Table A11.1: Optimized qRT-PCR temperatures for total PPARγ, PPARγ2, LPL and BAC amplification

Gene	Condition	Optimum conditions
PPARγ2	Initial denaturation	95°C for two minutes
	Denaturation	95°C for 20 seconds
	Annealing temperature	58.5°C for one minute
	Extension	60°C for one minute
	The amplification steps from denaturation to extension was	
Total PPARγ	Initial denaturation	95°C for two minutes
	Denaturation	95°C for 20 seconds
	Annealing temperature	55.6°C for one minute
	Extension	60°C for one minute
	The amplification steps from denaturation to extension was	
LPL/BAC	Initial denaturation	94°C for two minutes
	Denaturation	94°C for 20 seconds
	Annealing temperature	54.3°C for one minute
	Extension	62.5°C for one minute
	The amplification steps from denaturation to extension was	

APPENDIX 12

Preparation of buffers for 11β-HSD determination

Table A12.1: Composition of stock solutions used for 11β-HSD enzyme assay

Krebs-Ringer bicarbonate buffer (pH 7.4)	6.96g of NaCl, 0.29g of KCl, 0.38g of $CaCl_2.2H_2O$, 2.1g of $NaHCO_3$, 0.16g of KH_2PO_4, 0.29 g of $MgSO_4.7H_2O$ were dissolved in 1L of MiliQ water then gassed with carbogen for 1 hour.
HPLC mobile phase	20% methanol, 30% acetonitrile, 50% water 200ml of methanol, 300ml of acetonitrile and 500ml of MiliQ water was mixed and vacuum filtered through a 0.45µm Nylon filter membrane.

APPENDIX 13

Preparation of standards for the estimation of protein concentration

A protein standard curve was first established using a series of standards derived from a serial dilution of a 2 mg/ml stock bovine serum albumin in Krebs-Ringer buffer for the estimation of the protein concentration of tissue homogenates,. Samples with protein concentrations that were above the limit of the standard curve were diluted 2x or 5x and re-measured to ensure that the calculated value fell within the range of the standard curve.

Table A13.1: Preparation of protein standards.

Volume of stock (µl)	Volume of KR solution (µl)	Total volume (µl)	Concentration of standard (mg/ml)
0	100	100	0.0
15	85	100	0.3
30	70	100	0.6
45	55	100	0.9
60	40	100	1.2
75	25	100	1.5
90	10	100	1.8
100	0	100	2.0

$Conc_H$ x Vol_H	=	$Conc_A$ x Vol_A
Vol_H	=	($Conc_A$ x Vol_A) / ($Conc_H$)

Conc: Concentration, Vol: Volume, H: homogenate, A: assay

Figure A13.1: Determination of sampled volume for homogenates.

APPENDIX 14

Preparation of 17α-hydroxy-11-dehydrocorticosterone standards

17α-hydroxy-11-dehydrocorticosterone stock (1mM) was prepared by dissolving 0.34mg of 17α-hydroxy-11-dehydrocorticosterone powder in 1ml of mobile phase (20% methanol, 30% acetonitrile, 50% water). A series of 17α-hydroxy-11-dehydro-corticosterone standards with concentrations ranging from 1.0 to 9.0μM were prepared according to Table A7.1 to obtain a standard curve for determination of the amount of products formed by 11β-hydroxysteroid dehydrogenase 1 and 2.

Table A14.1: Preparation of 17α-hydroxy-11-dehydrocorticosterone standards.

Volume of stock (μl)	Volume of mobile phase (μl)	Total volume (μl)	Concentration of standard (μM)	Amount of standard (ρmole)
0.0	100.0	100.0	0.0	0.0
0.1	9.9	100.0	1.0	50
0.3	9.7	100.0	3.0	150
0.5	9.5	100.0	5.0	250
0.7	9.3	100.0	7.0	350
0.9	9.1	100.0	9.0	450

The standard curve was performed daily before assaying of samples to prevent day to day variation. Figures A13.1 a and b are randomly selected standard curves performed on different days that illustrate the consistency of the gradients and coefficient of variations done on different days.

(a)

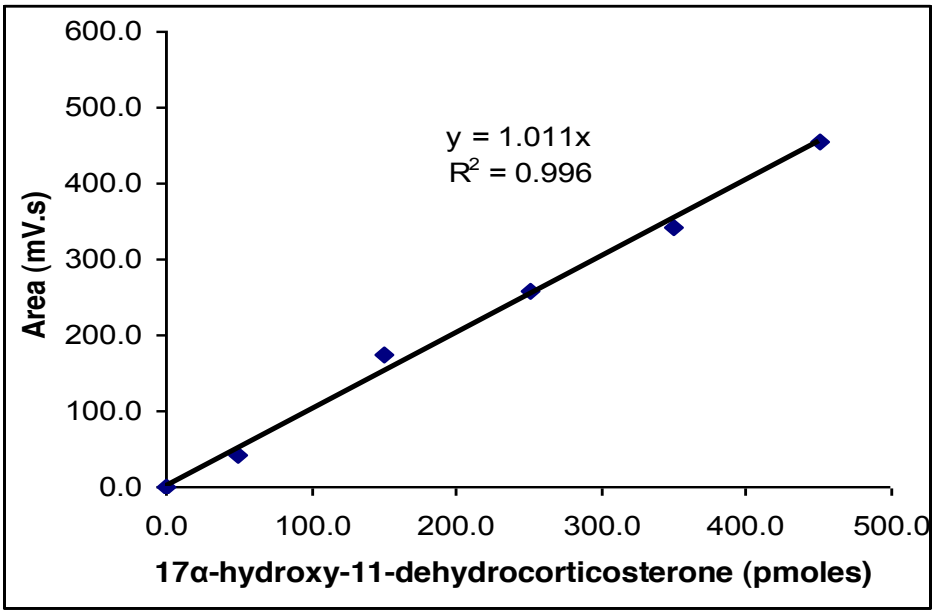

(b)

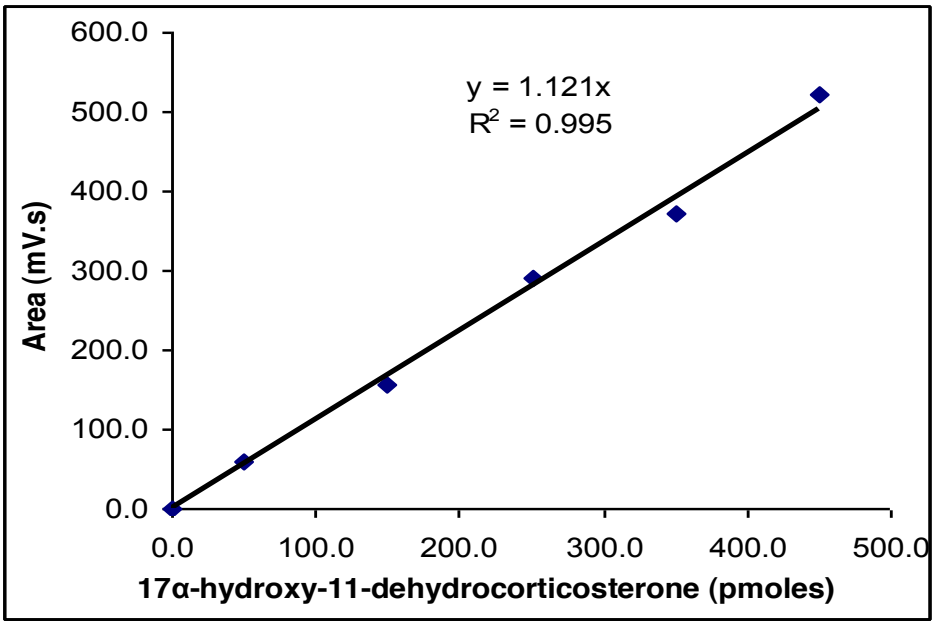

Figures A14.1a and b: Standard curves for 17α-hydroxy-11-dehydrocorticosterone estimation.

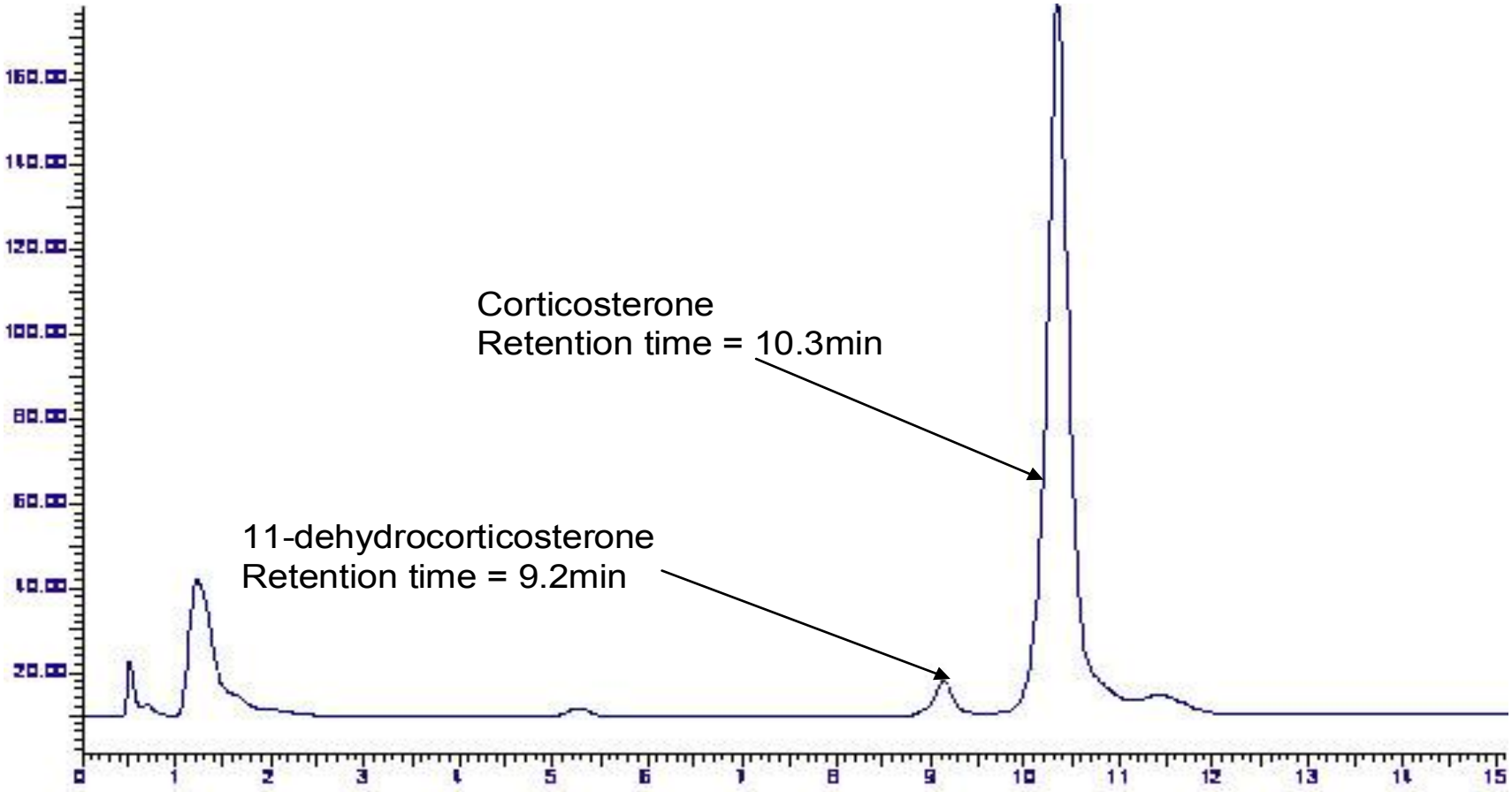

Figure A14.2: An example of a chromatogram accomplished by reverse phase chromatography (HPLC).

APPENDIX 15

Manuscript in-print

Effects of Glycyrrhizic acid on 11 β-Hydroxysteroid Dehydrogenase (11 βHSD1 and 2) Activities and HOMA-IR in Rats at Different Treatment Periods

Authors
C. Y. Yin[1], T. S. Ha[1], K. B. A. Kadir[2]

Affiliations
[1] School of Sciences, Monash University, Sunway Campus, Malaysia
[2] School of Medicine and Health Sciences, Monash University, Sunway Campus, Malaysia

Key words
- 11 β-hydroxysteroid dehydrogenase
- glucose
- glycyrrhizic acid
- insulin
- type 2 diabetes mellitus

Abstract

Glycyrrhizic acid (GA) has been reported to inhibit postprandial blood glucose rise and 11 β-hydroxysteroid dehydrogenase 1 (11 βHSD1) activity. As not much work has been done on GA effects on 11 βHSD1 and 2 and HOMA-IR at different treatment periods, this work was conducted. 60 male Sprague Dawley rats fed *ad libitum* were assigned into six groups of control and treated that were given GA at different duration namely 12, 24 and 48 h. Treated and control groups were intraperitoneally administered with GA (50 $mgkg^{-1}$) and saline respectively. Blood and subcutaneous (ATS) and visceral adipose tissue (ATV), abdominal (MA) and quadriceps femoris muscle (MT), liver (L) and kidney (K) were examined. HOMA-IR in GA-treated rats decreased in all groups ($p < 0.05$). In the 12-h and 24-h treated rats, 11 βHSD1 activities decreased in all tissues ($p < 0.05$) except MA and MT ($p > 0.05$) in the former and ATV ($p > 0.05$) in the latter. However, 11 βHSD1 activities decreased significantly in all tissues ($p < 0.05$) in the 48-h treated rats. Significant decrease in 11 βHSD2 ($p > 0.05$) activities were observed in the L of all treatment groups and K in the 24-h and 48-h treated rats ($p < 0.05$). Histological analysis on ATS showed increase in the number of small-size adipocytes while ATV adipocytes showed shrinkage after GA administration. Increased glycogen deposition in the L was observed in the GA-administered rats in all the treatment periods. In conclusion, GA treatment showed a decrease in the HOMA-IR and both 11 βHSD1 and 2 activities in all tissues, with more profound decrease in the 48-h treated rats.

Introduction

Glucocorticoids (GC) exert a diverse array of physiological roles and are important regulators of intermediary metabolism, possessing extensive influences on carbohydrate, protein and lipid metabolism. Alterations in GC metabolism are suggested to contribute to the development of obesity and insulin resistance (Mussig et al., 2008). Insulin resistance is also a characteristic in most patients with type 2 diabetes mellitus (T2DM) (Hammarstedtm et al., 2005).

T2DM involves the impairment of insulin action and secretion from the pancreatic β-cells. Both factors will collectively increase blood glucose levels (Schwartz, 1999). Researchers have proven that impaired insulin secretion together with peripheral insulin resistance is the main regulator behind the incidence of T2DM (Mahler and Adler, 1999). Current therapy for T2DM involves lifestyle intervention as well as pharmacotherapy with oral agents (e. g. biguanides, thiazolidenediones) (Mahler and Adler, 1999). The current therapies such as metformin and PPARγ agonist (rosiglitazone) had been documented to ameliorate the risk factors of T2DM and metabolic syndrome through the inhibition of 11 β-hydroxysteroid dehydrogenase (1 βHSD1) (Mahler and Adler, 1999; Anagnostis et al., 2009).

(11 βHSD) are microsomal enzymes which belong to the short-chain dehydrogenase/reductase superfamily. Two isoforms of the enzyme; 11 βHSD1 and 11 βHSD2, have been discovered (Steward, 1996). 11 βHSD1, which converts inactive GC to active GC in the cell, is expressed in many tissues, including liver and adipose tissue (Sandeep et al., 2005) as it plays a pivotal role in corticosteroid physiology by regulating the activation of glucocorticoid receptors (GR) as it affects the glucose and lipid metabolism as well as fat distribution (Rubis et al., 2006; Anagnostis et al., 2009). 11 βHSD2 converts active GC into inactive GC and it is localized in mineralocorti-

Bibliography
DOI 10.1055/s-0029-1237703
Exp Clin Endocrinol Diabetes 2009; 117: 1–8

ISSN 0947-7349

Correspondence
C. Y. Yin
Adeline
Monash University
Jalan Lagoon Selatan
Bandar Sunway
46150 Selangor Darul Ehsan
Malaysia
Tel.: +60/3/5514 60 00
Fax: +60/3/5514 60 01
adelinechia@gmail.com

coid-targeted cells such as the kidney, colon and salivary glands as it plays a role in regulating the activation of mineralocorticod (MR) receptors via stimulation by cortisol in renal tubes (Rubis et al., 2006; Anagnostis et al., 2009). The differential tissue expression of the two isozymes plays an important role in corticosteroid physiology by regulating the activation of (GR) and (MR) receptors (Steward, 1996). Tissue-specific expression of the two distinct isoforms (11 βHSD 1 and 2) plays a pivotal role in pre-receptor metabolism of corticosteroid hormones, thus regulating intracellular levels of GCs and MC activities in vivo and downstream activation of GR and MR (Shimoyama et al., 2003).

Glycyrrhizic acid (Glycyrrhizin or Glygyrrhizinate, GA) isolated from licorice, is known to possess a wide range of pharmacological effects such as anti-inflammatory and anti-tumorigenic activities (Draper and Steward, 2005). In animal studies, ethanolic licorice extract was found to have anti-diabetic effects on diabetic mice (Takii et al., 2001). GA and its metabolite glycyrrhetic acid (GE) exhibit nonselective competitive inhibition, the latter 200 to 1 000 times more potent than the former, of 11 βHSD activity (Isbrucker and Burdock, 2006). Both compounds were able to reduce 11 βHSD protein and messenger RNA levels in various organs (Draper and Steward, 2005). This would lead to lower glucocorticoid levels thus reducing the inhibitory effects of GC on the insulin-mediated translocation of glucose transporter to the cell membrane. Therefore it could lead to improve peripheral glucose uptake, a hallmark of enhanced insulin sensitivity (Ploeger et al., 2001).

The present study was therefore undertaken to investigate whether GA administration at different time periods will affect 11 βHSD1 and 2 activities as well as HOMA-IR in rats.

Materials and Methods

Animals

Male Sprague Dawley rats (*Rattus norvegicus*) (160–200 g) obtained from University Malaya's Animal House (University Malaya, Malaysia) were housed 3 or 4 per cage with free access to food and drinking water. They were maintained on a 12-h light-dark cycle in a room with controlled temperature (24 ± 1 °C) and humidity (55 ± 10 %). The use and handling procedure of animals had been approved by the Monash University Animal Ethics Committee according to the 2004 NHMRC Australian Code of Practice for the Case and Use of animal for Scientific purposes and relevant Victorian legislation [AEC: SOBSB/MY/2006/46].

In-vivo assay

The rats were divided into 6 groups (12, 24 or 48 h) [10 rats per group]. A 50 mg kg^{-1} dosage of GA (Sigma Chemical Co., St. Louis, MO, U.S.A.) was intraperitoneally (IP) administered to the rats. Control rats were given 0.9 % saline. The rats were fed *ad libitum* during the treatment periods. Upon completion of treatments (e.g. after 12 h of GA administration), rats were humanely sacrificed.

Blood was withdrawn from the apex of the heart for measurement of glucose and insulin levels. Tissues (subcutaneous and visceral adipose tissues, abdominal and quadriceps femoris muscle, liver and kidney) were harvested for measurement of 11 βHSD1 and 2 activities and histological analysis.

Laboratory assay

Whole blood glucose was analyzed by glucose oxidase method employing a Powerwave XS Microplate Scanning Spectophotometer (BIO-TEK, US). Enzyme immunoassay (LINCO-Millipore Corp., US) was used to measure serum insulin. For the estimation of insulin sensitivity, the homeostasis model assessment of insulin resistance (HOMA-IR) was calculated as (concentration of glucose × concentration of insulin/22.5) (van Wijk et al., 2005).

Extraction of 11 βHSD1 and 2

The subcutaneous and visceral adipose tissue (ATS and ATV), abdominal and quadriceps femoris muscle (MA and MT), liver (L) or kidney (K) were homogenized in cold Kreb's Ringer buffer (118 mM NaCl, 3.8 mM KCl, 1.19 mM KH_2PO_4, 2.54 mM $CaCl_2.2H_2O$, 1.19 mM $MgSO_4.7H_2O$, 25 mM $NaHCO_3$ gassed for 1 h with 95 % O_2/5 % CO_2) (Inoue et al., 2001). The homogenized lysates were centrifuged at 14 000 × g for 20 min at 4 °C.

Determination of 11 βHSD1 and 2 activities

The protein level of the supernatant (enzyme fraction – 50 mg of tissue protein) was measured by the Biuret method (Okutucu et al., 2007). Reaction buffer (500 µl) [0.1 mM of corticosterone, (0.35 mM of $NADP^+$ for 11 βHSD1 and 0.35 mM of NAD^+ for 11 βHSD2), 0.2 % of bovine serum albumin (w/v), 0.2 % of glucose (w/v) and 5 % of ethanol (v/v)] was added to the enzyme fraction and the mixture was incubated for 45 min at 37 °C.

Glucocorticoid extraction was carried out by adding 1.0 ml of ethyl acetate and the upper organic phase was evaporated and reconstituted with 0.5 ml of mobile phase (20 % methanol, 30 % acetonitrile and 50 % water). The 11-dehydrocorticosterone produced from corticosterone by the enzyme in the mixtures was quantitatively measured by HPLC using a reverse phase Waters Symmetry® C18 5 µm (3.9 × 150 mm) column (Waters Co., US) with a flow rate of 1 mL min^{-1} by UV absorbance at 254 nm. A Unit of 11 βHSD activity is defined as the amount of enzyme required for the formation of 1 pmol of 11-dehydrocorticosterone in 45 min per 50 mg of tissue protein (Boyer, 2006).

Histological analysis

Subcutaneous and visceral adipose tissue (ATS and ATV), abdominal and quadriceps femoris muscle (MA and MT), liver (L) or kidney (K) were fixed in 10 % neutral-buffered formalin and were then subjected to impregnation, infiltration, embedding and sectioning process. Tissue sections 5 µm thick were stain with Haematoxylin and Eosin (H&E) and Periodic acid Schiff's (PAS) stain. Images were then transferred to NIS-Element D2.30 software to measure the size of 100 adipocytes (μm^2) per field view per tissue section (Okuno et al., 1998).

Statistical analysis

Data were expressed as means ± standard error of means. Pearson correlations coeffiecients (r) between the continuous variables were calculated. Due to non-parametric distribution of the data, all subsequent analyses were performed using Mann-Whitney by SPSS version 16.0 (SPSS Inc., Chicago, IL, USA). A p value of ≤ 0.05 was considered significant.

Results

Rats administered with GA for 12, 24 or 48 h (fed *ad libitum*) showed a decrease in blood glucose levels compared to the control rats (0.9 % saline) and only the 24-and 48-h GA administered rats showed significant decrease (30 % and 34 % respectively) ($p < 0.05$) (**Fig. 1**). Lower insulin levels were also seen in all the treated rats when compared to the control rats (**Fig. 2**). Insulin resistance, calculated as HOMA-IR, was significantly lower in all the treated rats compared to the controls ($p < 0.05$) (**Fig. 3**). There was no significant decrease within the different treatment periods ($p > 0.05$).

Effects of GA on GC metabolism were determined by measuring 11 βHSD1 and 2 activities *in-vitro*. The 11 βHSD1 and 2 activities were lower in all tissues of GA-treated rats when compared to the control rats of identical treatment periods (12, 24 or 48 h).

All tissues showed significant decrease in 11 βHSD1 activities after 48 h ($p < 0.01$). However, all but MA and MT showed significant decrease after 12 h ($p < 0.01$) while all but ATV had significant decrease after 24 h when compared to their respective control groups ($p < 0.05$) (**Fig. 4a–c**).

The effects of GA on 11 βHSD2 activities are summarized in **Fig. 4** (**a, b, c**). Compared to the control groups, the 11 βHSD2 activities in GA-administered rats were lower in all tissues but only the L showed significant decrease at 12, 24 and 48 h along with the K at 24 and 48 h ($p < 0.03$).

As seen in **Fig. 5a**, 11 βHSD1 activities in all tissues except MA, L and K showed an increase at 24-h before decreasing to a level similar to that seen at the 12-h period However **Fig. 5b** shows that 11 βHSD2 activities in all tissues except MT and L had decreased at 24-h before increasing to a level similar to that seen at the 12-h period.

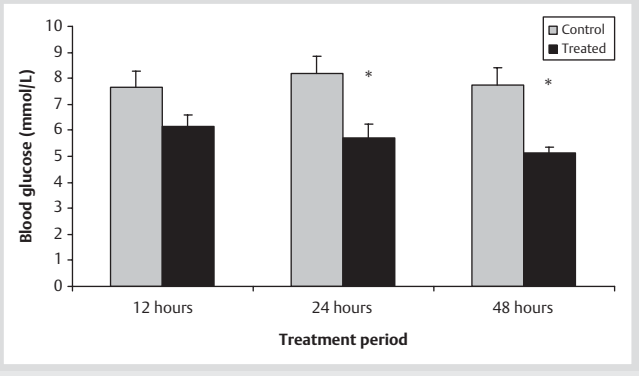

Fig. 1 Blood glucose of rats administered with GA (* $p < 0.03$; n = 10).

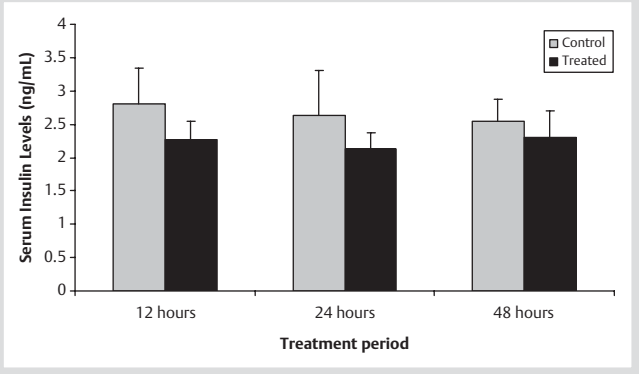

Fig. 2 Serum insulin levels of rats administered with GA (n = 10).

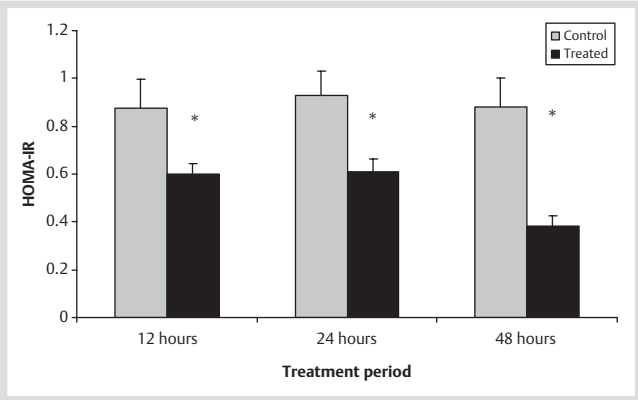

Fig. 3 HOMA index of rats administered with GA (* $p < 0.03$; n = 10).

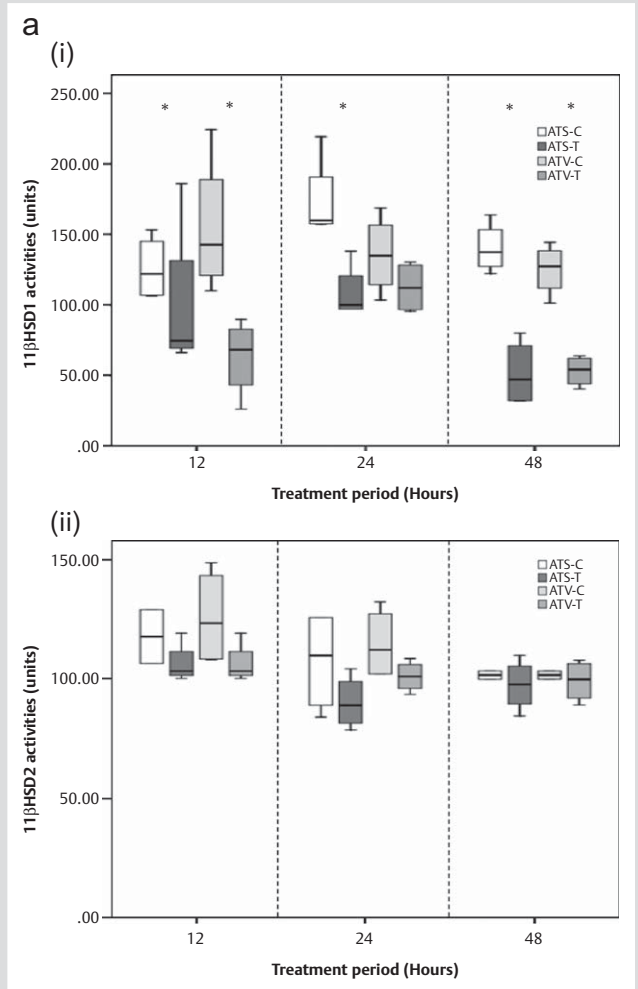

Fig. 4 ([**a**(i) and **a**(ii)], [**b**(i) and **b**(ii)], [**c**(i) and **c**(ii)]): 11 βHSD1 and 2 activities in control and GA-administered rats in durations of 12, 24 and 48 h (* indicates $p < 0.05$). Abbreviations: ATS-C: Subcutaneous adipose tissue-control; ATS-T: Subcutaneous adipose tissue-GA-administered; ATV-C: Visceral adipose tissue-control; ATV-T: Visceral adipose tissue-GA-administered; MA-C: Abdominal muscle-control; MA-T: Abdominal muscle-GA-administered; MT-C: Quadriceps femoris-control; MT-T: Quadriceps femoris-GA-administered; L-C: Liver-control; L-T: Liver-GA-administered; K-C: Kidney-control; K-T: Kidney-GA-administered.

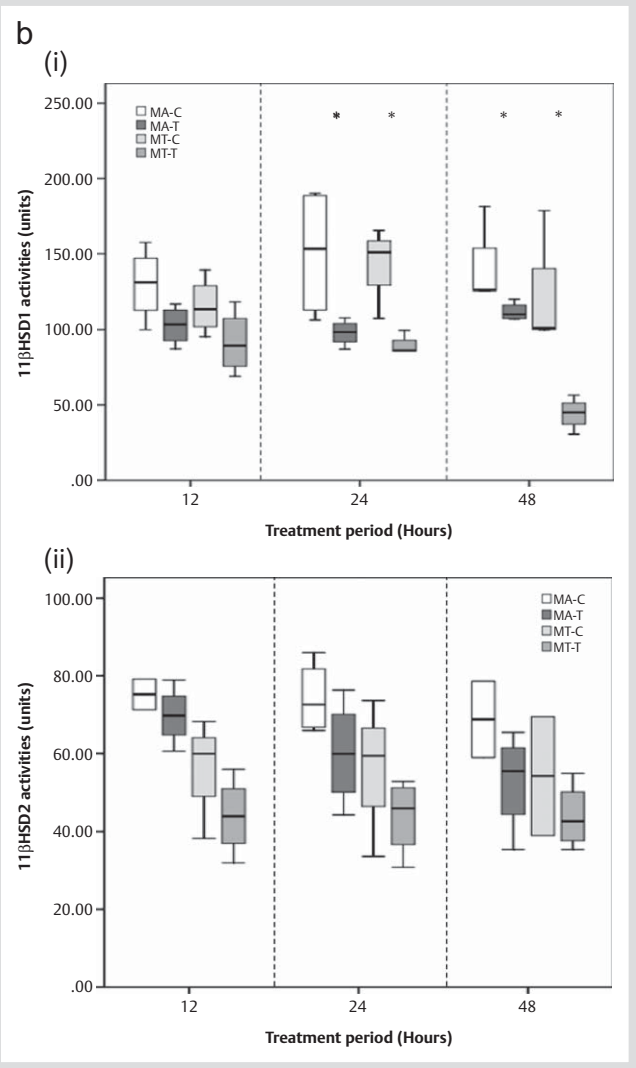

Fig. 4b (Continued).

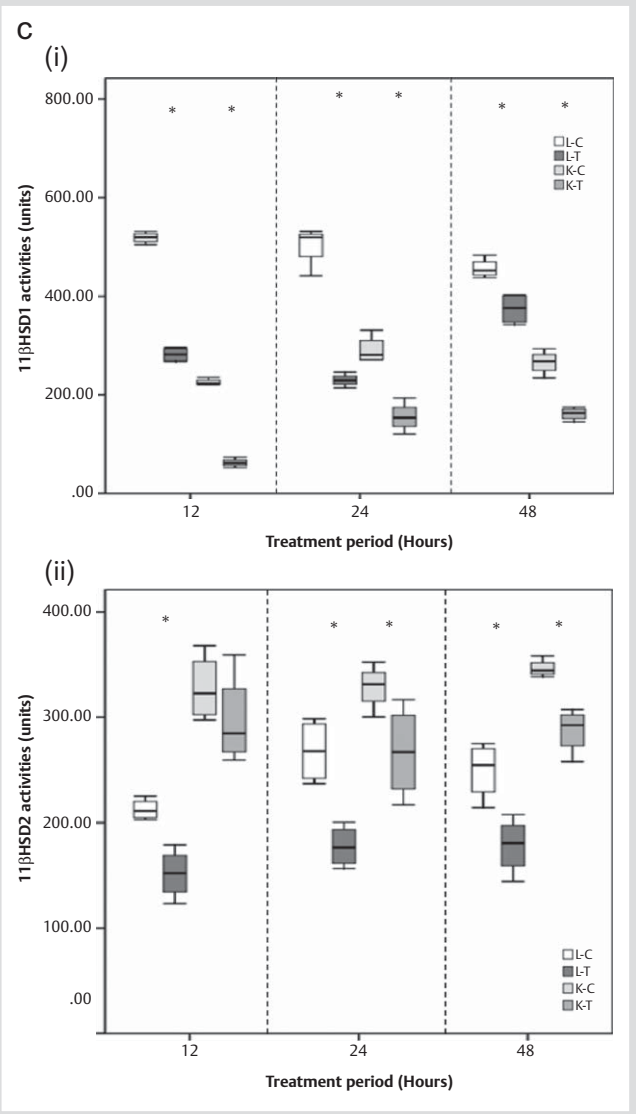

Fig. 4c (Continued).

Comparison between different treatment periods within the GA-treated rats showed significant increase in 11 βHSD1 activities by 25–54% in all tissues between the 12- and 24-h groups ($p<0.05$). However there was a non-significant decrease in 11 βHSD2 activities in all tissues except MT and L between the 12- and 24-h groups (10% - 15%) ($p>0.05$).

A significant increase in 11 βHSD1 activities (40% - 60%) was seen in the MA, L and K between the 12- and 48-h GA-treated rats ($p<0.01$) while a non-significant decrease in 11 βHSD2 activities (8–24%) was seen in the ATS, ATV and MA ($p>0.05$). A significant decrease (65%) was seen in 11 βHSD1 activities in ATS, ATV and MT between the 24- and 48-h GA-treated rats ($p<0.05$) (**Fig. 5a**). 11 βHSD2 activities however increased by only 7% in all tissues except MA and MT ($p>0.05$) (**Fig. 5b**). The effects of GA on 11 βHSD1 and 2 activities in different tissues, blood glucose, serum insulin and HOMA-IR at different treatment periods are summarized in **Table 1**.

Histological analysis on the kidney, abdominal and quadriceps femoris muscle did not show any morphological changes in the GA-administered rats. ATS in GA-administered rats in all treatment period showed an increase in the number of small size adipocytes with a non-significant decrease in the mean area. Mean area of ATS adipocytes in the control group in 12, 24 and 48-h were $391.20 \pm 150.38\,\mu m^2$, $407.00 \pm 120.37\,\mu m^2$ and $387.38 \pm 153.84\,\mu m^2$ respectively while that in the GA-administered rats were $374.04 \pm 191.91\,\mu m^2$, $287.45 \pm 112.10\,\mu m^2$ and $218.56 \pm 135.84\,\mu m^2$ respectively (4.34%, 29% and 43.67% respectively). There were no changes in the size of adipocytes for ATV in GA-administered rats compared to the control in all the treatment period. Mean area of ATV adipocytes in the control group in 12, 24 and 48-h were $395.20 \pm 185.38\,\mu m^2$, $377.50 \pm 167.37\,\mu m^2$ and $401.38 \pm 142.86\,\mu m^2$ respectively while that in the GA-administered rats were $384.04 \pm 191.91\,\mu m^2$, $367.45 \pm 112.10\,\mu m^2$ and $399.53 \pm 105.84\,\mu m^2$ respectively when stained with Heamatoxylin & Eosin stain (H&E stain) (**Fig. 6**). Darker magenta color and no structural differences were seen in the liver of GA-administered rats compared to the control. The liver in GA-administered rats for 48-h showed a greater intensity of magenta color compared to 12 and 24-h (**Fig. 7**).

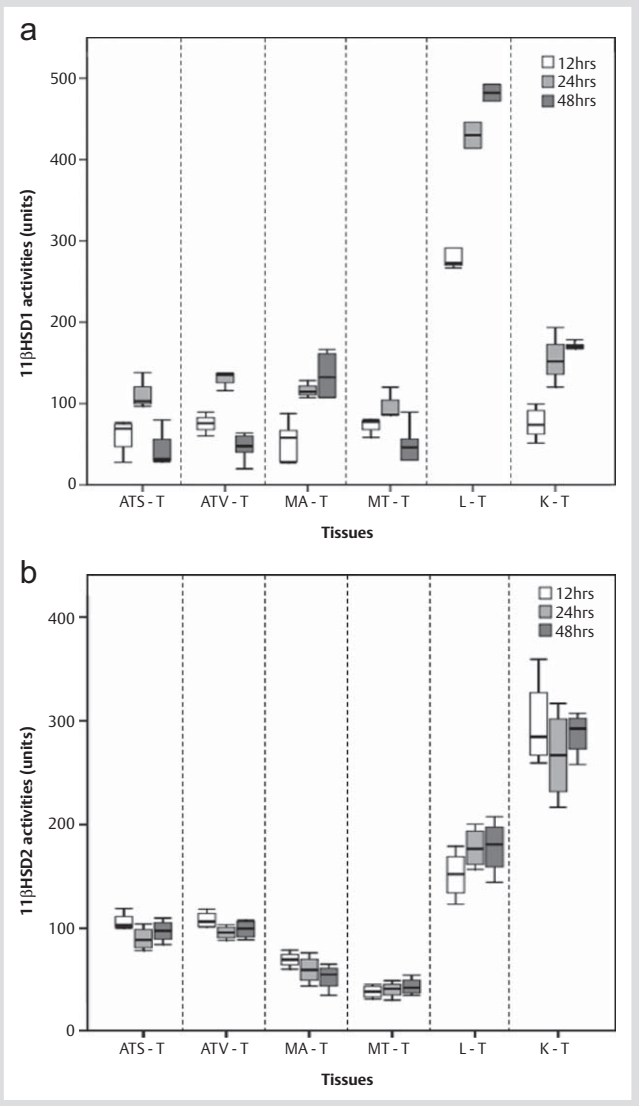

Fig. 5 **a:** 11 βHSD1 activities in GA-administered rats in different treatment periods.(a) Increase ($p<0.02$) in 11 βHSD1 activities was seen between the 12- and 24-h groups while decrease ($p<0.01$) was seen between the 24- and 48-h groups in subcutaneous and visceral adipose tissues and quadriceps femoris muscle. (b) Increase ($p<0.02$) in 11 βHSD1 activities was seen between the 12- and 24-h groups while non-significant increase was seen between the 24- and 48-h groups in abdominal muscle, liver and kidney ($p>0.05$). Abbreviations: ATS-T: Subcutaneous adipose tissue-GA-administered; ATV-T: Visceral adipose tissue-GA-administered; MA-T: Abdominal muscle-GA-administered; MT-T: Quadriceps femoris-GA-administered; L-T: Liver-GA-administered; K-T: Kidney-GA-administered. **b:** 11 βHSD2 activities in GA-administered rats in different treatment periods. Decrease ($p>0.05$) in 11 βHSD2 activities was seen between the 12- and 24-h groups in all tissues except quadriceps femoris and liver while increase ($p>0.05$) was seen between the 24- and 48-h groups in all except abdominal muscle. Abbreviations: ATS-T: Subcutaneous adipose tissue-GA-administered; ATV-T: Visceral adipose tissue-GA-administered; MA-T: Abdominal muscle-GA-administered; MT-T: Quadriceps femoris-GA-administered; L-T: Liver-GA-administered; K-T: Kidney-GA-administered.

Discussion

Excess tissue glucocorticoid action may underlie several characteristics of type 2 diabetes and metabolic syndrome (Draper and Steward, 2005). The absence of hyperglycaemia in all rats in the present study is in agreement with that reported by Andrews et al. (2003) who showed that 11 βHSD1 is lowered in fine-tuning blood glucose levels. It was postulated that the reduction in blood glucose levels in all three treatment periods was due to the inhibition of 11 βHSD1 in the skeletal muscles and adipose tissues (Ploeger et al., 2001). Lower active glucocorticoid levels in these tissues increase the translocation of glucose transporter isotype 4 and 2 (GLUT-4 and GLUT-2) to the cell membrane surface to facilitate the removal of glucose from the blood (Andrews et al., 2003).

The 11 βHSD1-mediated decrease in blood glucose could have caused a decrease in insulin levels in the GA-administered rats through a decrease in pancreatic glucose-stimulated insulin secretion and an increase in stability of glucose transporter isotype 2 (GLUT-2) respectively (Whorwood et al., 2002).

Significant decrease in HOMA-IR was seen in all the GA-administered rats. This could be due to the lowered insulin and glucose levels as HOMA-IR reflects the glucose output and insulin secretion (Wallace et al., 2004). A lower HOMA-IR indicates higher insulin sensitivity (Ahren and Pacini, 2004). Therefore selective inhibition of 11 βHSD1 blocks the activation of glucocorticoids and inhibition of 11 βHSD1 by GA could account for the reduction in blood glucose, serum insulin and HOMA-IR levels (Draper and Steward, 2005).

Evidence suggests that inhibition of 11 βHSD1 in subcutaneous and visceral adipose tissue will increase peripheral glucose uptake and suppress lipolysis (Andrews et al., 2003). This was supported by Masuzaki et al. (2001) who showed that the selective over-expression of 11 βHSD1 in adipose tissue led to increased adipose levels of corticosterone. Data from the present study suggests that GA inhibits conversion of 11-dehydrocorticosterone to corticosterone in adipose tissue as there was a decrease in 11 βHSD1 levels in both the subcutaneous and visceral adipose tissues. A decrease in 11 βHSD2 activities in the adipose tissues in this study could also help in preventing obesity as it decreases the proliferation activity in pre-adipocytes, where high levels of 11 βHSD2 are located (Lee et al., 2008). In the present study, the 11 βHSD1 activities were higher compared to 11 βHSD2 activities in both the subcutaneous and visceral adipose tissue of the control and the GA-administered rats. This was supported by Bujalska et al. (2002) who showed that 11 βHSD2 activities were extremely low or negligible in the adipose tissues compared to the 11 βHSD1 activities.

Both insulin and glucocorticoids have profound effects on the skeletal muscle, acting as potent anabolic and catabolic stimulus respectively (Whorwood et al., 2002). Studies have shown that 11 βHSD1-mediated regulation of intracellular conversion of cortisone to cortisol plays a key role in the etiology of insulin resistance. Our data showed decreased enzyme activities in all tissues of GA-administered rats especially in the 48-h group. This suggests that GA might have inhibited the action of 11 βHSD1, thus decreasing generation of active glucocorticoids, an antagonist of insulin. 11 βHSD2 activities were found to be lower in quadriceps femoris compared to the abdominal muscles. This could be due to a protective mechanism in order to prevent excessive activation of glucocorticoid receptor by increasing the turnover rate of active glucocorticoid since 11 βHSD2 has been reported to have protective effect on skeletal muscles (Jang et al., 2007). The 11 βHSD2 activities were lower than the 11 βHSD1 activities in abdominal and quadriceps femoris muscles in the present study. This is because 11 βHSD1 has a functional role in these tissues as previously mentioned.

Table 1 Effects of GA on 11βHSD1 and 2 activities in different tissues, blood glucose, serum insulin and HOMA-IR at different treatment periods.

	11 βHSD1 and 2 activities								
	ATS	ATV	MA	MT	L	K	Glucose	Insulin	HOMA-IR
12 h	↓	↓	↓	↓	↓	↓	↓	↓	↓
24 h	↓	↓	↓	↓	↓	↓	↓	↑	↑
48 h	↓	↓	↓	↓	↓	↓	↓	↑	↓

ATS, subcutaneous adipose tissue; ATV, visceral adipose tissue; MA, abdominal muscle; MT, quadricep femoris; L, liver; K, kidney

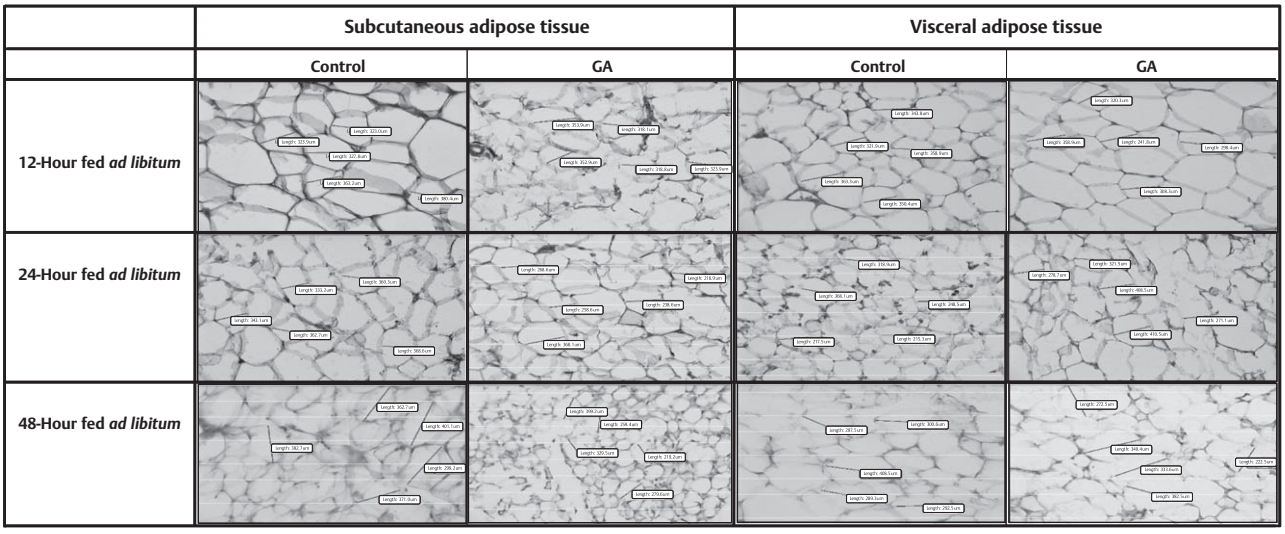

Fig. 6 Sections of subcutaneous and visceral adipose tissue with H&E stain (400x magnification).

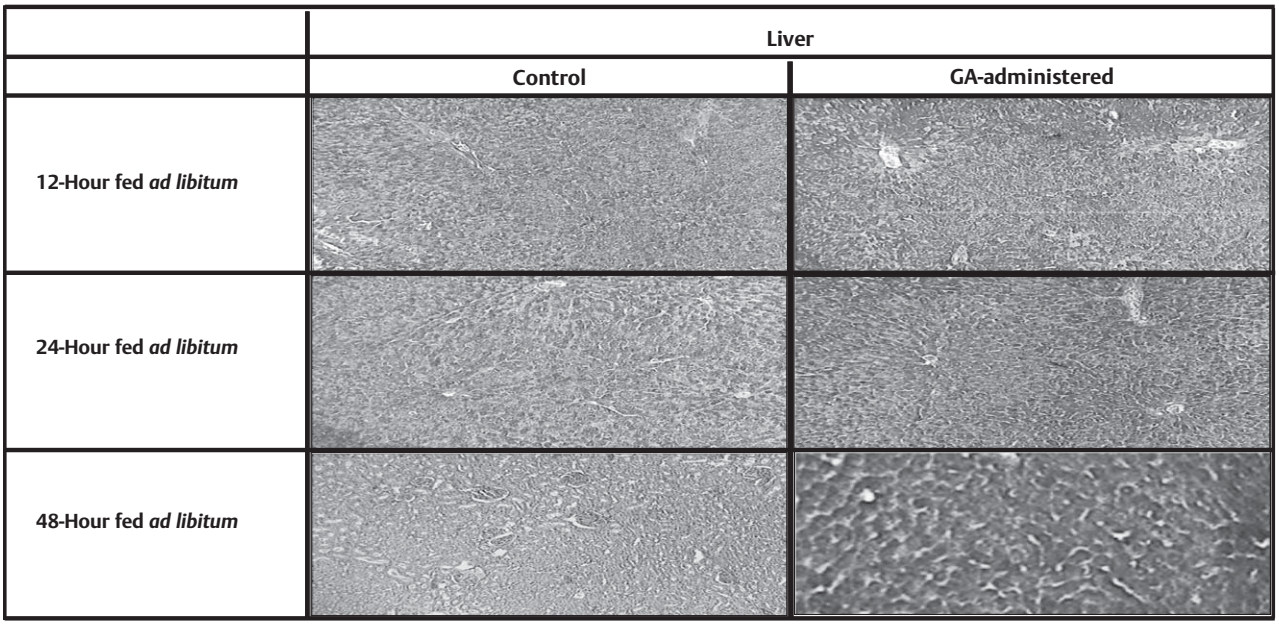

Fig. 7 Sections of liver with periodic acid Schiff's stain (PAS stain) (100x magnification).

The 11 βHSD1 activities in the liver were shown to be the highest among all the tissues. This is because the enzyme is highly expressed in metabolically active tissues to regenerate active corticosterone and acts predominantly as an oxo-reductase *in vivo* (Tomlinson et al., 2004). 11 βHSD1 activities were higher compared to 11 βHSD2 in the liver as it is a metabolically active tissue. The relatively low 11 βHSD2 activity in the liver might be due to the high density of blood vessels in the liver since epithelial cells of the blood vessel contain moderate amounts of 11 βHSD2 (Gong et al., 2008).

The levels of 11 βHSD1 activities in the kidney were significantly lower in all three treatment periods. This is consistent with GE, the metabolite of GA being reported to be a strong inhibitor of rat hepatic and renal 11 βHSDs (Draper and Steward, 2005). Highest 11 βHSD2 activities were also observed in the kidney compared to other tissues in all groups. The presence of 11 βHSD2 in the kidney is essential for protecting the mineralocorticoid receptor from non-specific binding of active glucocorticoid (Shimoyama et al., 2003). Data from the present study suggests that GA inhibits 11 βHSD2 activities in the kidney. Mussig et al. (2008) reported that there is a positive correlation in 11 βHSD2 activities with insulin resistance and obesity. Therefore it can be postulated that inhibition of renal 11 βHSD2 could prevent hepatic insulin resistance and reduce lipolysis in the adipose tissues as it prevents the inactive glucocorticoid supply to 11 βHSD1.

The observed increase in the number of small adipocytes in the subcutaneous adipose tissue is a result of adipocyte differentiation. Small adipocytes are found to be more sensitive to insulin and thus they can take in more glucose due to the high surface area which can actually decrease blood glucose levels (Okuno et al., 1998). However, in the visceral adipose tissue, the sizes of the adipocytes were similar in both the GA-administered and control rats. This was in agreement with Mori et al. (1999) who showed that the differentiation of pre-adipocytes into adipocytes only occurs in the subcutaneous adipose tissue. The increase in magenta color in the liver of GA-administered rats after PAS staining indicates that they have higher polysaccharide and carbohydrate contents as a result increased glucose uptake into hepatocytes for storage (Kiernan, 1999).

The greatest decrease in 11 βHSD1 activities in all tissues was seen after 48 h of GA treatment. This may be due to negligible urinary excretion of as GE undergoes enterohepatic recycling (Krähenbuhl et al., 1994). The delay in terminal clearance of GE would in turn continuously inhibit 11 βHSD1 activities.

11 βHSD1 activities in the various tissues studied showed significant decreases within the different treatment periods in the GA-administered rats. However no significant decreases were seen in 11 βHSD2 activities in the various tissues studied. The decrease in 11 βHSD1 is in agreement with an earlier study (Nwe et al., 2000), although the duration and route of GA administration were different. Our findings, together with those of Nwe et al. (2000) suggest that GA has a direct but weak glucocorticoid effect as there was only a minimal reduction in 11 βHSD1 activity. Our finding on the inhibition of 11 βHSD2 by GA is in agreement with those reported by Tanahashi et al. (2002) although the strain of rats, dosage and duration of GA administration were different.

Increased 11 βHSD1 activities in all tissues at 24 h could be due to the increase in stress levels caused by intraperitoneal injection. This is in agreement with Chapman and Seckl (2008) who showed that persistent environmental changes such as stress could disturb the levels of mediators that maintain allostasis including glucocorticoids. Studies have shown that an increase in 11-dehydrocorticosterone in rats was due to stress through activation of hypothalamo-pituitary-adrenal axis and the sympathetic nervous system (Harris et al., 2001). Thus it can be postulated that lower 11 βHSD1 activities observed at 48 h could be due to adaptation in response to stress levels which in turn reduces the production of 11 βHSD1.

Although the inhibition of 11 βHSD2 has been reported to cause hypertension and hypokalemia with suppressed plasma renin and aldosterone levels [Tanahashi et al., 2002], it was not observed in our study probably due to the short treatment duration. Therefore it would be appropriate to look into longer durations of GA administration to investigate the effects of GA towards 11 βHSD2 inhibition and hypertension.

In conclusion, we have demonstrated that GA lowered blood glucose, serum insulin, HOMA-IR, 11 βHSD1 and 2 activities in rats when compared to the control (**Table 1**). Results from the 48-h-treated rats displayed more prominent reduction, thus indicating that longer treatment period may yield better results with 50 $mgkg^{-1}$ of GA.

Acknowledgements

This work was funded by grants from the Ministry of Science, Technology and Innovation (MOSTI) [02-02-10-SF0003] and Monash University Minor grant [AS-2-4-06].

Author disclosure statement: No competing financial interests exist.

References

1 *Ahren B, Pacini G.* Importance of quantifying insulin secretion in relation to insulin sensitivity to accurately assess beta cell function in clinical studies. Eur J Endocrinol 2004; 150: 97–104
2 *Anagnostis P, Athyros VG, Tziomalos K et al.* The pathogenetic role of cortisol in the metabolic syndrome: A hypothesis. J Clin Endocrin Metab 2009, doi:10.1210/jc.2009-0370
3 *Andrews RC, Rooyackers O, Walker BR.* Effects of the 11 β-hydroxysteroid dehydrogenase inhibitor carbenoxolone on insulin sensitivity in men with type 2 diabetes. J Clin Endocrinol Metab 2003; 88 (1): 285–291
4 *Boyer R.* Biochemistry laboratory: Modern theory and techniques. San Francisco: Benjamin Cummings; 2006; 272
5 *Bujalska IJ, Walker EA, Hewison M et al.* A switch in dehydrogenase to reductase activity of 11 β-hydroxysteroid dehydroganse type 1 upon differentiation of human omental adipose stromal cells. J Clin Endocrinol Metab 2002; 87 (3): 1205–1210
6 *Chapman KE, Seckl JR.* 11 βHSD1, Inflammation, Metabolic disease and age-related cognitive (dys)function. Neurochem Res 2008; 33: 624–636
7 *Draper N, Stewart PM.* 11 β-hydroxysteroid dehydrogenase and the pre-receptor regulation of corticosteroid hormone action. J Endocrinol 2005; 186: 251–271
8 *Gong R, Morris DJ, Brem AS.* Variable expression of 11 β-hydroxysteroid dehydrogenase isoforms in vascular endothelial cells. Steroids 2008; 73: 1187–1196
9 *Hammarstedtm A, Anderson CX, Rotter S et al.* The effect of PPARγ ligands on the adipose tissue in insulin resistance. Prostaglandins Leukot Essent Fatty Acids 2005; 73: 65–75
10 *Harris HJ, Kotelevtsev Y, Mullins JJ et al.* Intracellular regeneration of glucocorticoids by 11 β-hydroxysteroid dehydrogenase (11 βHSD)-1 plays a key role in regulation of the hypothalamic-pituitary-adrenal axis; analysis of 11 βHSD-1 deficient mice. Endocrinology 2001; 142: 114–120
11 *Inoue H, Yokota H, Makino T et al.* Bisphenol a glucuronide, a major metabolite in rat bile after liver perfusion. Drug Metab Dispos 2001; 29 (8): 1084–1087
12 *Isbrucker RA, Burdock GA.* Risk and safety assessment on the consumption of licorice root (Glycyrrhiza sp. its extract and powder as a food ingredient, with emphasis on the pharmacology and toxicology of glycyrrhizin. Regul Toxicol Pharmacol 2006; 46: 167–192
13 *Jang C, Obeyesekere VR, Diley RJ et al.* Altered activity of 11 β-hydroxysteroid dehydrogenase types 1 and 2 in skeletal muscle confers metabolic protection in subjects with type 2 diabetes. ■ ■ ■ 2007; 92 (8): 2314–3320
14 *Kiernan JA.* Carbohydrate histochemistry. In Histological & Histochemical Methods: Theory & Practice. 3rd edition. Butterworth Heinemann, Oxford; 1999; 213–242

15 *Krähenbuhl S*, *Hasler F*, *Frey BM et al*. Kinetics and dynamics of orally administered 18β-glycyrrhetinic acid in humans. J Clin Endocrinol Metab 1994; 78: 581–585
16 *Lee MJ*, *Fried SK*, *Mundt SS et al*. Depot-specific regulation of the conversion of cortisone to cortisol in human adipose tissue. Obesity 2008; 16 (6): 1178–1185
17 *Mahler RJ*, *Adler ML*. Type 2 Diabetes Mellitus: Update on diagnosis, pathophysiology and treatment. J Clin Endocrinol Metab 1999; 84 (4): 1165–1171
18 *Masuzaki H*, *Paterson J*, *Shinyama H et al*. A transgenic model of visceral obesity and the metabolic syndrome. Science 2001; 294: 2166–2170
19 *Mori Y*, *Murakawa Y*, *Okada K et al*. Effects of troglitazone on body fat distribution in type 2 diabetic patients. Diabetes Care 1999; 22: 908–912
20 *Mussig K*, *Remer T*, *Haupt A et al*. 11β-hydroxysteroid dehydrogenase 2 activity is elevated in severe obesity and negatively associated with insulin sensitivity. Obesity 2008; 16 (6): 1256–1260
21 *Nwe KHH*, *Abdul Hamid*, *Morat PB et al*. Differential regulation of the oxidative 11β-hydroxysteroid dehydrogenase activity in testis and liver. Steroids 2000; 65: 40–45
22 *Okuno A*, *Tamemoto H*, *Tobe K et al*. Troglitazone increases the number of small adipocytes without the change of white adipose tissue mass in obese Zucker rats. J Clin Inves 1998; 101: 1354–1361
23 *Okutucu B*, *Dincer A*, *Habib Ö et al*. Comparison of five methods for determination of total plasma protein concentration. J Biochem Biophys Methods 2007; 70: 709–711
24 *Ploeger B*, *Mensinga T*, *Sips A et al*. The pharmacokinetics of glycyrrhizic acid evaluated by physiologically based pharmacokinetic modeling. Drug Metab Rev 2001; 33: 125–147
25 *Rubis B*, *Krozowski Z*, *Trzeciak WH*. Arginine vasopressin stimulates 11beta-hydroxysteroid dehydrogenase type 2 expression in the mineralocorticosteroid target cells. Mol Cell Endrocrinol 2006; 256: 17–22
26 *Sandeep TC*, *Andrew R*, *Homer NZM et al*. Increased in-vivo regeneration of cortisol in adipose tissue in human obesity and effects of the 11β-hydroxysteroid dehydrogenase type 1 inhibitor carbenoxolone. Diabetes 2005; 54: 872–879
27 *Schwartz MW*, *Kahn SE*. Insulin resistance and obesity. Nature 1999; 402: 860–861
28 *Shimoyama Y*, *Hirabyashi K*, *Matsumoto H et al*. Effects of glycyrrhetinic acid derivatives on hepatic and renal 11β-hydroxysteroid dehydrogenase activities in rats. J Pharm Pharmacol 2003; 55: 811–817
29 *Steward PM*. 11β- Hydroxysteroid dehydrogenase: Implications for clinical medicine. Clin Endocrinol 1996; 44: 493–499
30 *Takii H*, *Kometani T*, *Nishimura T et al*. Antidiabetic effect of glycyrrhizin in genetically diabetic KK-A^{y} Mice. Biol Pharm Bull 2001; 24: 484–487
31 *Tanahashi T*, *Mune T*, *Morita H et al*. Glycyrrhizic acid suppresses type 2 11β-hydroxysteroid dehydrogenase expression in vivo. J Steroid Biochem Mol Biol 2002; 80: 441–447
32 *Tomlinson JW*, *Walker EA*, *Bujalska IJ et al*. 11β-hydroxysteroid dehydrogenase type 1: A tissue-specific regulator of glucocorticoid response. Endocrine Rev 2004; 25 (5): 831–866
33 *van Wijk JPH*, *Cabezas MC*, *de Koning EJP et al*. Rosiglitazone imporves postprandialtriglyceride and free fatty acid metabolism in type 2 diabetes. Diabetes Care 2005; 28 (4): 844–849
34 *Wallace TM*, *Levy JC*, *Matthew DR*. use and abuse of HOMA modeling. Diabetes Care 2004; 27 (6): 1487–1495
35 *Whorwood CB*, *Donovan SJ*, *Flanagan D et al*. Increased glucocorticoid receptor expression in human skeletal muscle cells may contribute to the pathogenesis of the metabolic syndrome. Diabetes 2002; 51: 1066–1075

Lipoprotein lipase expression, serum lipid and tissue lipid deposition in orally-administered glycyrrhizic acid-treated rats

Wai Yen Alfred Lim[1], Yoke Yin Chia[1], Shih Yeen liong[1], So Ha Ton[1*], Khalid Abdul Kadir[2] and Sharifah Noor Akmal Syed Husain[3]

[1]School of Science, Monash University Sunway Campus, Jalan Lagoon Selatan, Bandar Sunway 46150, Selangor Darul Ehsan, Malaysia;
[2]School of Medicine and Health Sciences, Monash University Sunway Campus, Jalan Lagoon Selatan, Bandar Sunway 46150, Selangor Darul Ehsan, Malaysia;
[3]Cytopathology and Cytogenetics Unit, Department of Pathology, Universiti Kebangsaan Malaysia Medical Centre, Jalan Yaacob Latif, Bandar Tun Razak, Cheras 56000, Kuala Lumpur, Malaysia.

*Corresponding author

Email addresses:
LWYA: wylim3@student.monash.edu
CYY: ykchi4@student.monash.edu
LSY: sylio1@student.monash.edu
TSH: ton.so.ha@sci.monash.edu.my
KAK: khalid.kadir@med.monash.edu.my
SNASH: sharifah@mail.hukm.ukm.my

Abstract:

Background: The metabolic syndrome (MetS) is a cluster of metabolic abnormalities comprising visceral obesity, dyslipidaemia and insulin resistance (IR). With the onset of IR, the expression of lipoprotein lipase (LPL), a key regulator of lipoprotein metabolism, is reduced. Increased activation of glucocorticoid receptors results in MetS symptoms and is thus speculated to have a role in the pathophysiology of the MetS. Glycyrrhizic acid (GA), the bioactive constituent of licorice roots (*Glycyrrhiza glabra*) inhibits 11β-hydroxysteroid dehydrogenase type 1 that catalyzes the activation of glucocorticoids. Thus, oral administration of GA is postulated to ameliorate the MetS.

Results: In this study, daily oral administration of 50 mg/kg of GA for one week led to significant increase in LPL expression in the quadriceps femoris ($p<0.05$) but non-significant increase in the abdominal muscle, kidney, liver, heart and the subcutaneous and visceral adipose tissues ($p>0.05$) of the GA-treated rats compared to the control. Decrease in adipocyte size ($p>0.05$) in both the visceral and subcutaneous adipose tissue depots accompanies such selective induction of LPL expression. Consistent improvement in serum lipid parameters was also observed, with decrease in serum free fatty acid, triacylglycerol, total cholesterol and LDL-cholesterol but elevated HDL-cholesterol ($p>0.05$). Histological analysis using tissue lipid staining with Oil Red O showed significant decrease in lipid deposition in the abdominal muscle and quadriceps femoris ($p<0.05$) but non-significant decrease in the heart, kidney and liver ($p>0.05$).

Conclusion: Results from this study may imply that GA could counteract the development of visceral obesity and improve dyslipidaemia via selective induction of tissue LPL expression and a positive shift in serum lipid parameters respectively, and retard the development of IR associated with tissue steatosis.

Background:

Lipoprotein lipase (LPL) is the major enzyme responsible for the hydrolysis of circulating triacylglycerol (TAG) moiety of both classes of TAG-rich lipoproteins; the chylomicrons and very-low-density lipoprotein (VLDL), generating free fatty acids (FFA) that are either oxidized in the muscles or re-esterified in the adipose tissues, and glycerol that is returned to the liver. LPL plays a central role in overall lipoprotein metabolism, where (i) the successive interaction of VLDL with LPL generates the low-density lipoproteins (LDL) that are involved in forward cholesterol transport and (ii) the remnant lipoprotein particles so formed from LPL catalysis contributes to the maturation of high-density lipoprotein (HDL) precursors, the latter of which is then involved in reverse cholesterol transport [1, 2]. Perturbation in LPL activity could therefore lead to significant metabolic consequences and LPL has been implicated in pathophysiological conditions characterized by marked hypertriglyceridaemia, such as that observed in the metabolic syndrome (MetS).

The MetS refers to a constellation of metabolic abnormalities characterized by the co-existence of insulin resistance (IR), visceral obesity, hyperglycaemia, hypertension and dyslipidaemia. The syndrome has become a recognizable clinical cluster of risk factors that are predictive of the progression to cardiovascular disease and type 2 diabetes mellitus (T2DM) [3]. Both visceral obesity and IR are recognized as the major determinants in the development of the MetS [4] and in fact, over 80% of individuals with T2DM are obese and virtually all are insulin resistant [5]. Differing definitions of the syndrome have been put forward by various global health agencies such as the World Health Organization (WHO), the National Cholesterol Education Program Adult Treatment Panel III (NCEP ATP III) and the International Diabetes Federation (IDF) but all such definitions point to a common agreement that the syndrome results in increased atherogenesis and death from myocardial infarction [4]. Thus, increased attention has been channeled to the improvement of lipid abnormalities characteristic of the MetS.

Dyslipidaemia, the hallmark of the MetS which is manifested in the more severe form in T2DM, is characterized by (i) increased flux of FFA, (ii) elevated TAG level (hypertriglyceridaemia), (iii) reduced HDL level and (iv) a predominance of small, dense LDL. Elevated plasma FFA is viewed as the primary defect leading to the development of dyslipidaemia [6, 7] and IR [8]. With the ensuing IR, LPL expression is reduced and LPL activity becomes diminished [9, 10]. This amplifies the extent of the hypertriglyceridaemia by favouring the accumulation of TAG-rich chylomicrons and VLDL in the circulation. The increase in small, dense LDL and low HDL is secondary to this elevated TAG level, where through the action of cholesteryl ester transfer protein (CETP), TAG enrichment of both the HDL and LDL particles occurs. TAG-rich LDL particles are good substrate to be acted upon by hepatic lipase (HL), producing a population of small, dense, lipid-poor LDL. Similarly, HL-mediated hydrolysis of TAG-rich cholesterol-poor HDL leads to an accelerated degradation of apo A-I, the major protein of HDL. This causes the HDL to be rapidly cleared from the plasma

[6, 7, 11]. In addition to such serum lipid perturbations, studies have also indicated that tissue lipid accumulation is associated with obesity-related IR and T2DM where both conditions are associated with increased tissue lipid [12, 13].

Increased activation of glucocorticoid receptors has been implicated in the development of MetS symptoms such as visceral obesity and hyperlipidemia. Pharmacological inhibition of the enzyme 11β-hydroxysteroid dehydrogenase type 1 (11β-HSD1) that acts to regenerate active glucocorticoids from inactive 11-keto metabolites has been proposed as a therapeutic target for the treatment of MetS following the association of such inhibition with a cardioprotective lipid profile [14, 15]. Glycyrrhizic acid (GA), the primary bioactive constituent of the roots of the shrub *Glycyrrhiza glabra* and its pharmacologically active metabolite glycyrrhetic acid (GE) act as potent, non-selective inhibitors of both isoforms of 11β-HSD [16, 17]. To date however, the effects of orally-administered GA on LPL expression and on the modulation of serum lipid and tissue lipid deposition have yet to be conducted. The objectives of this study are therefore to determine and compare each of these parameters between GA-treated and non-treated rats following daily oral administration of GA for one week in the former.

Results:

GA treatment led to increase in LPL expression of all studied tissues. LPL expression in the GA-treated rats was increased in all studied tissues (Figure 1), of which included the heart, liver, kidney, quadriceps femoris (QF), abdominal muscle (AM), visceral adipose tissue (VAT) and subcutaneous adipose tissue (SAT). The QF demonstrated the highest increase with a fold difference of 2.02 ± 0.89, representing a significant 102% increase ($p<0.05$). This was followed by the AM (1.87 ± 1.61 fold; 87% increase), kidney (1.43 ± 0.93 fold; 43% increase), liver (1.29 ± 1.01 fold; 29% increase) and the VAT (1.08 ± 0.48 fold; 8%); all of which exhibited no significance difference between the control and GA-treated group ($p>0.05$). Increase in LPL expression was similar in the heart and SAT (1.04 ± 0.48; 4% increase) but these were not significant ($p>0.05$).

GA treatment reduced the size of adipocytes. Mean area of both VAT and SAT adipocytes showed non-significant decrease in the GA-treated group compared to the control ($p>0.05$) (Figure 2). In the VAT, mean adipocyte area in the control group was 1449.96 ± 156.58 μm^2 while that in the treated group was 1206.58 ± 239.48 μm^2. In the SAT, mean adipocyte area was 1419.91 ± 141.14 μm^2 in the control group, compared to a mean of 1161.18 ± 143.26 μm^2 in the treated group. These represented a 16.79% and 18.22% reduction in the area of adipocytes in VAT and SAT respectively. Sections of these tissues are shown in Figure 3.

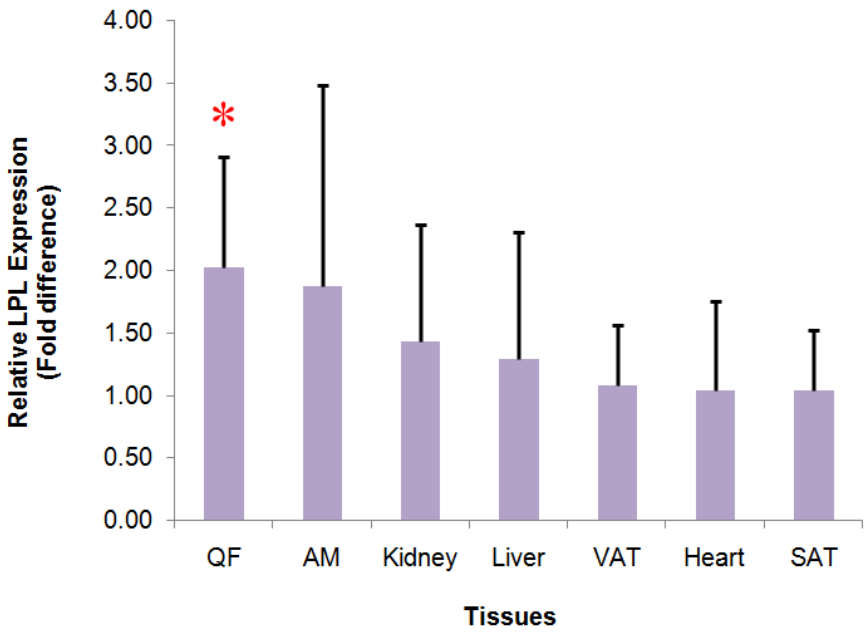

Figure 1: Fold difference in tissue LPL expression of the GA-treated group.
Relative tissue LPL expression following GA treatment is shown in decreasing order. In this analysis, β-actin (BAC) gene was used as the endogenous reference, GA-treated group as the target and control group as the calibrator. * denotes $p < 0.05$.

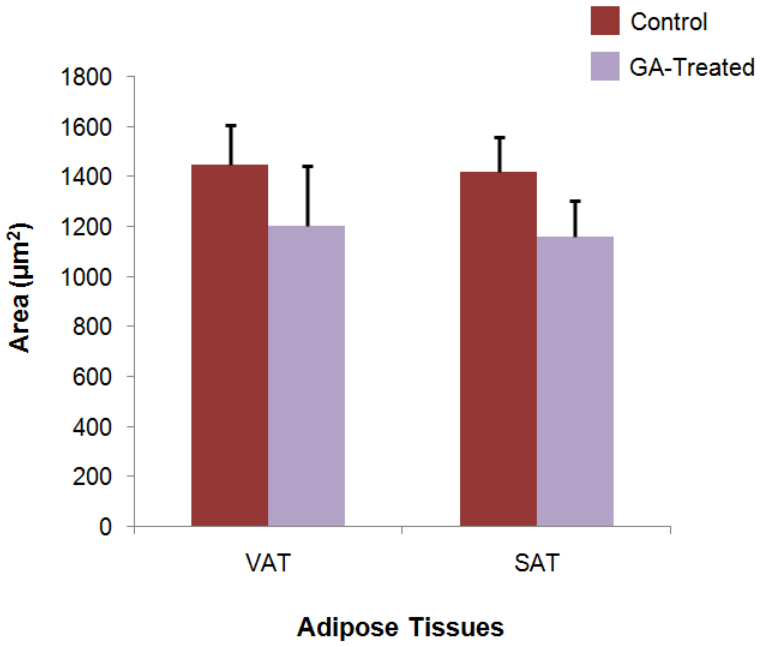

Figure 2: Mean area of adipocytes (μm^2) of control and GA-treated rats.
Size of adipocytes demonstrated a decrease in both the VAT and SAT depot after seven days of oral GA administration ($p>0.05$).

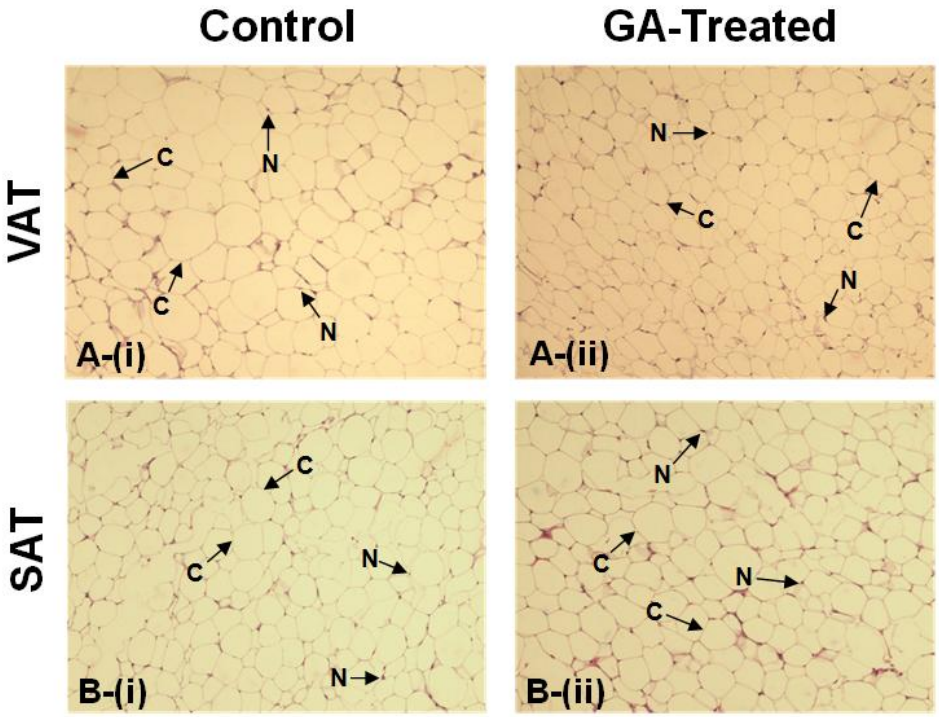

Figure 3: H & E-stained adipose tissues.
Representative sections of H&E-stained (A) VAT and (B) SAT in (i) control and (ii) GA-treated rats at 100× magnification. The adipocytes appear as empty, unstained vacuoles with the nucleus compressed to one side of the cell while the cytoplasm is reduced to only a small rim at the periphery of the cell. Arrows indicate examples of cytoplasm (C) and nucleus (N).

GA treatment led to improvement in all serum lipid parameters. Consistent improvement in all serum lipid parameters were observed in the GA-treated rats relative to the control (p>0.05) (Figure 4). Mean serum TAG showed a 14.73% reduction (control, 1.29 ± 0.31 mmol/L; treated, 1.10 ± 0.27 mmol/L) while that of total cholesterol charted a reduction of 12.99% (control, 3.31 ± 0.60 mmol/L; treated, 2.88 ± 0.43 mmol/L) and that of LDL-cholesterol a 36.96% reduction (control, 1.38 ± 0.34 mmol/L; treated, 0.87 ± 0.27 mmol/L). HDL-cholesterol on the other hand was elevated by 11.85% (control, 1.35 ± 0.19 mmol/L; treated, 1.51 ± 0.47 mmol/L). Serum FFA also exhibited a similar trend of improvement with a reduction of 8.51% in the treated group (control, 0.47 ± 0.07 mmol/L; treated, 0.43 ± 0.07 mmol/L).

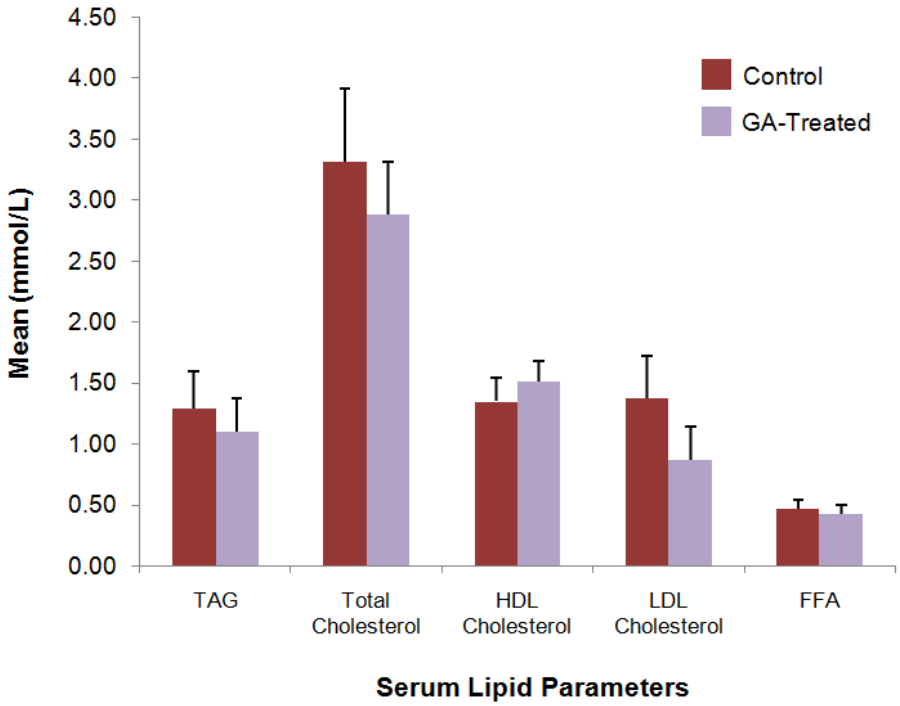

Figure 4: Serum lipid of control and GA-treated rats.
Mean serum TAG, total cholesterol, LDL-cholesterol and FFA (mmol/L) of GA- treated rats showed reduction after seven days of oral GA administration while that of HDL-cholesterol showed an increase ($p>0.05$ for all parameters).

GA treatment reduced tissue lipid deposition. Lipid deposition demonstrated a decrease across all studied tissues in the GA-treated group (Figure 5). Levels of lipid deposition was highest in the liver and recorded a 21.86% decrease (control, 582.44 (23.50-1939.66) AU; treated, 55.14 (23.13-1830.91) AU) following GA treatment. The kidney demonstrated a 25.11% decrease (control, 137.54 (11.55-392.10) AU; treated, 103.00 (13.10-228.00) AU). No significant difference between the control and treated groups were observed in both tissues ($p>0.05$). Among the muscles, the QF and the AM showed significantly reduced lipid deposition in the GA-treated group relative to the control ($p<0.05$), with a decrease of 42.21% and 33.96% in each tissue respectively (QF: control, 191.28 (28.85-606.17) AU; treated, 110.54 (12.21-594.28); AM: control, 141.29 (11.77-356.51) AU; treated, 93.31 (22.69-297.13) AU). Lastly, lipid deposition in the heart showed a non-significant 6.74% decrease (control, 149.56 (26.58-327.91) AU; treated, 139.48 (47.74-268.54) AU). Sections of these tissues are depicted in Figure 6.

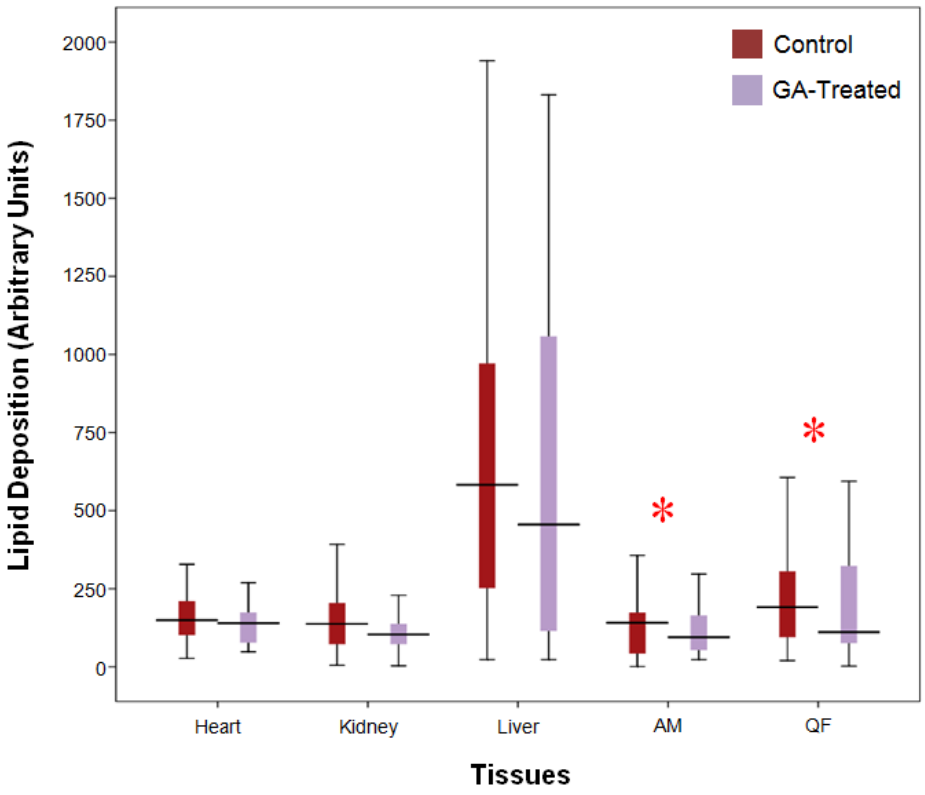

Figure 5: Levels of lipid deposition in non-adipose tissues.
Sections of ORO-stained tissues were converted to a grayscale each time for lipid staining quantification. * denotes $p < 0.05$.

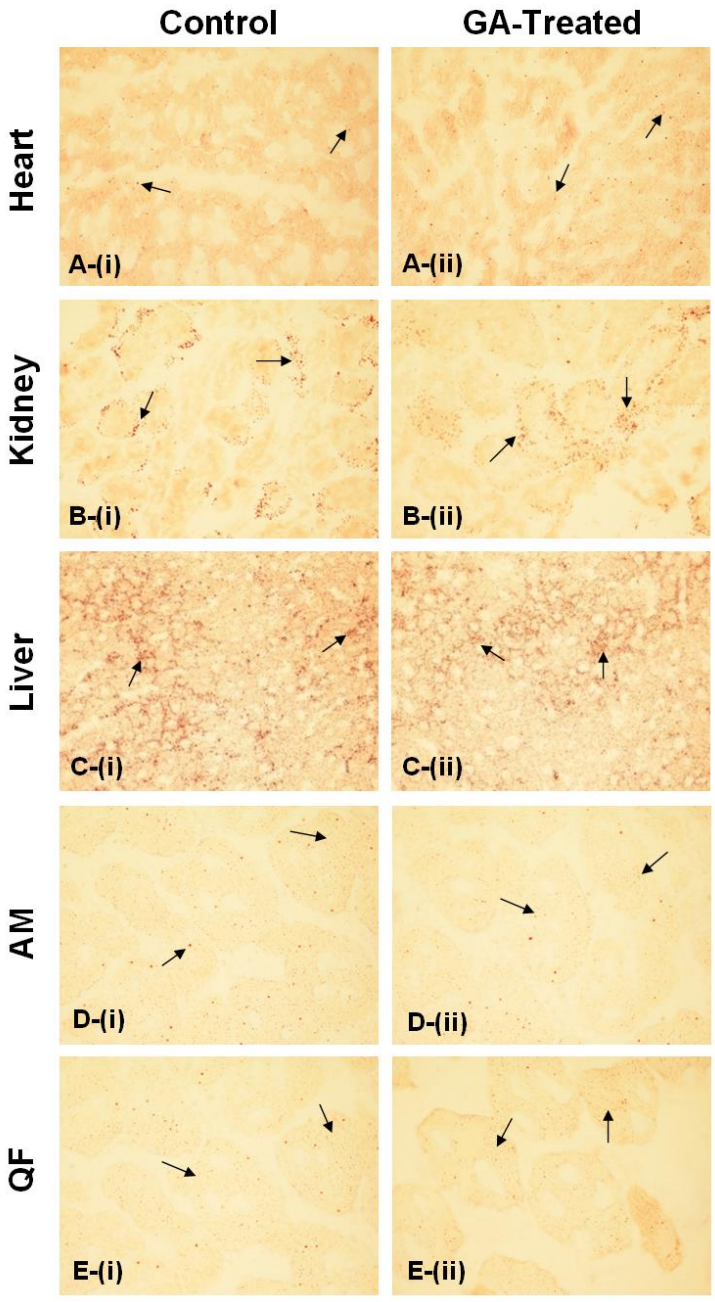

Figure 6: ORO-stained tissues.
Representative sections of ORO-stained (A) heart, (B) kidney, (C) liver, (D) AM and (E) QF in (i) control and (ii) treated rats at 400× magnification. Distinct spots of ORO-stained lipid were observed across all tissue sections with considerable heterogeneity in lipid content between tissues. Arrows indicate examples of lipid droplets.

GA treatment did not induce an increase in systolic blood pressure. Systolic blood pressure of control and GA-treated rats fluctuated within a narrow range throughout the duration of treatment (Figure 7). Systolic blood pressure of the control and GA-treated rats were compared on Days 0, 2, 4 and 6 of the treatment duration. No significant difference (p>0.05) in mean systolic blood pressure was observed between the control and treated groups and within each group on each of these days.

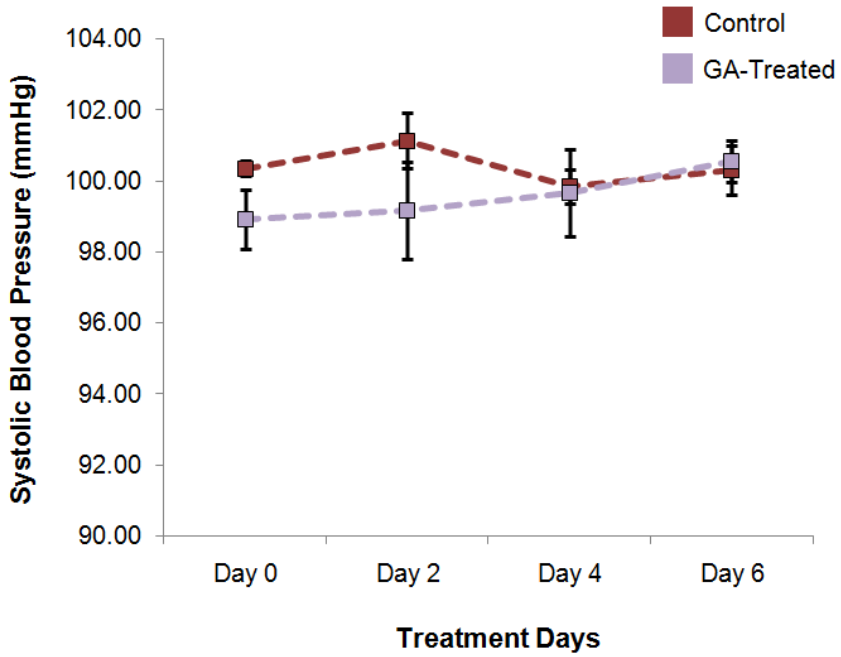

Figure 7: Evaluation of systolic blood pressure.
Day-to-day mean systolic blood pressure (mmHg) of control and treated rats over the duration of treatment. No significant difference was observed in each of the days between both groups and within each group (p>0.05).

Discussion:

IR has been recognized as the central component of the MetS which is associated with hyperinsulinaemia, glucose intolerance, dyslipidaemia and visceral obesity [4]. With the onset of IR, the activity of LPL, a key regulator of lipoprotein metabolism that is subject to insulin regulation, has been reported to be reduced both in the adipose tissues and muscles [18, 19]. Insulin has been implicated in the biosynthesis of LPL [10] where the insulin-signaling pathway activates the class of nuclear receptors known as the peroxisome proliferator-activator receptor (PPAR). The isoforms of these, PPARα and PPARγ, then bind to the peroxisome proliferator respondse element (PPRE) at the LPL gene promoter to up-regulate LPL expression [20].

In this study, inhibition of 11β-HSD1 by GA could not account adequately for the observed increase in tissue LPL expression. Despite the inhibitory effects of glucocorticoids on LPL protein synthesis and mRNA levels, such observations were only observed in the adipose tissues [21]. Therefore, the induction of LPL expression in this study points to a separate mode of action of GA where GA is postulated to activate the PPAR class of nuclear receptors. This is based on the consistency of several findings, where (i) triterpenoids have been reported to lead to the transactivation of PPAR-γ [22, 23] and more importantly (ii) PPAR-α and -γ agonists have been shown to reduce the expression and activity of 11β-HSD1 [24]. Thus, GA, both a triterpenoid and an 11β-HSD1 inhibitor may act as a ligand to the PPAR. Interestingly, 11β-HSD1 knock-out mice also show an elevation of PPAR-α mRNA. PPAR-α is physiologically induced by glucocorticoids and its elevation following 11β-HSD1 inhibition may have arisen from increased circulating plasma corticosterone due to impaired 11β-HSD1-mediated negative feedback upon the hypothalamic-pituitary-adrenal axis [14]. This increased PPARα may then act in return to up-regulate LPL. Thus, GA-mediated activation of the PPAR class of nuclear receptors may be direct or indirect.

PPAR-α plays a key role in regulating pathways of β-oxidation and is expressed abundantly in tissues metabolizing high amounts of FFA, such as the liver, kidney, heart and muscles while PPAR-γ is expressed primarily in the adipose tissues where it triggers adipocyte differentiation and lipogenesis [25, 26]. With reference to Figure 1, increased LPL expression was consistently higher in tissues characterized by high PPAR-α expression (QF, AM, kidney and liver) as compared to tissues in which PPAR-γ predominates (VAT and SAT). One exception however was seen in the heart that has a relative LPL expression comparable to that of the adipose tissues. Such discrepancy may be due to the lower distribution of GA into the heart as compared to all other tissues examined in this study [27]. The selective pattern of tissue LPL induction suggested that GA exhibits greater potency in activating PPAR-α than PPAR-γ. Such pattern of tissue LPL induction have been advocated for the correction of visceral obesity as it could lead to the competitive delivery of FFA away from the more pathogenic visceral fat depot to other less pathogenic depots [28].

This postulation was then confirmed in the study through the measurement of adipocyte size in both control and GA-treated rats. With reference to Figure 2, size of adipocytes exhibited a decrease in both the VAT and SAT following GA treatment. The overall results have therefore shown that by reducing visceral fat accumulation, GA has the potential to counteract the very fundamental abnormality that contributes to the development of the MetS, i.e. visceral obesity [8].

Accompanying the increase in tissue LPL expression and decrease in adipocyte size was the consistent improvement in serum lipid parameters of the GA-treated rats relative to the control; with a reduction in serum FFA, TAG, total cholesterol and LDL-cholesterol and elevation of HDL-cholesterol. The GA-induced decrease in serum FFA appears to be of critical importance due to the role of FFA in initiating the development of IR, β-cell dysfunction and dyslipidaemia [5, 7]. The observed decrease in serum FFA may be attributed to increased tissue uptake. Berthiaume *et al.* [29] has demonstrated that inhibition of 11β-HSD1 is associated with a concomitant increase in protein content of plasma membrane fatty acid-binding protein ($FABP_{pm}$) that facilitates the entry of FA into cells. In addition, PPAR-α agonists have also been reported to induce the activities of fatty acid transporter protein (FATP) and acyl-CoA synthetase [30],

where the former mediates FFA uptake and the latter is involved in the activation of FFA that then facilitates its β-oxidation [31, 32]. Activation of acyl-CoA synthetase therefore promotes the oxidation of FFA to prevent the saturation of cellular FA binding and transport [32]. This supports further the decrease in lipid deposition in the studied tissues despite increased FFA uptake.

The decrease in serum TAG did not appear secondary to the reduction in serum FFA and may be mostly attributed to the action of GA. Inhibition of 11β-HSD1 has been shown to reduce hepatic VLDL secretion [29] which may have been driven by increased hepatic FFA oxidation due to the induced expression of fat-catabolizing enzymes [14]. Hepatic VLDL secretion is regulated by the amount of lipids available for the assembly of VLDL [29]. Extracellular FFA entering the liver is either oxidized or esterified to form a cytosolic pool of TAG; the TAG required for VLDL assembly is recruited from this pool. Physiologically, extracellular FFA acts to boost VLDL secretion by expanding the size of this intrahepatic TAG pool [33]. With increased FA oxidation however, the drive for the VLDL assembly pathway is subsequently attenuated.

The increase in HDL-cholesterol following GA administration may be due to the increased production of apo A-I, the major protein of HDL that is subjected to accelerated catabolism in the MetS [7]. Apo A-I mRNA has been shown to be significantly elevated in 11β-HSD1 knock-out mice [14] and following PPAR-α activation [30]. Since the rate of HDL synthesis is dependent on the production of apo A-I [34], this has been speculated as the HDL-increasing mechanism of GA.

Despite lacking benefits of increased LPL expression in this study, such LPL induction by GA may be pivotal in the amelioration of lipid parameters in dyslipidaemic subjects. In the lean rats employed in this study, the serum TAG measured after a 12-h fast reflects only the VLDL fraction. Serum chylomicrons have a half life of 13-14 minutes and would be cleared from circulation within this fasting period [35]. In dyslipidaemic subjects however, hypertriglyceridaemia is attributed to the prolonged retention of both chylomicrons and VLDL due to inhibited lipolysis of both particles following decreased LPL levels [8]. Therefore, in the dyslipidaemic state, induced LPL may contribute to the increased clearance of such lipoproteins to reduce serum TAG. Furthermore, the development of small, dense LDL and the reduction in HDL seen in the dyslipidaemic state are attributed to CETP-mediated lipid exchange between both lipoprotein particles and TAG-enriched VLDL particles. Such exchange is substrate- rather than enzyme-driven [36]. The increased catabolism of TAG-enriched VLDL by LPL may thus serve to positively re-modulate HDL and LDL profile in dyslipidaemia.

The observed decrease in lipid deposition across all studied tissues may be consequential of increased lipid oxidation in these tissues following GA administration. Previous reports have suggested that increased tissue lipid content in the obese state is related to decreased activity of oxidative enzymes [12]. In this study, increase in enzymes of β-oxidation such as acyl-CoA synthetase, mitochondrial carnitine palmitoyltransferase-I and acyl-CoA oxidase were postulated to be induced through (i) direct activation of PPAR-α by GA, (ii) increased expression of PPAR-α following inhibition of 11β-HSD1 [14], or (iii) activation of PPAR-α by LPL-generated FFA that serves as natural PPAR-α ligands [37]. All the enzymes aforementioned carry a PPRE in the promoter region [30, 38, 39]. The last postulation showed consistency with the results of the

study where significant decrease in lipid deposition was observed in the AM and QF, in agreement with their higher increase in LPL expression compared to all other tissues. In addition to the current study, Berthiaume *et al.* [29] has also demonstrated that inhibition of 11β-HSD1 was associated with a reduction in tissue TAG content and increased FFA oxidation.

TAG is present in all cell types and intracellular storage of these neutral lipids occurs within lipid droplets. The adipose tissue and liver are the principal stores of TAG, explaining the high levels of lipid deposition in the liver, while other cell types store small quantities of these. Tissue TAG storage occurs in any quantities, and in the liver for example, TAG storage may range up to 10-fold [33]. This explains the large range of lipid deposition in tissues as observed in the study.

Obesity and T2DM has been associated with tissue lipid accumulation and such ectopic TAG accumulation, also known as tissue steatosis, is implicated in the impairment of insulin signaling [12, 13]. These lipotoxic effects are not exerted by TAG itself, but through TAG-derived bioactive lipid metabolites such as long chain fatty acyl-CoA, diacylglyerol and ceramide that activate several serine kinases to block insulin signal transduction [26]. In addition, lipid accumulation in the pancreatic islets would further impair insulin secretion where both ceramide and the nitric oxide generated from surplus unoxidized FFA induces β-cell apoptosis in the pancreatic islet [5]. T2DM has been postulated to only develop in such setting of concurrently occurring IR and β-cell failure [40]. With the demonstrated ability of GA to reduce tissue TAG accumulation therefore, GA exhibits the potential to revert such lipotoxicity exerted by tissue TAG excess and thereby serve to prevent the onset of T2DM.

The analysis of systolic blood pressure was conducted to determine the occurrence of the reported side effects of GA intake. Chronic administration of GA has been associated with the development of pseudoaldosteronism, of which includes symptoms such as electrolyte imbalance and increased blood pressure. This results from the non-selective nature of both GA and GE that inhibits not only 11β-HSD1 but also 11β-HSD2 [17]. In this study, one week administration of GA did not induce an increase in systolic blood pressure. The positive effects arising from the inhibition of 11β-HSD1, such as modulation of serum lipid, that is more readily observable compared to the side effects arising from the inhibition of 11β-HSD2, such as an increase in blood pressure, is possibly due to different potency of GA in inhibiting the two isoforms of the enzyme. Shimoyama *et al.* [41] has reported that GE, the active metabolite of GA, is more effective in inhibiting 11β-HSD1 than 11β-HSD2. The IC_{50} for the two enzymes are 0.09 μM and 0.36 μM respectively. This may signify that the impact of GA on systolic blood pressure may be observed if treatment duration was prolonged, or by increasing the treatment dosage within the same duration. Nevertheless, Quaschning *et al.* [42] has demonstrated that the use of aldosterone and endothelin receptor antagonists could normalize GA-induced blood pressure. The combinatorial use of GA and such antagonists may therefore represent a new therapeutic approach for patients with MetS; allowing patients to harbour the benefits from GA itself and simultaneously eliminating the possible side effects.

Conclusion:

Daily oral administration of 50 mg/kg of GA for a week led to increased LPL expression predominantly in the non-adipose tissues, with significant increase in the QF. Together with the reduction in size of adipocytes in both the VAT and SAT, this may suggest that GA could divert FFA away from the pathogenic visceral depot to the oxidative tissues, thus curbing visceral obesity. GA also modulated serum lipid and the consistent pattern of improvement of each lipid parameter; namely, serum FFA, TAG, total cholesterol, HDL-cholesterol and LDL-cholesterol, points to the ability of GA to cause a beneficial shift to a less atherogenic lipid profile. The decrease in tissue lipid deposition across all the non-adipose tissues studied indicated that lipid did not accumulate in these despite increased LPL expression, possibly due to an accompanying increase in β-oxidation. GA may therefore retard the development of IR associated with tissue steatosis.

Methods:

Animals and treatment. The use and handling procedure of animals in this research project had been approved by the Monash University Animal Ethics Committee (AEC Approval Number: SOBSB/MY/2007/22). 16 male *Rattus norvegicus* Sprague-Dawley rats weighing between 160-200g were supplied by Universiti Malaya Animal House (Malaysia) and were housed individually in polypropylene cages in a room kept at 23°C on a 12-h light: 12-h dark cycle (lights on at 0800 hours). The rats were randomly segregated into two groups of eight; representing the control and GA-treated groups. The GA-treated group was given 50 mg/kg of GA daily per oral (p.o.) while the control group given tap water without GA. All animals were fed *ad libitum* with free access to standard rat chow (Glenn Forrest Stockfeeder, Australia) and drinking water for the one week duration of treatment.

Systolic blood pressure measurement. Systolic blood pressure was measured by tail cuff plethysmography using the NIBP controller (ADInstruments, Australia). Conscious rats were placed into a plastic restrainer and a tail-cuff with a pulse transducer was applied onto the tail. The tail was heated using a table lamp. Rats were allowed to habituate to the procedure for 7 days prior to start of the experiment. The recording and determination of blood pressure were performed using the Chart recording software and a final reading was averaged out from at least 10 consecutive readings. This procedure was performed every alternate day.

Blood and tissue sampling. At the end of the treatment period, all rats were humanely sacrificed between 0800 to 1000 hours on the 8^{th} day of treatment after a 12-h fast. All rats were anaesthetized via intraperitoneal injection of 150 mg/kg of sodium pentobarbital (Nembutal) prior to exsanguination. Blood was drawn from the cardiac ventricle via the apex and was centrifuged at 12,000 × g for 10 minutes. The resulting serum supernatant was then rapidly aliquoted into microtubes and kept frozen at -80°C until required for analysis. The seven tissues of interest; heart, liver, kidney, AM, QF and VAT and SAT were promptly harvested, all of which were placed into individual cryovials (Nalgene, USA) and immediately snap-frozen in liquid nitrogen. These were then stored at -80°C until required for analysis. In addition, a fraction

of VAT and SAT were immersed in 10% neutral-buffered formalin in individual universal bottles for histological analysis.

Plasma lipid parameters. Total cholesterol, TAG and FFA were measured with Randox CH200 Cholesterol kit (Randox, UK), Wako Triglyceride E kit (Wako, Japan) and Randox FA115 Non-Esterified Fatty Acids kit (Randox, UK) respectively. To determine the level of HDL-cholesterol, HDL-cholesterol was first separated from the LDL and VLDL fraction by precipitation of the latter two using the Randox CH203 HDL Precipitant (Randox, UK), followed by a cholesterol assay using the Randox CH200 Cholesterol kit (Randox, UK). LDL-cholesterol was calculated using the Friedewald formula, using the levels of total cholesterol, TAG and HDL cholesterol obtained [43].

RNA extraction and cDNA synthesis. Total RNA extraction of the heart, liver, kidney, AM and QF was performed using the Qiagen RNeasy Mini Kit (Qiagen, USA) while that of the VAT and SAT with the Qiagen RNeasy Lipid Tissue Mini Kit. RNA purity was performed by measuring the absorbance of the diluted RNA at 260 and 280 nm. RNase-free DNase treatment was performed using Promega RQ1 RNase-free DNase (Promega, USA) and cDNA synthesis was performed using the Qiagen Omniscript Reverse Transcriptase kit (Qiagen, USA).

Real time reverse transcription polymerase chain reaction (qRT-PCR). The expression of LPL was determined by qRT-PCR using the LPL forward and reverse primers 5'-CAGCAAGGCATACAGGTG-3' and 5'- CGAGTCTTCAGGTACATCTTAC-3' and the probe 5'-(6-FAM) TTCTCTTGGCTCTGACC (BHQ1)-3' that are specific for *Rattus norvegicus* LPL mRNA [GenBank: BC081836] and normalized to the β-actin (BAC) gene with the forward and reverse primers 5'- GTATGGGTCAGAAGGACTCC-3' and 5'-GTTCAATGGGGTACTTCAGG-3' and the probe 5'-(TET) CCTCTCTTGCTCTGGGC (BHQ1)-3' specific for *Rattus norvegicus* BAC mRNA [GenBank: BC063166]. The comparison of LPL expression between control and GA-treated rats were performed using the Comparative Ct (ΔΔCt) Method, with BAC as reference, GA-treated group as target and control group as calibrator. Agarose gel electrophoresis was carried out on amplicons generated from qRT-PCR reaction to ensure primer specificity.

Tissue lipid staining. Frozen tissues were cut into small cubes of approximately $5 \times 5 \times 5$ mm on and embedded using the Optimal Cutting Temperature (OCT) Compound (Leica, Germany). Cryosectioning was performed at a temperature of -25°C where the embedded tissues were sectioned into 5 μm slices and adhered onto glass slides. Staining with Oil Red O (ORO) was performed in accordance to Koopman *et al.* [44] and captured at 400x magnification. Lipid deposition was quantified as specified by Goodpaster *et al.* [12]. Images were transferred to Image J software and converted to grayscale. Threshold for the intensity of staining was adjusted in order to pick up only the droplets of lipid; the full-range being from 0 to 255 arbitrary units (AU), where 0 represents complete staining and 255 represents no staining. For lipid quantification, pixels with intensities of $\leq 150 \pm 30$ AU were quantified. Lipid deposition were expressed in AU and calculated as:

$$\text{Lipid Deposition} = \frac{\text{Percentage of area stained} \times \text{Mean intensity of staining}}{10^6}$$

Eight contiguous views per tissue section were captured and analyzed for the lipid content. The level of lipid deposition of each tissue section was calculated as the average of these eight values.

Morphometric analysis of adipocytes. Adipose tissues that were fixed in 10% neutral-buffered formalin as aforementioned were processed by a Leica TP 1020 Automatic Tissue Processor and embedded in paraffin. 5 μm thick tissue sections were then stained with haematoxylin and eosin (H&E) followed by the measurement of the size of 100 adipocytes (μm^2) per field view per tissue section at 100x magnification.

Statistical analysis. Statistical analysis of LPL expression was performed using the Relative Expression Software Tool (REST©) MCS Beta 2006 while that of all other parameters was performed using the Statistical Package for the Social Sciences (SPSS) Version 16.0. Data distribution was analyzed using the Kolmogorov-Smirnov test. Parametric data were then analyzed with independent t-test and are presented as mean ± standard error while non-parametric with Mann-Whitney U-test and are reported as median (minimum – maximum). In all analyses, a p-value ≤ 0.05 was considered significant.

Abbreviations:

11β-HSD: 11β-hydroxysteroid dehydrogenase; AM: abdominal muscle; CETP: cholesteryl ester transfer protein; FFA: free fatty acids; GA: glycyrrhizic acid; GE: glycyrrhetic acid; H&E: haematoxylin and eosin; HL: hepatic lipase; HDL: high-density lipoprotein; IR: insulin resistance; LDL: low-density lipoprotein; LPL: lipoprotein lipase; MetS: metabolic syndrome; ORO: Oil Red O; PPAR: peroxisome proliferator-activator receptor; PPRE: peroxisome proliferator response element; QF: quadriceps femoris; SAT: subcutaneous adipose tissue; T2DM: type 2 diabetes mellitus; TAG: triacylglycerol; VAT: visceral adipose tissue; VLDL: very-low-density lipoprotein.

Competing interests:

The authors declare that they have no competing interests.

Authors' contributions:

LWYA was involved in all bench work, data acquisition, analysis and interpretation and manuscript preparation. CYY had part in the optimization of the qRT-PCR conditions and LSY had part in histological work. TSH, KAK and SNASH participated in the coordination of the study and helped in drafting the manuscript. All authors read and approved the final manuscript.

Acknowledgements:

The study is funded in part by a grant from the Malaysian Ministry of Science, Technology and Innovation (02-02-10-SF0003).

References:

1. Preiss-Landi K, Zimmermann R, Hammerle G, Zechner R: Lipoprotein lipase: the regulation of tissue specific expression and its role in lipid and energy metabolism. *Curr Opin Lipidol* 2002, 13(5):471-481.
2. Pillarisetti S, Saxena U: Lipoprotein lipase as a therapeutic target for dyslipidemia. *Front Biosci* 2003, 8:d238-241.
3. Balkau B, Valensi P, Eschwege E, Slama G: A review of the metabolic syndrome. *Diabetes Metab* 2007, 33:405-413.
4. Fulop T, Tessier D, Carpentier A: The metabolic syndrome. *Pathologie Biologie* 2006, 54:375-386.
5. Boden G, Shulman GI: Free fatty acids in obesity and type 2 diabetes: defining their role in the development of insulin resistance and beta-cell dysfunction. *Eur J Clin Invest* 2002, 32(3):14-23.
6. Krauss R: Lipids and Lipoproteins in Patients With Type 2 Diabetes. *Diabetes Care* 2004, 27(6):1496-1504.
7. Kolovou GD, Anagnostopoulou KK, Cokkinos DV: Pathophysiology of dyslipidaemia in the metabolic syndrome. *Postgrad Med J* 2005, 81:358-366.
8. Lann D, LeRoith D: Insulin Resistance as the Underlying Cause for the Metabolic Syndrome. *Med Clin N Am* 2007, 91:1063-1077.
9. Mead JR, Irvine SA, Ramji DP: Lipoprotein lipase: structure, function, regulation and role in disease. *J Mol Med* 2002, 80:753-769.
10. Kageyama H, Hirano T, Okada K, Ebara T, Kageyama A, Murakami T, Shioda S, Adachi M: Lipoprotein lipase mRNA in white adipose tissue but not in skeletal muscle is increased by pioglitazone through PPAR-gamma. *Biochem Biophys Res Commun* 2003, 305:22-27.
11. Aguilera CM, Gil-Campos M, Canete R, Gil A Alterations in plasma and tissue lipids associated with obesity and the metabolic syndrome. *Clin Sci* 2008, 114:183-193.
12. Goodpaster BH, Theriault R, Watkins SC, Kelley DE: Intramuscular Lipid Content Is Increased in Obesity and Decreased by Weight Loss. *Metabolism* 2000, 49(4):467-472.
13. Athenstaedt K, Daum G The life cycle of neutral lipids: synthesis, storage and degradation. *Cellular and Molecular Life Sciences* 2006, 63:1355-1369.
14. Morton MM, Holmes MC, Fievet C, Staels B, Tailleux A, Mullins JJ, Seckl JR: Improved Lipid and Lipoprotein Profile, Hepatic Insulin Sensitivity and Glucose Tolerance in 11beta-Hydroxysteroid Dehydrogenase Type 1 Null Mice. *J Biol Chem* 2001, 276(44):41293-41300.
15. Livingstone DEW, Walker BR: Is 11beta-Hydroxysteroid Dehydrogenase Type 1 a Therapeutic Target? Effects of Carbenoxolone in Lean and Obese Zucker Rats. *J Pharmacol Exp Ther* 2003, 305(1):167-172.

16. Alberts P, Engblom L, Edling N, Forsgren M, Klingstrom G, Larsson C, Ronquist-Nii Y, Ohman B, Abrahmsen L: Selective inhibition of 11beta-hydroysteroid dehydrogenase type 1 decreases blood glucose concentrations in hyperglycaemic mice. *Diabetologia* 2002, 45:1528-1532.
17. Wamil M, Seckl JR: Inhibition of 11beta-hydroxysteroid dehydrogenase type 1 as a promising therapeutic target. *Drug Discov Today* 2007, 12(13/14):504-520.
18. Pollare T, Vessby B, Lithell H: Lipoprotein lipase activity in the skeletal muscle is related to insulin sensitivity. *Arterioscler Thromb Vasc Biol* 1991, 11:1192-1203.
19. Kern P: Potential Role of TNF-alpha and Lipoprotein Lipase as Candidate Genes for Obesity. *J Nutr* 1997, 127:1917S-1922S.
20. Hanyu O, Miida T, Obayashi K, Ikarashi T, Soda S, Kaneko S, Hirayama S, Suzuki K, Nakamura Y, Yamatani K, Aizawa Y: Lipoprotein lipase (LPL) mass in preheparin serum reflects insulin sensitivity. *Atherosclerosis* 2004, 174:385-390.
21. Enerback S, Gimble JM: Lipoprotein lipase gene expression: physiological regulators at the transcriptional and post-transcriptional level. *Biochim Biophys Acta* 1993, 1169:107-125.
22. Wang Y, Porter WW, Suh N, Honda T, Gribble GW, Leesnitzer LM, Plunket KD, Mangelsdorf DJ, Blanchard, SG, Willson TM, Sporn MB: A Synthetic Triterpenoid, 2-Cyano-3,12-dioxooleana-1,9-dien-28-oic Acid (CDDO) , Is A Ligand for the Peroxisome Proliferator-Activated Receptor Gamma. *Mol Endocrinol* 2000, 14(10):1550-1556.
23. Sato M, Tai T, Nunoura Y, Yajima Y, Kawashima S, Tanaka K: Dehydrotrametenolic Acid Induces Preadipocyte Differentiation and Sensitizes Animal Models of Noninsulin-Dependent Diabetes Mellitus to Insulin. *Biol Pharm Bull* 2002, 15(1):81-86.
24. Hermanowski-Vosatka A, Balkovec JM, Cheng K, Chen HY, Hernandez M, Koo GC, Le Grand CB, Li Z, Metzger JM, Mundt SS, Noonan, H, Nunes, C N, Olson SH, Pikounis B, Ren N, Robertson N, Schaeffer JM, Shah K, Springer MS, Strack AM, Strowski M, Wu K, Wu T, Xiao J, Zhang BB, Wright SD, Thieringer R: 11beta-HSD1 inhibition ameliorates metabolic syndrome and prevents progression of atherosclerosis in mice. *J Exp Med* 2005, 202(4):517-527.
25. Berger J, Tanen M, Elbrecht A, Hermanowski-Vosatka A, Moller DE, Wright SD, Thieringer R: Peroxisome Proliferator-activated Receptor-gamma Ligands Inhibit Adipocyte 11beta-Hydroxysteroid Dehydrogenase Type 1 Expression and Activity. *J Biol Chem* 2001, 276(16):12629-12635.
26. Muoio DM, Newgard CB: Obesity-Related Derangements in Metabolic Regulation. *Annu Rev Biochem* 2006, 75:367-401.
27. Ishida S, Sakiya Y, Ichikawa T, Taira Z, Awazu S: Prediction of Glycyrrhizin Disposition in Rat and Man by a Physiologically Based Pharmacokinetic Model. *Chem Pharm Bull* 1990, 38(1):212-218.
28. McCarty M: Modulation of adipocyte lipoprotein lipase expression as a strategy for preventing or treating visceral obesity. *Med Hypotheses* 2001, 57(2):192-200.
29. Berthiaume M, Laplante M, Festuccia WT, Cianflone K, Turcotte LP, Joanisse DR, Olivecrona G, Thieringer R, Deshaies Y: 11beta-HSD1 inhibition improves triglyceridaemia through reduced liver VLDL secretion and partitions lipids towards oxidative tissues. *Am J Physiol Endocrinol Metab* 2007, 293:E1045-E1052.

30. Staels B, Dallongeville J, Auwerx J, Schoojans K, Leitersdorf E, Fruchart JC: Mechanisms of Action of Fibrates on Lipid and Lipoprotein Metabolism. *Circulation* 1998, 98:2088-2093.
31. Elliot WH, Elliot DC: Energy release from fat. In: *Biochemistry and Molecular Biology.* 3rd edn. Oxford: Oxford University Press; 2005: 226-232.
32. Doege H, Stahl A: Protein-Mediated Fatty Acid Uptake: Novel Insights from In Vivo Models. *Physiology* 2006, 21:259-268.
33. Gibbons GF, Islam K, Pease RJ: Mobilisation of triacylglycerol stores. *Biochim Biophys Acta* 2000, 1483:37-57.
34. Dullens SPJ, Plat J, Mensink RP: Increasing apo A-I production as a target for CHD risk reduction. *Nutr Metab Cardiovas* 2007, 17:616-628.
35. Gurr MI, Harwood JL, Frayn KN: Lipid transport. In: *Lipid Biochemistry: An Introduction.* 5th edn. Oxford: Blackwell Science; 2002: 170-212.
36. Tan KCB, Shiu SWM, Chu BYM: Roles of hepatic lipase and cholesteryl ester transfer protein in determining low density lipoprotein subfraction distribution in Chinese patients with non-insulin-dependent diabetes mellitus. *Atherosclerosis* 1999, 145:273-278.
37. Koike T, Liang J, Wang X, Ichikawa T, Shiomi M, Liu G, Sun H, Kitajima S, Morimoto M, Watanabe T, Yamada N, Fan J: Overexpression of Lipoprotein Lipase in Transgenic Watanabe Heritable Hyperlipidemic Rabbits Improves Hyperlipidemia and Obesity. *J Biol Chem* 2004, 279(9):7521-7529.
38. van der Leiji FR, Huijkman NCA, Boomsma C, Kuipers JRG, Bartelds B: Genomics of the Human Carnitine Acyltransferase Genes. *Mol Genet Metab* 2000, 71:139-153.
39. Kane CD, Francone OL, Stevens KA: Differential regulation of the cynomolgus, human, and rat acyl-CoA oxidase promoters by PPAR-alpha. *Gene* 2006, 380:84-94.
40. Kim H, Ahn Y: Role of Peroxisome Proliferator-Activated Receptor-gamma in the Glucose-sensing Apparatus of Liver and Beta-cells. *Diabetes* 2004, 53(1):S60-S65.
41. Shimoyama Y, Hirabayashi K, Matsumoto H, Sato T, Shibata S, Inoue H: Effects of glycyrrhetinic acid derivatives on hepatic and renal 11beta-hydroxysteroid dehydrogenase activities in rats. *J Pharm Pharmacol* 2003, 55:811-817.
42. Quaschning T, Ruschitzka F, Niggli B, Lunt CMB, Shaw S, Christ M, Wehling M, Luscher TF: Influence of aldosterone *vs* endothelin receptor antagonism on renovascular function in liquorice-induced hypertension. *Nephrol Dial Transplant* 2001, 16:2146-2151.
43. Friedewald WT, Levy RI, Fredrickson DS: Estimation of the concentration of LDL-cholesterol in plasma without use of the preparative ultracentrifuge. *Clin Chem* 1972, 18:499-502.
44. Koopman R, Schaart G, Hesselink MKC: Optimisation of Oil Red O staining permits combination with immunofluorescence and automated quantification of lipids. *Histochem Cell Biol* 2001, 116:63-68.

Response's to Professor Lee's comments:

General comment:

(1) Manuscript is in-print.

Specific comments:

p 16 Section 1.3.1: Comment:	It is possible that GA absorption could occur if a dose of 150 mg/kg was administered.
p 49 Section 2.1.4: Comment:	Source, formulation and purity of GA – Sigma Aldrich, 100% by weight, >75% HPLC grade.
p 95 Figure 3.10: Comment:	It is valid to combine and tabulate all the values for all the control rats in the different treatment groups. Different control values for the different dosages were presented to show the data range of each group but all the individual control values were still within the normal range (e.g.: 8 – 12 mmol/L for blood glucose).

Response's to Professor Sheila's comments:

General comment:

(1) p viii: Add title of Appendices in Table of Contents:

Appendix 1 –	Calculation of sample size
Appendix 2 –	Preparation and standard curve of glucose, insulin, TAG, cholesterol and HDL-cholesterol
Appendix 3 –	Protocol of total RNA extraction from liver and kidney
Appendix 4 –	Protocol of total RNA extraction from abdominal and quadriceps femoris muscle
Appendix 5 –	Protocol of total RNA extraction from subcutaneous and visceral adipose tissue
Appendix 6 –	Rnase-free DNase treatment
Appendix 7 –	cDNA synthesis
Appendix 8 –	Characteristics of primers and probes for total PPARγ, PPARγ2, LPL and BAC amplification
Appendix 9 –	Optimized reaction mixtures for qRT-PCR
Appendix 10 –	Standard curve construction for quantification of total PPARγ and PPARγ2 expression
Appendix 11 –	Optimized qRT-PCR temperatures
Appendix 12 –	Preparation of buffers for 11β-HSD determination
Appendix 13 –	Preparation of standards for protein concentration
Appendix 14 –	Preparation of 17α-OH-11-dehydrocorticosterone standards
Appendix 15 –	Manuscript in-print

(2) Graphs were blurry as they were copied from the statistic software.

(3) Typographical errors:

p 179 line 8:	"was" for "were"
p 189 line 11:	"is" for "are"
p 191 line 16:	"is" for "are"
p 193 line 7:	"tissues" for "tissue"
p 229 line 6:	Add at the end of the sentence: 23 – 33
p 252 line 7:	Add at the end of the Journal title: USA

(4) Appendices had been referred in the main text in the thesis

(5) Abstract does not need to be revised as there were no changes made in the thesis.

Specific comments:

p 12 Table 1.3: Comment: Mastura *et al* (2008) referred to the Malaysian population

p 26 Figure 1.7: Add at the end of the sentence:

"Despite having only two protein isoforms, there are four possible mRNA isoforms arising from the PPARγ gene. The PPARγ1, PPARγ3 and 4 mRNA encodes for the PPARγ1 protein while the PPARγ2 mRNA encodes for PPARγ2 protein".

p 31 Figure 1.9: Add at the end of the sentence:

"The NH,-terminal domain contains the active-site residues and apoC-I1 interaction site that covers the catalytic cleft. The COOH terminal domain contains the Ab epitope and heparin-binding region required for lipolysis. They are positioned in close proximity to the active-site region on the other subunit".

p 45 Section 1.7: Comment: The eventual candidate for the GA treatment would be the diabetics as it could help them control the risk factors for metabolic syndrome. However, the results of my study also indicate that those at risk of diabetes could also be targeted as the GA treatment managed to successfully control the blood glucose and lipid levels in rats. This study was not performed using diabetic rats as the main objective was to determine the effects of GA towards PPARγ, 11β-HSD and LPL levels. Thus, lean rats were selected in this study. The use of diabetic rats would be considered in future work as this work was done to ascertain the relationship between GA and the three mentioned parameters. The data of my study is important as it highlights the role of GA to ameliorate hyperglycaemia, insulin resistance, visceral obesity and dyslipidaemia, all risk factors for metabolic syndrome. Individuals with metabolic syndrome have been known to have a high risk for the development of type 2 diabetes mellitus and cardiovascular diseases.

p 49 Section 2.1.4: Comment: No positive control was included as the main objective was to determine the effects of GA on the parameters studied and not to compare the effects of GA with the available synthetic drugs in the market. Research has already been done on the effects of the synthetic drugs and it would not be feasible to repeat it in my study. Data of daily food and fluid consumption were not documented because the data used was to ensure that the rats did not suffer a sudden loss in appetite which might affect their physiology and to determine the amount of GA consumed a day. Data showed that the rats took an average of 25g of rat chow and consumed 30ml of GA daily.

p 51 Section 2.2.1: Add at the end of the subtitle: (Varley *et al*., 1980)

p 57 line 3: delete "total mRNA" and read "for the total RNA extraction…"

p 64 para 2 and 3: Comment: The beginning of a sentence with a numeral was used to state the amount of compound required. The format used was similar to those in the published papers

p 66 Section 2.5: Add at the end of the subtitle: (Okuno *et al*., 1998)

p 68 Figure 2.3: Comment: Figure was placed at this page because it was also mentioned in the main text in page 67.

P 74 Table 3.1: Comment: Table was presented to indicate the p-values and the range of the data for Figures 3.1, 3.2 and 3.3.

p 75 Figure 3.1: Comment: Standard errors cannot be indicated in a median graph (box plot). However it was stated in a mean graph (histogram). The number of experiments was not stated as it was clearly understood that eight rats were used in each group.

p 78 Section 3.1.2.1: Comment: This section was included as a short section to explain how the data was obtained. The method in which the copy numbers were obtained had been included in the thesis at page 62.

p 89 Table 3.5: Comment: % decrease is relative to the control rats. Data in Figure 3.8 was re-calculated and found to be similar as reported in the thesis.

p 95 Figure 3.10: Comment: Reduction in blood glucose levels at 75mg GA is significantly different. The data presented (box plot) represents the lower quartile, median and the upper quartile. Thus the overlapping seen could be due to the wide data range. All the data queried were again subjected to statistical analysis and the data was found to be as reported in the thesis.

p 156 Figure 3.49: Comment: Lim *et al* (2009) used 50 mg/kg GA while the data in this figure represents the effects of the administration of 100mg/kg GA, thus leading to different results.

p 170 para 2: Add at the end of the para 2:

"The subcutaneous adipose tissue in the GA-administered rats showed an increase in the number of small size adipocytes".

p 177 Section 4.1: Comment: There were no significant differences observed between oral and IP routes due to the short duration of treatment (12 hours) and the low dose of GA (50 mg/kg) administered. Professor Lee commented that it could be due to the small number of animals in each group. However the amount of samples/animals used were approved by the Monash Animal Ethics committee and were calculated as shown in page 253. The preparation of GA in my study was similar to those in the reported literature and was also administered through the oral route. However, my study is expanded to determine the effects of GA on various other parameters as compared to the literature which only focused on the properties of GA. The study of the bioavailability of GA has been carried out by various researchers (Ploeger *et al*., 2001; Ishbrucker and Burdock, 2006). The LD_{50} values of GA were not examined as it has already been reported by Ishbrucker and Burdock (2006) and was found to be between the range of 1220 – 12,700 mg/kg.

p 190 para 2 line 10: Sentence was replaced with:

"Thus, this represents the potential glucoregulatory regulation in the skeletal muscles by PPARγ".

p 195 para 2: Comment: A new paragraph was made beginning from "LPL is a key…"

p 195 para 3: Comment: The main text was written not with the aim to postulate but to emphasize that the findings in my study were similar to those found by Fried *et al* (1993).

p 198 Section 4.6: Comment: Last sentence of para 1 was removed – "It was reported… ".

p 200 para 3 line 1: Comment: The higher 11β-HSD2 activity in the visceral adipose tissue was compared to subcutaneous adipose tissue and this was in agreement with the findings of Milagro *et al* (2007).

p 201 line 3: Comment:	Refer to amendments for page 170.
p 205 para 3: Comment:	Delete “excess” and read “the removal of glucose”.
p 210-213: Comment:	Data for blood pressure was presented in page 167-168 while discussion on the measurement were in page 210-213 (as in the thesis).
p 214 Section 4.10: Comment:	The text in this section is already a summary of the overall postulated effects of GA on the various parameters examined and is simplified into Figure 4.10.
p 218 & 219: Comment:	Oral route was stated as the most effective as it is a safer route of administration, simple, safe, cheap and it does not cause an increase in the stress levels of the rats. This is crucial as this study involves the analysis of GC levels. The main aim of this study was to investigate the short term effects of GA on the various studied parameters in rats. Upon carrying out the research, 12, 24 and 48 hours as well as seven days were determined as the treatment duration. Comparing between the treatment durations, the seven day treatment duration resulted in the optimal improvement in the various parameters studied. Future work in this study would involve lengthening the duration of the treatment to determine the effects of GA given long term to rats. In this study, the insulin and lipid profile were stated to be non-significant. There were only two postulations made in the conclusion chapter. Therefore it does not seem to be overly postulated.

p 221 Future work: Add to the end of the para 2:

“The potential use of state-of-the-art technologies such as microarrays can be used to address the genome wide analysis of the studied genes following GA administration”.

p 259, 260 & 261 Appendix 3, 4 & 5: delete “total mRNA” and read “for total RNA extraction…”